

NN31157.150

Agricultural Research Department  
Winand Staring Centre for Integrated Land, Soil and Water

# Relationships between forest condition and natural and anthropogenic stress factors on the European scale; pilot study

J.M. Klap (SC-DLO), W. de Vries (SC-DLO),

J.W. Erisman (RIVM) and E.P. van Leeuwen (RIVM)

(Editors)

sc-dlo



**rivm**  
research for  
man and environment

SC REPORT 150

RIVM REPORT 722108022

Wageningen (The Netherlands), 1997

32/447(150) 2<sup>e</sup> ex

BIBLIOTHEEK  
STARINGGEBOUW

**Relationships between forest condition and natural and  
anthropogenic stress factors on the European scale; pilot study**

**J.M. Klap (SC-DLO)  
W. de Vries (SC-DLO)  
J.W. Erisman (RIVM)  
E.P. van Leeuwen (RIVM)**

**(Editors)**

**SC Report 150  
RIVM Report 722108022**



23 DEC. 1997

**DLO Winand Staring Centre, Wageningen (The Netherlands), 1997**

15ng48900\*



## ABSTRACT

J.M Klap, W. de Vries, J.W. Erisman & E.P. van Leeuwen (Editors), 1997. Relationships between forest condition and natural and anthropogenic stress factors on the European scale; pilot study. Wageningen (The Netherlands), DLO Winand Staring Centre. Report 150. 245 pp.; 54 Figs; 33 Tables; 236 Refs; 5 Annexes.

Ten years of defoliation data for six tree species of the systematic forest condition monitoring network have been correlated with site-specific estimations of various stress factors, both natural and anthropogenic. The stress factors include available and interpolated soil data, interpolated and modelled meteorological data and modelled air pollution and deposition data. Various threshold values were included, e.g. site-specific estimations for the critical deposition levels. The results were highly affected by methodological differences the different countries. On top of this effect, age is an important factor, followed by different natural and anthropogenic stress factors, depending on the tree species.

Keywords: vitality, defoliation, drought, temperature, air pollution, atmospheric deposition, threshold values, *Pinus sylvestris*, *Picea abies*, *Quercus robur*, *Quercus petraea*, *Fagus sylvatica*, *Quercus ilex*

ISSN 0927-4537

© 1997 DLO Winand Staring Centre for Integrated Land, Soil and Water Research (SC-DLO)  
P.O. Box 125, NL-6700 AC Wageningen (The Netherlands).  
Phone: +31 317474200; fax: +31 317424812; e-mail: postkamer@sc.dlo.nl

No part of this publication may be reproduced or published in any form or by any means, or stored in a data base or retrieval system, without the written permission of the DLO Winand Staring Centre.

The DLO Winand Staring Centre assumes no liability for any losses resulting from the use of this document.

Projects 7438/7536

## Contents

Preface	9
Summary	11
1 Introduction	19
1.1 Background and Aims	19
1.1.1 Background of this report	19
1.1.2 Aims of this study	20
1.2 Hypotheses explaining forest decline	21
1.3 Tree species and stress factors considered in this study	23
1.4 Contents of this report	24
2 The selected response variables in the correlative study	25
2.1 Introduction	25
2.1.1 Response variables considered	25
2.1.2 Aims and contents of Chapter 2	26
2.2 Methods	26
2.3 Results	27
2.3.1 Numbers of observations	27
2.3.2 Actual defoliation	29
2.3.3 Changes in defoliation	30
2.3.4 Trends in defoliation	32
2.4 Discussion and conclusions	34
3 Stand and site characteristics and chemical soil composition	37
3.1 Introduction	37
3.1.1 Stand and site characteristics	37
3.1.2 Chemical soil composition	37
3.1.3 Aim and contents of Chapter 3	38
3.2 Methods and data	38
3.2.1 Observation and derivation of stand and site characteristics	38
3.2.2 Observation of the chemical soil composition	39
3.2.2.1 Sampling	40
3.2.2.2 Sample Preparation	40
3.2.2.3 Sample Storage	40
3.2.2.4 Soil Analysis	41
3.2.2.5 Quality control	41
3.2.3 Amount of data received	42
3.2.4 Clustering of soil type information and extrapolation of soil chemical data	43
3.2.4.1 Clustering	43
3.2.4.2 Extrapolation	45
3.3 Results and discussion	45
3.3.1 Site and stand characteristics	45
3.3.2 Chemical composition of the humus layer	47
3.3.3 Chemical composition of the mineral layer	48



3.4 Conclusions	52
4 Calculation of natural meteorological stress	55
4.1 Introduction	55
4.2 Input data and methods	56
4.2.1 Estimation of site-specific meteorological data	56
4.2.2 Temperature stress indices	57
4.2.3 Relative transpiration	59
4.2.4 Calculation of the water balance components	61
4.3 Results and discussion	63
4.3.1 Meteorological data	63
4.3.2 Temperature stress indices	63
4.3.2.1 Overall variation	63
4.3.2.2 Temporal variation	65
4.3.2.3 Spatial variation	66
4.3.3 Relative transpiration	69
4.3.3.1 Overall variation	69
4.3.3.2 Temporal variation	70
4.3.3.3 Spatial variation	70
4.4 Uncertainties	71
4.4.1 Meteorological data	71
4.4.2 Temperature stress indices	72
4.4.3 Relative transpiration	72
4.5 Conclusions	73
5 Calculation of anthropogenic air pollution stress	75
5.1 Introduction	75
5.2 Concentrations and present loads of sulphur and nitrogen compounds and loads of base cations	76
5.2.1 Introduction	76
5.2.2 Methods	76
5.2.2.1 The EDACS model	76
5.2.2.2 Model validation procedures	77
5.2.3 Results and discussion	78
5.2.3.1 Concentration levels	78
5.2.3.2 Deposition levels of sulphur and nitrogen compounds	83
5.2.3.3 Deposition levels of base cations	86
5.2.4 Uncertainties in the concentration and deposition estimates	88
5.2.4.1 Concentration levels	88
5.2.4.2 Deposition levels	88
5.3 Ozone concentrations	92
5.3.1 Introduction	92
5.3.2 Methods	93
5.3.3 Results and discussion	94
5.3.3.1 Overall variation	94
5.3.3.2 Temporal variation	95
5.3.3.3 Spatial variation	95
5.3.4 Uncertainties	97
5.4 Conclusions	97

6 Critical thresholds for sulphur and nitrogen compounds and ozone	101
6.1 Introduction	101
6.1.1 Critical concentration levels	101
6.1.2 Critical deposition levels	101
6.1.3 Aims and contents of Chapter 6	102
6.2 Methods to derive critical deposition levels for sulphur and nitrogen compounds	103
6.2.1 The simple mass balance approach	103
6.2.2 Adaptations of the simple mass balance approach	105
6.3 Results and discussion	106
6.3.1 Critical concentration levels for sulphur and nitrogen compounds and ozone and calculated exceedance at the monitoring plots	106
6.3.1.1 Sulphur and nitrogen compounds	106
6.3.1.2 Ozone	107
6.3.2 Critical deposition levels for sulphur and nitrogen compounds and calculated exceedances at the monitoring plots	108
6.3.2.1 The eutrophying impact of nitrogen	108
6.3.2.2 The acidifying impact of sulphur and nitrogen	111
6.4 Uncertainties	114
6.4.1 Derivation of critical levels	114
6.4.2 Calculation of critical deposition levels for nitrogen	115
6.4.3 Calculation of critical deposition levels for acidity	116
6.5 Conclusions	118
7 Relationships between crown condition and stress factors	121
7.1 Introduction	121
7.2 Methodological approach	122
7.2.1 Statistical method	122
7.2.1.1 Regression model	122
7.2.1.2 Temporal and spatial correlations	124
7.2.1.3 Data set used	124
7.2.2 Response variables considered	125
7.2.3 Predictor variables included	126
7.2.3.1 Key factors considered	126
7.2.3.2 Temporal aggregation and lagged effects	128
7.2.3.3 Correlations between predictor variables	129
7.2.3.4 Included interactions	130
7.2.3.5 Threshold values	130
7.2.4 The investigated relationships between response and predictor variables	131
7.2.4.1 Models used	131
7.2.4.2 Sets of predictor variables used in the various models	132
7.2.4.3 Strategy of model selection	134
7.3 Results	136
7.3.1 Correlation between predictor variables	136
7.3.2 Analysis of actual defoliation data (Model A)	137
7.3.2.1 Reference models	137
7.3.2.2 Additional tests	139
7.3.2.3 Separation of country effects and stress factors	139
7.3.3 Analysis of the changes in defoliation (Model B)	146



7.3.4 Analysis of trends in defoliation (Model C)	147
7.4 Discussion and recommendations	148
7.5 Conclusions	151
8 Discussion	153
8.1 Introduction	153
8.2 Quality of stress data	154
8.2.1 Introduction	154
8.2.2 Site characteristics	154
8.2.3 Meteorological stress	155
8.2.4 Air pollution	155
8.3 Relationships between crown condition data and stress	157
8.3.1 Correlative studies with European data	157
8.3.2 Evaluation of relationships and comparison with existing hypothesis on forest decline	158
8.3.3 Final remarks	160
9 Conclusions	161
9.1 Stand and site characteristics	161
9.2 Chemical soil composition	161
9.3 Meteorological stress	162
9.4 Air pollution	163
9.5 Relationships between crown condition and environmental stress factors	164
9.6 Overall conclusions	165
10 Uncertainties and recommendations	167
References	169
Annexes: Technical details on assessment methods and additional results	189
Annex 1 Interpolation of meteorological data	191
Annex 2 Calculation of evapotranspiration, transpiration, interception and soil evaporation	195
Annex 3 Calculation of concentration and deposition levels of acidifying compounds, base cations and ozone	201
Annex 4 Calculation of model inputs to derive critical deposition levels	221
Annex 5 Detailed results of the statistical analyses	231

## Preface

The present report is the result of a pilot study in which preliminary relationships were assessed between forest condition (crown condition in terms of defoliation) and various stress factors on the European scale at the so-called Level 1 sites. These sites form a systematic network of monitoring plots, distributed all over Europe, including some 30 countries, both EU and non-EU. This monitoring network is an initiative of the European Commission (DG VI) and ICP Forests of UN-ECE.

This report is part of a series of reports handling about forest condition:

- Assessment of the possibilities to derive relationships between stress factors and forest condition for The Netherlands (Report 147);
- Relationships between forest condition and stress factors in The Netherlands (Report 148);
- Assessment of the possibilities to derive relationships between stress factors and forest condition for Europe (Report 149);
- Relationships between forest condition and natural and anthropogenic stress factors on the European scale; pilot study (Report 150);
- Relationships between forest condition and natural and anthropogenic stress factors on the European scale; comprehensive study (Report 151).

Reports 147 and 148 are dealing with the forest condition in The Netherlands. Reports 149, 150, and 151 are dealing with the forest condition in Europe. In Reports 147 and 149 data availability and possible methods to analyse forest condition data are reported. In Reports 148, 150 and 151 the results are described of the execution of the proposed methods (Reports 147 and 149). The studies on The Netherlands and European scale were executed simultaneously. The execution phase on the European scale is divided into a pilot study (the present report: Report 150) and a comprehensive study (Report 151)

This pilot study on the European level was carried out separately in this report, but was also incorporated in the overall evaluation of ten years of crown condition monitoring at the Level 1 sites. This overall evaluation was an initiative of the 11<sup>th</sup> Task Force Meeting of ICP Forests. The combination of the current study with this evaluation offered the opportunity to broaden the view of the current project and to enrich this evaluation with an analysis of the relationship between the observed crown condition with various possible stress factors. In this respect, most of the contents of this separate report was also issued as the Part B of the Technical Background Document of the Common Overview Report of UN/ECE and EC 'Ten years of forest condition monitoring in Europe: studies on temporal development, spatial distribution and impacts of natural and anthropogenic stress factors' (UN/ECE & EC, 1997a; Müller-Edzards et al., 1997). The most important difference (besides various editorial differences) between the two versions is, that the present report had to accommodate for the fact that the presentation of crown condition data of Part A of the '10 Years Overview Report' is not available for the reader of the present report. Therefore, an additional chapter (Chapter 2) was included in this issue, which gives in short an



overview of the defoliation data, concentrated on the way these data were included in the correlative study.

The correlative study (and the ongoing study as a whole) is mainly an initiative of SC-DLO and RIVM. The editors Klap and De Vries are affiliated with SC-DLO, whereas the editors Erisman and Van Leeuwen are affiliated with RIVM. There are, however, various other institutes involved in the pilot phase of the correlative study and the preceding derivation of site-specific estimations of stress factors, namely:

- Federal Institute for Forest Research and Forest Products (BFH / PCC-West, Hamburg, Germany; Chr. Müller-Edzards; Chapter 1: imbedding in Overview Report),
- Laboratory of Soil Science, Gent University (FSCC, Gent, Belgium; L Van-mechelen, E. van Ranst; Chapter 3: chemical soil composition),
- Swedish Environmental Research Centre (IVL, Göteborg, Sweden; G. Lövblad; Chapter 5: validation of deposition estimates),
- Norwegian Meteorological Institute (DNMI, Oslo, Norway; D. Simpson; Chapter 5: validation of air pollution concentration estimates) and
- Centre for Biometry Wageningen (CBW, Wageningen, The Netherlands, J. Oude Voshaar, Chapter 7: development of statistical models).

## Summary

### **Background and aims of the study**

In order to obtain more insight in the possible causes of forest decline (in terms of defoliation and discolouration) a pilot study was carried out, in which the observed data on crown condition are correlated with site-specific estimations of various natural and anthropogenic stress factors. This pilot study was also imbedded in the evaluation of 10 years of forest condition monitoring at the Level 1 plots. In this framework, the work of this pilot study was focused on the derivation of stress factors and the correlative study using the available crown condition data.

The general aim of the pilot study was to gain insight in or to derive information on:

1. temporal and spatial patterns of forest condition (in terms of defoliation) in Europe;
2. soil characteristics related to atmospheric deposition of S and N compounds and base cation inputs (based on the results of a recent soil survey);
3. stress factors (modelled) with respect to meteorology (temperature stress and water stress) and air pollution (concentrations and deposition levels of S and N compounds and ozone);
4. threshold values (modelled) for air pollution (critical deposition levels for N and acidity) and
5. the correlation between the temporal trends and spatial patterns of forest condition, the effects of stand and site characteristics, and the above mentioned natural and anthropogenic stress factors.

The study was focused on six major tree species for which the number of trees was large enough to perform sound statistical analyses: *Pinus sylvestris*, *Picea abies*, *Quercus robur* and *Q. petraea*, *Fagus sylvatica* and *Quercus ilex*.

### **Temporal and spatial trends in crown condition**

Analyses with respect to temporal changes and spatial patterns in crown condition focused on the effect parameters in the correlative study, which were derived from the available data on defoliation, namely the actual defoliation, the change in defoliation (compared to the previous observation) and the trend in defoliation. The calculated mean defoliation values per plot were analysed on a logit transformed scale.

The number of plots and observations decrease strongly according to *Pinus sylvestris*; *Picea abies* > *Quercus robur* + *Quercus Petraea*; *Fagus sylvatica* > *Quercus ilex*. Furthermore, there is a considerable increase in the number of plots during the considered period, especially for the most common tree species *Pinus sylvestris* and *Picea abies*. The actual defoliation data show a variation which is wide enough for a sound statistical analysis.

There is a declining tendency in the crown condition (increase in defoliation), although it is more clear for the non-coniferous tree species (*Quercus robur*, *Quercus petraea*, *Fagus sylvatica* and *Quercus ilex*) than for the coniferous tree species (*Pinus sylvestris*, *Picea abies*). Annual changes in defoliation vary mostly between plus or



minus 10%, whereas average trends in defoliation vary generally between plus or minus 5% per year. Positive trends (increased defoliation) occurred at about an equal number of plots as negative trends. The median value is close to 0, which means that the overall deterioration in crown condition over the monitoring period is not large. However, distinct cluster of large deterioration occurs in Central and Eastern Europe, where air pollution is high, such a cluster also occurs in Spain, where the reverse is true but meteorological stress is high. Extreme changes in defoliation up to 30% (both as deterioration and recovery) do occur, but such changes may, however be due to (i) extreme meteorological events, (ii) to certain pests or diseases (not included in the statistical analyses due to a lack of data) or (iii) to a learning effect in the beginning of the monitoring period (not accounted for in the statistical analyses).

### ***Stand and site characteristics***

General stand and site characteristics (soil type, main tree species, tree age, altitude, humus type and water availability) were assessed during the crown condition assessment. The number of plots for which such parameters were available varied between 2227 and 5843. Other relevant stand characteristics, such as tree height, influencing atmospheric (dry) deposition, and evapotranspiration, have not been recorded. Therefore, this stand characteristic was derived as a function of tree species, tree age, climatic zone and site quality characteristics using yield tables.

Results of the distribution of tree species over major stand and site characteristics, show that (i) stand ages between 20 and 100 years are evenly distributed over the various tree species (an exception is *Quercus ilex*, where most stands are relatively young), (ii) the coniferous tree species (*Pinus sylvestris* and *Picea abies*) and the *Quercus* species (*Q. robur* and *Q. petraea*) mainly occur in the lowlands below 500 m (approximately 70-90% of the sites), whereas *Fagus sylvatica* and *Quercus ilex* are quite evenly distributed over the altitudes between < 250 m up to 1500 m and (iii) the coniferous tree species occur mainly on coarse textured poorly buffered sandy soils, whereas the deciduous tree species occur more frequently on fine textured clay soils and on calcareous soils.

### ***Chemical soil composition***

This report presents the major results of a recent soil survey, by limiting the chemical soil composition to parameters that affect the forest condition and/or reflect the impact of atmospheric deposition. Soil chemical parameters thus included are the pH, base saturation and C/N ratio. The information for mineral topsoil includes measured values whenever the soil condition plots coincide with the crown condition plots. For those crown condition plots where no soil data were available (e.g. Italy, Poland, Sweden) soil properties were extrapolated using the FAO soil map. The extrapolation procedure was performed since data for base saturation and C/N ratio in the mineral soil were needed to calculate critical deposition levels for all Level I plots.

Measured values of the pH(CaCl<sub>2</sub>) in the humus layer are generally 0.5 pH unit lower than in the mineral topsoil. Inversely, the base saturation is generally much higher in the humus layer compared to the mineral soil. Acid topsoil conditions, i.e. a pH(CaCl<sub>2</sub>) below 3.5 in the humus layer and below 4.0 in the mineral topsoil, and a base saturation below 25% in the mineral soil, occurs at approximately 40-50% of the sites. It is likely

that acid inputs to these soils is buffered by the release of toxic aluminium. Extremely acid topsoil conditions, namely a  $\text{pH}(\text{CaCl}_2)$  below 3.5 and a base saturation below 10% occurs at less than 10% of the sites. At those sites, acidic deposition will certainly be buffered by the mobilisation of toxic Al. C/N ratios are mostly lower in the humus layer compared to the mineral soil. C/N ratios in the humus layer below 20, which might indicate enhanced N accumulation, occurred at 10% of the sites.

The FAO soil type explained 68% of the variation in pH and 49% of the variation in base saturation. Using soil clusters, the explanation decreased to 50% and 37%, respectively. The spatial pattern of pH and base saturation and C/N ratio over Europe is thus strongly correlated with soil type (parent material class). To a lesser extent, this is also true for the C/N ratio, where soil type explained only 11% of the variation. Fine textured (clay) soils and calcareous soil with a high pH and base saturation and a low C/N ratio mainly occur in Southern Europe. An impact of acid deposition levels on the soils could not be substantiated on the European scale.

### ***Meteorological stress***

Meteorological stress parameters include temperature stress and drought stress. Temperature stress indices used in this study were (i) a winter index (the sum of daily mean temperatures below 0°C between October 1 and April 1), (ii) a late frost index (the lowest minimum temperature below 0°C starting 15 days before bud burst and ending at June 30), (iii) a heat index (the sum of daily maximum temperatures above 35°C during the growing season) and (iv) a summer index (the sum of daily mean temperatures above 5°C during the dependent growing season). The growing season varied between tree species and the climatic region. Temperature stress indices were derived from the interpolation of 6 hour averaged air temperature data from available meteorological databases in the period 1980-1995 (the database was extended to 1980 in order to describe lagged effects). The water stress parameter used in this study was the relative transpiration (transpiration reduction), which gives insight in the tree species specific drought stress. Relative transpiration was calculated with a combined meteorological/hydrological model using interpolated data for precipitation, cloud cover, air temperature, dew point temperature and wind speed obtained from the meteorological databases mentioned above.

As expected, results showed that the spatial variation of temperature indices coincides with the climatic regions in Europe. A low winter index and high heat index was calculated for sites in southern Europe, where mainly deciduous trees occur, whereas the sites in northern Europe (mainly coniferous trees), experience a high winter index and a low heat index. The largest temporal variation was calculated for the winter index, coinciding with warm and cold years. Relative transpiration is lower for deciduous trees in the South of Europe than for the coniferous trees in the North. It shows a complex spatial pattern, coinciding to a large extent with patterns of rainfall and temperature, which both are important parameters for the calculation of transpiration.



### ***Air pollution***

Air pollution data were calculated with two recently developed models for the calculation of concentration and deposition levels of S and N compounds and base cations (EDACS) and for the calculation of ozone concentration levels (EDEOS) in combination with models developed at EMEP. With respect to S and N compounds, wet deposition data derived with the EMEP model at a resolution of  $150 \times 150 \text{ km}^2$  were used. The data were combined with site specific dry deposition estimates derived with the EDACS model, using air concentration fields, calculated with the EMEP model, in combination with stand characteristics and meteorological data. For base cations a similar approach was used, but calculations were limited to the period between 1989 and 1993, for which detailed air concentration fields were available. Data were extrapolated to the period between 1986 and 1995 using a trend in base cation concentrations in precipitation obtained from the EMEP monitoring network.

Present concentration levels of S and N compounds were compared with critical levels for these compounds. Critical concentration levels, related to the direct above-ground effects of an exposure of  $\text{SO}_2$ ,  $\text{NO}_2$  and  $\text{NH}_3$  on the forest condition, were derived from the literature and were used independent of location, tree species and/or soil type.

Calculated annual average  $\text{SO}_2$  concentrations for all the monitoring sites between 1986 and 1995 varied mainly between 2 and  $50 \mu\text{g m}^{-3}$ . The critical concentration of  $20 \mu\text{g m}^{-3}$  was exceeded at 20% of the monitoring sites, mainly in Central Europe. A clear reduction in exposure of  $\text{SO}_2$  concentration (and  $\text{SO}_2$  deposition) is shown between 1986 to 1992. Calculated maximum annual average concentrations of  $\text{NO}_2$  and  $\text{NH}_3$  were 27 and  $3 \mu\text{g m}^{-3}$ , which is lower than the critical levels of 30 and  $8 \mu\text{g m}^{-3}$ , respectively. Even though the calculated concentration levels of N compounds ( $\text{NO}_2$  and  $\text{NH}_3$ ) are strongly underestimated in and near source areas, direct above-ground effects only play a role on the local scale but not on a European scale.  $\text{NH}_3$  concentrations show no clear trend during the ten years, whereas  $\text{NO}_2$  concentrations decreased very little.

Ozone concentration levels were only calculated for 1990, since emission data from the various countries came available at a very late stage. The calculation for one year was done to have at least some insight in the spatial pattern of ozone stress, to be included in the correlation between crown condition and stress parameters. Hourly ozone concentrations at canopy level were calculated with the EDEOS model using air concentration fields of  $\text{O}_3$  at 50 m above the surface, calculated with the EMEP model, in combination with  $\text{NO}_2$  and NO stand characteristics, and meteorological and orographic data. Critical levels for ozone have been defined by the sum of differences between the hourly ozone concentrations in ppb during daylight hours and a threshold value of 40 ppb during a six-month growing season commencing at the first of April. For forests, a critical accumulated ozone exposure over a threshold of 40 ppb, called AOT40, has been set at 10 ppm.hours independent of the tree species considered. AOT30 and AOT60 values were also calculated for use in the correlative study.

Calculated annual average AOT40 values for  $\text{O}_3$  in 1990 exceeded the long-term critical AOT level of 10 ppm.h at more than 90% of the monitoring sites. It must be



emphasised that 1990 was a year with relatively high O<sub>3</sub> concentrations and might therefore not be representative for other years. The critical level was exceeded to a large extent for all deciduous forest stands (*Quercus robur* + *Quercus petraea* and *Fagus sylvatica*) and for *Quercus ilex* and at approximately 80% of the coniferous forest stands (*Pinus sylvestris* and *Picea abies*). Exposure is different for the different tree species as the result of the spatial distribution of species and of O<sub>3</sub> concentrations. The coniferous trees are mainly located in the Northern part of Europe, where ozone concentrations are relatively low. *Quercus robur* + *Q. petraea* and *Quercus ilex* occur mainly in Southern Europe where the ozone concentrations are higher than in Northern Europe. *Fagus sylvatica* is mainly located in Central Europe, where ozone concentrations are highest, specifically in mountainous areas.

### ***Exceedances of critical deposition levels***

Critical deposition levels, related to the indirect soil-mediated effects of atmospheric deposition on forest condition, were calculated for each monitoring site with an adapted version of the simple mass balance model for the acidifying impact of both S and N compounds assuming that a tree species specific, critical Al/(Ca+Mg+K) ratio in soil solution is not exceeded at the bottom of the root zone. Separate critical deposition levels for nitrogen as a nutrient were derived by requiring that an assumed critical N content in foliage is not exceeded to avoid an increased sensitivity to natural stress. The calculation of a long-term critical load used in policy making assumes a steady-state situation, that may occur in the future. In this study however, the actual threshold at the time of consideration is relevant. This led to adaptations of the model application. Critical deposition levels were only calculated for soils with a base saturation below 25%. Below this value, Al release is considered to start and a critical Al/(Ca+Mg+K) ratio is the basis for the critical deposition level calculation. Stands with a base saturation of less than 25% covered 42% of all the monitoring plots. For the other plots the critical deposition level was assumed to equal the present load. Furthermore, the calculation of the model inputs was based on base cation deposition, and uptake and precipitation data for the time period 1985-1995, instead of long-term averages in order to account for these processes at the time of consideration.

The range in calculated present N loads was comparable to the range in calculated critical N deposition levels related to possible vegetation changes in the ground vegetation. Values varied mostly (ca 90%) between 100 and 1000 mol<sub>c</sub> ha<sup>-1</sup> a<sup>-1</sup>. The percentage of plots where these critical N deposition levels were exceeded equalled 25%. These plots mainly occurred in Central and Western Europe, such as Germany, Poland, the Czech Republic and The Netherlands, where present N loads are high. The range in calculated critical N deposition levels related to effects on trees, such as nutrient imbalances and increased susceptibility to drought, frost and diseases/pests was much higher than those related to vegetation changes. Values varied mostly between 1500 and 2500 mol<sub>c</sub> ha<sup>-1</sup> a<sup>-1</sup>. Calculated current deposition levels during the considered period hardly ever exceeded these critical thresholds. The calculated deposition levels of N compounds are, however, seriously underestimated. Available data for high N deposition areas indicate that elevated N deposition is a serious problem in relation to forest condition (nutrient imbalances, elevated susceptibility to natural stress factors etc.).

As with the concentration levels of SO<sub>2</sub>, NO<sub>2</sub> and NH<sub>3</sub>, highest deposition levels for acidity (the sum of S and N compounds) were calculated in Central and Western Europe. Calculated base cation deposition was largest in coastal areas due to sea salt and in Southern Europe due to soil (Sahara) dust. Base cation deposition compensated almost entirely for the potential acid input in the South of Europe, whereas in Central Europe it equalled about 25% of the potential acid input. Potential acid deposition decreased between 1986 and 1992, but remained fairly constant after 1992. The strong decrease is mainly the result of the decrease in SO<sub>x</sub> deposition, and to a small decrease in NO<sub>y</sub> deposition. Calculated critical deposition levels for acidity varied in the same range as the calculated present loads (mostly between 1000 and 8000 mol<sub>c</sub> ha<sup>-1</sup> a<sup>-1</sup>). The number of plots where critical acid deposition levels are exceeded equalled 12% of all plots. These plots were mainly located in Central and Western Europe.

#### ***Relationship between forest condition and environmental stress factors***

The relationship between the observed crown condition (response variable) of five major tree species (*Pinus sylvestris*, *Picea abies*, *Quercus robur* + *Quercus petraea*, *Fagus sylvatica* and *Quercus ilex*) and the measured and modelled stress factors (predictor variables) was investigated by using multiple regression analyses. *Quercus robur* and *Quercus petraea* were lumped in the correlative study because of the limited number of stands and the partly comparable autecology. The response variables for the considered tree species were limited to three defoliation measures, namely (i) the average actual defoliation at each plot, (ii) the change in the defoliation compared to the observation in the previous year and (iii) the trend in defoliation during the observation period. The change and the trend in defoliation were added as response variables to accommodate for the effect of country on the observed defoliation, which is the result of different standards for the reference trees and the systematic observer variation between countries. The predictor variables include time-independent (constant) site and stand characteristics and chemical soil parameters and time-dependent modelled data on meteorological variables and air pollution. In the latter case, the exceedance of critical deposition levels were also used as predictor variables. The possible impact of the time-dependent predictor variables was extended with 'lagged' effects years after the occurrence of certain events. Furthermore, the annual deviation of the modelled meteorological stress variables from the mean values in the considered 10 year period were used as predictor variables, because these deviations are less confounded with countries than the absolute values.

Country as a predictor variable explained 33-39% of the actual defoliation, and age explained additional 2 and 13% of defoliation. Other stress factors that obviously explained the increase in defoliation for the considered species to a certain degree, were relative transpiration (*Pinus sylvestris*, *Quercus robur* + *Q. petraea*, *Fagus sylvatica* and *Quercus ilex*), the concentration of NO<sub>2</sub> (*Quercus robur* + *Quercus petraea*, *Fagus sylvatica* and *Quercus ilex*), the SO<sub>2</sub> concentration (*Fagus sylvatica*) and the ozone concentration (*Quercus ilex*). When using changes and trends in defoliation, the effect of country appeared to be much less significant, still explaining up to 10% of the defoliation. This implies that the different application of the methodology (the use of different reference trees) may affect changes and trends in defoliation. Excluding country as an explaining variable, altitude, various meteorological stress parameters



(relative transpiration, late frost, summer index and winter index), and air pollution stress factors ( $\text{NO}_2$  and  $\text{NH}_3$  concentrations, AOT30 and acid deposition) explained mostly less than 10% of the changes and trends in defoliation. Note that it is not suggested here that the AOT30 or AOT60 values should be used, instead of the AOT40 as critical levels for ozone.

### ***Overall conclusions and recommendations***

Several modelled stress factors showed a significant relationship with forest condition but the explanation of the variability in the current defoliation and changes and trends in defoliation was generally low. Results using current year defoliation data as response variable showed a strong relationship between defoliation and countries (an explanation of 35-40% of the variation) and age (an increase in the explanation between 4 and 15%). Various other stress factors, both natural and anthropogenic, appeared sometimes to be significant, depending on the tree species.

There are several reasons for the limited explanation by the empirical relationships between the defoliation data and the various stress factors, including (i) the inspecificity of the response variable with respect to the predictor variables (stress factors), (ii) the limited comparability of crown condition data between countries, (iii) the large uncertainties in the derivation of environmental stress factors on the local scale, (iv) neglecting several factors influencing crown condition such as mechanical damage (e.g. wind-break, snowbreak, fire etc.) and biotic stress (insect attacks, fungi diseases, game and grazing, action of man), due to limited data availability, (v) the non-specific character of defoliation as vitality indicator with respect to air pollution, (vi) the occurrence of interactions of air pollution with natural stress (meteorological stress and diseases/pests), age and other tree characteristics and (vii) the relatively short considered period that does not take into account long-term effects of anthropogenic stress factors and (viii) the limited time frame in which this pilot study was executed, preventing the possibilities to improve the available methods.

Part of these drawbacks will be solved in the comprehensive study, which is following this pilot study.



# 1 Introduction

*Wim De Vries<sup>1)</sup>, Jaco Klap<sup>1)</sup>, Jan Willem Erisman,<sup>2)</sup> Christian Müller-Edzards<sup>3)</sup>*

<sup>1)</sup> DLO Winand Staring Centre (SC-DLO), Wageningen, The Netherlands

<sup>2)</sup> National Institute of Public Health and the Environment (RIVM), Bilthoven, The Netherlands

<sup>3)</sup> Programme Coordinating Centre-West (PCC West), BFH, Hamburg, Germany

## 1.1 Background and Aims

### 1.1.1 Background of this report

In order to obtain more insight in the possible causes of forest decline (in terms of defoliation and discolouration) a pilot study was carried out, in which the observed data on crown condition in Europe, monitored since 1986 at a systematic 16 x 16 km grid, the so-called Level 1 plots, were correlated with site-specific estimations of various natural and anthropogenic stress factors.

This pilot study was imbedded in an overall evaluation of 10 years of forest condition monitoring at the Level 1 plots. The necessity of such an evaluation was decided upon at the eleventh Task Force Meeting of ICP Forests of UN/ECE. The overall evaluation is presented in the so-called Technical Background Document of the '10 Years Overview Report' (Müller-Edzards et al., 1997), further denoted as the 'Overview Report'. This Overview Report contains (i) an analysis of the forest condition development in Europe between 1986 and 1995, including national reports outlining the forest condition and the relationship with air pollution in the participating countries (Part A of the Overview Report) and (ii) the current pilot study on the assessment of site-specific stress factors and a preliminary correlative study on the relationships between forest condition and the various environmental stress factors (Part B of the Overview Report). Besides this the methods and results of both parts were summarised in a much shorter, policy-aimed document (the '10 Years Overview Report'; UN/ECE and EC, 1997a). The results from this 'Overview Report' were combined in an executive report (UN/ECE and EC, 1997b) with a summary of the results of a soil chemical survey and a foliar composition survey at a selection of plots of the same Level 1 monitoring network and results of the Intensive Monitoring Programme.

This report can be considered as an adapted version of the pilot study presented in Part B of the Overview Report. The major difference is the inclusion of an additional chapter (Chapter 2) which gives an overview of the spatial and temporal variation in the crown condition data, with the emphasis on the way they were investigated in the correlative study.

This work was mostly carried out by SC-DLO and RIVM, in co-operation with PCC-West, IVL and DNMI. This pilot study is part of an ongoing project carried out by SC-DLO and RIVM. In this framework, this pilot study fits in between a Definition study and a Comprehensive Study. The Definition Study (Klap et al., 1997) was carried out in order to investigate all possible relationships between crown condition and stress

factors in view of the availability and quality of data. The comprehensive study will be carried out as a continuation of the ongoing project and will include all aspects which were omitted in the pilot study.

This pilot study was carried out in 1996 and 1997 and dealt with the forest condition data that were gathered in the period 1988-1995. The derivation of site-specific estimations for various stress factors was done for a longer period, starting with the year 1981.

### **1.1.2 Aims of this study**

The major aim of this correlative study is to derive empirical relations between forest condition and natural and anthropogenic stress factors. Furthermore, it is aimed to contribute to the interpretation of the variation in the crown condition data presented in Part A of the Overview Report. The latter was achieved by the inclusion of this report as the already mentioned Part B in the Overview Report and its implications for the Synthesis and the Conclusion of the Overview Report.

The aims of the present report are to:

- Make an analysis of the temporal and spatial variation in the defoliation data in the form they were included in the statistical analysis (additional to Part B of the Overview Report).
- Apply the results of a recent soil survey to considered locations with emphasis on soil characteristics that are related to atmospheric deposition of S and N compounds.
- Model site-specific estimations for stress factors with respect to meteorology (temperature stress and water stress) and air pollution (concentration and deposition levels of S and N compounds and ozone).
- Assign or model threshold values for air pollution (critical concentration and deposition levels).
- Explore the possibilities for the statistical analysis of 10 year of observed crown condition data and the trends in these data with the above mentioned natural and anthropogenic stress factors, while accounting for the effect of stand and site characteristics (including the chemical soil composition).

To achieve these aims, modelled water stress, air pollutant concentrations and data collected for soil condition assessments in Europe were added to the crown condition data by means of statistical methods. Our attempt is to assess possible relationships between natural and anthropogenic stress factors and forest condition. The preliminary results of this exercise will further be elaborated by improving the input data and the statistical methods, based on the finding presented in this report. The current study is therefore also indicated as a 'pilot study', since much is expected from these further elaborations.



## 1.2 Hypotheses explaining forest decline

To gain insight in the stress factors to be included in a statistical analyses, an overview is first given of the various hypotheses explaining forest decline.

Different hypotheses were proposed to explain the occurrence of forest decline. Auclair et al. (1992) blamed unfavourable weather conditions, especially drought for damaging the forests. Some authors suggested that pest infestations or fungi attacks following drought periods cause the overall deterioration of forest health (e.g. Houston, 1981; 1992). The role of forest management practices as adversely influencing forest health was discussed by Van Goor (1985), Nys (1989) and several others.

Although undoubtedly fungi may severely affect trees, the hypotheses that fungi are a major agent affecting forests, as supposed by Kandler (1992; 1994), failed explaining the widespread occurrence of forest decline. Research performed to evaluate the impact of insects on forests generally gave evidence that especially trees already affected proved sensitive to insect attacks (e.g. Speight and Wainhouse, 1989). The oxidising effect of strong acids on leaf cuticles as explaining forest decline as well had to be rejected, although in extremely polluted areas this effect had been observed (review given e.g. by Innes, 1993).

In contrast to these hypotheses which interpreted the deterioration of forest health as a natural or management related phenomenon, other scientists proposed that air pollution might cause defoliation and yellowing of leaves and needles. Burton et al. (1983) proposed heavy metals as impairing forest health. Manion (1981) and Evans (1984) suggested that the oxidation of SO<sub>2</sub> and NO<sub>x</sub> to strong acids might directly destroy the leaf cuticle and thus cause damage to trees. Smith (1981) discussed SO<sub>2</sub> and NO<sub>x</sub> as responsible for affecting biochemical pathways and so damaging foliage. Bruck (1985) proposed increased susceptibility towards frost, induced by nitrogen deposition. Matyssek et al. (1990) proposed ozone as agent damaging foliage.

Other authors considered soil acidification, associated with a decrease in pH and base cation saturation as well as an increase of the concentration of Al<sup>3+</sup> in the soil solution, responsible for recent forest decline (for example Ulrich et al., 1979, Hutchinson et al., 1986; Tamm and Hallbäcken, 1986) since Al<sup>3+</sup> is very likely to be toxic to plant roots (Cronan and Gregal, 1995; Marschner, 1990; Mengel, 1991). Several authors (e.g. Roelofs et al., 1985; Schulze 1989) suggested that acidification of soil and excessive N inputs causes nutrient imbalances. This coincided with field observations and foliage analyses that deficiencies of Mg and K caused yellowing of needles of Norway spruce (Bosch et al., 1983; Zöttl and Mies, 1983; Zech and Popp, 1983). The hypotheses on air pollution and its effects on soil chemistry took into account the well-known reaction of plants to nutrient deficiencies (for details see Marschner, 1990). The role of nitrogen as fertilising agent was considered as causing forest damage by several authors (e.g. Nihlgård 1985). In this respect Ulrich et al. (1979), Ellenberg (Jr.) (1983, 1985 and 1991) and Tamm (1991) stressed that the increase of nitrogen in the environment leads to changes in vegetation as well as damage to trees. A continuous high input of N, may cause damage to forests due to: (i) water shortage, since a high N input favours growth



of canopy biomass, whereas root growth is relatively unaffected (De Visser, 1994), (ii) nutrient imbalances, since the increase in canopy biomass also causes an increased demand of base cation nutrients (Ca, Mg, K) whereas the uptake of these cations is reduced by increased levels of dissolved  $\text{NH}_4$  (Boxman et al., 1988) and (iii) an increased sensitivity to natural stress factors such as frost (Aronsson, 1980; Bruck, 1985) and attacks by fungi (Roelofs et al., 1985). An excess input of N can finally cause pollution of ground water due to  $\text{NO}_3$  leaching.

Hypotheses which refer to air pollution as causing forest damage are still discussed controversially. Effects of air pollution might show up with a considerable time delay, especially where concentrations are low (UN/ECE, 1991). However, some authors deny any relationship between deterioration of forest health and air pollution (e.g. Kandler, 1992 and 1994). Yet, most scientists agree that forest condition is influenced by a multitude of different stress factors including air pollution (e.g. FBW, 1989; Schulze, 1989; UBA, 1994; Landmann and Bonneau, 1995), the dynamics of which are partly not understood for their non-linear characteristics.

Hypotheses which took into account indirect effects of air pollutants, however, still give evidence for affecting forest health, and thus have to be considered as important, since many of the affected forest stands were located far away from sources of acidifying compounds, long-range transboundary air pollution was suspected to play an important role in deteriorating ecosystems in Europe (UN/ECE, 1979). First evidence for the impact of air pollution as impairing the stability of ecosystems was found in Scandinavia, where lakes and soils showed severe changes in their chemical constitution, especially due to increasing  $\text{SO}_4^{2-}$ -concentrations accompanied by increasing acidification. The monitored lakes and soils, however, were located very distant from known sources of  $\text{SO}_4^{2+}$  which led to first evidence for the risk of long-range transboundary air pollution.

Under the scope of the programme on large scale monitoring on Level I, crown condition and the occurrence of easily identifiable damage as biotic or climatic stress are assessed annually. Furthermore, soil condition data and foliar element contents were recorded at part of the monitoring plots. Until now no thorough study has been performed to derive causal relationships between forest vitality in Europe on the one hand and natural and anthropogenic stress on the other hand. Several studies, however, used national data to search for empirical relations between the two (e.g. Mather, 1994; Nellesmann and Frogner, 1994; Hendriks et al., 1994). In 1991 an Interim report on cause-effect relationships in forest decline was prepared for the Programme Coordination Centres with the assistance of the United Nations Environment Programme (UNEP) and the Secretariat of the United Nations Economic Commission for Europe. This report concluded that 'the methods assessing and reporting forest health have provided a valuable overview of forest condition in Europe but are not designed to clarify cause-effect relationships'. The main reasons for this were that for a better understanding of these relationships, the basic survey should be extended with intensive monitoring of hydrology, biology and chemistry.

### 1.3 Tree species and stress factors considered in this study

More than 100 tree species are assessed annually at the Level 1 plots. However, only few species occur in considerable numbers. A limited number of tree species was selected to be included in the correlative study. This selection was based on the number of plots at which these species were found and on the representativeness of the species. The distribution of tree species at the Level 1 plots can be considered as a representative sample of the European forests, since this network consists of a systematic grid. For this correlative study the two most common coniferous tree species (*Pinus sylvestris* and *Picea abies*) and the two most common and most wide-spread deciduous tree species (*Quercus robur* and *Q. petraea* and *Fagus sylvatica*) were selected. *Quercus ilex* was added as a representative of the Mediterranean tree species.

The selected species account for more than two thirds of all trees, and the analysed sample can thus be considered as representative for most European forests. The number of trees for the other species is generally too small for sound statistical analysis. The statistical analyses performed in this part requires sufficient observations to reveal statistically significant relationships between the various predictor variables (stress factors) and forest condition. The two deciduous oak species were analysed together in the same analyses. The applied statistical models were adapted to account for possible differences between the two species.

Table 1 Factors influencing forest condition, their source and main aspects (after Klap et al., 1997)

Factor	Data source	Main aspects	In this study
Stand characteristics	Stand characteristics	Tree species, age, canopy closure	yes
Management	(Historical) management data	Management system/thinning regime, fertilisation	no
Water availability	Site characteristics	Water retention capacity	yes
	Meteorological data	Precipitation, temperature, evaporation	yes
	physiological processes	Water uptake, transpiration	yes
Temperature	Meteorological data	Heat, cold, winter frost, late frost	yes
Insects, fungi, bacteria, viruses	Local observation	Insect attacks, fungal etc. infestations (resp. 'pests' and 'diseases')	no
	Forest sanity data bases	-	no
Chemical foliar composition	Foliar chemical data	N, P, Ca, Mg, K contents in foliage	no
Chemical soil composition	Soil chemical data	pH, base saturation, nutrient availability, heavy metal, aluminium concentrations	yes
	Site characteristics	Soil type, hydrology	yes
Exposure to gaseous agents	Ambient composition	O <sub>3</sub> , SO <sub>2</sub> , NH <sub>3</sub> , CO <sub>2</sub> , VOC's, HF	yes
Deposition of atmospheric compounds (and exceedances of critical levels)	Ambient composition	Distance to sources, transport processes	yes
	Stand characteristics	Tree height, canopy closure, dist. to forest edge	yes
	Site characteristics	Orography, chem. soil composition, roughness	yes
	Meteorological data	Precipitation, temperature, wind speed, radiation	yes
Mechanical damage	(Historical) management data	Accidents, miss-management	no
	Meteorological data	Storms, snow cover, glazed rain	no

The general trends in vitality parameters can not be explained by current known monocausal relations. Thus in order to detect empirical relations, nearly all known and possible stress factors have to be derived for each site for all the years. An overview of



these factors and data is given in Table 1. Table 1 displays the data which are in principle necessary for each site (and for each year) in order to test and develop statistical models and the data used in this pilot study. The required temporal scale is different for the different parameters (Klap et al., 1997; Chapter 6).

The focus of this pilot study was the derivation of meteorological data and both current and critical concentration/deposition levels of S and N compounds and ozone and its correlation with trends in defoliation for the period 1986 to 1995. The correlative study was limited to five major tree species, since the number of stands is too small for an in-depth analysis for the other species (Section 7.2.1). Data on the foliar composition were not yet used. Furthermore, data on insects, fungi etc. and on management were too scarce to be used in this study. More information on the stress factors used in this study is given in Section 7.2.

## **1.4 Contents of this report**

Chapter 2 gives an overview of the response variables that were selected from the available defoliation data. These response variables include the actual defoliation and the changes and trends in defoliation at all Level 1 plots.

Stand and site characteristics and relevant soil data (pH, base saturation and C/N ratio) of the Level I plots, used in the correlative study, are presented in Chapter 3. This includes measured data at approximately 50-60% of the plots, depending on the parameter considered, and data that are assigned based on extrapolations with soil type. In Chapters 4 and 5, the various stress factors which might impair forest health and the methods of their assessment are given. This includes meteorological stress factors (Chapter 4) as well as anthropogenic stress due to increased concentrations and depositions of S- and N-compounds and ozone (Chapter 5). In Chapter 6, the calculated stress factors for air pollution are compared with calculated site-specific estimations for the critical concentration and deposition levels.

In Chapter 7 relationships between crown condition and stress factors are given. This includes a regression analysis that correlates defoliation data of five major tree species with stand/ site characteristics, measured and extrapolated soil data and modelled data of stress factors.

After a discussion of the results (Chapter 8), conclusions and recommendations for future activities are drawn (Chapter 9). Supplementary information explaining the methods and models used in Chapter 4, 5 and 6 is given in the Annexes 1-4, whereas additional results from the statistical analysis are given in Annex 5.



## 2 The selected response variables in the correlative study

*Jaco Klap, Wim de Vries*

*DLO Winand Staring Centre (SC-DLO), Wageningen, The Netherlands*

### 2.1 Introduction

#### 2.1.1 Response variables considered

This chapter describes the selected response variables that were used for the statistical analysis of the six considered tree species. The selected response variables were derived from the defoliation data that were presented more extensively in Part A of the Technical Background Document of the '10 Years Overview Report' (Müller-Edzards et al., 1997). All peculiarities and limitations of that data base, therefore, also apply for the data presented here (Chapter 2-4 of Part A of the Technical Background Document; Müller-Edzards et al., 1997). The defoliation data used in the statistical analysis, however, differ from the data presented in Part A of that report due to (i) the use of transformed values of the defoliation data and (ii) slight differences in the calculated changes and trends in defoliation data.

Various response variables can be calculated from the available crown condition data. In the pilot study, however, the response variable for each of the six considered tree species was limited to three defoliation measures, namely : (i) the average actual defoliation at each plot, (ii) the change in the average defoliation compared to the observation in the previous year and (iii) the average estimated trend in defoliation during the observation period. In an analysis of the actual defoliation differences between countries should be accounted for, since different reference trees are used to determine the degree of defoliation (Chapter 6). This effect is likely to be limited with respect to changes and trends in defoliation. That was the reason to include these response variables.

*Table 2 Expected advantages and disadvantages of using the actual forest condition or the change or trend in forest condition as response variable*

Response variable	Advantage	Disadvantage
Actual forest condition	- Response variable is likely to be sensitive for the effect of stress factors	- Different standards for reference tree - Only within-country variation of stress factors is used
Change in forest condition	- Effect of different reference trees is limited - Large range in stress factors by neglecting country effects	- Response variable is likely to be less sensitive to stress factors
Trend in forest condition	- Effect of different reference trees is limited - Large range in stress factors by neglecting country effects - Better opportunities for revealing 'long term' trends	- Response variable is likely to be less sensitive to stress factors - Loss of year-to-year variation (within-plot differences)

Besides the actual defoliation, it can be expected that changes and trends also respond to stress (the predictor variables). For example, a certain stress in the current or previous year may cause defoliation increase in that year (change). Or a continuously

high stress during several decades may have a lagged effect that results in a deterioration trend in the observation period. It is, however, likely that changes and trends in defoliation are less sensitive indicators for stress by e.g. air pollution. A stand with high defoliation in high deposition area, for example, may not change much from the present bad situation, whereas such changes may occur at a lower deposition level for healthier stands. The (expected) advantages and disadvantages of the approaches are summarised in Table 2.

## 2.1.2 Aims and contents of Chapter 2

The aim of this chapter is to give an overview of the response variables used in the correlative study. The selected values for the actual defoliation and the changes and trends in defoliation are thus presented on the logit scale used in the statistical analysis. Data on the original percentage scale used in the field observations are also presented for intercomparison.

This chapter first gives a short overview of the methods used (Section 2.2) followed by an overview of the resulting data (Section 2.3). First, the numbers of available data are presented for the three response variables (Section 2.3.1). Then, overviews are given of the spatial and/or temporal variation of the actual defoliation (Section 2.3.2), the change in defoliation (Section 2.3.3) and the trend in defoliation (Section 2.3.4). Finally some conclusions are given (Section 2.4) in relation to the applicability of the data for the statistical analysis.

## 2.2 Methods

Defoliation data are determined for at least 20 individual trees at each Level 1 plot. For plots with a mixed species composition, a lower number of individual trees was available for the analysis. In the analyses we used, however, average values for each tree species at the plot, since no information is available on the difference between predictor variables on the individual tree level. The calculation of average values for the current defoliation and of the change and trend in defoliation was done after a logit transformation of the observed values for the individual trees. The equation used for this transformation is :

$$\text{logit(defoliation)} = \text{Ln} \left( \frac{\text{defoliation}}{1 - \text{defoliation}} \right) \quad (\text{Eq.1})$$

where:

defoliation = the defoliation on the scale between 0 and 1 (i.e. percentage / 100)

The logit transformation was made to make a meaningful use of additive aspects of predictor variables (Section 7.2.1). Actual defoliation values (and changes and trends) at the boundaries of the original scale (near 0 and 100%) get more weight at the transformed scale than values in the middle of the scale. Note that (i) the logit value



equals 0 at an original defoliation of 50%, negative below this value and positive above this value and (ii) the logit transformation can not be applied on negative values. The latter constraint implies that it is essential to first transform the original defoliation data, since changes and trends can be negative.

The change in defoliation was calculated as the deviation of the defoliation in the current year, compared to the defoliation in the previous year. Unlike the presented values in Chapter 3 of Part A, the change was thus calculated (and used as a response variable) independent of the (5% or 10%) defoliation classes in which the previous year defoliation occurred. The trend in defoliation was calculated as the coefficient (i.e. the 'slope') in a regression with the plot-mean defoliation values as the Y variable and the year as the X variable for plots with at least two observations. Again, this differs from the calculation of trends presented in Section 4.2 of Part A of the '10 Years Overview report', where an index of trends was calculated as the Spearmans rank correlation between the actual defoliation of all individual trees at each plot and years. In calculating trends, it was assumed that the tree species composition at the plots did not change. As with the actual defoliation, the changes and the trends in the annual mean defoliation were also used on the logit scale in the statistical analysis. The values at the original percent scale used in the field assessments are, however, added in this chapter for reasons of comparison.

The following sections give an overview of the number of observations for the three response variables for the considered six tree species (Section 2.3.1), the overall variation in the three response variables for the considered six tree species by means of a cumulative frequency distribution (Section 2.3.2), the temporal (annual) variation in the actual defoliation and the changes in defoliation by means of graphs (Section 2.3.3) and the spatial distribution of trends by means of a map irrespective of tree species (Section 2.3.4).

## 2.3 Results

### 2.3.1 Numbers of observations

This section gives an overview of the numbers of plots and observations (plot-year combinations) per tree species that were available for the statistical analysis. In principle all available reliable observations were used in the analyses (Table 3). The total number of plots refer to the plots which have been assessed at least once, which is more than the most recent assessment because some plots were abandoned within the considered time period. The observations for the actual defoliation and changes in defoliation include the data that were available for all plots for all the years of observation. For the trends in defoliation, the observations equal the number of included plots.

Results show that the number of plots and observations decrease strongly according to *Pinus sylvestris*; *Picea abies* > *Quercus robur* + *Q. Petraea*; *Fagus sylvatica* >

*Quercus ilex*. Especially for the last tree species, the number of plots and observations is at the border for a reliable statistical analyses.

Table 3 The available number of plots and observations for the selected response variables for the analysed tree species

Species	Actual defoliation		Change in defoliation		Trend in defoliation (plots/values)
	Plots	Observ. <sup>1)</sup>	Plots	Observ. <sup>1)</sup>	
<i>Pinus sylvestris</i>	2433	9164	1798	6471	1825
<i>Picea abies</i>	2089	7362	1513	4745	1576
<i>Quercus robur</i>	497 2)	together:	432 3)	together	together
<i>Quercus petraea</i>	422 2)	4563	376 3)	3555	823
<i>Fagus sylvatica</i>	846	3945	735	2933	765
<i>Quercus ilex</i>	215	1481	207	1263	206

<sup>1)</sup> The number of observations equals the number of plot-year combinations

<sup>2)</sup> The total number of plots with at least one of the two species equals 836. In the consecutive sections, the observations for *Quercus robur* and *Quercus petraea* are presented separately. Note, however, that the values in the statistical analyses were averaged over both species.

<sup>3)</sup> The total number of plots with at least one of the two species equals 734.

The first year of defoliation data included in the analysis was 1988. The data base with defoliation data contains also data for the year 1987 but this year was left out from the analysis because (i) for many countries this was the first year of observation, for which the results are less comparable with the results of later years, due to learning effects and (ii) the 1987 assessment contained relatively few locations, which partly do not coincide with later assessments.

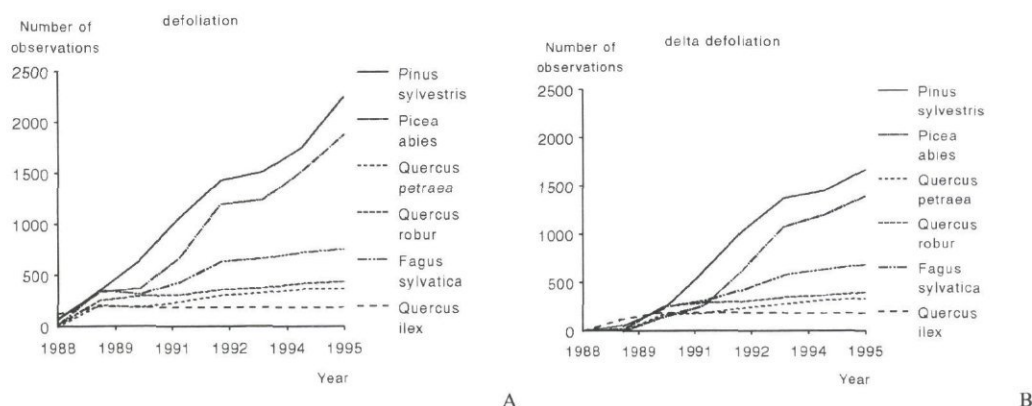


Fig. 1 Temporal variation in the number of available data for the actual defoliation (A) and the change in defoliation (B) for the six investigated tree species

There is a large increase in the number of included plots during the considered time period between 1988 and 1995, both for the actual defoliation data and for the changes in defoliation compared the previous year, specifically for *Pinus sylvestris* and *Picea abies* (Fig. 1). This means that there is a large variability in the length of the time series, which may be aggravated by the occurrence of missing years within the time series for a considerable number of plots. In the applied regression model, however, the analysis of locations with unequal time series did not cause limitations in the derivation of relationships between response and explaining variables. Therefore all observations



were included. Although the number of observations on defoliation was small in the first years, the inclusion of these years was considered useful to have longer time series for at least part of the plots.

### 2.3.2 Actual defoliation

These results for the actual defoliation were investigated by means of cumulative frequency distributions of the actual defoliation for the six investigated tree species for all plot-year combinations both on the original scale used in the field assessments (%) and on the logit scale used in the statistical analysis (Fig. 2).

Results show that the percentage of stands with a defoliation above 25% (stands that are considered to be damaged) increases according to sclerophyllous tree species (*Quercus ilex*) > deciduous tree species (*Fagus sylvatica*, *Quercus robur* and *Quercus petraea*) > coniferous tree species (*Pinus sylvestris*, *Picea abies*). Values varied from approximately 10% for *Quercus ilex* to approximately 30% for *Picea abies* (Figure 2A). On the logit scale, values are mostly negative (Figure 2B) since the absolute defoliation is nearly always below 50% for all tree species considered (see the explanation on the logit transformation given before).

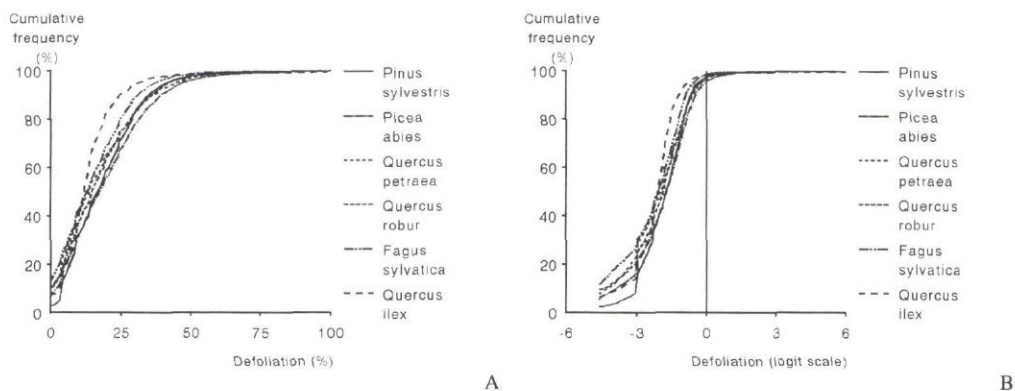


Fig. 2 Cumulative frequency distributions of the actual defoliation for the six considered tree species on the original percent scale (A) and on the logit scale used in the statistical analysis (B)

The results for the defoliation data in terms of the development of the distribution over the different 5% classes (Fig. 3) continuously increased during the observed, which means that the data of two consecutive years are not completely comparable (Section 2.3.1). These figures, however, do give a first impression of the results that will be analysed in the next section. The conclusions that can be derived from these figures are in line with those given in Part A of the Overview Report (EC/UN-ECE, 1997). There is a clear decline in the crown condition (increase in defoliation) over the whole considered time period for the non-coniferous tree species (*Quercus robur*, *Quercus petraea*, *Fagus sylvatica* and *Quercus ilex*). In general the largest changes are found between 1988 and 1990. Note, however, that the number of plots increases strongly in this period. This may also have influenced the seemingly strong increase in defoliation

for *Pinus sylvestris* in this period. From 1990 onwards the actual defoliation does not strongly change for the coniferous tree species.

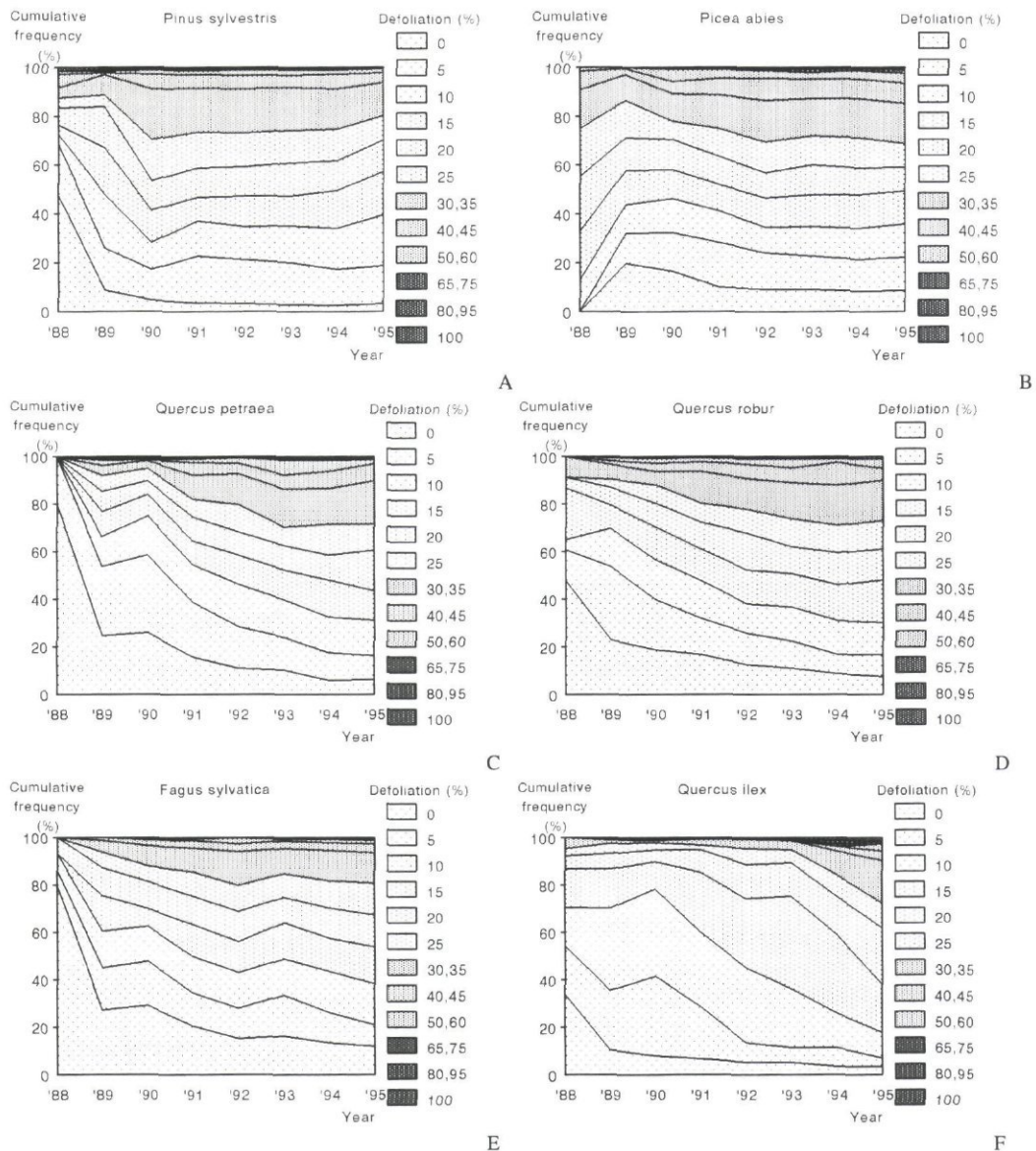


Fig. 3 Temporal development of the 5% defoliation classes for the six considered tree species (Note that the number of plots varies through the years)

### 2.3.3 Changes in defoliation

The results on the calculated changes between two consecutive years are presented in this section by means of cumulative frequency distributions of all data per tree species (Fig. 4) and the temporal development of the yearly changes (Fig. 5).



The cumulative frequency distributions are presented both on the percent scale of the actual observations (Fig. 4A) and on the transformed scale on which the statistical analysis were conducted (Fig. 4B). The figures lump all available data of the calculated changes, irrespectively over which consecutive years they were calculated. Positive values in the figure indicate an increased defoliation (decreased crown condition), whereas negative values indicate the reverse.

Results show that annual changes in defoliation vary mostly between plus or minus 10% (Fig. 4). Extreme changes up to 30% (both as deterioration and recovery) do, however, occur. This may be due to extreme meteorological events or to certain pests or diseases, but it may also partly be due to a learning effect in the beginning of the monitoring period. In general an increase in defoliation (positive values) occurs more often than a decrease (negative values) even though the median changes are close to zero for all the tree species considered. As stated before, the cumulative frequency distributions indicate that a (slight) decrease in crown condition (increase in defoliation) is larger going from *Pinus sylvestris* < *Picea abies* < *Fagus sylvatica* < *Quercus robur*, *Quercus petraea* < *Quercus ilex*. This is in accordance with the results presented in Chapter 3 of Part A of the '10 Years Overview Report' (EC/UN-ECE, 1997).

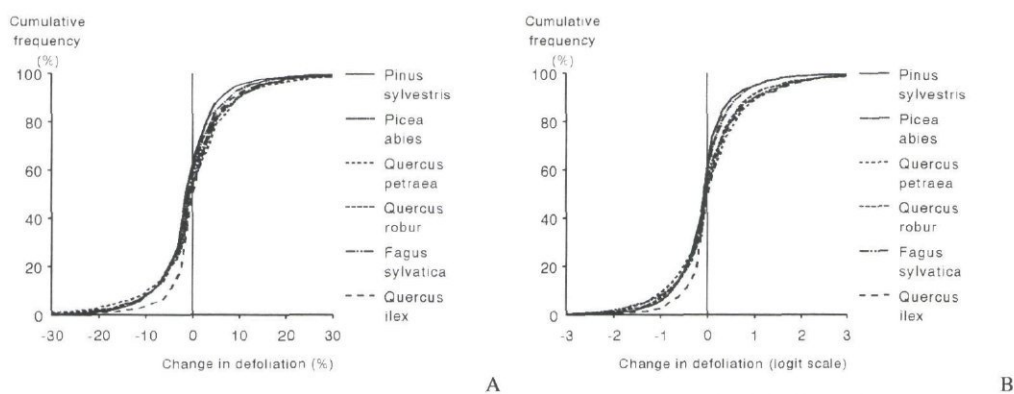


Fig. 4 Cumulative frequency distributions of the calculated changes in defoliation between two consecutive years for the six considered tree species on the original percent scale (A) and on the logit scale used in the statistical analysis(B)

The results of the temporal development of the changes between two consecutive years are also affected by the varying number of plots through the years, which puts limitations on the interpretability of the results (Fig. 5). The results, however, give a good impression about the relative number of positive and negative changes in the various years. The conclusions that can be derived from these figures are comparable to those related to Figure 3 and 4. There is a stronger decline in the crown condition (increase in defoliation) for the non-coniferous tree species (*Quercus robur*, *Quercus petraea*, *Fagus sylvatica* and *Quercus ilex*) than for the coniferous tree species (*Pinus sylvestris* and *Picea abies*) and in general the largest changes are found between 1988 and 1990.

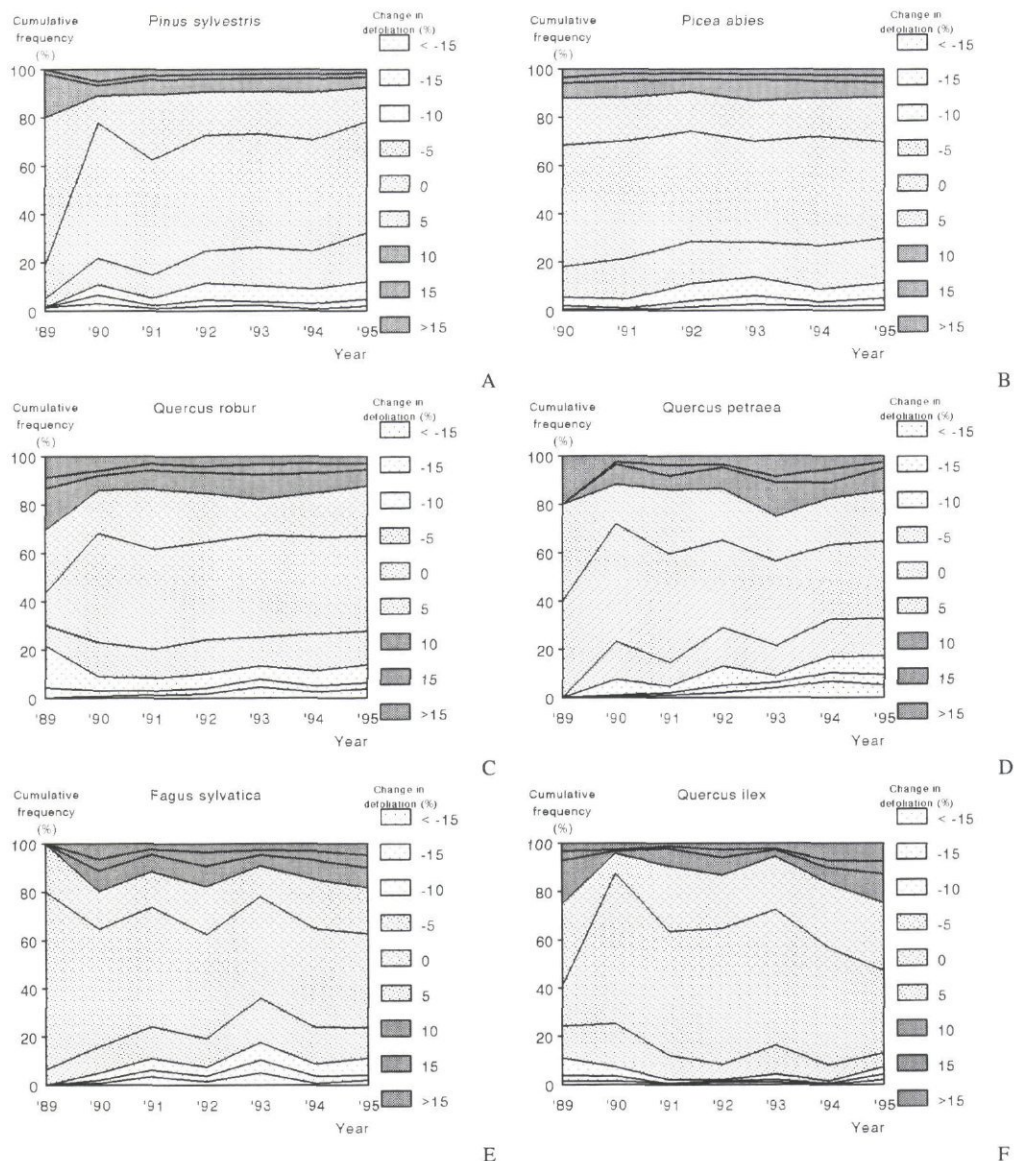


Fig. 5 Temporal development of the changes in the 5% defoliation classes compared to the previous year for the six considered tree species (Note that the number of plots varies through the years)

### 2.3.4 Trends in defoliation

The calculated trends are presented by means of cumulative frequency distributions of all data (both on the original percent and on the logit transformed scale; Fig. 6) and by means of a map with the spatial distribution of the results (Fig. 7). Here these results are presented irrespective of the tree species considered, whereas in the statistical analysis (Chapter 7) the results are analyses of all species separately.

Average trends in defoliation vary generally between plus or minus 5% per year (Fig. 6). Extreme values up to 15% per year are due to calculated trends in short time



series (less than 4 year). Again, this figure shows that a positive trend (increased defoliation) occurs more often than a negative trend, but the difference is very small. The median value is close to 0, which means that the overall deterioration in crown condition over the monitoring period is not very large.

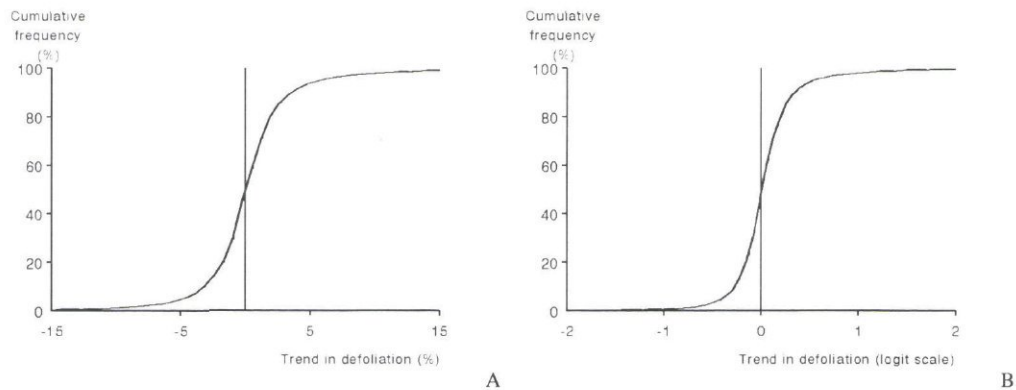


Fig. 6 Cumulative frequency distributions of the calculated trends in the defoliation for the six considered tree species on the original percent scale and on the logit scale used in the statistical analysis

It should be noted that the above results, do not imply that there may not be a clear problem with respect to forest vitality in relation to e.g. air pollution problems. The investigated stands in large parts of Europe are not exposed to severe air pollution (Chapter 5). In this context it is relevant to see what the spatial distribution is of the calculated trends. This is illustrated in Fig. 7. These results show a rather scattered pattern of positive and negative trends for the most of Europe. This indicates that differences occur within short distances and that local conditions and specific stand characteristics have a strong impact on the results.

There are, however, distinct clusters of plots with a positive trend in defoliation throughout the whole of Europe. The spatial distribution of these clusters is in accordance with the spatial distribution in the differently calculated trend indices in Chapter 4 of Part A of the '10 Years overview Report' (Müller-Edzards et al., 1997). The map (Fig. 7) is quite comparable to the map with sites with an increase in defoliation that is at least moderately larger (kriged residuals greater than the 75th percentile) than expected from geographic location, altitude and climatic zone. As with that map, Fig. 7 shows a distinct cluster of large deterioration (brown and red squares) in Central and eastern Europe and in Spain. It is well known that the air pollution differs strongly between both regions (Chapter 5), indicating that other factors than air pollution alone (as mentioned in Chapter 1) must be responsible for this decrease. There is however a clear coincidence with the high air pollution in Central Europe and the high deposition of acidity (specifically sulphur), exceeding critical loads in this area (Chapter 6).



Fig. 7 Trend in defoliation per plot on the logit scale over all observed years including all tree species

## 2.4 Discussion and conclusions

Conclusions related to the applicability of the defoliation data (response variables) for use in the statistical analysis presented in Chapter 7 are as follows.

1. The number of plots and observations decrease strongly according to *Pinus sylvestris*; *Picea abies* > *Quercus robur* + *Quercus Petraea*; *Fagus sylvatica* > *Quercus ilex*. Especially for the last tree species, the number of plots and observations is rather low for a reliable statistical analyses.
2. There is a large increase in the number of plots during the considered time period (1988-1995) specifically for *Pinus sylvestris* and *Picea abies*. This means that there is a large variability in the length of the time series. Even though (i) the inclusion of all relevant data is useful, in order to have longer time series for at least part of the plots and (ii) unequal time series can be accounted for in the statistical analyses, the different length of time series affects the calculation of trends.
3. There is a declining tendency in the crown condition (increase in defoliation), although it is more clear for the non-coniferous tree species (*Quercus robur*, *Quercus petraea*, *Fagus sylvatica* and *Quercus ilex*) than for the coniferous tree species (*Pinus sylvestris*, *Picea abies*). This is in accordance with the results given in Chapter 3 of Part A of the Overview Report. In general the largest changes are



found between 1988 and 1990, but the number of plots increased strongly in this period. This may also have influenced the seemingly strong increase in defoliation for this period and thus the statistical analyses.

4. Annual changes in defoliation vary mostly between plus or minus 10%, whereas average trends in defoliation vary generally between plus or minus 5% per year. Positive trends (increased defoliation) occurred at about an equal number of plots as negative trends. The median value is close to 0, which means that the overall deterioration in crown condition over the monitoring period is not large, although a distinct decreasing trend has been observed in the lowest 10% defoliation class (Chapter 3 of Part A of the Overview Report (Müller-Edzards et al., 1997)). It is thus unlikely that the use of changes and trends in defoliation over the whole of Europe will give a clear relationship with stress factors. Even though a distinct cluster of large deterioration occurs in Central and Eastern Europe, where air pollution is high, such a cluster also occurs in Spain, where the reverse is true but meteorological stress is high (in accordance with Chapter 4 of Part A). It is also questionable whether a clear relationship between these stress factors and trends or changes in defoliation can be derived in specific parts of Europe with a clear deterioration in crown condition.
5. Extreme changes in defoliation up to 30% (both as deterioration and recovery) do occur. It is unlikely that such changes, which may be due to (i) extreme meteorological events (only approximated at the sites by interpolation from meteorological databases) or (ii) to certain pests or diseases (not included in the statistical analyses due to a lack of data) or (iii) to a learning effect in the beginning of the monitoring period (not accounted for in the statistical analyses) can be explained by the stress factors included in the statistical analyses.

### 3 Stand and site characteristics and chemical soil composition

Wim de Vries<sup>1)</sup>, Gert Jan Reinds<sup>1)</sup>, Jaco Klap<sup>1)</sup>, Lucas Vanmechelen<sup>2)</sup> and Eric van Ranst<sup>2)</sup>

<sup>1)</sup> DLO Winand Staring Centre (SC-DLO), Wageningen, The Netherlands

<sup>2)</sup> FSCC, Gent University, Gent, Belgium

#### 3.1 Introduction

##### 3.1.1 Stand and site characteristics

As stated in Chapter 1 (Table 1), there are several stand and site characteristics, such as tree species, tree age, altitude, soil type and water availability that influence forest condition (defoliation and/or discoloration) (UN/ECE and EC, 1996). Stand and site characteristics that are assessed during the crown condition assessment include the main tree species, tree age and altitude. These data have been assessed for a total number of 5843 plots.

Additional soil related site characteristics, such as humus type and soil type have been recorded during a soil survey carried out by 15 EU member states and 8 non-EU countries in the period between 1990 and 1995. The European *Forest Soil Condition Database* presently contains information on 4532 plots in 23 countries, and will be extended with more than 1000 plots from 8 countries in the coming years, with the possibility for more data from other countries. Most observation plots (ca 3000) are situated at the intersection points of a 16 x 16 km<sup>2</sup> grid, and are shared with the *Forest Crown Condition Database*. The main objective of this European-wide soil survey is the assessment of basic information on the chemical soil status and on other soil properties determining the vulnerability of the soil to air pollution.

The relatively large number of soil survey plots that do not coincide with the crown condition monitoring plots is mainly due to the fact that all soil survey plots in Sweden (1200) completely differ from the forest condition plots (700). For the whole of Sweden, interpolated values for the latter plots were used.

##### 3.1.2 Chemical soil composition

For each plot, the database consists of general information, such as FAO soil classification name, and chemical and physical data of organic and mineral soil layers. The mineral soil was sampled at two or three fixed depths between 0 and 20 cm. Data are available in the majority of plots for the following parameters: pH(CaCl<sub>2</sub>), organic carbon, nitrogen for both mineral and organic layers, and total amounts of P, K, Ca and Mg for organic layers. Total concentrations of Na, Al, Fe, Cr, Ni, Mn, Zn, Cu, Pb and Cd and cation exchange properties were less frequently reported. In addition, information on soil parent material and some physical soil properties (texture, coarse fragments content and bulk density) was provided on a voluntary basis (FSCC, 1997).



Here we report the major results of this soil survey, by limiting the chemical soil composition to parameters that reflect the impact of atmospheric deposition and/or affect the forest condition. Soil chemical parameters thus included are pH, base saturation and C/N ratio (compare FSCC, 1997). Unlike the FSCC report, measured data are limited to soil survey plots coinciding with the crown condition monitoring plots, thus excluding approximately 1500 plots. Furthermore, maps are presented for the mineral topsoil that do not only include measured values but also extrapolated values for all the crown condition monitoring plots. This extrapolation was performed since (i) data for the base saturation and the C/N ratio in the mineral topsoil were needed to calculate critical deposition levels for the monitoring plots (Section 6.2 and Annex 4) and (ii) data for pH, base saturation and C/N ratio were included as explaining variables (stress factors) in the correlative study between forest crown condition and stress factors (Chapter 7).

### **3.1.3 Aim and contents of Chapter 3**

The aim of this chapter is to present (i) the distribution of major tree species over stand and site characteristics that are known to affect forest condition and (ii) the range in and spatial distribution of the relevant soil chemical parameters. The methods and data that were used to measure and/or derive stand and site characteristics and the chemical soil composition are presented in Section 3.2. The distribution of the five major tree species over major stand and site characteristics (tree age, altitude and soil properties) is discussed in Section 3.3.1. Measured values for pH, base saturation and C/N ratio in the humus layer at a limited number of crown condition plots are presented and discussed in relation to possible impacts of atmospheric deposition in Section 3.3.2. Section 3.3.3 includes a presentation and discussion of the range in and spatial pattern of the measured and extrapolated values of the above-mentioned key parameters in the mineral topsoil for all monitoring plots. Conclusions with respect to the range in and spatial distribution of pH, base saturation and C/N ratio in relation to the calculated present and critical atmospheric deposition levels of nitrogen and acidity are given in Section 3.4.

## **3.2 Methods and data**

### **3.2.1 Observation and derivation of stand and site characteristics**

An overview of the stand and site characteristics, observed or calculated, at either all or part of the plots is given in Table 4. The maximum number of locations is 5843, which all have been assessed at least once in the period 1990 to 1995. In this Chapter, however, the presentation of the data will be related to the most recent observations. With respect to the forest condition, the number of locations included is related to the 1995 forest condition assessment. In the statistical analysis (Chapter 7) all locations have been included.

Apart from tree species, the only stand characteristic recorded at the plot is the age of the forest (in classes of 20 years). Relevant stand characteristics influencing atmospheric (dry) deposition and evapotranspiration, such as tree height (e.g. Stevens, 1987) and canopy coverage (e.g. Draaijers et al., 1992), have not been recorded. Especially tree height is a crucial parameter in calculating potential evapotranspiration (Chapter 4 and Annex 2) and dry deposition of S, N and base cations (Chapter 5 and Annex 3). Therefore, this stand characteristic was derived as a function of tree species, tree age, climatic zone and site quality characteristics, such as water availability, drainage status and nutrient availability (indicated by the C/N ratio), which are mainly related to soil type. A similar approach was used to derive growth rates, which influence the critical deposition levels of S and N compounds. More information on the procedure, used to derive tree heights and growth rates, is given in Annex 4.

*Table 4 Stand and site characteristics observed or calculated at the monitoring plots*

Characteristic	Classification	Derivation	Number of plots	
			Latest assessment <sup>1)</sup>	Total <sup>1)</sup>
Tree species	Name	Observed	5421	5843
Tree age	20 a interval	"	5421	5843
Tree height	Value in m.	Calculated		5843
Altitude	50 m. interval	Observed	5421	5843
Water availability	3 classes	"	4592	
Humus type	7 classes	"	4592	
Soil type	FAO classification	"	4592	
Parent material	FAO classification	"	2227	
Texture class	3 classes	"	3326	

<sup>1)</sup> The total numbers include all locations which have been assessed at least once; the difference with the numbers for the latest assessment are the plots that had not been assessed in 1995.

Site characteristics that have been recorded at each plot include the altitude (in classes of 50 m), humus type (in seven classes, i.e. mull, moder, mor, anmor, peat, raw and other) and water availability (in three classes, i.e. insufficient, sufficient and excessive). At part of the plots (4592), soil type has been recorded according to the recently updated FAO classification (FAO, 1988). At a subset of the plots where soil type has been recorded, information is also given about the parent material (2227 plots), using the classification given in Table 4, and the texture class (in three classes, defined as coarse (class 1), medium (class 2) and fine (class 3), with clay contents below 18%, between 18 and 35% and above 30%, respectively (3326 plots)).

### **3.2.2 Observation of the chemical soil composition**

In this section the measurements of the chemical soil composition, including soil sampling, sample preparation and storage, analyses and quality control are described.



### **3.2.2.1 Sampling**

The actual sampling area was selected in a homogeneous part of the study plot, that was representative in terms of ground vegetation, forest floor and slope conditions. The organic top layer was sampled separately. A distinction was made between O- and H-horizons, defined in the FAO-guidelines for soil description (FAO, 1990).

After removal of the organic layer, the mineral soil was sampled by genetic horizons or by layers with predetermined depths. When samples were taken according to horizons, depth and thickness of the horizons were also recorded. The method using predetermined depth layers was preferred because it facilitates comparison between soils. When sampling was done by fixed depth, results were reported for the following layers:

- 0 to 10 cm; it was advised to sample 0 to 5 cm and 5 to 10 cm separately (mineral surface layers);
- 10 to 20 cm; Germany reported results on the 10 to 30 cm layer (subsurface layers).

For every sampled layer or horizon, one representative composite sample or several separate samples were collected. The number of subsamples collected per composite was reported and varies between 1 and 36. Pritchett and Fisher (1987) found that a composite of 12 to 15 subsamples usually forms an adequate sample for operational purposes. In the composite depth sampling method the whole soil core was homogenised and a subsample was taken for laboratory analysis.

### **3.2.2.2 Sample Preparation**

Macroscopic roots, stones and gravel were manually removed at the sampling location. In the laboratory, the samples were air-dried at a temperature not higher than 40°C. After drying, the samples were ground and sieved through a 2 mm sieve. The fraction < 2 mm ('air-dried fine earth') was homogenised and constitutes the sample that was subjected to the laboratory analyses. The calculation of the results of soil analysis was done on basis of 'oven-dry' soil. The moisture content of air-dried soil was determined prior to soil analysis by overnight heating of an accurately weighed subsample in an oven at 105°C.

### **3.2.2.3 Sample Storage**

It was advised to store the soil samples in a soil bank for eventual reanalysis in the future. The nutrient content, in particular ammonium-N and P, may change when samples were stored for a prolonged period at temperatures above 40°C or below freezing (Bates, 1993). Storage conditions within this temperature range and at a reasonably low humidity will have little or no influence on the nutrient contents of soil samples. The soil material should have been kept in the dark.

### 3.2.2.4 Soil Analysis

The parameters of the forest soil condition inventory and their reference analysis methods, as described in the Programme Manual (UN/ECE, 1994) and in Commission Regulation (EEC) No. 926/93 (EC, 1993), are given in Table 5.

*Table 5 Mandatory (M) and Optional (O) parameters of the level I Forest Soil Condition Survey*

Parameter	Unit	Reference method	Organic layer	Mineral layer
pH		extractant: 0.01 M CaCl <sub>2</sub> measurement: pH-electrode	M	M
Org. C	g kg <sup>-1</sup>	dry combustion	M	M
Total N	g kg <sup>-1</sup>	dry combustion	M	M
P, K, Ca, Mg	mg kg <sup>-1</sup>	digestion in aqua regia	M	O
CaCO <sub>3</sub>	g kg <sup>-1</sup>	calcimeter (if pH>6)	O	M
Weight of the organic layer	kg m <sup>-2</sup>	volume (cylindrical) - dry weight	M	
Na, Al, Fe, Cr, Ni, Mn, Zn, Cu, Pb, Cd	mg kg <sup>-1</sup>	digestion in aqua regia	O	
Exchangeable acidity (AcExc)	cmol <sup>+</sup> kg <sup>-1</sup>	titration of a 0.1 M BaCl <sub>2</sub> extraction to pH 7.8		O
Acid exchangeable cations (ACE)	cmol <sup>+</sup> kg <sup>-1</sup>	sum of Al <sup>3+</sup> , Fe <sup>2+</sup> , Mn <sup>2+</sup> and H <sup>+</sup> measured in a 0.1M BaCl <sub>2</sub> extraction		O
Basic exchangeable cations (BCE)	cmol <sup>+</sup> kg <sup>-1</sup>	sum of Ca <sup>2+</sup> , Mg <sup>2+</sup> , K <sup>+</sup> and Na <sup>+</sup> measured in a 0.1M BaCl <sub>2</sub> extraction		O
Cation exchange capacity	cmol <sup>+</sup> kg <sup>-1</sup>	BCE + ACE, or BCE + AcExc		O
Base saturation	%	100 x BCE/CEC		O

### 3.2.2.5 Quality control

Although a common methodology for sampling and analysis was adopted before the start of the monitoring activities in most countries, differences in national methods exist. In order to verify the data quality of the reported analysis results, two standard samples were provided to all laboratories, participating in the survey. The results of the standard samples showed a moderate to high variability even among laboratories using the same methods. Fortunately, a relatively low interlaboratory variability was observed for the most relevant parameters in this study (23% for pH, 10% for base saturation and 10% for the C/N ratio).

The quality of the chemical data was further controlled by subjecting the national data files to an integrity check. Integrity rules were defined by plausible value ranges and acceptable differences between overlying layers, taking soil type specific properties into account. Reported data, violating one or more integrity rules, were flagged and cross-checked by the National Focal Centre (FSCC, 1997).



### 3.2.3 Amount of data received

Information on mandatory parameters was provided for most or all parameters by the 23 countries involved. Data on optional chemical parameters are more scarcely available. Table 6 presents the availability of soil condition results in the current European database. It shows that especially in central and eastern Europe, the availability of data is limited. Information on physical soil parameters, such as parent material, texture, coarse fragments and bulk density, were provided on a voluntary basis. Table 7 lists the countries that submitted such information.

More information about the availability of data is given in the FSCC report (FSCC, 1997).

Table 6 Availability of soil condition results in the 23 countries<sup>1)</sup>

Country	Number of soil unit Plots	Soil unit	pH (Org)	C-Org, C/N (Min)	CaCO <sub>3</sub> (Min)	P		K,Ca,Mg		Optional aqua regia extractions (Org)	Cation Exch. Properties (Min)
						Org	Min	Org	Min		
Austria	131	1	1	1	1	1	1	1	1	Al, Fe, Cr, Ni, Mn, Zn, Cu, Pb, Cd	1
Belgium	31	1	1	1	1	1	0	1	0		(1)
Croatia	87	1	(1)	1	1	(1)	0	(1)	0	(Fe, Mn, Zn)	0
Czech Rep.	100	1	(1)	(1)	1	1	0	1	0		0
Denmark	25	1	1	1	1	1	1	1	1	Na	0
Finland	442	1	1	1	1	1	0	1	0	Na, Al, Fe, Cr, Ni, Mn, Zn, Cu, Pb, Cd	1
France	517	1	1	1	1	1	0	1	0		1
Germany	416	1	1	1	1	1	(1)	1	(1)	(Na), Al, (Fe, Cr, Ni, Mn), Zn, Cu, Pb, Cd	1
Greece	15	1	1	1	1	1	0	1	0		0
Hungary	67	1	1	1	1	1	0	1	0	Al, Fe, Mn	(1)
Ireland	22	0	1	1	1	1	1	1	1		0
Italy	20	0	1	1	1	1	0	1	0		0
Lithuania	74	1	(1)	(1)	1	0	0	0	0	Fe, Cr, Ni, Mn, Zn, Cu, Pb, Cd	1
Luxembourg	4	1	1	1	1	1	0	1	0	Mn	1
Netherlands	11	1	1	1	1	1	1	1	1	Na, Al, Fe, Cr, Ni, Mn, Zn, Cu	1
Norway	440	(1)	1	1	1	0	0	0	0		1
Portugal	157	1	1	1	1	1	0	1	1	Na, Al, Fe, Cr, Ni, Mn, Zn, Cu, Pb, Cd	1
Slovak Rep.	111	1	1	1	1	1	0	1	1	Na, Al, Fe, Mn, Zn, Cu	1
Slovenia	34	1	1	1	1	0	0	1	0		1
Spain	464	1	1	1	1	1	0	1	0		0
Sweden	1249	(1)	1	1	1	0	0	0	0		(1)
Switzerland	48	1	(1)	(1)	1	1	1	1	1	Na, Al, Fe, Cr, Ni, Mn, Zn, Cu, Pb, Cd	1
United Kingdom	67	1	1	1	1	1	0	1	0	Na, Al, Fe, Cr, Ni, Mn, Zn, Cu, Pb, Cd	0
Total	4532	95%	81%	93%	84%	56%	13%	56%	11%	20 - 31%	62%

<sup>1)</sup> Available for at least 90% of the plots; (1): available for less than 90% of the plots; 0: unavailable; Org: organic layer; Min: mineral layer.

<sup>2)</sup> Percentages express the relative availability in comparison to the total number of plots.

Table 7 Availability of supplementary soil information on parent material, texture, coarse fragments and bulk density<sup>1)</sup>

Country	Parent Material	Texture	Coarse Fragments	Bulk Density
Austria	1	1 J	1 J	0
Belgium	(1)	(1) J	(1) J	(1) M
Denmark	1	1 M	1 J	1 M
Finland	0	1 M	1 M	1 M, E
France	1	1 J	1 J	(1) M
Germany	(1)	(1) J	(1) M	(1) M
Greece	1	1 J	0	0
Hungary	1	1 J	1 J	1 M
Ireland	1	0	(1) J	1 M
Luxembourg	1	1 J	0	0
Netherlands	1	1 J	1 M	1 E
Norway	(1)	1 J	(1) J	1 J
Spain	1	1 M	1 M	1 M, E
Sweden	1	1 J	0	0
Switzerland	1	1 J	1 J	0
United Kingdom	1	1 J	0	0
Total	30%	73%	48%	45%

<sup>1)</sup> available for at least 90% of the plots; (1): available for less than 90% of the plots; 0: unavailable; M: measured data; J: expert judgement; E: derived from pedotransfer function.

<sup>2)</sup> percentages in last line express the relative availability in comparison to the total number of plots.

### 3.2.4 Clustering of soil type information and extrapolation of soil chemical data

#### 3.2.4.1 Clustering

In order to present the soil data as a function of soil type, a clustering of soil types (according to FAO, 1988) is needed. The proposed clustering of FAO soil types is based on the parent material which is related to the weathering rate (buffer rate) of the soil (De Vries et al., 1994; De Vries, 1996a), as indicated in Table 8. This is because (i) the parent material strongly affects the chemical soil conditions (such as pH, base saturation and C/N ratio) and (ii) the weathering rate has a large influence on the critical acid deposition level of the soil (Section 6.3).

Table 8 The considered soil clusters and associated parent material classes in relation to their parent material

Parent material class Soil cluster	Weathering rate class	Parent material
0 (peat)	very low	Peat soils <sup>1)</sup>
1 (sand)	low	Mainly acidic soils with a sandy texture <sup>2)</sup>
2 (clay)	intermediate	Mainly slightly acidic soils with a loamy or clayey texture <sup>3)</sup>
3 (volcanic)	high	Mainly volcanic soils <sup>4)</sup>
4 (calcareous)	very high	Generally calcareous soils or saline soils with a high pH and an extremely high weathering rate <sup>5)</sup>

<sup>1)</sup> All soils with more than 30% of organic matter

<sup>2)</sup> Sand (stone), gravel, granite, quartzite, gneiss

<sup>3)</sup> Granodiorite, Gabbro, loess, fluvial and marine sediment (schist, shale, greywacke, glacial till)

<sup>4)</sup> Basalt, Volcanic deposits

<sup>5)</sup> Calcite, Dolomite, gypsum, salt



In order to cluster the soil types in one of the five parent material classes, the following procedure was used. First a rough assignment was made for each major soil grouping according to soil characteristics, such as organic matter content, texture, base saturation, and the occurrence of basic materials, such as calcium carbonate (Table 9).

*Table 9 A rough classification of major soil groupings in parent material classes based on dominant soil characteristics*

Soil characteristics	Major soil grouping	Parent material class
High organic matter content	Histosols	0
Coarse texture and/or low base saturation	Regosols, Leptosols, Arenosols, Planosols, Podsoluvisols, Podzols, Acrisols, Ferralsols, Plinthosols, Alisols, Nitisols	1
Fine texture and/or high base saturation	Fluvisols <sup>1)</sup> , Gleysols <sup>1)</sup> , Vertisols Cambisols, Kastanozems, Chernozems, Pheaozems, Greyzems, Luvisols, Lixisols	2
Volcanic material	Andosols	3
Occurrence of calcium carbonate, calcium- sulphate or salt	Calcisols, Gypsisols, Solonetz, Solonchaks	4

<sup>1)</sup> Sometimes these soils have a sandy texture and/or a low base saturation.

A further refinement of the soils in the parent material classes 1 and 2 was based on their diagnostic properties, as indicated in Table 10. Diagnostic properties that are not included in Table 10 (cf. the legend of the FAO soil map of the world; FAO, 1988), were considered not relevant to refine the parent material classes.

The assumed relationship between parent material class and the soil type according to the updated FAO classification (FAO, 1988) based on Table 9 and 10 is given in De Vries et al. (1997). For ca 2200 plots additional data on parent material were available (Section 3.2.3) which were sent on a voluntary basis. In this case a direct relationship between the parent material code, indicated on the submission forms and a parent material class is possible as indicated in the Forest Soil Coordinating Centre (FSCC) report (FSCC, 1997). This relationship was used to check the parent material classes assigned from soil type at these plots.

*Table 10 Refinement of the classification of major soil groupings in parent material classes 1 and 2 based on diagnostic properties*

Diagnostic properties	Soil characteristic	Parent material class
Lithic	Shallow soil	1
Gelic 1)	Permafrost	1
Albic	Leached	1
Dystric, Umbric 1)	Low base saturation	1
Vertic, Luvic	Fine textured	2
Eutric, Mollic	High base saturation	2
Vitric, Andic	Volcanic material	3
Calcic, Calcic, Gypsic, Salic, Rendzic, Petrocalcic, Petrogypsic	Occurrence of calcium carbonate, calcium sulphate or salt	4

<sup>1)</sup> In combination with Andosols or soil with a high salt content, the weathering class is set at 2

Other possibilities are a clustering based on soil properties related to the so-called epipedon or on texture class as presented in the Forest Soil Condition Report (FSCC, 1997). Here, we limited the presentation to the above mentioned soil clusters since (i) the soil epipedon is considered less relevant in relation to weathering, and (ii) there is a strong correlation between parent material and texture. Acidic parent material is mainly associated with a coarse texture (clay content less than 18%), whereas slightly acidic parent material is mainly correlated with the texture classes medium (clay content between 18 and 35%) and fine (clay content above 35%). However, in deriving weathering rates, the impact of texture class on the weathering rates in the various parent material classes was accounted for (Annex 4).

For the correlative study, soil type information and soil data were also derived for those plots where no data on these parameters have been recorded. An indication of soil type was derived from an overlay with the FAO Soil Map of Europe using the old classification (FAO, 1981). The relationship between these soil types and the parent material class is given in De Vries (1991).

#### **3.2.4.2 Extrapolation**

The values for pH, base saturation and C/N ratio at plots where no data were available (ca 45% of the plots), were derived by either using the median value of the FAO soil type or of the soil cluster (peat, sand, clay, calcareous) occurring at the plot (Section 3.2.4). The latter approach was used when there were no other data available for the specific FAO soil type observed at the plot. This approach seems very reasonable for pH(CaCl<sub>2</sub>) and base saturation, since FAO soil type alone explained 68 % and 49 % of the variation of both parameters in the mineral topsoil. For the C/N ratio, the explanation was only 11 % and therefore other factors seem to be more important. Use of soil clusters caused a decline in the variation explained for pH(CaCl<sub>2</sub>), base saturation and C/N ratio of 50 %, 37 % and 8 %, respectively. Actually, various other stand and site characteristics that may influence the chemical soil composition, including the estimated atmospheric deposition levels, were included in the regression analyses, but only soil type appeared to have a significant influence (Sections 3.3.2 and 3.3.3). Note that the soil type may also be an interpolated value from the soil map, in case the FAO soil type was not given (Section 3.2.1). In calculating median values, use was made of all the data reported to the EC, even though a large number of soil survey plots do not coincide with the forest condition plots.

### **3.3 Results and discussion**

#### **3.3.1 Site and stand characteristics**

The distribution of the five major tree species over stand and site characteristics included in the statistical analysis (Table 25: tree age, altitude and soil cluster) is given in Tables 11-13. The number of plots for each tree species equals 2433 for *Pinus*



*sylvestris*, 2090 for *Picea abies*, 840 for *Quercus robur* and/or *Q. petraea*, 849 for *Fagus sylvatica* and 215 for *Quercus ilex*.

Except for *Quercus ilex* stands, which are mostly relatively young, stand ages between 20 and 100 years are evenly distributed over the various tree species (Table 11). The well known impact of tree age on crown condition thus seems to be quite comparable for most species.

Table 11 Distribution of the five major tree species over the mean age classes (%)

Mean age (year)	<i>Pinus</i>	<i>Picea</i>	<i>Quercus spec.</i>		<i>Fagus</i>	<i>Quercus</i>
	<i>sylvestris</i>	<i>abies</i>	<i>Q. robur</i>	<i>Q. petraea</i>	<i>sylvatica</i>	<i>ilex</i>
<20	5.5	5.5	5.5	2.6	4.3	16.3
21 - 40	14.2	15.0	14.0	16.7	11.8	29.3
41 - 60	18.6	16.9	19.9	22.9	17.7	17.2
61 - 80	20.6	18.0	18.3	15.4	17.1	11.2
81 - 100	15.8	15.9	15.2	16.7	18.8	6.0
101 - 120	8.2	8.5	7.6	6.2	11.7	2.3
>120	9.6	10.5	2.2	6.9	9.5	1.4
irregular	7.6	9.6	13.3	12.6	9.3	16.3

The coniferous tree species (*Pinus sylvestris* and *Picea abies*) and the *Quercus species* (*Q. robur* and *Q. petraea*) mainly occur in the lowlands below 500 m (approximately 70-90 % of the plots; compare Table 12). Inversely, *Fagus sylvatica* and *Quercus ilex* are quite evenly distributed over the altitudes between < 250 m up to 1500 m. Negative impacts of higher altitudes on the crown condition may thus be larger for these species.

Table 12 Distribution of the five major tree species over the altitude classes (%)

Altitude (m)	<i>Pinus</i>	<i>Picea</i>	<i>Quercus spec.</i>		<i>Fagus</i>	<i>Quercus</i>
	<i>sylvestris</i>	<i>abies</i>	<i>Q. robur</i>	<i>Q. petraea</i>	<i>sylvatica</i>	<i>ilex</i>
< 250	67.2	45.9	65.2	31.7	16.8	14.9
250 - 500	18.3	23.4	22.1	45.3	30.6	24.7
500 - 750	6.8	15.6	9.5	14.3	23.7	21.9
750 - 1000	2.8	6.8	1.6	4.9	15.2	22.3
1000 - 1500	2.8	6.6	1.4	3.5	12.8	16.3
> 1500	1.2	1.5	0.0	0.2	0.7	0.0
unknown	0.9	0.1	0.2	0.0	0.1	0.0

The coniferous tree species occur mainly on coarse textured soils (indicated as sand), whereas the deciduous tree species occur more frequently on fine textured soils (indicated as clay; Table 13). Hardly any monitoring plot is situated on volcanic soils. The occurrence of tree species on peat soils is also very low and limited to coniferous species. Finally, the deciduous species occur more often on calcareous soils, especially *Quercus ilex*. This reflects the distribution of the tree species over Europe. In general deciduous species are more concentrated in the Mediterranean countries with a large percentage of calcareous soils. The more frequent occurrence of deciduous tree species on well buffered soils (clay soils, calcareous soils) implies that the same level of acid deposition will have less impact on the soil chemistry below deciduous tree species, compared to the coniferous tree species.

Table 13 Distribution of the five major tree species over the soil clusters (%)

Soil cluster	<i>Pinus</i>	<i>Picea</i>	<i>Quercus spec.</i>		<i>Fagus</i>	<i>Quercus</i>
	<i>sylvestris</i>	<i>abies</i>	<i>Q. robur</i>	<i>Q. petraea</i>	<i>sylvatica</i>	<i>ilex</i>
peat	3.2	2.3	0.0	0.0	0.0	0.0
sand	63.8	65.3	31.0	26.9	36.4	40.0
clay	27.3	26.0	54.5	62.5	45.7	33.0
volcanic	0.0	0.0	0.4	0.0	0.1	0.0
calcareous	5.7	6.5	14.1	10.6	17.8	27.0

### 3.3.2 Chemical composition of the humus layer

Information on the overall variation of the measured pH(CaCl<sub>2</sub>), base saturation and C/N ratio as a function of soil cluster is given in Tables 14 and 15. The information is limited to plots where both the crown condition and chemical soil composition has been observed (Section 3.1). The results thus exclude data for ca 1500 plots (mainly in Sweden) where the soil survey plots do not coincide with the crown condition plots. In case of base saturation, the amount of data was limited to 363 plots coinciding with the crown condition plots (since this was not even considered as an optional parameter) and all measurements were made in humus layers on acid sandy soils. Results have therefore not been presented in a separate table.

Table 14 Minimum, maximum, 5, 50 and 95 percentile values of measured pH(CaCl<sub>2</sub>) values in the humus layer as a function of soil cluster

Statistic	Peat	Sand	Clay	Calcareous	Unknown	All
N	73	1356	474	172	115	2190
minimum	2.7	2.2	2.6	3.3	2.7	2.2
5 percentile	2.8	2.9	3.1	4.1	2.9	3.0
50 percentile	3.4	3.5	4.7	5.9	3.6	3.7
95 percentile	4.5	5.3	6.4	6.8	6.8	6.3
maximum	5.5	6.9	7.1	7.4	7.4	7.4

Results for the pH measured in a 0.1 M CaCl<sub>2</sub> extract, show a clear increase according to peat < sand < clay. Median values in these layers equal 3.4, 3.5 and 4.7, respectively (Table 14). 90% of the pH values occurred in a range between 3.0 and 6.3, coinciding with a base saturation between 41 and 89%. This seems high and it was therefore stated that exchangeable cation pools in humus layers are extremely important in buffering the pH of acid forest soil (James and Riha, 1986). It should be noted, however, that a constant supply of base cations by litterfall, followed by mineralisation, and by foliar exudation prevents a large base cation release from the adsorption complex, even at low pH (De Vries, 1994). Even though pH values are lowest in humus layers on sandy soils, they are generally higher than those observed in sandy soils where potential acid deposition is high. pH values in 150 humus layers of acid sandy forest soils in The Netherlands for example range mostly between 2.6 (5 percentile) and 3.5 (95 percentile) (De Vries and Leeters, 1996).

The base saturation at the level 1 monitoring plots is also higher than values observed in the above-mentioned 150 humus layers in The Netherlands. This might be an indication of the influence of acid deposition on the pH and base saturation in the



humus layer. The correlation coefficient between the calculated annual average acid deposition over the considered 10 year period (Chapter 5) and measured pH values below 3.5 (which occur at 42% of the plots and may indicate acidification), however, appeared to be negligible. Use of other thresholds for either the pH (e.g. below 4.0) and/or the acid deposition level (e.g. above 2000 mol<sub>e</sub> ha<sup>-1</sup> a<sup>-1</sup>) did not improve the correlation. Correlations with the measured base saturation values were also negligible. There is thus no clear indication of the effect of acid deposition on the spatial distribution of actual pH and base saturation values. This can, however, be expected considering the overwhelming effect of soil type (and climate) on soil chemical properties. When changes in soil properties, such as pH, become available through repeated soil surveys, a relationship is more probable.

The C/N ratio appeared to decrease according to peat > sand > clay and calcareous soils (Table 15). 90% of the values ranged between 17 and 47. C/N ratios in the humus layer below 20, which might be indicative for elevated N accumulation, were observed at approximately 10% of the plots. The impact of N deposition was not substantiated by a correlation between the calculated annual average N deposition over the considered 10 year period and measured C/N ratios below 20. Use of other thresholds for either the C/N ratio (e.g. below 15; occurring at 3% of all plots) and/or the nitrogen deposition level (e.g. above 1000 mol<sub>e</sub> ha<sup>-1</sup> a<sup>-1</sup>) did not improve the correlation. Again, a relationship between N accumulation and N deposition is more likely than a relationship with the actual C/N ratio.

*Table 15 Minimum, maximum, 5, 50 and 95 percentile values of measured C/N ratio values in the humus layer as a function of soil cluster*

Statistic	Peat	Sand	Clay	Calcareous	Unknown	All
N	73	1356	472	174	482	2559
minimum	16	8.4	5.4	12	15	5.4
5 percentile	18	18	15	16	19	17
50 percentile	29	28	24	27	30	28
95 percentile	49	48	39	45	49	47
maximum	73	97	66	75	85	97

### 3.3.3 Chemical composition of the mineral layer

Information on the overall variation of the measured pH(CaCl<sub>2</sub>), base saturation and C/N ratio at the crown condition monitoring plots as a function of soil cluster is given in Tables 16-18. As with the humus layers, data for volcanic soils were lacking, except for four plots that did not coincide with the crown condition plots. The number of plots where both crown condition and soil chemical parameters have been measured equals 2773 for pH, 2029 for base saturation and 2752 for C/N ratio (compare Tables 16, 17 and 18). The total number of plots where pH, base saturation and C/N ratio in the mineral topsoil has been measured is much larger, especially for pH (4097) and C/N ratio (4069) and to a lesser extent for base saturation (2761). As stated before, these data were used for the extrapolation of the data to other plots.

Table 16 Minimum, maximum, 5, 50 and 95 percentile values of measured values for the pH(CaCl<sub>2</sub>) in the mineral topsoil (0-20 cm) as a function of soil cluster

Statistic	Peat	Sand	Clay	Calcareous	Unknown	All
N	18	1465	538	216	545	2773
minimum	2.5	2.7	2.9	3.3	2.9	2.5
5 percentile	3.0	3.3	3.5	4.6	3.5	3.4
50 percentile	4.2	4.0	4.5	7.2	4.4	4.2
95 percentile	5.5	5.2	7.5	7.7	7.5	7.5
maximum	5.7	7.4	7.9	7.9	7.8	7.9

Table 17 Minimum, maximum, 5, 50 and 95 percentile values of measured values for the base saturation in the mineral topsoil (0-20 cm) as a function of soil cluster

Statistic	Peat	Sand	Clay	Calcareous	Unknown	All
N	16	2077	343	79	514	2029
minimum	9.0	2.5	4.0	75	4.0	2.5
5 percentile	11	3.3	10	90	9.0	8.0
50 percentile	48	24	76	100	70	32
95 percentile	99	86	100	100	100	100
maximum	100	100	100	100	100	100

Ninety percent of the pH values vary between 3.4 and 7.5 with a base saturation varying between 8 and 100%. 95 percentile values and maximum values for pH in the sand and clay soils (7.4 and 7.9 respectively) reveal that most likely calcareous soils are included in these soil clusters, whereas the minimum values for calcareous soils (3.2) implies that this soil cluster includes plots where the mineral topsoil is decalcified. pH(CaCl<sub>2</sub>) values below 4.0, which are indicative for the occurrence of Al mobilisation in response to acid inputs, were measured at 53% of the plots. Note that pH values measured in a CaCl<sub>2</sub> extract are slightly lower than those measured in soil solution. Generally a pH of 4.2 in soil solution is considered as the threshold value below which Al buffering becomes significant (Ulrich, 1983). Extremely low pH values, below 3.5, occurred at 8% of the plots. A base saturation less than 25 %, which is also used as a threshold value for Al mobilisation (Section 6.2 and De Vries, 1994), was observed in the mineral topsoil at 42% of the plots. At less than 10% of the plots, extremely low base saturation values, below 10%, were measured.

Table 18 Minimum, maximum, 5, 50 and 95 percentile values of measured values for the C/N ratio in the mineral topsoil (0-20 cm) as a function of soil cluster

Statistic	Peat	Sand	Clay	Calcareous	Unknown	All
N	17	1443	534	215	545	2752
minimum	7.0	5.0	3.3	2.5	4.4	2.5
5 percentile	7.7	10	9.5	7.3	11	10
50 percentile	30	20	15	13	15	17
95 percentile	56	39	30	21	26	35
maximum	64	230	77	35	61	230

Ninety percent of the C/N ratios varied between 10 and 38. Extremely low C/N ratios (below 10) occurred at approximately 5% of the plots, especially in the peat, clay and calcareous soils. Note, however, that extreme values such as 2.5 (minimum) are likely



to be unreliable because they are calculated for plots where both the C content and N content were extremely low. This holds even more for the observed maximum values.

pH and base saturation clearly increase according to coarse textured soil types with acidic parent material (indicated as sand) < peat < finer textured soil types with more basic parent material (indicated as clay) < calcareous soils. This increase in pH and base saturation is reasonably correlated with a decrease in C/N ratio according to peat > sand > clay > calcareous.

As with the humus layers a clear impact of atmospheric deposition on mineral soil properties could not be derived. Calculated correlation coefficients between the annual average deposition of acidity and nitrogen over the considered 10 year period and the measured values for pH, base saturation and C/N ratio (in the range below respectively 4.0, 25% and 20) were nearly always negligible (Chapter 7). Again, pH changes, which have been reported in various countries, such as Sweden (e.g. Falkengren-Grerup et al., 1987; Hallbäck and Tamm, 1986), Scotland (e.g. Billet et al., 1988), Germany (e.g. Ulrich et al., 1980; Butzke, 1988) and Austria (e.g. Glatzel and Kazda, 1985) likely show a much better relationship with acid deposition than actual pH values. The same holds for changes in pools of base cations and nitrogen.

The spatial distribution of the measured and interpolated pH values (Fig. 8) shows that low pH values (<4.0) mainly occur in Central and Northern Europe. Note, however, that the pH values in large parts of Central Europe (Poland, Romania, Bulgaria, Estonia, Latvia, Moldova and Russia) and Northern Europe (e.g. the whole of Sweden) are extrapolated based on the soil type occurring on the FAO soil map of Europe 1 : 5 000 000 (FAO, 1981). The relatively poor quality of this soil map influences the spatial distribution of the pH in these countries. According to this map, for example, nearly all soils in Sweden are podzolic soils, which have a median pH between 3.5 and 4.0. The distribution of measured pH values most likely coincides with that of Norway and Finland with higher pH values (between 4.0 and 5.0) going from south to north. pH values above 7.0, which are indicative for calcareous topsoils, mainly occur in Southern Europe, specifically in large parts of France and Spain. Intermediate pH values between 4.0 and 5.0 occur throughout the whole of Europe, but hardly in Central and Western Europe (The Netherlands, Germany, Poland, Czech Republic) where acid deposition is highest. Values between 5.0 and 7.0 are few (Fig. 8).

The spatial distribution of measured and interpolated base saturation values (Fig. 9) largely coincides with that of the pH. Base saturation below 25% generally occurs at plots where pH values are below 4.0. Again the uniform legend for Sweden is likely to be an artefact of the interpolation procedure. Base saturation values above 90% mostly coincide with the calcareous soils where pH is above 7.0. A base saturation between 25 and 50% mostly occurs at plots with a pH between 4.0 and 5.0. As with the pH range between 5 and 7, base saturation values between 50 and 90% were measured infrequently (compare Fig. 8 and 9).

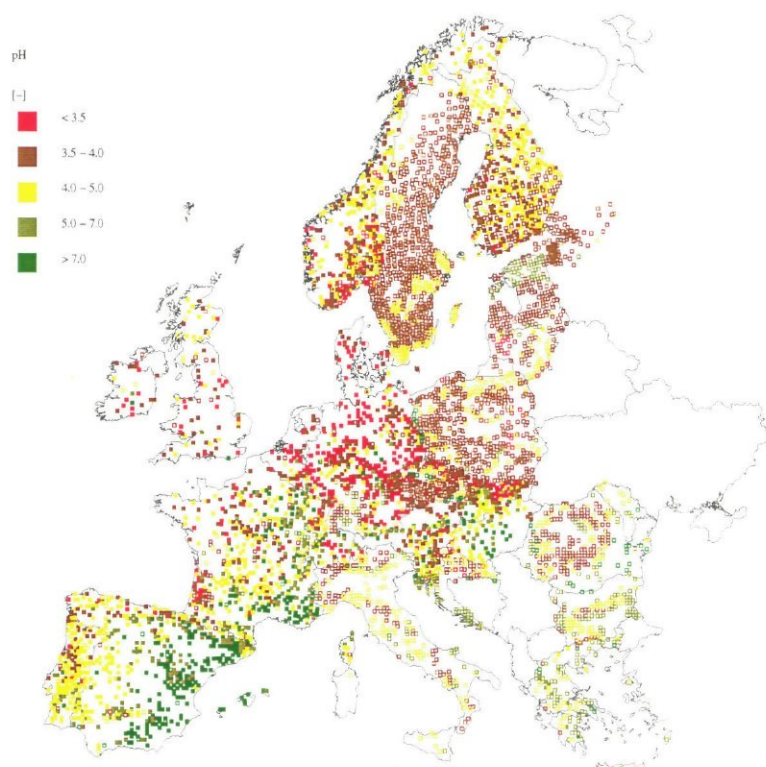


Fig. 8 Measured and interpolated pH values for the mineral topsoil of all monitoring plots (measured values are indicated as solid squares and interpolated values as open squares).

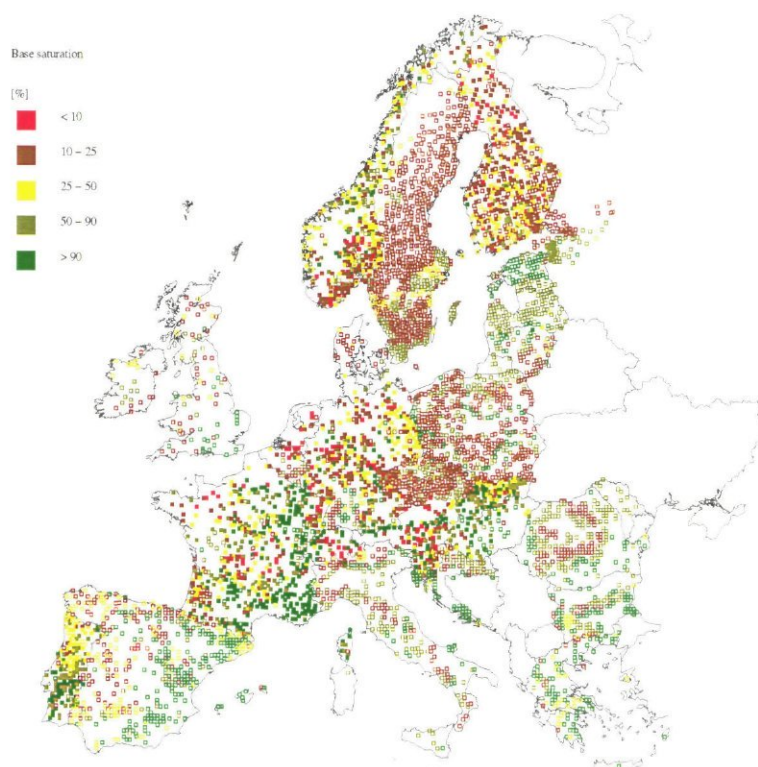


Fig. 9 Measured and interpolated base saturation values for the mineral topsoil of all monitoring plots (measured values are indicated as solid squares and interpolated values as open squares).



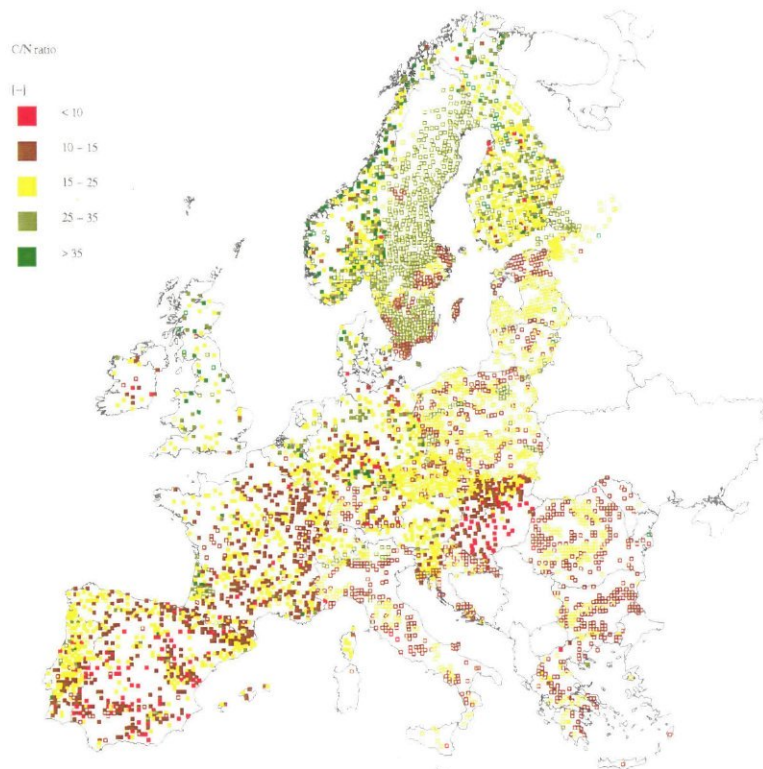


Fig. 10 Measured and interpolated C/N ratio values for the mineral topsoil of all monitoring plots (measured values are indicated as solid squares and interpolated values as open squares).

The spatial distribution of measured and interpolated C/N ratios (Fig. 10) also shows a correlation with the pH distribution, although smaller than with the base saturation. Low C/N ratios are often measured in calcareous soils, which are mainly distributed in the Southern part of Europe and in large parts of central Europe (specifically in Hungary). C/N ratios above 25 mainly occur in the Nordic countries at acidic soil types. Again the spatial distribution in Sweden is an artefact of the interpolation procedure and it is likely that C/N ratios between 15-25 occur more often in the southern part of the country. Values below 15 or even 10 are mainly recorded at plots where the pH is above 7.0 and the base saturation above 90%.

### 3.4 Conclusions

With respect to the distribution of tree species over major stand and site characteristics, the following conclusions can be drawn:

1. Stand ages between 20 and 100 years are evenly distributed over the various tree species, except for *Quercus ilex*, where most stands are relatively young.
2. The coniferous tree species (*Pinus sylvestris* and *Picea abies*) and the *Quercus* species (*Q. robur* and *Q. petraea*) mainly occur in the lowlands below 500 m (approximately 70-90 % of the plots). Inversely, *Fagus sylvatica* and *Quercus ilex* are quite evenly distributed over the altitudes between < 250 m up to 1500 m.

Negative impacts of higher altitudes on the crown condition may thus be larger for these species.

3. The coniferous tree species occur mainly on coarse textured poorly buffered sandy soils, whereas the deciduous tree species occur more frequently on fine textured well buffered clay soils and on calcareous soils.

The following conclusions can be drawn with respect to the range in and spatial distribution of pH, base saturation and C/N ratios in humus layers and mineral topsoils:

1. Measured values of the  $\text{pH}(\text{CaCl}_2)$  in the humus layer are generally 0.5 pH unit lower than in the mineral topsoil. Median values for example equal 3.7 and 4.2. Inversely, the base saturation is generally much higher in the humus layer (median value of 65%) compared to the mineral soil (median value of 32%), due to the constant supply of base cations by litterfall and throughfall. C/N ratios are mostly higher in the humus layer compared to the mineral soil. Median values in both layers equal 28 and 17, respectively.
2. pH values in the humus layer below 3.5, which might indicate enhanced acidification, occurred at 42% of the plots. C/N ratios in the humus layer below 20, which might indicate enhanced N accumulation, occurred at 10% of the plots.
3. Acid topsoil conditions, i.e. a  $\text{pH}(\text{CaCl}_2)$  below 4.0 and a base saturation below 25% occurs at 53% and 42% of the plots, respectively. It is thus likely that about half of the level I plots occur on soils in the aluminium buffer range. Extremely acid topsoil conditions, namely a  $\text{pH}(\text{CaCl}_2)$  below 3.5 occurs at 8% of the plots. Similarly, a base saturation below 10% occurs at 3% of the plots. At those plots, acidic deposition will certainly be buffered by the mobilisation of toxic Al.
4. The FAO soil type explained 68% of the variation in pH and 49% of the variation in base saturation. Using soil clusters, the explanation decreased to 50% and 37% respectively. The spatial pattern of pH and base saturation over Europe is thus strongly correlated with soil type (parent material class). To a lesser extent, this is also true for the C/N ratio, where soil type explained 11% of the variation. Fine textured (clay) soils and calcareous soil with a high pH and base saturation and a low C/N ratio mainly occur in Southern Europe. The increase in pH and base saturation in non-calcareous soils from north to south and west to east in Europe also follows the climate gradient of a precipitation surplus in North-western Europe to an evapotranspiration deficit in Eastern Europe and the Mediterranean areas.
5. An impact of acid deposition levels on actual pH and base saturation values could not be substantiated on a European scale. The same holds for C/N ratios in relation to N deposition levels. This can be expected considering the overwhelming effect of soil type and climate on the chemical soil properties. A relationship between changes in soil chemical properties and atmospheric deposition is much more probable.



6. Extrapolation of pH, base saturation and C/N ratios to plots where no measurements were taken is hampered when soil type information is lacking. This holds specifically for areas where soil types are interpolated from the FAO soil map of Europe 1 : 5 000 000. This may affect the spatial pattern of calculated critical acid deposition level in these areas.

## 4 Calculation of natural meteorological stress

*Kees Hendriks<sup>1)</sup>, Jaco Klap<sup>1)</sup>, Erik de Jong<sup>2)</sup>, Erik van Leeuwen<sup>2)</sup>, Wim de Vries<sup>1)</sup>*

<sup>1)</sup> DLO Winand Staring Centre (SC-DLO), Wageningen, The Netherlands

<sup>2)</sup> National Institute of Public Health and the Environment (RIVM), Bilthoven, The Netherlands

### 4.1 Introduction

#### *Identification of stress factors*

In order to derive relationships between forest condition and natural and anthropogenic stress, stress factors, as described in Section 1.3, need to be quantified. It is generally accepted that changes in forest condition are not related to one single factor, rather than to the interaction of a mixture of stress, which can intensify or compensate for forest condition changes. The meteorological stress factors are related to the occurrence of rare meteorological events, such as low and/or high temperatures in specific periods, drought, storms, etc. Although the occurrence of such rare events might be influenced by climatic change, the meteorological stress is considered as natural stress here. Anthropogenic stress is caused by air pollution exposure and deposition loads. Air pollution was found to enhance the occurrence of natural stress or to lead to direct or indirect effects. This is the result of exposure to toxic levels of gases, such as NH<sub>3</sub>, NO<sub>2</sub>, SO<sub>2</sub> and O<sub>3</sub>, and/or of high atmospheric inputs of acid or acid forming compounds and nitrogen compounds.

As already mentioned in Chapter 1 most natural and anthropogenic stress factors are not measured directly at the Level 1 plots. In assessing the causal relationships, quantitative site specific data are needed. Recent development on compilation of meteorological data bases with data covering all of Europe (Potma et al., 1993), and model development to determine site specific meteorological stress factors (Hendriks et al., 1997) made it possible to provide site specific estimates of such parameters for the first time. The stress factors that were considered in this study will be discussed in the next sections.

Unfavourable meteorological conditions can be a serious cause of stress for forest trees, and affect forest condition. Besides negative aspects, meteorological condition can also cause positive effects. Meteorological stress factors include drought stress, temperature stress (cold, frost, heat), radiation stress (lower level of global radiation than the potential level) and mechanic stress (storms, snow, glazed frost). In this pilot study we focus on temperature stress and drought stress.

Both low and high temperatures can cause stress. High temperatures mainly affect transpiration rates and activity of enzymes. Influence of high temperatures, self-evident, may occur during the growing season. Low temperatures can cause damage in cases of severe or incessant winter frost through freezing or dehydration of needles and buds by which they can be damaged or die off. Late night-frosts in spring can cause severe damage or die off of just flushing buds (Hellinga, 1983).



Water stress is considered to be very important with respect to forest condition. Innes (1993) mentioned that the most alarming and frequent observations of a decrease in forest condition in Central Europe coincided with the dry years 1982 and 1983. Landmann (1995) mentioned that defoliation appears to be highest in soils poorly supplied with water and/or in stands in which trees, at some stage of development, have suffered from competition for water. The effects of water stress may diverge from yellowing of the foliage, foliage necrosis, to complete defoliation following extreme drought events (Innes, 1993; Landmann, 1995).

#### ***Aims and contents of chapter 4***

The aims of this chapter are to present information on the overall range, the temporal trends, the spatial distribution and the reliability of calculated natural (meteorological) stress factors. The meteorological stress factors calculated are presented in Section 4.2. A distinction was made in factors indicating temperature stress (winter index, late frost, heat index and summer index) and water stress (relative transpiration). In Section 4.2 first the methods (the models and their input data) that were used to calculate site-specific stress factors are described, followed by a description of the results in terms of the overall range, temporal trends and spatial distribution (Section 4.3), while ending with an overview of the uncertainties associated with the modelling (Section 4.4). This chapter ends with conclusions (Section 4.5) that are related to the aims described above.

## **4.2 Input data and methods**

One of the main focuses in this preliminary study is the derivation of meteorological stress factors (e.g. frost, drought) using available meteorological data bases. Besides for the calculation of such factors, meteorological data are needed to calculate deposition loads. The assessment of meteorological parameters is not included in the EU/ICP Forests Level I Monitoring Programme. Therefore, all meteorological information was derived from external data bases. In the following sections, the procedure to derive site-specific meteorological data is described (Section 4.2.1). Secondly the selected temperature stress indices are defined and the method by which they are calculated (Section 4.2.2). Then the procedure is described to calculate the relative transpiration as an indicator for drought stress and the precipitation excess, followed by a more detailed description of the water balance of a forest and its components (Section 4.2.3).

### **4.2.1 Estimation of site-specific meteorological data**

Interpolation of meteorological data from regular synoptic stations in Europe is the most suitable method to estimate site specific meteorological parameters. One consistent data base for the whole period 1980-1995 (including a memory term for the calculation of drought stress) was not available. Therefore data from several sources

were used. Mainly, three different databases were used, generally containing data from the same meteorological stations on the same time resolution. For the period 1980 to 1989, a data base of the WMO (World Meteorological Organisation) on a global scale archived by ECMWF (European Centre for Medium-range Weather Forecasts), Reading, UK was used. This so-called ODS (Observational Data Set) data set contains 6 hourly averaged meteorological observations at 00, 06, 12, 18 GMT measured at 1306 stations over Europe (of which 4 are observations carried out on ships). For the period 1990 to 1995, data from essentially the same stations on the same temporal resolution were obtained from NCAR (National Centre for Atmospheric Research), Boulder, USA. As NCAR does not archive precipitation amounts for Europe, these missing data were obtained from the German Weather Service (Deutscher Wetter Dienst, DWD). Parameters derived in this study are summarised in Table 19.

Table 19 Meteorological variables extracted from the ODS (1980-1989) and NCAR + DWD (1990-1995) data bases

Variable	measurement height	units
Wind speed	10 m	m s <sup>-1</sup>
Total cloud cover	-	octa
Air temperature	1.5 m	0.1 °C
Dew point temperature	1.5 m	0.1 °C
Precipitation	0.5 m	0.1 mm

Site-specific meteorological data were obtained through interpolation of measurements, except for precipitation amounts for which the value from the nearest meteorological station was taken. Interpolation to each site was performed using a simple inverse distance weighting procedure from a maximum of four meteorological stations located in the immediate surroundings of the site. Most emphasis in the method is put on data quality by selection of the most representative stations to be used for the interpolation to each site. The selection procedure was based on the method described by Van der Voet *et al.* (1994) and is extensively described in Annex 1.

#### 4.2.2 Temperature stress indices

##### *Definition*

The following key factors related to temperature stress were selected, based on the analysis of relevant factors and the availability of data (Klap *et al.*, 1997):

- Winter index: indication of severeness of the winter. This index equals the sum of daily mean temperatures below 0 °C in the period from 1 October to 1 April (degree days below 0 °C).
- Late frost: late night-frost in spring can cause serious damage to trees when growth has just started and the buds and young shoots are very sensitive to frost. This key parameter was defined by the lowest minimum temperature (below 0 °C) in a period starting at 15 days before the growing season started and ending at June 30.
- Heat index: the possible occurrence of damage by high temperatures was estimated by the so-called heat index, which equals the sum of differences between daily maximum temperatures in the growing season and a threshold value of 35 °C



(degree days above 35 °C). The threshold of 35 °C is rather arbitrary, since no information on such a threshold value was found in literature.

- Summer index: the quality of the growing season was included, as it affects the possibilities of photosynthetic activity and the possibility of the tree to produce reserve assimilates for purposes of defence and growth in the beginning of the next season. This key factor was expressed as an effective temperature sum, which equals the sum of differences between daily mean temperatures during the growing season and a (preliminary) threshold of 5 °C (degree days above 5 °C).

Besides the temperature indices used in this pilot study, also temperature changes can possibly affect tree condition (e.g. Hartmann 1996). Such an index, however, was not included in this study.

### Aggregation

Aggregation of meteorological data comprises aggregation over the growing season or winter period, which varies per climatic region and tree species. In general, the demarcation of the growing season is important for all stress factors which affect the level of physiological activity of the tree, such as the winter- and summer index but also the exposure to ozone (i.e. AOT40, Section 5.3), and the calculations of the water stress (drought). The demarcation of the growing season is also used to determine the period of bud burst, in which trees are vulnerable for late frost, starting 15 days before bud burst and ending on June 30.

Table 20 Start of the growing and dormant season per tree species for climatic regions

Climatic region <sup>1)</sup>	Starting date growing season			Starting date dormant season (all species)
	<i>Q. petraea</i>	<i>P. sylvestris</i> <i>Q. robur</i> <i>Q. ilex</i>	<i>P. abies</i> <i>F. sylvatica</i>	
Boreal (Lat. > 65° N)	May 1	May 16	June 1	September 16
Boreal (Lat. < 65° N)	April 16	May 1	May 16	September 16
Boreal Temperate	April 1	April 16	May 1	September 16
Mountainous N. (Alt. > 500m or Lat. > 65° N)	April 16	May 1	May 16	September 16
Mountainous N. (Alt. < 500 m and Lat. < 65° N)	April 1	April 16	May 1	September 16
Sub-Atlantic	March 16	April 1	April 16	October 1
Continental	March 16	April 1	April 16	October 1
Atlantic North	March 16	April 1	April 16	October 1
Atlantic South	March 1	March 16	April 1	October 16
Mountainous South (Alt. < 1500 m)	March 16	April 1	April 16	October 1
Mountainous South (Alt. > 1500 m)	April 1	April 16	May 1	October 16
Mediterranean Lower	Feb. 15	March 1	March 16	October 16
Mediterranean Higher	March 1	March 16	April 1	October 16

<sup>1)</sup> Based on the regions used in the annual Forest Condition Reports (e.g. UN-ECE, EC, 1996).

The demarcation of the growing season is determined by climatic factors, day length, and tree species. In this pilot study, however, the begin and end of the growing season were set to fixed dates, depending on bio-geographic region and tree species. In the consecutive comprehensive study the moment of flourishing and the start of the winter

rest period will also be linked to meteorological data (which will result in a floating date, depending on the weather). In that stage, also the photosynthetic activity of evergreen trees during mild episodes in the winter period will be taken into account.

Table 20 shows selected dates for the beginning of the growing season. The beginning of the growing season first starts in the southern regions and then moves northwards, whereas the end of the growing season has the opposite trend. The beginning of the growing season was considered to be species-dependent. *Quercus petraea* was considered to be an 'early' species, whereas *Fagus sylvatica* and *Picea abies* were considered to be 'late' species.

### 4.2.3 Relative transpiration

#### **Definition**

The variation in transpiration of a forest is strongly determined by the soil moisture supply and vegetation characteristics (Monteith, 1965). Thus, at first sight, parameters like soil moisture supply and precipitation deficit seem usable indicators for drought stress. Both parameters, however, do not take effects of vegetation on the evapotranspiration into account. Transpiration therefore, can be considered as a more reliable key parameter indicating drought stress.

Drought stress occurs in situations where the actual transpiration is less than the maximum, or potential transpiration. Thus a ratio or absolute difference between actual and potential levels can be used as indicator for drought stress. Relative transpiration ( $RE_T$  = actual transpiration/potential transpiration) was chosen as key parameter, because drought stress is expected to be better correlated with relative transpiration than with relative evapotranspiration ( $RET$  = actual evapotranspiration/ potential evapotranspiration) as the latter term also includes evaporation of intercepted precipitation and soil evaporation. The growing season is the most appropriate time scale to calculate the  $RE_T$ . A mean  $RE_T$  for the growing season was derived per year for use in the statistical model.

#### **Procedure to calculate relative transpiration and precipitation excess**

The procedure to calculate the relative transpiration ( $RE_T$ ) is illustrated in Fig. 11. The first step in the calculation is that of the potential evapotranspiration ( $ET_p$ ) by use of the Penman-Monteith equation (described in Annex 2.1). Secondly, the interception ( $E_I$ ) is calculated, for which the model of Gash (1995) was used. As a third step soil evaporation is calculated according to Van den Broek and Kabat (1996). Next, potential transpiration is calculated by subtraction of interception and potential soil evaporation. Finally, actual transpiration is calculated depending on the potential transpiration and the soil moisture content. For this latter it is necessary to simulate the forest water balance, which is shortly explained in the next section. More detail on the calculation of the relative transpiration can be found in Hendriks et al. (1997) and in Annex 2.



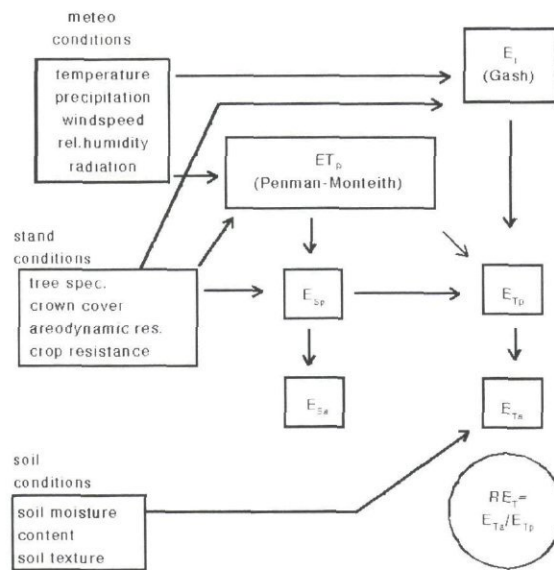


Fig. 11 Procedure to calculate the relative transpiration ( $RET$ )

### Calculation of the water balance

The water balance of a forest can be calculated according to:

$$\Theta_{i+1} = \Theta_i + P_i - Q_{S,i} - E_{T,i} - E_{I,i} - E_{S,i} - Q_{D,i} \quad (\text{Eq. 2})$$

where:

- $\Theta_i$  = soil moisture content on day  $i$  (mm)
- $P_i$  = precipitation (mm d<sup>-1</sup>)
- $Q_{S,i}$  = surface run-off (mm d<sup>-1</sup>)
- $E_{T,i}$  = actual transpiration (mm d<sup>-1</sup>)
- $E_{I,i}$  = interception (mm d<sup>-1</sup>)
- $E_{S,i}$  = actual soil evaporation (mm d<sup>-1</sup>)
- $Q_{D,i}$  = drainage (mm d<sup>-1</sup>)
- $I$  = day number (-)

Eq. 2 is the basis of most hydrological simulation models (e.g. SWACROP, Kabat et al., 1992; SOIL, Jansson, 1991). The soil water content is used as an intermediate pool between storage in the soil and uptake by the trees. In the simulation models soil water fluxes are calculated depending on many soil physical, meteorological and crop specific factors. Because the lack of required soil physical data which are needed for detailed hydrological models on the one hand and inaccuracies for the estimates of the other missing parameters on the other hand, the application of such detailed models is not very useful. For this reason a simple bucket model was used, which, assuming a fixed bucket size, predicts soil moisture contents, run-off, drainage, transpiration, interception and soil evaporation (Fig. 12). The principle of the bucket model is based on the models of Boughton (1984) and Kalma et al. (1995). The water balance model was implemented as a subroutine in the EDACS deposition model (Section 5.2.1.1). In the following the components of the water balance are briefly explained.

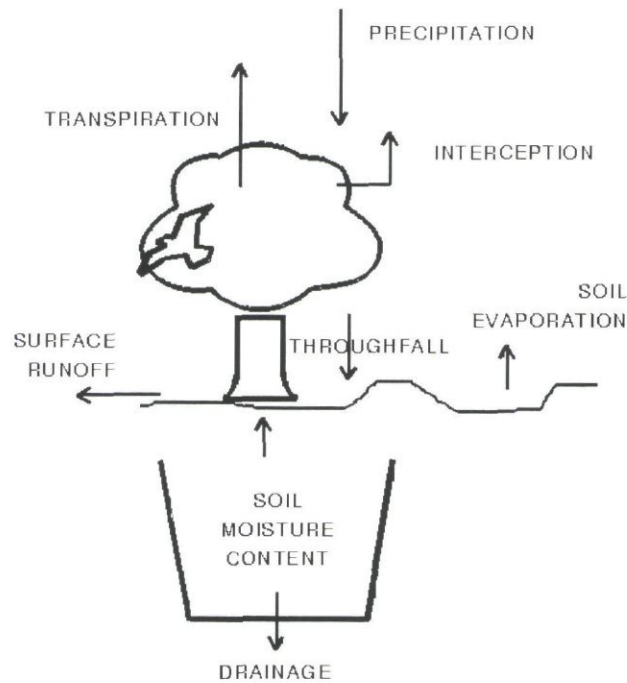


Fig. 12 The bucket model representing the forest water balance

#### 4.2.4 Calculation of the water balance components

##### *Soil moisture content and drainage*

Since soil physical characteristics are not measured at the Level 1 plots, and supplemental measurements are excluded in this study, information on available soil water was derived from the results of a study by Van Dam *et al.*, (1994) on the available water capacity for the soil units of the EC soil map. Based on soil physical properties, Van Dam *et al.* (1994) calculated the available water capacity (AWC) for the soil units of the EC soil map at a scale 1 : 1 000 000. These values could be extrapolated to the Level 1 plots since the soil units are known for these plots (Section 3.2.3). The value for the AWC given by Van Dam *et al.* (1994) was used as a bucket size, assuming that when the bucket is filled, the surplus of water will percolate to deeper soil layers and can be considered as the precipitation excess. The annual precipitation excess, thus calculated, was used in the derivation of critical deposition levels for S and N (Section 6.3 and Annex 4). In the bucket model this excess is indicated by the drainage flux  $Q_d$  (Fig. 12).

##### *Surface run-off*

Surface run-off depends on slope, vegetation and soil texture classes (Driessen, 1986). In forests, however, run-off is often limited because of the presence of a litter layer and interception of precipitation through the crowns and ground vegetation, which causes a lessened precipitation intensity to the forest floor. Therefore run-off is neglected by assuming  $Q_s = 0$ .



### ***Rates of potential transpiration, interception and soil evaporation***

Potential evapotranspiration,  $ET_p$ , was calculated using the Penman-Monteith equation (Monteith, 1965). In general, this equation gives reliable estimates of the evapotranspiration (Federer, 1982; Moors et al., 1996) and required site specific meteorological parameters were available through interpolation from the meteorological data base (see above). The calculation of the  $ET_p$  from the meteorological parameters is explained extensively in Annex 2.1.

Potential transpiration ( $E_{Tp}$ ) is calculated according to Eq. 3:

$$E_{Tp} = ET_p - E_I - E_{Sp} \quad (\text{Eq. 3})$$

where:

$E_I$  = evaporation of intercepted precipitation

$E_{Sp}$  = soil evaporation

$E_I$  can be calculated with models (e.g. Gash, 1995; Rutter et al., 1975), or as a fraction of gross precipitation (e.g. Calder, 1986). Dolman and Moors (1994) showed that the fraction of  $E_I$  as percentage of gross precipitation depends strongly on tree species, storm intensity, and storm duration. An error of more than 100% may occur when using estimates as a fraction of gross precipitation (Moors et al., 1996). Moors et al. (1996) stated that  $E_I$  can be estimated satisfactory only for time periods of one day or shorter, and only process orientated models should be used. Therefore the model of Gash (1995) was used to calculate the interception (Annex 2, Section A2.2). Potential soil evaporation ( $E_{Sp}$ ) was calculated according to Van den Broek and Kabat (1996) as a function of  $ET_p$  and  $LAI$ . Actual soil evaporation ( $E_{Sa}$ ) was then calculated as a function of the potential rate and the time since the last rainfall event (Annex 2, Section A2.3).

### ***Actual rates of transpiration***

Actual transpiration ( $E_{Ta}$ ) is usually calculated as a function of both  $E_{Tp}$  and the soil moisture content (Andersson and Harding, 1991; Federer, 1982; Van Keulen, 1986). We used a slightly modified version of the model of Van Keulen (1986) in which  $E_{Ta}$  equals  $E_{Tp}$ , when the available amount of soil moisture is adequate to supply sufficient water to the plant roots. In the model a critical soil moisture,  $SMC_{cr}$ , content was used, above which roots can freely take up water from the soil, depending on soil characteristics and atmospheric demands.  $SMC_{cr}$  was calculated depending on a critical pressure head ( $h_{cr} = -1000$  cm). In Annex 2 (Section A2.4) the method to derive  $E_{Ta}$  is given in more detail.

### ***Relative transpiration***

The relative transpiration ( $RE_T$ ) was calculated for the growing season. Since the length of the growing season differs per climatic region (Table 20), the period for which  $E_{Ta}$  and  $E_{Tp}$  was calculated also differs. Both  $E_{Ta}$  and  $E_{Tp}$  were calculated as the sum of the daily values of their fluxes over the growing season. Finally,  $RE_T$  was calculated by dividing  $E_{Ta}$  by  $E_{Tp}$ .

### ***Derivation of other input data***

Besides meteorological data, also tree physiological data such as crop resistance ( $r_b$ ), Leaf Area Index ( $LAI$ ), crown storage capacity ( $S$ ) and throughfall coefficient ( $p$ ) are required for the computation of transpiration. Mean values for these tree species specific data were derived from literature (Annex 2). If a Level 1 plot contained more than one tree species, the values for the physiological parameters were averaged, taking into account the coverage of each tree species in the stand.

Mean values for required soil and stand characteristics, such as soil texture and soil type, were derived from the available data base at the Level 1 plots, from literature or from expert judgement (Annex 2).

## **4.3 Results and discussion**

### **4.3.1 Meteorological data**

As expected, lowest temperatures are found in northern and eastern Europe, and highest temperatures in southern Europe. Conform climatic data, highest precipitation amounts are found in the coastal areas (especially in Norway, Ireland and the north-western part of the Iberian peninsula) and mountainous areas (Alps, Italy and Croatia). Relatively dry years were 1985, 1986, 1989, 1994 and 1995. Wet years were 1990 to 1992. The warmest year for the plots was 1992.

In general the precipitation values are higher than expected, though in other areas (e.g. France) the precipitation sum seems to be underestimated. These results are mainly due to the uncertainty in the (invalidated) meteorological data bases used, the way missing values are treated and the procedure used to derive precipitation amounts at the plots (Section 4.2.3). Due to the random nature of precipitation, this method is not straightforward.

Though the absolute values have uncertainty, the impact on the calculation of the drought stress is not expected to be very large. For this purpose the relative transpiration is calculated. In this ratio, the precipitation amount is used, both in the numerator and the denominator. This, to some extent, levels out the large precipitation values.

### **4.3.2 Temperature stress indices**

#### **4.3.2.1 Overall variation**

The overall variation in temperature indices, calculated for all plots in the considered 10 year period, is given in Fig. 13. Results for the separate indices are discussed below.



### Winter index

The calculated overall average winter index for all tree species is 203 degree days. Three major groups in tree species can be distinguished (Fig. 13A). At plots of the first group, containing *Quercus ilex*, only a low percentage of all plots (less than 40% of total observation, which probable is about 4% of total plots) show winter temperatures below zero. The second group is that of *Quercus robur* and *Fagus sylvatica* with an average winter index of about 100 degree days. The third group, containing *Picea abies* and *Pinus sylvestris*, has an average winter index of about 240 degree days.

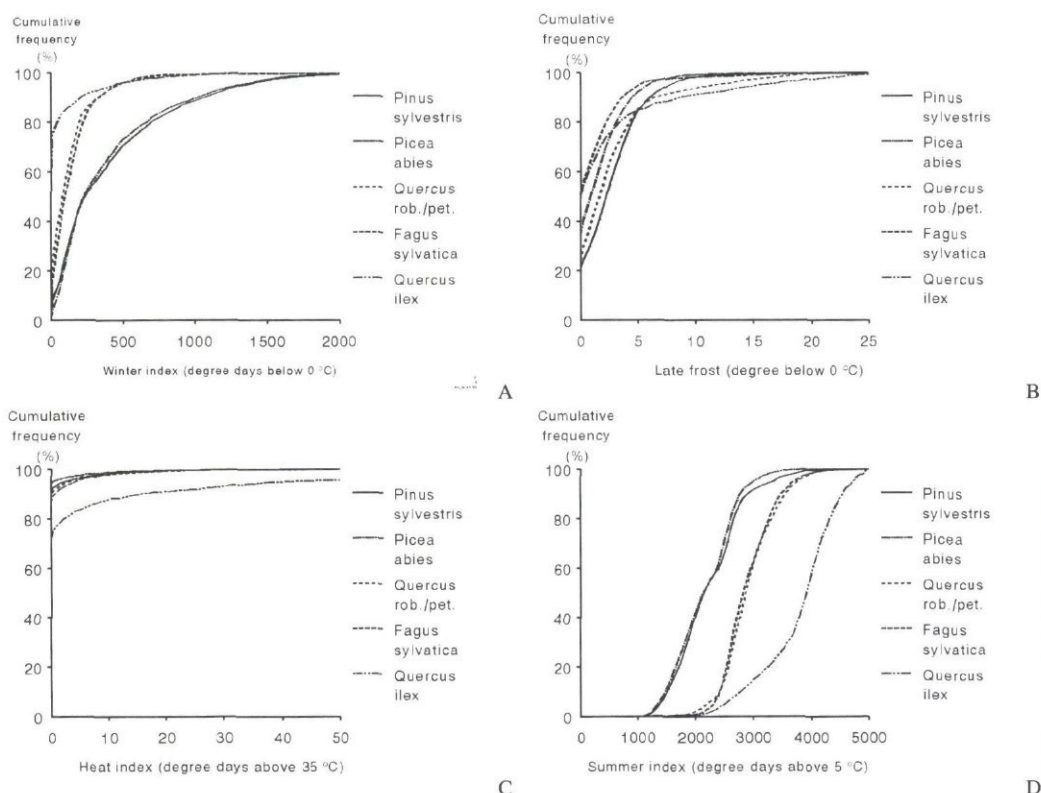


Fig. 13 Cumulative frequency distributions of the winter index (A), late frost (B), heat index (C) and Summer index (D) for the five major tree species in this study

### Late frost

The overall average late frost index equals 1.58 below 0 °C. No large differences were found for the groups of tree species (Fig. 13B). Plots with *Quercus robur* and *Pinus sylvestris*, have a somewhat lower late frost index compared to the other tree species.

### Heat index

The overall average of the heat index is 0.70 degree days, which means that on the average the temperature for only few, on the average about 10%, level 1 plots exceeds 35 °C for one or more days. On the average, only 3% of the total number of observations have a heat index of 10 degree days or more (Fig. 13C). In about 20% of the *Quercus ilex* plots, the heat index is higher than for the other tree species.

### ***Summer index***

An overall average summer index of 2413 degree days was calculated for all plots and all tree species. Just as for the winter index, three groups of tree species could be distinguished having the same distribution of the summer index (Fig. 13D). The groups of *Quercus ilex*, of *Quercus robur* and *Fagus sylvatica*, and of *Pinus sylvestris* and *Picea abies* have an average overall summer index of respectively 3925, 2850 and 2100 degree days above 5 °C.

### **4.3.2.2 Temporal variation**

Temporal variation in calculated annual average values for the various temperature indices are given in Fig. 14.

### ***Winter index***

Per year a rather large variation in winter index is calculated, with average values ranging from 530 degree days in 1987 to 155 degree days in 1992. On the average about 20% of the level 1 plots have a winter index higher than 500 degree days (Fig. 14A). However, a large yearly variation exists, ranging from 5% in 1991 and 1992 to more than 40% in 1985 and 1987. About 10% of the plots have a winter index less than 0.1 degree day which can be interpreted as plots where it does not freeze in the winter period.

### ***Late frost***

The temporal variation of the late frost index is not very large. Average values range from 1.46 °C in 1994 to 3.42 °C in 1986. Most level 1 plots, on the average 43%, have a late frost index in the range from 1 to 5 °C below zero. Only about 3% of the plots have a late frost index of more than 10 °C, and about 30% of less than 0.1 °C (Fig. 14B)

### ***Heat index***

As shown in Fig. 14C, very little temporal variation in heat index was calculated. The years 1990 and 1991 were relative hot years, showing a modest percentage of plots with a heat index larger than 30 degree days.

### ***Summer index***

Temporal variation of the summer index is small, with average values ranging from 2596 degree days in 1985 to 2769 degree days in 1995. About 50% of the level 1 plots have a Summer index between 2000 and 3000 degree days above 5°C, with only a small variation per year (Fig. 14D).



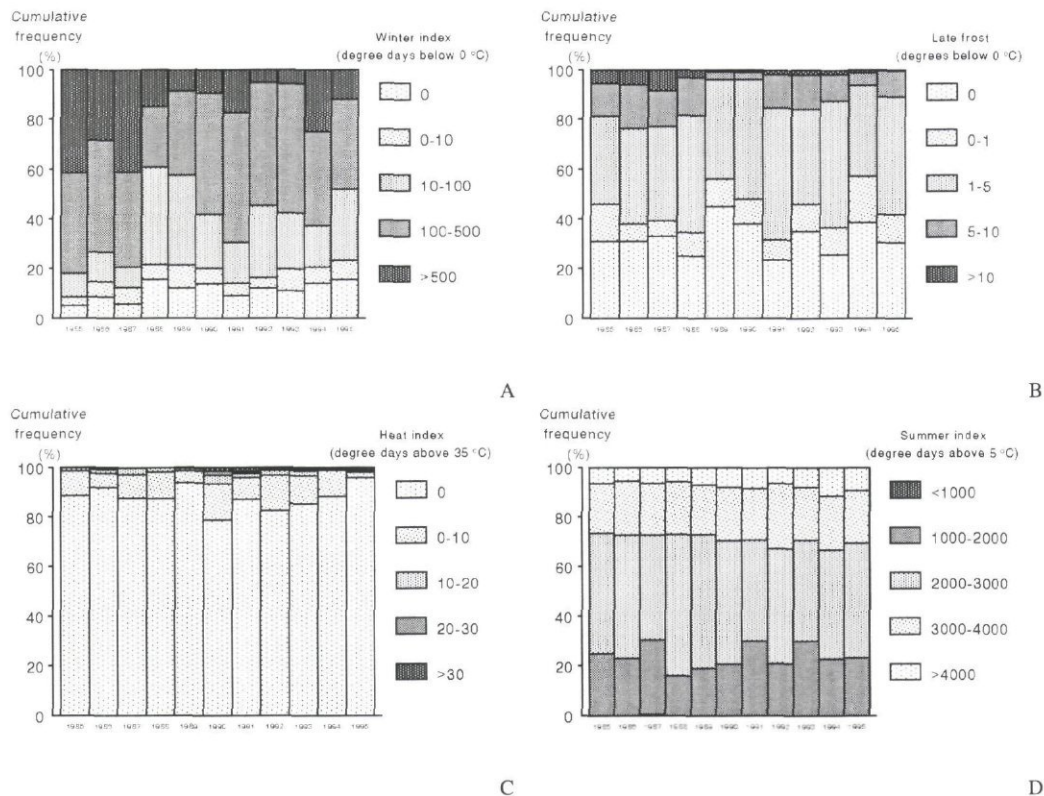


Fig. 14 Trends in the annual average winter index (A), late frost (B), heat index (C) and Summer index (D) for the five major tree species considered in this study

#### 4.3.2.3 Spatial variation

##### **Winter index**

The averaged winter index for the period 1985 to 1995 shows a clear pattern over the Level 1 plots in Europe (Fig. 15) which is related to the climatic regions in Europe. The northern and eastern part of the boreal region have an average winter index of more than 500 degree days. The southern boreal region and the continental region have an average winter index ranging from 100 to 500. The winter index in the Atlantic region largely ranges between 10 and 100 degree days, whereas in the Mediterranean region it is mostly less than 10 degree days.

##### **Late frost**

The late frost index (or spring frost index) shows the most complicated pattern of the temperature indices used in this study. The largest area has a late frost index between 1 and 5 °C (Fig. 16). In the southern regions no, or hardly any late frost occurs, while in the northern regions more plots with a late frost index of more than 5 °C occur. Also mountainous areas have a late frost index of more than 5 °C.

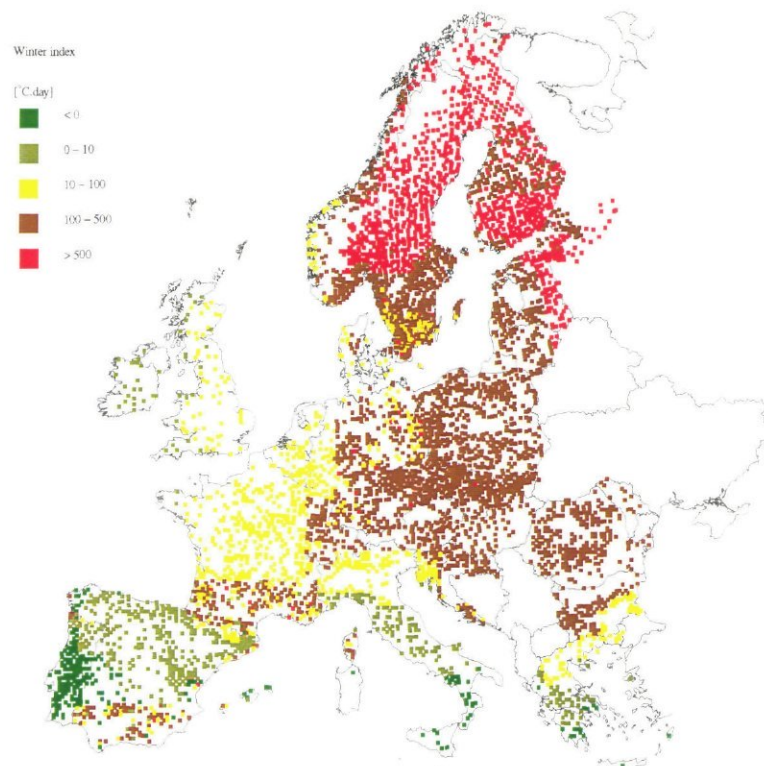


Fig. 15 The calculated 10 years average winter index for all monitoring plots

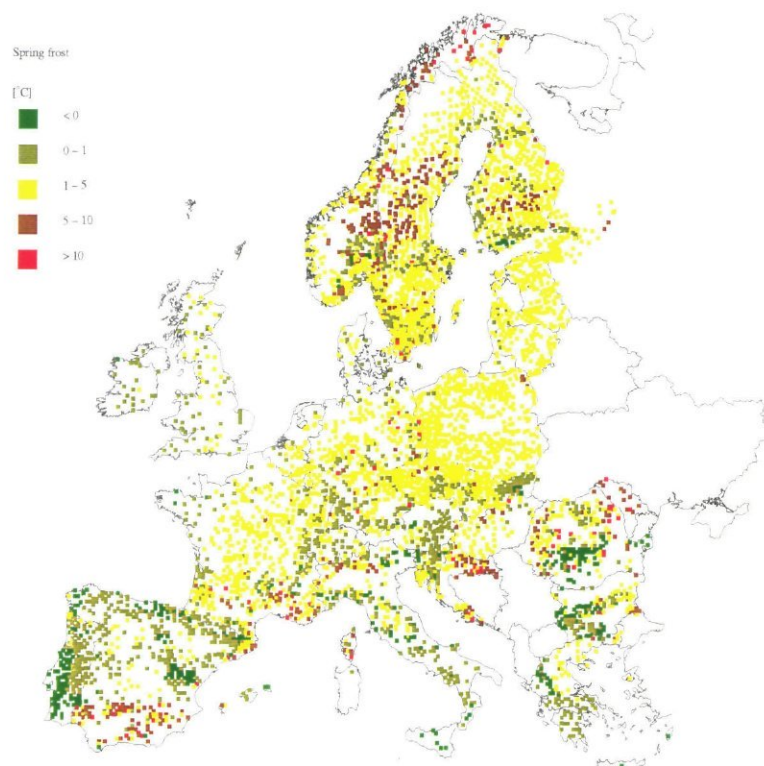


Fig. 16 The calculated 10 years average spring frost for all monitoring plots



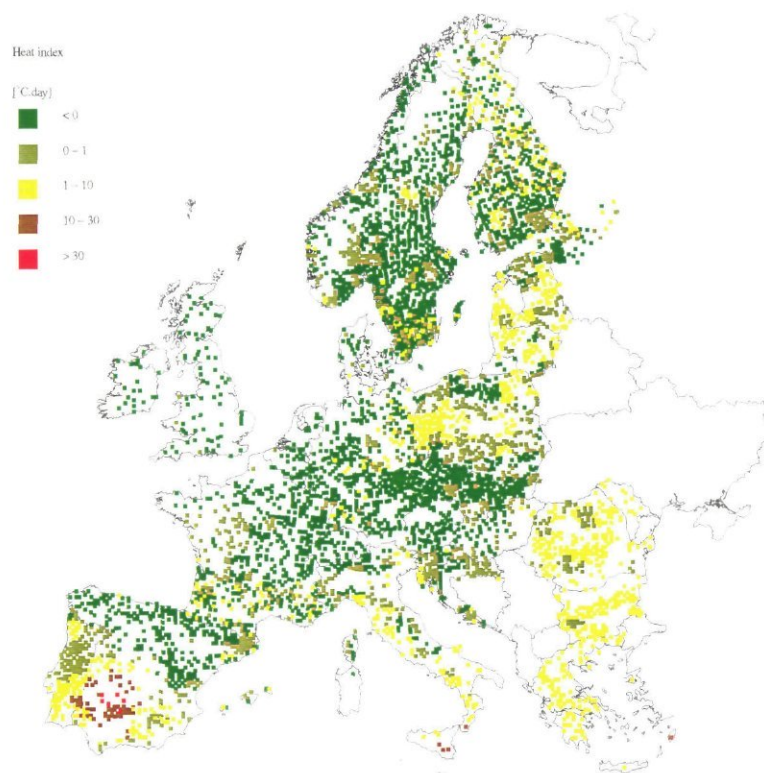


Fig. 17 The calculated 10 years average heat index for all monitoring plots

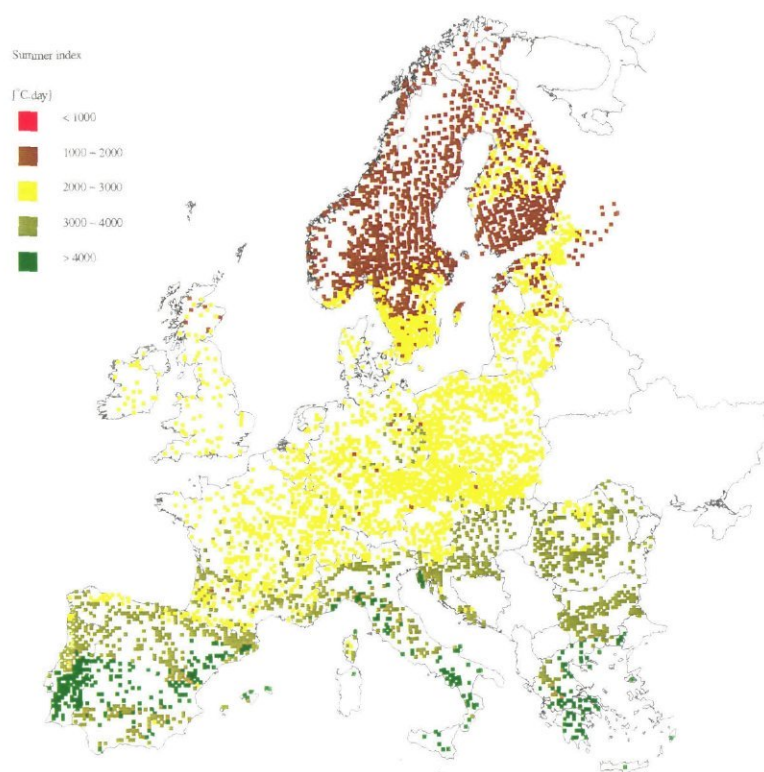


Fig. 18 The calculated 10 years average summer index for all monitoring plots

### Heat index

The average heat index only reaches high values in Central Spain, where it is more than 30 degree days (Fig. 17).

### Summer index

Just as the winter index, the summer index shows a clear geographical pattern throughout Europe. It changes from a relatively low summer index in between 1000 and 2000 degree days in the northern boreal regions, to 2000 and 3000 degree days along west and north-eastern Europe. In the northern Mediterranean and the continental regions the summer index is 3000 to 4000 degree days, whereas in the southern Mediterranean region it reaches values up to 4000 degree days (Fig. 18).

## 4.3.3 Relative transpiration

### 4.3.3.1 Overall variation

On the average, relative transpiration  $RE_T$  for all Level 1 plots and for all years equals 0.8, which might be considered rather high. Considerable differences in  $RE_T$  exist between the tree species (Fig. 19). 50% of the observations for *Quercus ilex* have more than 50% transpiration reduction, while for *Quercus robur* and *Fagus sylvatica*, and for *Pinus sylvestris* and *Picea abies* the percentages are about 15 and 5 respectively. Only about 10% of the *Quercus ilex* observations have a  $RE_T$  higher than 80%, while for *Quercus robur* and *Fagus sylvatica* on 40% and for *Pinus sylvestris* and *Picea abies* on 80% of the observations a  $RE_T$  of 80% is exceeded.

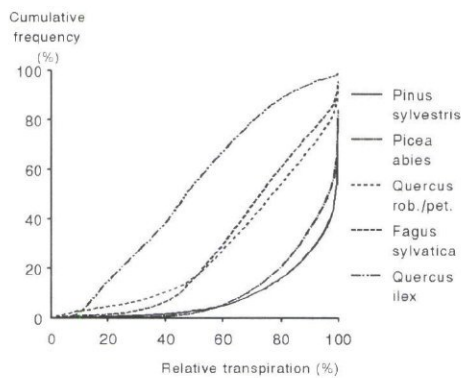


Fig. 19 Cumulative frequency distribution of the relative transpiration for the five major tree species considered in this study



#### 4.3.3.2 Temporal variation

The temporal variation in the average  $RE_T$  varies from 0.72 in 1994 to 0.86 in 1987. On about 15% of the level 1 plots  $RE_T$  equals 1.0, meaning that actual transpiration equals the potential level, while on about 65% of the plots  $RE_T$  is less than 0.5. Especially for 1987 and 1993 a low  $RE_T$  was calculated for a large percentage of the plots: respectively 60% and 50% have a  $RE_T$  lower than 0.5 (Fig. 20).

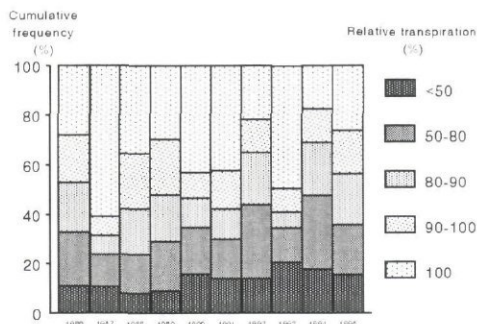


Fig. 20 Trends in the annual relative transpiration for the five major tree species considered in this study

#### 4.3.3.3 Spatial variation

The geographical distribution of the  $RE_T$  shows a decreasing  $RE_T$  from the north towards the south of Europe (Fig. 21). As expected, high  $RE_T$  is calculated for Ireland, Scotland, western and northern Norway, north Finland, and Estonia, which are all regions with a large amount of precipitation. In the southern regions, including Portugal, Spain, large parts of France, Italy, Croatia, Hungary, Rumania, and Bulgaria, the average  $RE_T$  in general is lower than 0.75, which also was expected because of the low precipitation and high potential evapotranspiration in these regions. Leenmans and Cramer (1990) found  $RE_t$  to be 0.9 to 1.0 for the Nordic countries, between 0.6 and 0.8 for the North-western part of Europe, and between 0.4 and 0.5 for the Mediterranean regions. Our results, especially in the Mediterranean region show higher values compared to Leenmans and Cramer (1990).

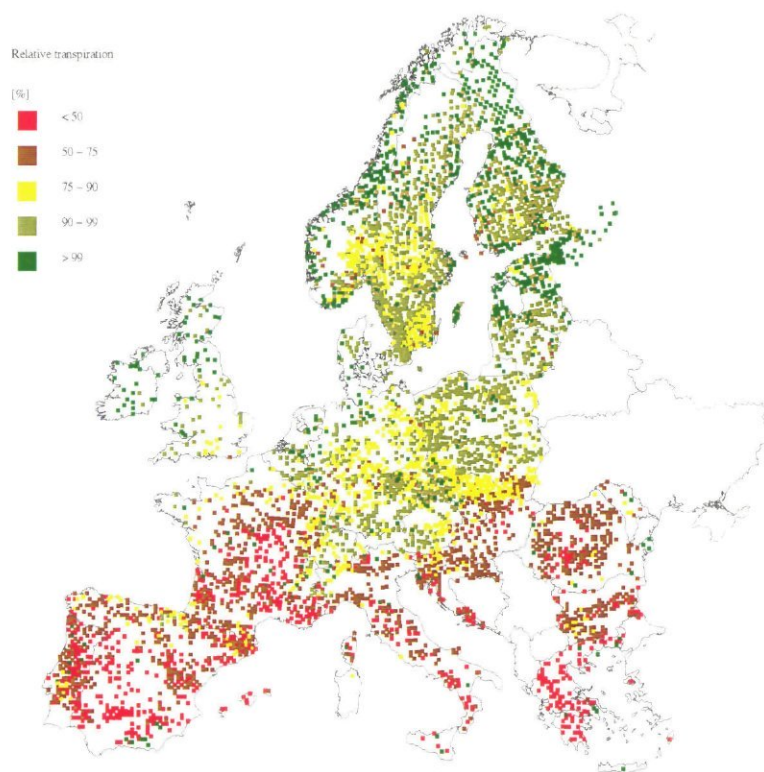


Fig. 21 The calculated 10 years average relative transpiration for all monitoring plots

## 4.4 Uncertainties

### 4.4.1 Meteorological data

In this section a brief description of uncertainty in the meteorological data is given. Uncertainty numbers are presented on the one standard deviation ( $\sigma$ ) level as percentages. In Annex 1 (Section A1.2) the method used to quantify the uncertainty associated with the interpolation of the meteorological data is described and results are discussed in more detail. It is very hard to quantify the total uncertainty in the interpolated meteorological parameters accurately, because uncertainty arises from several factors:

- errors in the selection procedure (interpolation errors),
- errors in the meteorological measurements and data transmission and handling, and
- the use of (three different) invalidated data sets from ECMWF, NCAR and DWD (meaning that they are not screened for errors and unrealistic values), in which moreover quite some missing data values are archived.



The last error source contributes to the total uncertainty to a large extent. The uncertainty as obtained with cross validation can be considerable, especially for parameters showing strong regional differences, such as precipitation amount. Air temperature and relative humidity perform good in large parts of Europe (average uncertainty about 25%), but for individual plots uncertainty can be large (up to 100%). Wind speed, cloud cover and dew point temperature seem to perform fairly good (average uncertainty about 50%), but for individual plots uncertainty can amount 200%. Largest uncertainty is associated with the interpolated precipitation amounts (average uncertainty about 100%), though locally uncertainty can be much higher. Considering the meteorological databases available on a European scale, better estimates than the values obtained in this study are not available.

#### **4.4.2 Temperature stress indices**

The uncertainties in temperature key parameters can be divided into two groups of causes. At first, uncertainties result from inaccuracies in the meteorological data and the interpolation procedure (Section 4.2.1). The second uncertainty source is a physiological one. Based on available knowledge, threshold values were chosen for the temperature key parameters: 0 °C for the winter index, 5 °C for the summer index, and 35 °C for the heat index. Effects of chosen threshold values on the relationships with defoliation are unknown. Furthermore, no difference was made between sensitivity per tree species, which also introduced some uncertainty.

#### **4.4.3 Relative transpiration**

The uncertainties in the calculated relative transpiration have many causes. First, the uncertainty in the basic meteorological input data play a role in the accuracy of the calculated  $RE_T$ . Several estimations are needed to calculate global radiation, and the meteorological conditions at crown height (Annex 2). As mentioned, derivation of site-specific precipitation data is very difficult and leads to high uncertainty. Besides uncertainties in input data, also the calculation method yields uncertainties. Several assumptions were needed to calculate process parameters such as the soil moisture content, stomatal resistance, plant available water, and drainage. Furthermore, because of lack of local data, large-scale, long-term average data had to be used. For instance a mean evaporation during rainfall was calculated per climatic region, and not per plot. All these uncertainties together may be large. The pattern in  $RE_T$  as shown in Fig. 21, however, is in accordance to the expectation, which supports the reliability.

## 4.5 Conclusions

The following conclusions can be drawn with respect to the overall, temporal and spatial variation of calculated meteorological stress factors.

1. The overall variation of temperature indices varies between 0 and 2500 degree days below 0 °C for the winter index, between 0 and 50 degree days below 0 °C for late frost, between 0 and 90 degree days for the heat index and between 0 and 5200 degree days for the summer index. Relative transpiration is lower for deciduous trees in the South of Europe than for the coniferous trees in the North.
2. The temperature stress indices do not show much variation in time for the period 1985 to 1995. The winter index is the key parameter with the most temporal variation, coinciding with warm and cold years.
3. Clear spatial patterns were found for the winter index, and the summer index. In general trends are north-south orientated, going from colder northern regions, both in summer and in winter, to warmer southern regions. The relative transpiration also shows a clear, but more complex pattern, coinciding to a large extent with patterns of rainfall and temperature, which both are important parameters in the Penman-Monteith equation to calculate transpiration. The absolute values, however, deviate from long-term mean values as used in other pan-European studies. This holds especially for precipitation, which is generally high as compared to other meteorological data sets. Because precipitation is a very important input parameter for many of the calculations in this study, the uncertainty in this parameter is an important source of the uncertainty in the resulting parameters.
4. The calculated indices for temperature and drought stress, contain uncertainties which largely depend on the reliability of the site specific meteorological data. The latter depends mainly on the reliability of the meteorological data base and on the interpolation method used to generate site specific data. The site specific meteorological data followed in general the geographical patterns as expected.



## 5 Calculation of anthropogenic air pollution stress

*Erik van Leeuwen<sup>1)</sup>, Gun Lövblad<sup>2)</sup>, David Simpson<sup>3)</sup>, Wim de Vries<sup>4)</sup>, Erik de Jong<sup>1)</sup>, and Jan Willem Erisman<sup>1)</sup>*

<sup>1)</sup> National Institute of Public Health and the Environment (RIVM), Bilthoven, The Netherlands

<sup>2)</sup> Swedish Environmental Research Centre (IVL), Göteborg, Sweden

<sup>3)</sup> Norwegian Meteorological Institute (DNMI), Oslo, Norway

<sup>4)</sup> DLO Winand Staring Centre (SC-DLO), Wageningen, The Netherlands

### 5.1 Introduction

#### *Identification of stress factors*

In Europe, sulphur and reduced and oxidised nitrogen compounds are found to acidify soils and surface waters. Furthermore, nitrogen deposition causes eutrophication. Base-cations such as  $\text{Na}^+$ ,  $\text{Mg}^{2+}$ ,  $\text{Ca}^{2+}$  and  $\text{K}^+$  also play an integral role in the chemical processes of acid deposition since the acidity of any material is a function of both its acidic and basic compounds. Besides their ability to neutralise acid, base-cations are important nutrient elements for ecosystems. The deposition of atmospheric pollutants includes both deposition of gaseous compounds and aerosols. They can be transferred to soil, vegetation and water surfaces by dry deposition, wet deposition, and cloud and fog deposition. The latter was not taken into account in this study.

#### *General approach*

Air pollution can damage trees either directly, by exposure of the leaves to elevated concentrations of  $\text{SO}_2$ ,  $\text{NO}_2$  and/or  $\text{NH}_3$ , or indirectly by deposition to soils initiating complex processes in the soil(solution) which negatively influence forest vitality. Up to now, concentration and/or deposition measurements are not included in the EU/ICP Forests Level 1 Monitoring Programme. Recent model development to determine site specific concentration and deposition levels (Van Pul et al., 1995, Erisman et al., 1995) made it possible to provide site specific estimates of such parameters for the first time. As there is some serious lack of knowledge regarding deposition modelling on the small scale in Europe (Lövsblad et al., 1993; Erisman and Draaijers, 1995), an important part of the research was focused on evaluation of model results. For this, throughfall data were collected by IVL (Sweden), obtained at several forest stands in Europe. Modelled results were compared with throughfall data, which were corrected for canopy interactions. In this way, uncertainty in modelled estimates was determined.

#### *Aims and contents of Chapter 5*

The aims of this chapter are to present information on the overall range, the temporal trends, the spatial distribution and the reliability of calculated and anthropogenic (air pollution) stress factors. Section 5.2 focuses on the calculated annual average concentration and deposition levels for  $\text{SO}_2$ ,  $\text{NO}_2$  and  $\text{NH}_3$  and the deposition levels of  $\text{Na}^+$ ,  $\text{Mg}^{2+}$ ,  $\text{K}^+$  and  $\text{Ca}^{2+}$ . Calculated annual average ozone levels for the year 1990 are presented in Section 5.3. Each section first describes the methods (the models and their input data) that were used to calculate site-specific stress factors, followed by a



description of the results in terms of the overall range, temporal trends and spatial distribution, while ending with an overview of the uncertainties associated with the modelling. This chapter ends with conclusions (Section 5.4) that are related to the aims described above.

## **5.2 Concentrations and present loads of sulphur and nitrogen compounds and loads of base cations**

### **5.2.1 Introduction**

In Europe, the large-scale concentration and deposition distribution of acidifying components is commonly described with the EMEP model (e.g. Tuovinen *et al.*, 1994). For estimating site-specific estimates the model resolution of  $150 \times 150 \text{ km}^2$  is much too coarse. Therefore the EDACS model (European Deposition of Acidifying Components on a Small scale) was developed, which is used to estimate site-specific dry deposition fluxes of acidifying components (i.e.  $\text{SO}_x$ ,  $\text{NO}_y$  and  $\text{NH}_x$ ) and base cations. In this section the method is presented. A more extended description of the EDACS model as well as the derivation of wet deposition estimates can be found in Van Pul *et al.* (1995), Erisman *et al.* (1995) and in Annex 3. In the second part of this section, the throughfall measurements which are used to evaluate the site-specific deposition estimates are described. A data base with most of the European throughfall measurements was compiled by IVL for this purpose. The model validation procedure is explained.

### **5.2.2 Methods**

#### **5.2.2.1 The EDACS model**

Dry deposition estimates of the acidifying components are obtained using ambient air concentrations calculated with the EMEP long-range transport model (daily averages), which in turn are based on emissions of  $\text{SO}_2$ ,  $\text{NO}_x$  and  $\text{NH}_3$  (e.g. Tuovinen *et al.*, 1994), together with parametrised dry deposition velocities (Van Pul *et al.*, 1995). The acidifying components considered are  $\text{SO}_2$  and  $\text{SO}_4^{2-}$ -aerosol ( $\text{SO}_x$ );  $\text{NO}$ ,  $\text{NO}_2$  ( $\text{NO}_x$ );  $\text{HNO}_3$  and  $\text{NO}_3$ -aerosol;  $\text{NH}_3$  and  $\text{NH}_4^+$ -aerosol ( $\text{NH}_x$ ). Concentrations at 50m above the surface are used. At this height it is assumed that concentrations and meteorological parameters are not influenced by surface properties to a large extent. Dry deposition velocities of gases and particles at this height are calculated for each site using stand information, routinely available meteorological information and the inferential technique (Erisman *et al.*, 1994; Van Pul *et al.*, 1995). Derivation of meteorological data is described in Annex 1. The dry deposition velocity fields (calculated for every 6 hourly period) are averaged to daily values and combined with concentration fields from the EMEP-model. Daily fluxes are subsequently summed to annual totals. In order to estimate total deposition at each site, wet deposition obtained from the EMEP model is added to the dry deposition.

For estimating dry deposition of base cations ( $\text{Na}^+$ ,  $\text{Mg}^{2+}$ ,  $\text{Ca}^{2+}$  and  $\text{K}^+$ ) essentially the same method is used. Unlike the acidifying components, for base cations 6-hourly dry deposition velocity fields are aggregated to annual means before they are combined with annual mean concentration fields (Draaijers et al., 1996). Currently, reliable information on the spatial and temporal variation of base cation emissions is not available hampering accurate concentration modelling with long-range transport models. For this reason, surface-level air concentrations are estimated from precipitation concentrations and scavenging ratios (Draaijers et al., 1996). Annual mean precipitation concentrations are used to infer annual mean air concentrations of  $\text{Na}^+$ ,  $\text{Mg}^{2+}$ ,  $\text{Ca}^{2+}$  and  $\text{K}^+$ . Detailed precipitation concentration fields for 1989 and 1993 were obtained from Van Leeuwen et al. (1995). These concentration fields were extrapolated to the whole period 1986 to 1995, using a trend in base cation precipitation concentrations obtained from the EMEP measurement network (Schaug et al., 1993). The method used to derive base cation air concentrations and deposition estimates is further elaborated in Draaijers et al. (1996) and in Annex 3.

#### 5.2.2.2 Model validation procedures

Throughfall and stemflow measurements were used to evaluate the modelled deposition estimates. A major limitation of such measurements is that information to distinguish between in-canopy and atmospheric sources of chemical compounds often is lacking, thereby hampering accurate deposition estimation. To overcome this limitation, in this study a canopy budget model was applied.

Results of throughfall, stemflow and bulk precipitation measurements for several years were obtained from national organisations responsible for throughfall and stemflow monitoring in their countries which were gathered via the chairwoman of the Expert Panel on Deposition (G. Lövblad, pers. communication). In total, results from 296 different throughfall measurement plots were obtained. Table 21 lists the countries from which data were obtained, as well as the type of forest and the maximum measurement period within the country. At several of the plots only data on one year were obtained. The measurement plots are not equally distributed over Europe, as most plots are located in Scandinavia, Germany, The Netherlands, France, Ireland and Switzerland. The majority of the plots (82%) is situated in coniferous forest stands; only 11% in deciduous forest stands and 7% in mixed forest stands. Monitoring took place between 1986 and 1995 for a period of at least one year. At most plots stemflow was not measured as it generally contributes only a small fraction of the total flux to the forest floor (Ivens, 1990). In that case, the stemflow flux was computed as a percentage of the throughfall flux using a parametrisation on tree species and stand age described by Ivens (1990). Wet deposition was estimated from bulk precipitation measurements by applying bulk to wet-only correction factors presented by Van Leeuwen et al. (1995).

A canopy budget model initially developed by Ulrich (1983) was used to estimate the impact of canopy leaching on throughfall and stemflow fluxes of  $\text{Mg}^{2+}$ ,  $\text{Ca}^{2+}$  and  $\text{K}^+$ .



An extensive description and uncertainty analysis of the model used is presented by Draaijers and Erisman (1995). In the model,  $\text{Na}^+$  is assumed not to be influenced by canopy exchange. Dry deposition of  $\text{Na}^+$  was thus calculated by subtracting wet deposition from the throughfall+stemflow flux (Annex 3, Section A3.4). Particles containing  $\text{Mg}^{2+}$ ,  $\text{Ca}^{2+}$  and  $\text{K}^+$  were assumed to have the same mass median diameter as  $\text{Na}^+$  containing particles.

Table 21 The number of throughfall monitoring locations and the measuring period in coniferous, deciduous and mixed forest stands used for model validation

Country	Coniferous	Deciduous	Mixed	Measurement period
Czech Republic	8	3		1985-1995
Denmark		1		1992
Finland	27		9	1990-1994
France	18	8		1993-1994
Germany	63	12	2	1989
Hungary	1			1990-1993
Ireland	3		1	1989-1994
Netherlands	22	2	4	1987-1991
Norway	19			1992-1995
Poland			1	1992-1994
Russian Federation		2		1990-1993
Sweden	69		4	1988-1995
Switzerland	12	5		1989-1992

Empty boxes indicate that no data were available for this category in that country

Deposition estimates derived from throughfall and bulk precipitation measurements were compared to modelled deposition estimates for all measurement plots. For this purpose, the model was run using stand-specific roughness lengths which were derived from available data on stand height or stand age. The impact of canopy closure on the roughness length was not be taken into account due to lack of data.

## 5.2.3 Results and discussion

### 5.2.3.1 Concentration levels

#### *Overall variation*

The cumulative frequency distributions of  $\text{SO}_2$ ,  $\text{NO}_2$  and  $\text{NH}_3$  concentrations for all tree species together averaged over the period 1986 to 1995 (Fig. 22A) shows that for  $\text{SO}_2$ , the critical level of  $20 \mu\text{g m}^{-3}$  is exceeded at about 20% of the plots. The critical concentration levels of  $\text{NO}_2$  and  $\text{NH}_3$  ( $30$  and  $8 \mu\text{g m}^{-3}$  respectively) are not exceeded.

Concerning the  $\text{SO}_2$  concentration for each tree species separately, the cumulative frequency distribution averaged over the period 1986 to 1995 (Fig. 22B) shows that the defined critical concentration level of  $20 \mu\text{g m}^{-3}$  is exceeded at about 20% of the plots for all tree species except *Quercus ilex* for which the critical concentration level is not



exceeded at all. At about 10% of the plots the  $\text{SO}_2$  concentration is larger than  $30 \mu\text{g m}^{-3}$  and at 5% it is larger than  $40 \mu\text{g m}^{-3}$ . Fig. 22B also shows that the cumulative frequency distribution of *Pinus sylvestris* resembles the one of *Picea abies* (Group 1), with most trees being located at the lower concentration levels. The same holds for *Quercus robur* and *Fagus sylvatica* (Group 2), which are mostly experiencing slightly higher concentration levels. *Quercus ilex* (Group 3) is generally exposed to very low  $\text{SO}_2$  concentrations.

The cumulative frequency distributions of  $\text{NO}_2$  concentrations (Fig. 22C) show that the critical concentration level of  $30 \mu\text{g m}^{-3}$  is exceeded for none of the tree species (the maximum concentration is  $27 \mu\text{g m}^{-3}$ ). All plots are exposed to concentrations lower than  $20 \mu\text{g m}^{-3}$ . For *Quercus ilex*, there are even no plots that are exposed to a concentration larger than about  $7 \mu\text{g m}^{-3}$ . Again, the different groups described above can be distinguished.

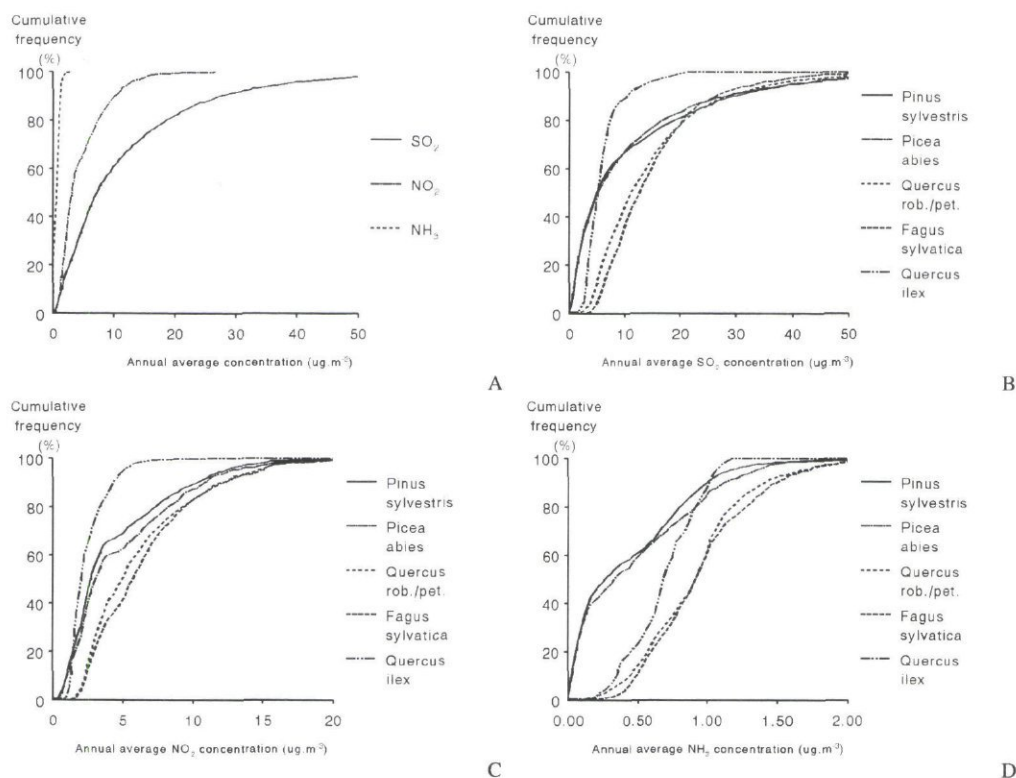


Fig. 22 Cumulative frequency distributions of (A)  $\text{SO}_2$ ,  $\text{NO}_2$  and  $\text{NH}_3$  concentrations for all tree species, for  $\text{SO}_2$  (B),  $\text{NO}_2$  (C) and  $\text{NH}_3$  (D) for the five tree species considered in this study

Concerning the  $\text{NH}_3$  concentration, the cumulative frequency distributions (Fig. 22D) show that the critical level of  $8 \mu\text{g m}^{-3}$  is not exceeded at all.  $\text{NH}_3$  concentrations do hardly exceed  $2 \mu\text{g m}^{-3}$  (with a maximum of  $3 \mu\text{g m}^{-3}$ ). These low concentrations were obtained from the EMEP-LRT model. This model does not describe local variation in  $\text{NH}_x$  emissions (caused by agricultural activities), and hence local variation in air concentrations. From the large EMEP grid cells (with a resolution of  $150 \times 150 \text{ km}^2$ )

the locally high concentrations are not found as the model calculates the average concentration for the whole grid cell. Though Group 1 (with most trees being located at the lower concentration levels) and Group 2 (with most trees being located at the higher concentration levels) behave the same as with regard to the  $\text{SO}_2$  and  $\text{NO}_2$  concentration levels, *Quercus ilex* (Group 3) is now situated in between both groups.

### Temporal variation

The results for the  $\text{SO}_2$  concentrations per year are presented in a bar diagram showing the number of locations (in percentage of the total number of plots) above certain levels, for all tree species together (Fig. 23A). The resulting figure shows a trend towards smaller percentages of plots exceeding the critical concentration level from 1986 to 1995, 1989 being the only exception. In 1986 about 25% of all plots exceeded the critical  $\text{SO}_2$  concentration of  $20 \mu\text{g m}^{-3}$ , whereas in 1995 this was only the case at 10% of the plots. This temporal variation follows the large-scale emission reductions introduced after 1986.

Little variation was observed in  $\text{NO}_2$  concentrations in the period 1986 to 1995 (Fig. 23B). There is a slight trend towards lower concentrations. Like for the  $\text{SO}_2$  concentrations, in 1989 a little break in the trend can be seen. Even for single years, the critical level was exceeded at none of the plots.

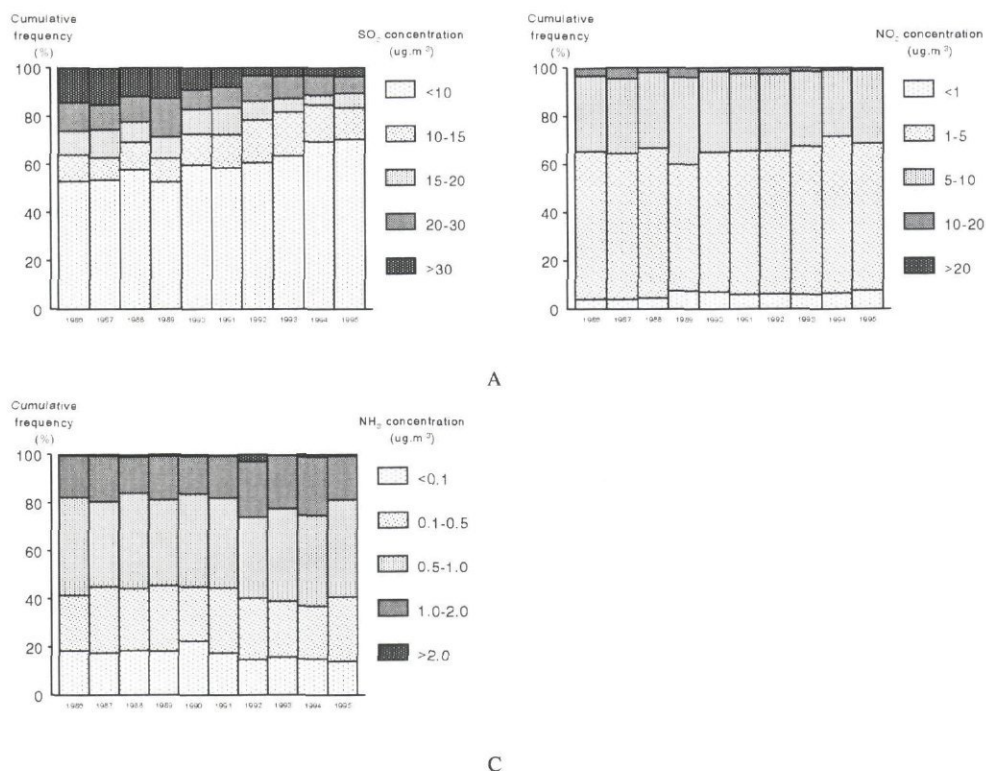


Fig. 23 Temporal variation of  $\text{SO}_2$  (A),  $\text{NO}_2$  (B) and  $\text{NH}_3$  (C) concentrations for all tree species



No specific trend was observed in the temporal variation of the  $\text{NH}_3$  concentrations averaged over all plots (Fig. 23C). Even for single years, a concentrations of  $2 \mu\text{g m}^{-3}$  was exceeded at only a very small percentage of the plots

### ***Spatial variation***

The spatial distribution over Europe in the modelled  $\text{SO}_2$   $\text{NO}_2$  and  $\text{NH}_3$  concentrations is presented by means of maps of the average concentrations of all Level 1 plots over the period 1986 to 1995 (Fig. 24-26).

The plots where the critical  $\text{SO}_2$  concentration level of  $20 \mu\text{g m}^{-3}$  is exceeded are mostly located in eastern Germany, Poland and the Czech and Slovak Republics (Fig. 24). Here concentrations of up to  $50 \mu\text{g m}^{-3}$  are found. Also in Hungary, Rumania, Bulgaria, The Netherlands, United Kingdom and Spain the critical concentration level is sometimes exceeded.

The highest average  $\text{NO}_2$  concentrations are found in Germany and The Netherlands, though the concentrations are still below the critical level (Fig. 25). The EMEP grid resolution is clearly shown in central Europe.

The  $\text{NH}_3$  concentration map (Fig. 26) shows largest concentrations (though still below the critical level) in The Netherlands, Belgium, western Germany and northern Italy.

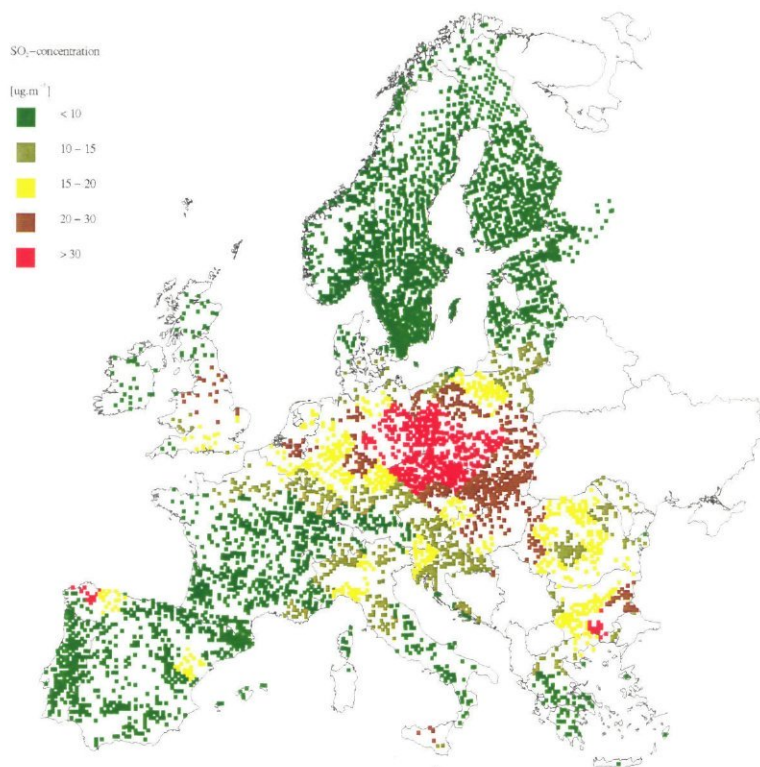


Fig. 24 The calculated 10 years average  $\text{SO}_2$  concentration for all monitoring plots.

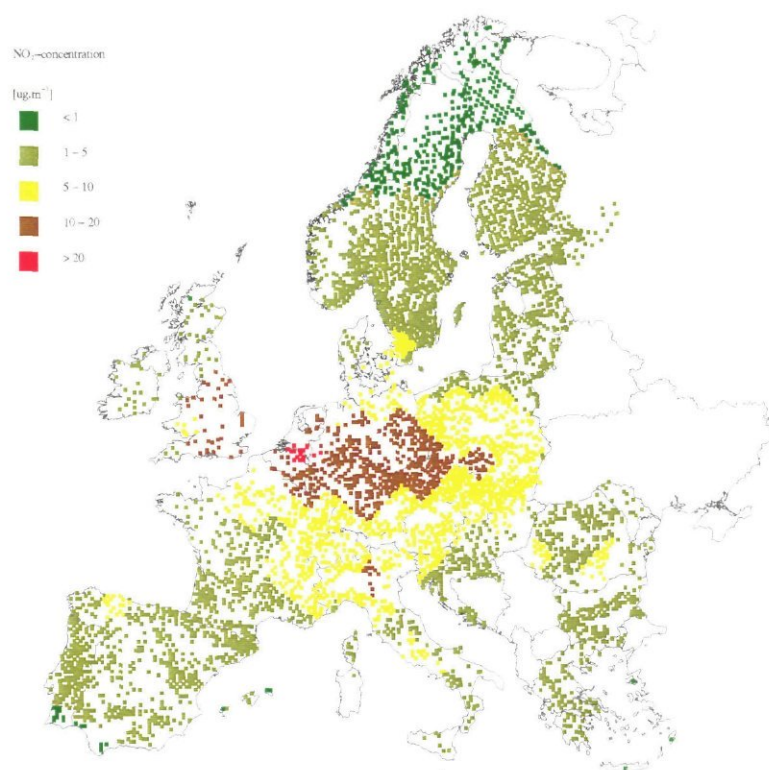


Fig. 25 The calculated 10 years average NO<sub>2</sub> concentration for all monitoring plots.

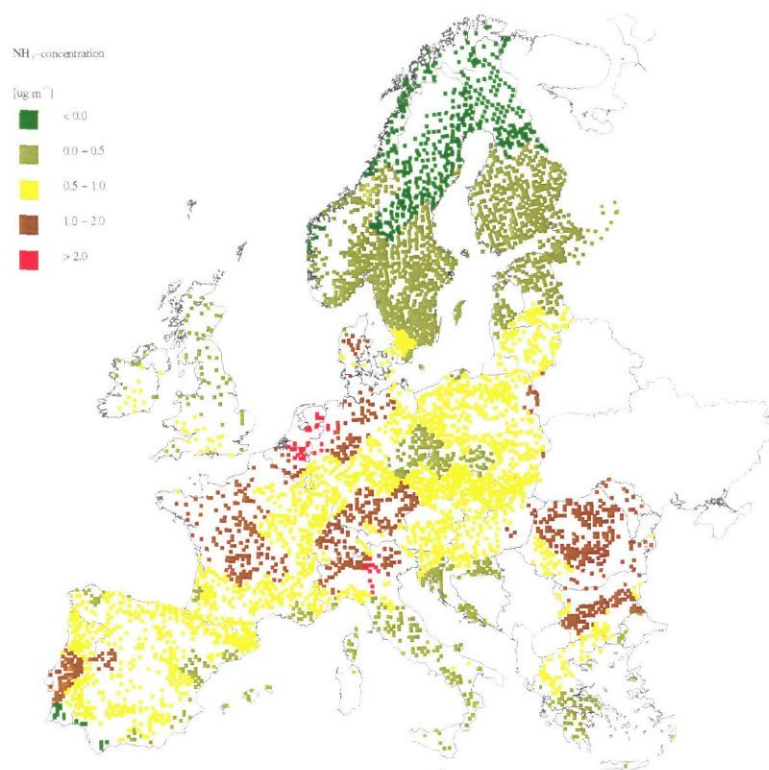


Fig. 26 The calculated 10 years average NH<sub>3</sub> concentration for all monitoring plots.

### 5.2.3.2 Deposition levels of sulphur and nitrogen compounds

#### Overall variation

The cumulative frequency distributions of the total nitrogen load ( $\text{NO}_y$  and  $\text{NH}_x$ ) for all tree species separately averaged over the period 1986 to 1995 (Fig. 27A) show that a deposition load of  $1000 \text{ mol}_c \text{ ha}^{-1} \text{ a}^{-1}$  is exceeded at about 20% of the plots for all tree species except *Quercus ilex*, for which at all plots nitrogen loads are smaller than  $600 \text{ mol}_c \text{ ha}^{-1} \text{ a}^{-1}$ . A deposition load of  $1500 \text{ mol}_c \text{ ha}^{-1} \text{ a}^{-1}$  is exceeded at about 5% of the plots. Comparison of the actual loads with the critical deposition levels will be made in Section 5.3. The low deposition numbers found here are caused by using the large scale  $\text{NO}_x$  and  $\text{NH}_x$  air concentration fields generated by the EMEP-LRT model to obtain the dry deposition estimates. As explained in Section 5.2.1.1, dry deposition is calculated by multiplying the dry deposition velocity at the plots with these air concentration fields, which results in underestimation of the nitrogen loads.

The cumulative frequency distributions of total potential acid deposition (sulphur and nitrogen loads; Fig. 27B) shows that a load of  $2000 \text{ mol}_c \text{ ha}^{-1} \text{ a}^{-1}$  is exceeded in a very large percentage of the plots. For *Quercus robur* and *Fagus sylvatica* this load is exceeded at about 60% of the plots and for *Picea abies* and *Pinus sylvestris* at about 40% of the plots. For *Quercus ilex* the acid deposition load does not exceed  $1500 \text{ mol}_c \text{ ha}^{-1} \text{ a}^{-1}$ . Exceedances of critical deposition levels for total acid are described in Section 5.3. The groups distinguished in Section 5.2.2.1 can also be recognised in Fig. 27A and B.

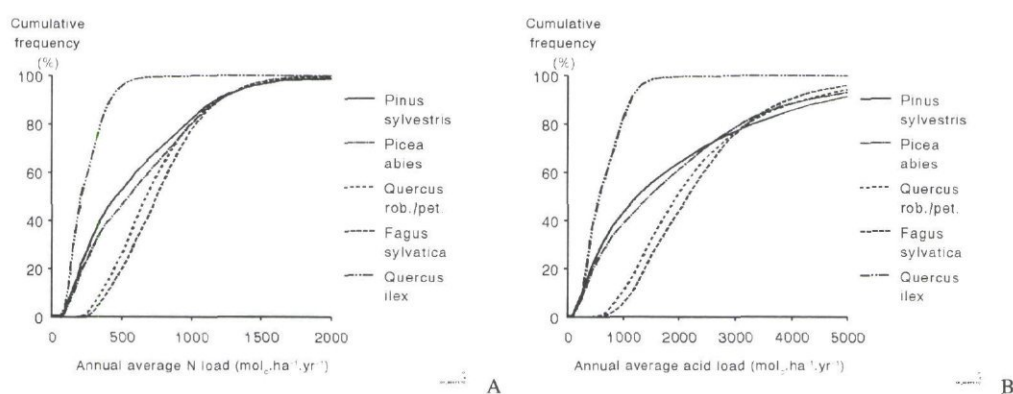


Fig. 27 Cumulative frequency distributions of total nitrogen deposition (A) and potential acid deposition (B) for the five major tree species considered in this study

#### Temporal variation

The bar diagram (Fig. 28A) in general shows a trend towards smaller percentages of plots with high nitrogen loads. This is mainly due to a (small) decrease in  $\text{NO}_2$  concentration and deposition. For example, exceedance of a total nitrogen load of  $1500 \text{ mol}_c \text{ ha}^{-1} \text{ a}^{-1}$  declines from about 5% in 1986 to about 1% in 1995. A total



nitrogen load of  $1000 \text{ mol}_c \text{ ha}^{-1} \text{ a}^{-1}$  is exceeded in about 20% of the plots in 1986 and in about 10% of the plots in 1995.

The temporal variation of total acid deposition averaged over the tree species (Fig. 28B) in general shows a trend towards smaller percentages of plots exceeding high deposition loads. This is the result of the reduction in  $\text{SO}_2$  emissions in Europe after 1986. The percentage of plots exceeding an acid load of  $1000 \text{ mol}_c \text{ ha}^{-1} \text{ a}^{-1}$  declines from about 75% in 1986 to about 55% in 1995. In the last three years an opposite trend might be the case. The 2000 (and 4000 between brackets)  $\text{mol}_c \text{ ha}^{-1} \text{ a}^{-1}$  acid deposition load is exceeded in about 50% (15%) of the plots in 1986 and in 30% (5%) of the plots in 1995.

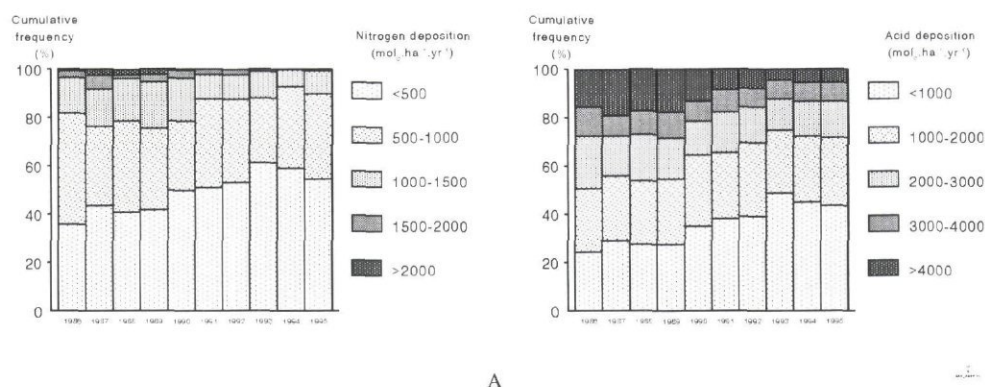


Fig. 28 Temporal variation in annual average deposition of total nitrogen (A) and potential acid (B) for all tree species together

### Spatial variation

The map presenting the average total deposition for the considered time period (Fig. 29) shows that highest nitrogen loads are found in Germany, Poland, Czech Republic and The Netherlands.

The map presenting the potential acid deposition averaged over the period 1986 to 1995 (Fig. 30) shows that an acid deposition load of  $1000 \text{ mol}_c \text{ ha}^{-1} \text{ a}^{-1}$  is not exceeded in Scandinavia (except the southern part) and the largest part of the Iberian peninsula (except the northern part). Also in parts of the United Kingdom, Ireland, France, Italy and Greece this load is not exceeded. However, especially in Central Europe (in particular Poland, Germany, Czech and Slovak Republics) and The Netherlands and Belgium potential acid deposition loads up to  $5000 \text{ mol}_c \text{ ha}^{-1} \text{ a}^{-1}$  are found.

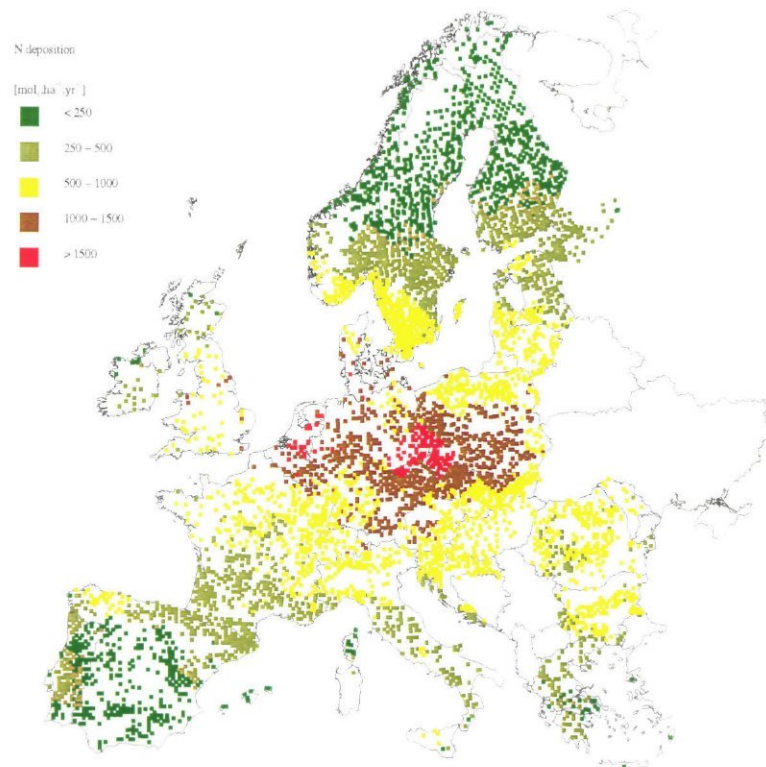


Fig. 29 The calculated 10 years average N deposition for all monitoring plots

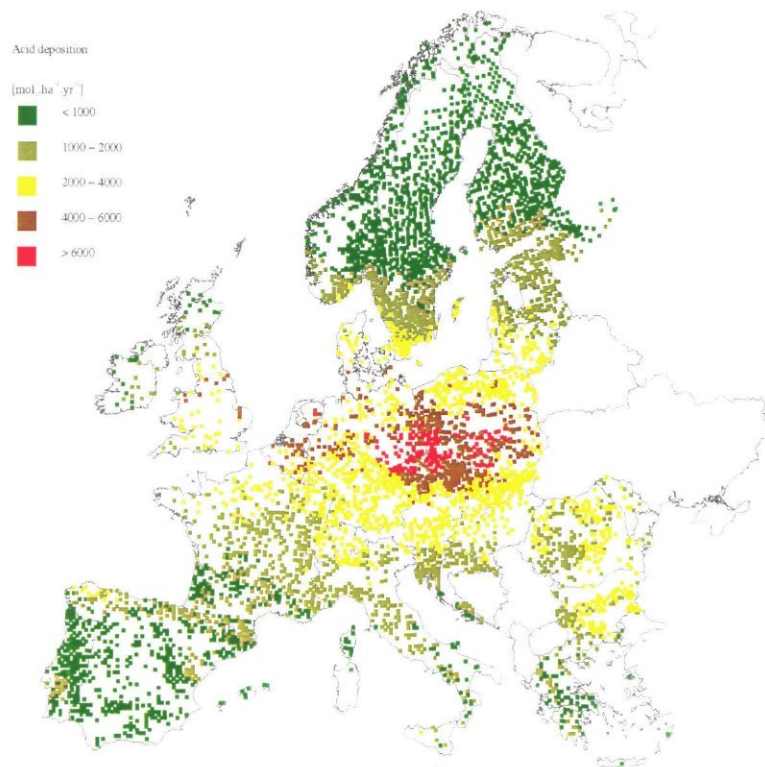


Fig. 30 The calculated 10 years average acid deposition for all monitoring plots

### 5.2.3.3 Deposition levels of base cations

#### Overall variation

The overall variation in the  $\text{Na}^+$ ,  $\text{Mg}^{2+}$ ,  $\text{K}^+$  and  $\text{Ca}^{2+}$  deposition (separately) is presented in cumulative frequency distribution of the results for these variables for the five tree species which are considered in this study (Fig. 31A). The  $\text{K}^+$  deposition is lowest and  $\text{Na}^+$  deposition is highest, especially in coastal areas. The total base cation deposition (i.e. the sum of the  $\text{Mg}^{2+}$ ,  $\text{K}^+$  and  $\text{Ca}^{2+}$  deposition) can be considered as a measure for the acid neutralisation capacity of the potential acid deposition, which is considered in the previous section (e.g. Draaijers et al., 1996a). Base cation deposition is highest for *Quercus robur* and *Fagus sylvatica*, both occurring most in the south of Europe (Fig. 31B). The base cation deposition increases from coniferous forest, which are more common in northern Europe, to deciduous species, generally occurring in the south.

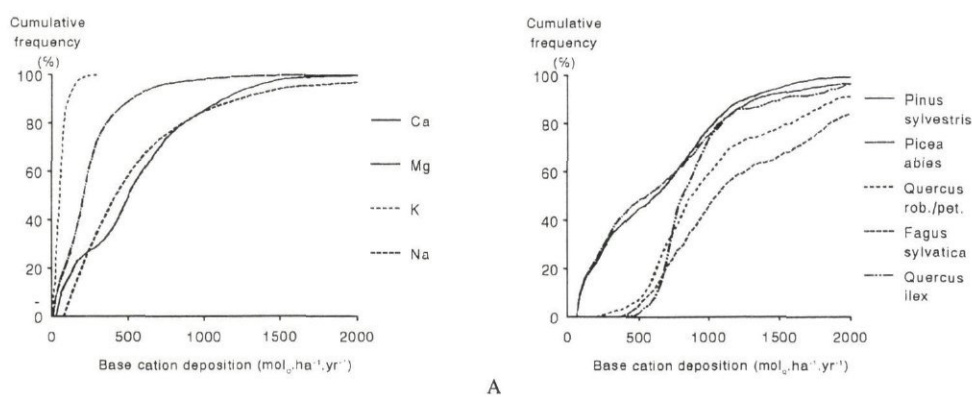


Fig. 31 Cumulative frequency distributions of  $\text{Na}^+$ ,  $\text{Mg}^{2+}$ ,  $\text{K}^+$  and  $\text{Ca}^{2+}$  deposition for all tree species together (A) and total base cation deposition (without  $\text{Na}^+$ ) (B) for the five major tree species considered in this study

#### Temporal variation

The temporal variation in the averaged base cation (all without Na) deposition for all tree species together shows that there is a slight trend towards lower base cation inputs, especially in those areas where the inputs are low (Fig. 32). Besides meteorological factors affecting deposition, the decrease is due to the reduction in industrial emission in central Europe during the ten years. The highest values do not show a trend because these are mainly the result of natural sources, such as sea salt and soil dust, which are not expected to change much.

#### Spatial variation

The highest base cation deposition (all without  $\text{Na}^+$ ) for the ten year period is found in southern Europe (Fig. 33). The deposition of soil dust of calcareous soils and of Sahara dust contributes most to the total deposition. Draaijers et al. (1996a) estimated the total base cation inputs in these regions are nearly equal to potential acid inputs. Base cation deposition is also high in coastal areas, due to the sea salt deposition. Lowest base cation deposition is found in Scandinavia, where values are below 500 mol<sub>c</sub> ha<sup>-1</sup> a<sup>-1</sup>. In central Europe, base cation input equals about 25% of the total potential acid inputs. The relatively high inputs in the eastern part of Europe are probably due to an



potential acid inputs. The relatively high inputs in the eastern part of Europe are probably due to an overestimation. In these areas, the deposition estimates are based on interpolation of only few measurements showing quite large deposition values (van Leeuwen et al., 1996).

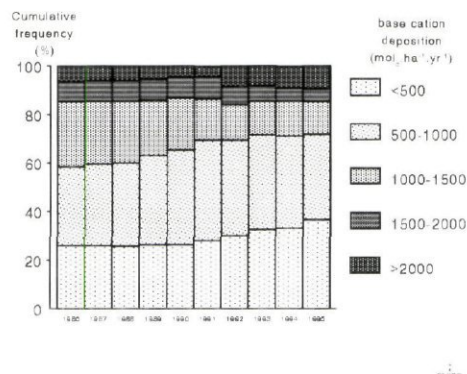


Fig. 32 Temporal variation in annual average deposition of the sum of the  $Mg^{2+}$ ,  $K^{+}$  and  $Ca^{2+}$  deposition, for all tree species together

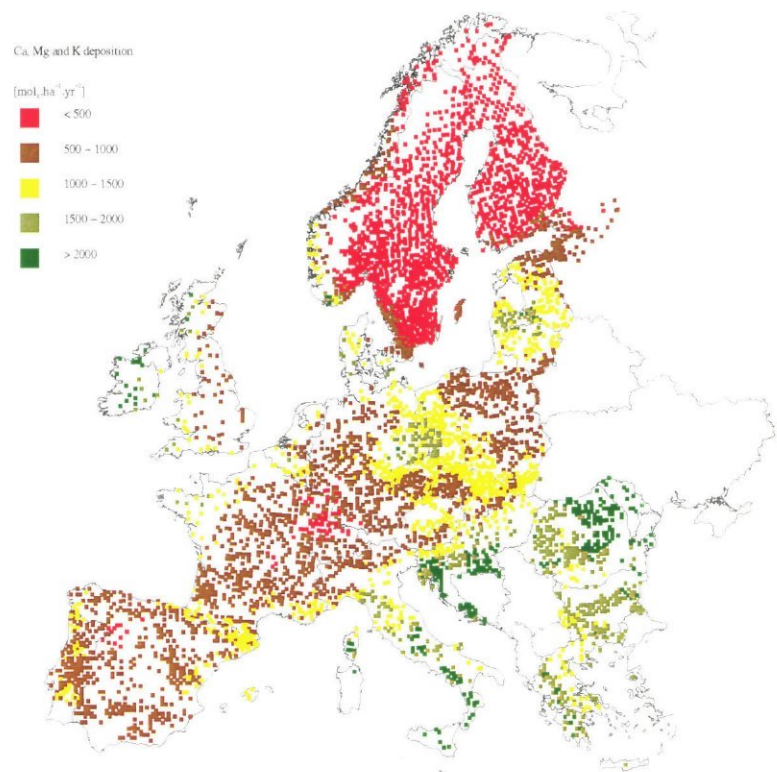


Fig. 33 The calculated 10 years average sum of Ca, Mg and K deposition for all monitoring plots

## **5.2.4 Uncertainties in the concentration and deposition estimates**

### **5.2.4.1 Concentration levels**

From a statistical analysis with measurements it was concluded that the uncertainty (on the one  $\sigma$  level) in the air concentrations derived from the EMEP-LRT model equals 40-70% (Krüger, 1993). It is assumed that the concentration distribution within a grid cell ( $150 \times 150 \text{ km}^2$ ) is homogeneous. In background areas with low concentrations this assumption is valid and the uncertainty in concentrations is therefore low. This assumption is, however, not valid in grid cells which contain industrialised areas or many scattered sources such as intensive animal husbandry farms and/or roads. For such conditions, sub-grid concentration variations will be present and the uncertainty in site specific concentrations will be large, usually resulting in underestimates. The uncertainties are largest for components with many scattered low level sources, such as  $\text{NO}_2$  and  $\text{NH}_3$ . Especially for  $\text{NH}_3$ , because of its relatively high conversion rate and dry deposition velocities, this might lead to serious underestimates. Asman and van Jaarsveld (1992) showed that when using a model resolution of  $5 \times 5 \text{ km}^2$ , modelled concentrations compared reasonably well with observations. When the model resolution was set to  $75 \times 75 \text{ km}^2$ , however, modelled concentrations were a factor of two lower than the measured ones.

An other factor introducing systematic underestimation in or near source areas is the use of 24 h averaged data. Peak values at different periods of the day for different components are levelled down. Finally, also the use of modelled concentrations at 50m height might introduce further systematic deviations of concentrations for components with low level sources. For  $\text{SO}_2$  this will not introduce systematic deviations.

In conclusion it is clear that  $\text{NH}_3$  concentrations are seriously underestimated, especially in areas with livestock breeding. On an annual basis this underestimation can reach an order of magnitude.  $\text{SO}_2$  concentrations are underestimated in or near source areas. Furthermore, peak values are levelled down.  $\text{NO}_2$  concentrations are underestimated, but to a lesser extend than  $\text{SO}_2$  and  $\text{NH}_3$ , because of the relatively small dry deposition velocity and low conversion rate.

### **5.2.4.2 Deposition levels**

In the first part of this section, uncertainty in the total deposition estimates will be briefly described. At the end of the section, the comparison of modelled deposition with throughfall measurements will be presented. The uncertainty in EDACS results is derived from Draaijers et al. (1996) concerning dry deposition of base cations, Erisman (1993) and Van Pul et al. (1995) concerning dry deposition of acidifying compounds, and Van Leeuwen et al. (1995) concerning wet deposition of acidifying compounds and base cations. In these publications and in Annex 3 (Section A3.4), a more extended description of the uncertainty estimates can be found. These can be interpreted as general limitations in model results.



**Regional scale uncertainty**

The uncertainty in regional scale deposition estimates strongly depends on the pollution climate and on landscape complexity of the area under study. The uncertainty in total deposition is determined by the uncertainty in wet, dry and cloud and fog deposition. Fog and cloud water deposition is not taken into account. Therefore, deposition estimates are more uncertain in areas with complex terrain where fog and cloud deposition might be important. Deposition estimates are also more uncertain in areas with strong horizontal concentration gradients, e.g. in source areas.

Using error propagation methods and assuming that presented uncertainties in deposition velocities and air concentrations represent random errors, the total uncertainty in dry deposition for a grid cell (on the one  $\sigma$  level) was roughly estimated to amount ca. 80-120% on average (Draaijers et al., 1996), both for acidifying components and base cations. Van Leeuwen et al. (1995) estimated the uncertainty in wet deposition at 50-70% on average. The uncertainty in total deposition can be calculated to amount 90-140% (Draaijers et al., 1996).

**Comparison of modelled deposition with throughfall data**

Long term mean modelled and measured wet, dry and total deposition fluxes were compared separately. For total deposition, the comparisons are presented in scatter plots for each component (Fig. 34A-G). These figures include all data with periods ranging from 1 year to 10 years (1986 to 1995). Table 21 lists the number of measurements used to calculate the long term-mean deposition estimates. At 36 plots the mean deposition over one year was used, at 41 plots the mean deposition over 2 years, etc. Only 7 stations collected throughfall during 10 years.

*Table 21 Number of throughfall measurements used to calculate the long-term mean deposition estimates*

Number of years	1	2	3	4	5	6	7	8	9	10
Number of plots	36	41	26	36	8	24	4	12	2	7

Table 22 presents the correlation coefficients of linear regression equations between modelled and measured total deposition. Additional data for wet and dry deposition are presented in Annex 3. The results of a ‘paired two sample for means’ t-test show that the averages of modelled data are significantly different from throughfall data. The table also presents the relative standard error, giving a measure of the relative uncertainty. The relative standard error is the predicted y-value (model estimate) for each x value (throughfall estimate) in the regression, divided by the average of the x values.

The averages of the deposition measurements and the deposition estimates are different on the  $p<0.05$  level and there is considerable scatter, although there is usually a high correlation (except for  $\text{NO}_y$ ) and significant regression equations ( $p<0.05$ ) were found (Fig. 34A-G and Table 22). Estimates might differ significantly if at the higher deposition levels some outliers are found (e.g. Fig. 34C), influencing the results to a large extent. This means that in general the model performs well, but for individual plots the deviation from the measured level can be large. To a large extent this can be attributed to the large uncertainty in air concentrations. Air concentrations of acidifying



components are based on the EMEP model which has a poor spatial resolution ( $150 \times 150 \text{ km}^2$ ) and only accounts for the long-range transported fraction, whereas air concentrations of base cations are based on a simple scavenging model. The scatter in the results can also be attributed to uncertainty in the throughfall measurements (Draaijers et al., 1996a).

Table 22 Pearson correlation coefficients of linear regression equations between modelled and measured total deposition. Moreover results of a 'paired two sample for means' t-test to see whether both estimates are equal on the average or not, and the relative standard error are presented (RelSE). \* denotes both estimates differ significantly ( $p < 0.05$ ). n denotes the number of measurements used in the comparison

		SO <sub>x</sub>	NO <sub>y</sub>	NH <sub>x</sub>	Na <sup>+</sup>	Mg <sup>2+</sup>	Ca <sup>2+</sup>	K <sup>+</sup>	Acid	Total N
Total deposition	r	0.49	0.13	0.72	0.79	0.54	0.69	0.28	0.63	0.68
	t-test	*	*	*	*	*	*	*	*	*
	RelSE	82%	67%	49%	109%	90%	56%	49%	64%	51%
	n	292	292	296	236	236	236	236	292	292

For SO<sub>x</sub> and NO<sub>y</sub> two groups of plots can be distinguished (Fig. 34A and B); one group scattering around the 1:1 line (which is included in each plot), where both model and measured estimates are low, and another group where modelled values are high, whereas measured data are much lower. For NO<sub>y</sub> this might be explained by canopy uptake. For SO<sub>x</sub> this has probably to do with the use of surface resistance parametrisations which were derived from measurements at plots with high NH<sub>3</sub> concentrations, promoting SO<sub>2</sub> deposition (Erisman et al., 1994a). By using these parametrisations in areas with low NH<sub>3</sub> concentrations this leads to overestimates of the SO<sub>2</sub> deposition.

Most throughfall measurements are obtained in relatively low NH<sub>x</sub> deposition areas. At stands where the deposition is higher than about  $1500 \text{ mol}_c \text{ ha}^{-1} \text{ a}^{-1}$ , the throughfall estimates are much higher than the modelled estimates, despite the expected canopy uptake. This is caused by underestimation in high emission areas of the concentrations resulting from the EMEP model resolution.

For Ca<sup>2+</sup> and K<sup>+</sup> (Fig. 34F and G) the same is observed as for NH<sub>x</sub>. The model seems to underestimate total deposition at higher deposition levels. This is probably due to the fact that 'background' air concentrations are used. If forests are located near local sources such as e.g. agricultural fields or unpaved roads, they will receive an additional input of NH<sub>x</sub>, Ca<sup>2+</sup> and K<sup>+</sup>. For NH<sub>x</sub> and especially NO<sub>y</sub> negative net throughfall fluxes were found for several plots, denoting canopy uptake. The negative net throughfall fluxes are mostly measured at plots located far away from nitrogen sources (e.g. Scandinavia).

A comparison of total deposition for potential acid and total nitrogen (Fig. 35) shows that the correlation between modelled and measured estimates is high, with r being 0.63 and 0.68, respectively (Table 22). Total nitrogen estimates scatter around the 1:1 line. For total acid estimates, modelled values are higher than measured values at modelled acid loads above  $4000 \text{ mol}_c \text{ ha}^{-1} \text{ a}^{-1}$ .

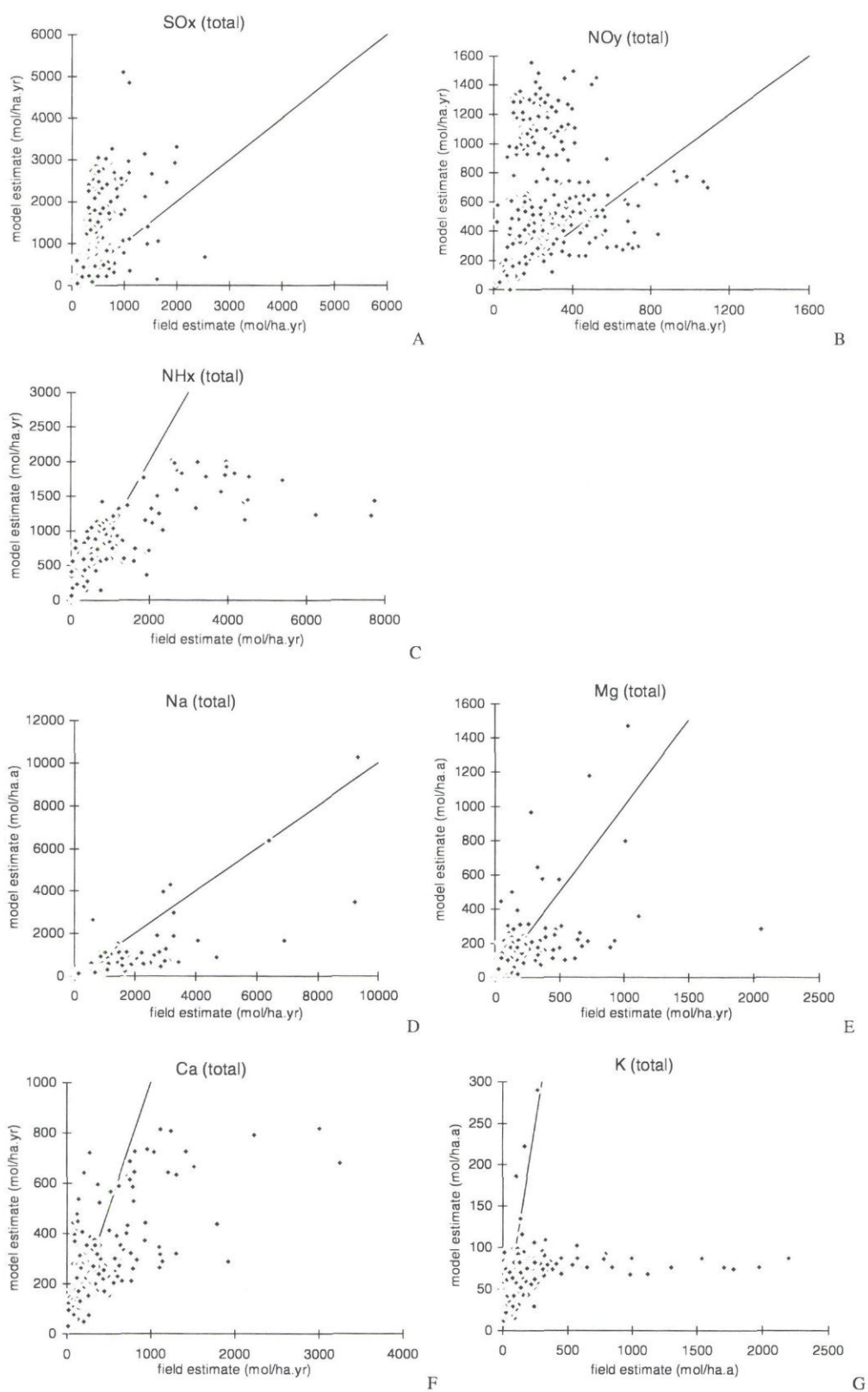


Fig. 34 Comparison between modelled total deposition and total deposition estimated from through-fall and bulk precipitation measurements for SO<sub>x</sub> (A), NO<sub>y</sub> (B), NH<sub>x</sub> (C), Na<sup>+</sup> (D), Mg<sup>2+</sup> (E), Ca<sup>2+</sup> (F) and K<sup>+</sup> (G). In each plot the line  $y = x$  is presented

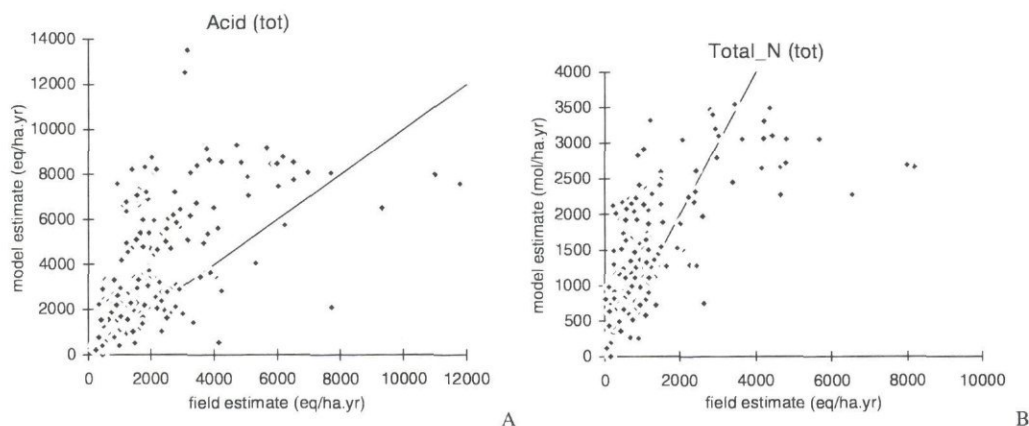


Fig. 35 Comparison between modelled total deposition of potential acid (A) and total nitrogen (B), and total deposition estimated from throughfall and bulk precipitation measurements. In each plot the line  $y = x$  is presented.

Before drawing firm conclusions from this comparison, it must be emphasised that the throughfall measurements also have uncertainty. This has mainly to do with the canopy interactions, but also with the error sources related to the way representative samples are obtained and samples are handled (Draaijers et al., 1996b). The uncertainty in atmospheric deposition estimated from throughfall, stemflow and precipitation measurements is estimated to be 30% for sulphur and 40% for nitrogen and base cations, provided that state-of-the-art measurements and analytical techniques are used in combination with a sufficiently large number of replicate samplers (Draaijers et al., 1996b).

The relative standard error, as listed in Table 22 can be considered as an average difference between modelled total deposition values and those derived from throughfall measurements. The average difference ranges from 49% for  $\text{NH}_x$  and  $\text{K}^+$  to 109% for  $\text{Na}^+$ . These values are within the range of the uncertainty estimates determined by error propagation.

## 5.3 Ozone concentrations

### 5.3.1 Introduction

Direct damage to trees can occur by exposure of the leaves to elevated concentrations of ozone. For forest trees a critical level of ozone has been defined which is expressed as the cumulative hourly exposure over a threshold of 40 ppb during daylight hours, accumulated over six month. This index is referred to as AOT40 and should not exceed 10 000 ppb.h, (Section 6.3.1.2). As ozone concentrations show a large spatial variability over Europe, it is important to map the exceedances of the critical levels with a resolution as high as possible. Currently, at RIVM a procedure named EDEOS (European Deposition and Exposure of Ozone on a Small scale), based on the EDACS



model, is developed aiming at mapping the ozone exposure in Europe on a resolution of  $1/6^\circ \times 1/6^\circ$  lat/lon (ca.  $12 \times 20 \text{ km}^2$ ) (Eleveld et al., 1997 in prep). The EDEOS model was applied to estimate ozone stress for each plot.

Some major problems in applying the EDEOS method within the framework of this study are:

- emission data became available at a very late stage, resulting in a lack of EMEP ozone concentration fields for the whole period 1986 to 1995, and
- the model has been under development continuously and is yet very recently applicable.

This necessitates a simplified approach concerning the calculation of ozone stress. Ozone concentrations and AOT40 values were calculated for the growing season of one year only (1990). These values were used in the statistical model in order to at least describe the spatial variation in ozone stress.

### 5.3.2 Methods

In the EDEOS model various sources of data are used as input. First, 6-hr average concentration fields of ozone, NO and NO<sub>2</sub> at 50 m height on a coarse grid of  $150 \times 150 \text{ km}^2$  provided by the EMEP Lagrangian long-range transport model (Simpson et al. 1993) are used. These ozone concentrations are transformed to values at canopy height by correcting for deposition of ozone and chemical interactions between ozone and NO. Deposition fluxes and deposition velocities are calculated using the same procedure and the same land use and meteorological information as used in EDACS (Van Pul et al., 1995). For the NO correction with the photostationary equilibrium detailed NO emission maps were used.

The EDEOS model reconstructs hourly ozone concentrations based on ozone concentration fields at 00.00, 06.00, 12.00 and 18.00 hours. Furthermore, the model accounts for the dependence of ozone concentrations on local orography. This dependence is modelled based on data from the EUROTRAC-TOR and EMEP programmes as well as on literature results, and combined with orographic data (on a  $1/6^\circ \times 1/6^\circ$  resolution) provided by EPA (Environmental Protection Agency, USA). All ozone measurements which were made at different altitudes in the USA and Europe were plotted as a function of altitude. The best fit through the values provided a function to correct for the height dependence of ozone concentrations. This way the concentration of ozone at the surface is obtained. From the modelled surface concentrations the exceedances of AOT40 levels at each monitoring site can be obtained. For more details on the methods used the reader is referred to Annex 3 and Eleveld et al. (1997, in prep).

### 5.3.3 Results and discussion

#### 5.3.3.1 Overall variation

The overall variation of the various ozone indicators is presented in a cumulative frequency distribution concentrations per tree species considered in this study, averaged over the growing season of 1990 (Fig. 36).

The average ozone concentration exceeds a concentration level of 40 ppb at almost all plots (Fig 36A). For *Quercus robur* + *Q. petraea*, *Quercus ilex* and *Fagus sylvatica* this level is exceeded at all plots, whereas for *Pinus sylvestris* and *Picea abies* it is exceeded in about 80% of the plots. Concentrations up to 100 ppb were calculated. The high average ozone concentrations result in high modelled AOT40 values (the cumulative exposure over the threshold concentration of 40 ppb calculated over the growing season for daylight hours only). The critical ozone level (AOT40) of 10 000 ppb.h (hence 10 ppm.h in the figure) is exceeded at all plots for *Quercus robur* + *Q. petraea*, *Quercus ilex* and *Fagus sylvatica*, and at about 80% and 75% of the plots for *Picea abies* and *Pinus sylvestris*, respectively (Fig 36B). AOT40 values of five times the critical level is exceeded at about 60% of the plots for *Fagus sylvatica*, 30% for *Quercus robur* + *Q. petraea*, *Quercus ilex* and *Picea abies* and 10% for *Pinus sylvestris*.

The cumulative frequency distributions of *Pinus sylvestris* resemble the ones of *Picea abies* (though at the higher levels the graphs deviate, with *Picea abies* having larger percentages of plots exceeding the AOT40), with most trees being located at the lower levels. Both tree species are mostly located in northern Europe where ozone concentrations are generally low. The cumulative frequency distributions of *Quercus robur* + *Q. petraea* resemble the ones of *Quercus ilex*, with most trees being located at the intermediate levels as they are located in southern areas where ozone concentrations are generally higher than in northern Europe. *Fagus sylvatica* behaves differently, as these trees are exposed to the highest ozone levels. This tree species is mostly located in Central Europe where ozone concentrations are highest.

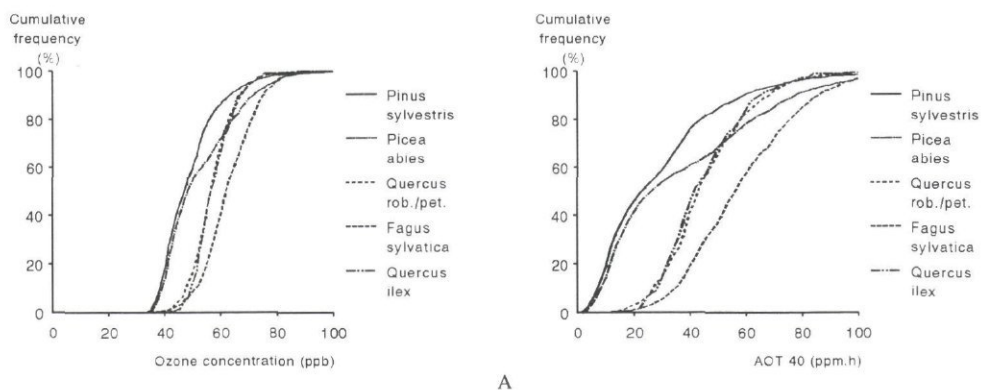


Fig. 36 Cumulative frequency distributions of (A) ozone concentrations and (B) AOT40 values for the five major tree species considered in this study

A comparison between the AOT40 and the AOT30 and AOT60 was made for all species together (Fig. 37). These alternative ozone levels were calculated to see whether AOT values other than the commonly used AOT40 are better related to forest condition (Chapter 7). Especially in the Nordic countries, AOT30 seems to be more appropriate, as in these areas effects have already been observed at lower (30 ppb) ozone concentrations (Führer, 1996).

The 95th percentiles, (i.e. the values that are exceeded at 5% of the plots) of the AOT40 are 75 ppm.h, i.e. 7½ times the critical value, for *Pinus sylvestris*, *Quercus robur* + *Q. petraea* and *Quercus ilex*. For *Picea abies* and *Fagus sylvatica* this percentile is about 95 ppm.h, whereas for all tree species together it is about 85 ppm.h. From these numbers it can also be concluded that the trees at the ICP plots are exposed to severe ozone stress.

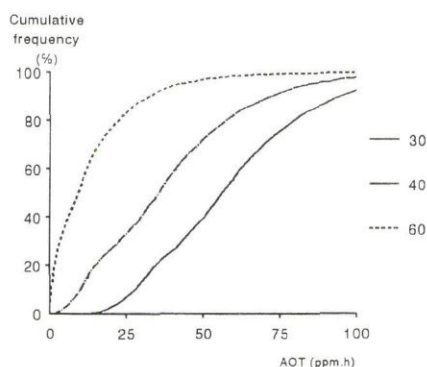


Fig. 37 Cumulative frequency distributions of AOT30, AOT40 and AOT60 for all tree species together

### 5.3.3.2 Temporal variation

At the very end of the project, also ozone exposure calculations for the growing seasons of 1985, 1989, 1992, 1993 and 1994 have been made. As these values have not been incorporated in the statistical analysis, they will not be presented in the figures here as well. However, it should be stressed here that there was considerable variation between years, with the calculated AOT40 values for most years being considerably lower than the 1990 values.

### 5.3.3.3 Spatial variation

The spatial variation in the ozone concentrations (averaged over the daylight hours in the growing season of 1990) and the AOT40 (estimated for the same period) is presented in two separate maps (Fig. 38 and 39, respectively). The lowest O<sub>3</sub>



concentrations ( $< 40$  ppb) are found in parts of (northern) Scandinavia and the United Kingdom (Fig. 38).

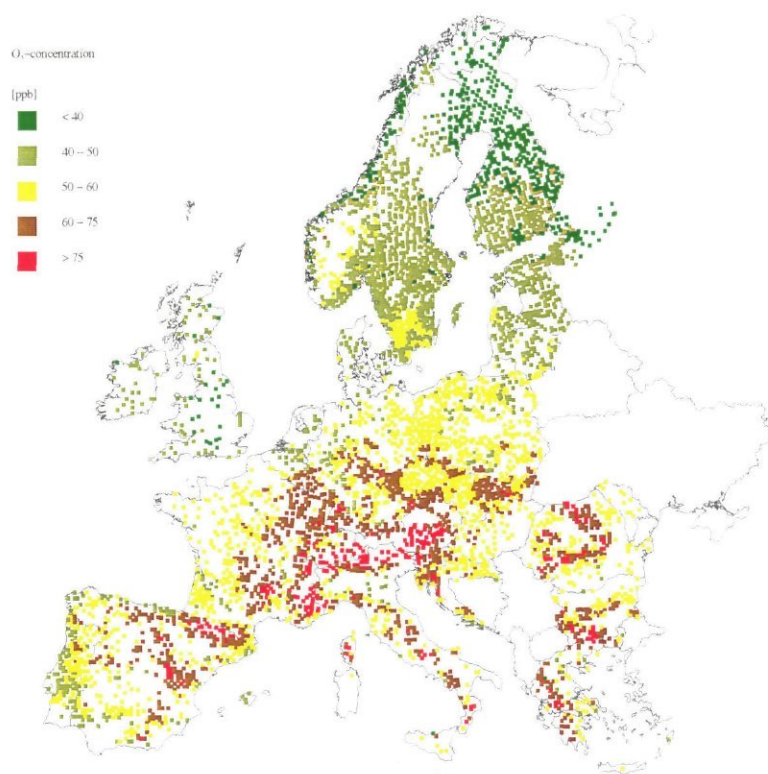


Fig. 38 Site specific modelled ozone concentrations averaged over the growing season of 1990

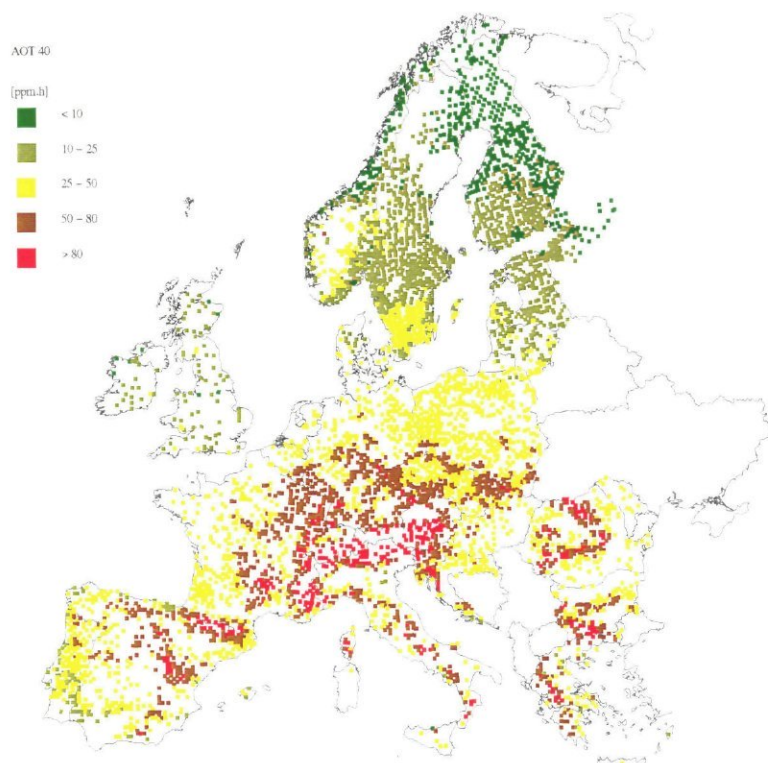


Fig. 39 Site specific modelled AOT40 values calculated over the growing season of 1990

In the remaining of the continent concentrations are fairly high (ranging between 50 and 75 ppb), whereas highest concentrations (> 75 ppb) are estimated at high altitudes in mountainous areas (e.g. Alps and Pyrenees). The AOT40 values show the same spatial pattern as the ozone concentrations, with highest values being estimated in Southern and Central Europe and in mountainous areas (Fig. 39).

### 5.3.4 Uncertainties

EDEOS was just finished at the end of this pilot study. The outcome of the model was only very roughly validated with measurements. Hence, no accurate uncertainty estimates in the ozone concentrations are available. A first comparison between calculated EDEOS and hourly measured ozone concentrations from the TOR network, i.e. the Tropospheric Ozone Research programme within the BIATEX framework, (both averaged over the growing season, daylight hours only) showed a reasonably good agreement. Though only nine measurement stations were involved in the comparison, results scattered around the 1:1 line closely.

In EDEOS uncertainties mainly arise from (i) the assumption that photostationary equilibrium exists, (ii) the separate treatment of deposition and the chemical interaction between ozone and NO, whereas they should be treated simultaneously as both processes are mutually dependent, (iii) the use of annual NO<sub>x</sub> emissions per area and the neglectance of VOC emissions, and (iv) uncertainty in the parametrisation of the elevation dependence on ozone concentrations. Eleveld et al. (1997, in prep) mention the latter to be very important. Furthermore, they state that in the largest areas in Europe the deposition correction was dominant over the correction due to the photochemical equilibrium between ozone and NO, hence giving information on which parts of the procedure contribute the most to the overall uncertainty. This gives an idea where future improvements to the model should be made.

## 5.4 Conclusions

The following conclusions can be drawn with respect to the overall, temporal and spatial variation of calculated anthropogenic stress factors.

### *Concentration levels of SO<sub>2</sub>, NO<sub>2</sub> and NH<sub>3</sub>*

1. The concentration levels for NO<sub>2</sub> and NH<sub>3</sub> estimated for the plots are low. Values ranges between 0 and 27 µg m<sup>-3</sup> for NO<sub>2</sub> and between 0 and 3 µg m<sup>-3</sup> for NH<sub>3</sub>, which are all below the critical levels for these gases (Chapter 5). Concentration levels for SO<sub>2</sub> vary mainly between 2 and 50 µg m<sup>-3</sup>, the latter value exceeds the critical level of 20 µg m<sup>-3</sup>.



2. A clear reduction in exposure of SO<sub>2</sub> concentration is shown between 1986 to 1995. During the last three years the concentration remained constant. NH<sub>3</sub> concentrations show no clear trend during the ten years, whereas NO<sub>2</sub> concentrations decreased very little.
3. Spatial variation of calculated concentration levels show high concentrations for SO<sub>2</sub>, NO<sub>2</sub> and NH<sub>3</sub> in Central and Western Europe. Highest SO<sub>2</sub> concentrations occur in Germany, Poland and the Czech Republic, whereas NO<sub>2</sub> and NH<sub>3</sub> concentrations are highest in The Netherlands, Belgium and Western Germany.
4. The uncertainty in the calculated concentration levels is large because the concentrations are underestimated to a large extent for plots located in or near to source areas. The underestimation is largest for NH<sub>3</sub> because of the many scattered low level sources and by using 50 m height model results. The underestimation can be an order of magnitude.

#### ***Deposition of S and N compounds and base cations***

1. The calculated N deposition values mostly range between 100 and 1000 mol<sub>c</sub> ha<sup>-1</sup> a<sup>-1</sup>, whereas the potential acid load vary mostly between 500 and 5000 mol<sub>c</sub> ha<sup>-1</sup> a<sup>-1</sup>. Total nitrogen and potential acid input is lowest for *Quercus ilex*, mainly occurring in Mediterranean areas. The other tree species show similar values. Nitrogen deposition decreased somewhat between the ten years. This is mainly due to a small decrease in NO<sub>y</sub> deposition. Potential acid deposition decreased between 1986 and 1992, but remained fairly constant after 1992. The strong decrease is mainly the result of the decrease in SO<sub>x</sub> deposition, and to a small decrease in NO<sub>y</sub> deposition.
2. The spatial distribution of the S and N deposition largely resembles the source area distribution. As with the concentration levels of SO<sub>2</sub>, NO<sub>2</sub> and NH<sub>3</sub>, highest deposition levels are observed in Central and Western Europe.
3. Base cation deposition is largest in coastal areas and in southern Europe. This is mainly due to the main sources, i.e. soil dust, Sahara dust and sea salt. In the eastern part of Europe the high base cation deposition is the result of uncertainty in wet deposition measurements. Base cation deposition can compensate almost entirely for the potential inputs in the south of Europe, whereas in central Europe it equals about 25% of the potential acid input.

Because of the underestimation of the ambient reduced and oxidised nitrogen concentration, the deposition of total nitrogen is underestimated in or near to source areas. The uncertainty in regional scale estimates of deposition was estimated by error propagation and amounts to 90-140%, depending on the compound and the region. Uncertainty was determined with throughfall data collected for as many plots in Europe and as many years as possible. A comparison between site specific modelled deposition and deposition derived from throughfall data showed that correlation between the two is significant for all compounds, although the average of the two differ significantly for almost all. The good correlation shows that the model calculates high or low values when the measurements show high or low values, but the absolute number is not right,



as shown by the t-test. In the correlative study (Chapter 7), the deposition estimates are therefore useful if used in a relative sense. If used as absolute values, in the case of critical deposition level exceedances, the outcome might be disturbed by the uncertainty in the model results. The total acid deposition is usually overestimated by the model, whereas the total nitrogen deposition is underestimated at plots with high nitrogen loads. The uncertainties, estimated as the standard error shows that these are somewhat lower than obtained by error propagation. One has to keep in mind that throughfall measurements in itself provide an estimate of the deposition with large uncertainty, especially for components with a strong canopy interaction, such as nitrogen and base cations.

### ***Ozone concentrations***

1. Ozone concentrations, averaged over the daylight hours in the growing season of 1990, vary between 30 and 100 ppb. AOT40 values vary between 1,000 and 100 000 ppb.h. For *Quercus robur* + *Q. petraea*, *Quercus ilex* and *Fagus sylvatica* the AOT40 is exceeded at all plots, whereas for *Pinus sylvestris* and *Picea abies* it is exceeded at about 75% of the plots.
2. Lowest ozone concentrations are found in parts of (Northern) Scandinavia and the United Kingdom. In the remaining of the continent concentrations range between 50 and 75 ppb, whereas highest concentrations are estimated at high altitudes in mountainous areas (e.g. Alps and Pyrenees). The spatial pattern in the modelled AOT40 values resembles the pattern of the ozone concentrations.
3. Up to now, EDEOS was validated with measurements only very roughly. However, a first comparison between ozone concentrations calculated by EDEOS and measured ozone concentrations showed a reasonably good agreement.

## 6 Critical thresholds for sulphur and nitrogen compounds and ozone

*Wim de Vries<sup>1)</sup>, Gert Jan Reinds<sup>1)</sup>, Jaco Klap<sup>1)</sup>, Erik van Leeuwen<sup>2)</sup> and Jan Willem Erisman<sup>2)</sup>*

<sup>1)</sup> DLO Winand Staring Centre (SC-DLO), Wageningen, The Netherlands

<sup>2)</sup> National Institute of Public Health and the Environment (RIVM), Bilthoven, the Netherlands

### 6.1 Introduction

In assessing the relationship between forest condition and stress factors, it is relevant to have information on threshold values below which the effect of a stress factor is considered to be insignificant. With respect to stress factors related to air pollution, the concept of critical levels and critical loads has been introduced in this context (Nilsson, 1986). These thresholds are defined as ‘a quantitative estimate of an exposure to one or more pollutants below which significant harmful effects of specified sensitive elements of the environment do not occur according to present knowledge’ (Nilsson and Grennfelt, 1988). In this text we do, however use the term critical deposition levels instead of critical loads, since the values that are calculated refer to the actual thresholds at the monitoring plots during the time of consideration. The term critical loads is only used when we refer to long-term acceptable values. More information on the difference is given in Section 6.2.2.

#### 6.1.1 Critical concentration levels

Critical (concentration) levels are thresholds related to the direct above-ground effects of an exposure of gaseous air pollutants, such as SO<sub>2</sub>, NO<sub>2</sub>, NH<sub>3</sub> and O<sub>3</sub>, on the forest condition. Such (apparent) no-adverse effect levels have been derived for forests from a compilation of literature on dose (the product of pollutant concentration and duration of exposure) response relationships (e.g. Ashmore and Wilson, 1994; UN/ECE 1989, 1995, 1996). Even though critical levels are influenced by climatic conditions (temperature, relative humidity, soil water content) and internal growth factors (leaf age, stand of development), values are presently defined independent of location, tree species and/or soil type. The only differentiation relates to exposure duration, i.e. ‘acute’ effects of short-term exposures (1 hour or 1 day mean values) and ‘chronic’ effects of long-term exposures (annual mean values) (UN/ECE, 1996).

#### 6.1.2 Critical deposition levels

Critical deposition levels (loads) are threshold values related to the indirect soil-mediated effects of atmospheric deposition (loads) on forest condition, such as nutrient imbalances caused by soil acidification and N accumulation (Section 1.1). Critical deposition levels aim to prevent a decrease in biodiversity and vitality of the forests. Literature information suggests that indirect soil-mediated effects of air pollutants on



the vitality of forests are generally more important than direct effects (Roberts et al., 1989; Heij and Schneider, 1995). The decrease in forest vitality, due to (relative) deficiencies in cation nutrients such as Mg, is considered to be at least partly caused by the mobilisation of Al in soils in response to S and N inputs (Heij *et al.*, 1991). Numerous studies, both in the laboratory and in the field, have shown that nutrient imbalances resulting from high concentrations of Al and N (NH<sub>4</sub>) as compared to (divalent) base cations such as Ca and Mg, have a negative influence on root elongation and root uptake (Sverdrup et al., 1990; Heij et al., 1991; De Vries, 1991 and Sverdrup and Warfvinge, 1993 for summarising overviews).

In this context critical Al/(Ca+Mg+K) ratios have been derived for various tree species (Sverdrup and Warfvinge, 1993). A strong decrease in pH in response to depletion of readily available secondary Al compounds may also play a role (Houdijk, 1994). Furthermore, elevated N inputs increases the N content of foliage and soil humus, which in turn may lead to an increased susceptibility of forests to natural stresses, such as fungal diseases, drought and frost (Aronsson, 1980; Roelofs et al., 1985; Boxman et al., 1986; De Visser, 1994) and vegetation changes in forest understorey (Hommel et al., 1990; Van Dobben et al., 1994; Bobbink et al., 1992; 1995).

### 6.1.3 Aims and contents of Chapter 6

The aims of this chapter are to present information on the order of magnitude and/or range, the spatial distribution and the reliability of calculated thresholds and exceedances of

- annual average concentration levels for SO<sub>2</sub>, NO<sub>2</sub>, NH<sub>3</sub> and O<sub>3</sub>,
- deposition levels for N related to the eutrophying effect of this compound and
- deposition levels for the acidifying impact of both S and N.

This chapter first describes the methods that have been used to calculate site-specific critical S and N deposition levels related to acidification and critical N deposition levels related to eutrophication (Section 6.2). Unlike critical levels, critical deposition levels were calculated for each stand while accounting for effects of location, tree species and soil type. as stated before, the critical deposition levels used in this study, do not refer, however, to long-term acceptable loads, used for policy making (e.g. Posch et al., 1995a; 1995b) but to actual thresholds at the monitoring plots for the time of consideration (1985-1995). The assumed steady-state situation in deriving long-term critical loads was thus not applied. The standard approach in deriving long-term critical loads and the adaptations used to obtain actual critical deposition levels are described in Section 6.2.1. and 6.2.2, respectively. Literature based critical levels for air pollutants used in this study are presented and discussed in Section 6.3.1. The results that have been calculated for critical deposition levels of N and acidity are given in Section 6.3.2. A critical review of the reliability of the literature-derived (site-independent) critical levels for SO<sub>2</sub>, NO<sub>2</sub>, NH<sub>3</sub> and O<sub>3</sub> and the calculated critical deposition levels for N and acidity is given in Section 6.4. This chapter ends with conclusions (Section 6.5) that are related to the aims described above.



## 6.2 Methods to derive critical deposition levels for sulphur and nitrogen compounds

Critical (concentration) levels used in this study were based on literature information on this topic (e.g. UN/ECE, 1989, 1995, 1996). These results were used independent of the considered site, even though meteorological factors may influence the critical levels (Section 6.4).

Critical deposition levels were calculated for each monitoring site with an adapted version of the simple mass balance (SMB) model (e.g. De Vries, 1991, 1993; Sverdrup and De Vries, 1994). The SMB model has widely been used throughout Europe to produce critical load maps since 1991 (Hettelingh et al., 1991; Downing et al., 1993; Posch et al., 1995b), as it is part of a 'Manual on Mapping Critical Loads and levels and their exceedances' (UN/ECE, 1996).

Critical deposition levels for the acidifying impact of both S and N compounds were calculated by requiring that an assumed, tree species specific, critical Al/ (Ca + Mg + K) ratio in soil solution is not exceeded at the bottom of the root zone. Separate critical deposition levels for nitrogen as a nutrient have also been derived by requiring that an assumed critical N content in foliage is not exceeded to avoid an increased sensitivity to natural stress. Here, we first describe the standard SMB model (Section 6.2.1) and then the adaptations to the model used in this study (Section 6.2.2). In Section 6.2.1, we still use the term critical loads, whereas in Section 6.2.2 on the adaptations, the term critical deposition level is used. The way in which model inputs were derived is given in Annex 4.

### 6.2.1 The simple mass balance approach

The principle of the SMB model is that it calculates critical loads by including processes influencing acid production and consumption during infinite time only. This implies that dynamic processes such as cation exchange, adsorption/desorption of SO<sub>4</sub> and NH<sub>4</sub> and mineralisation/ immobilisation dynamics of N, S and base cations (BC) are not considered in the assessment of a long-term acceptable (critical) load (UN-ECE, 1996). Further assumptions in the SMB model are:

1. negligible N fixation,
2. no NH<sub>4</sub> leaching and
3. negligible reduction and precipitation of SO<sub>4</sub>.

A justification of these assumptions has been given in De Vries (1993).

The SMB model calculates critical loads for the acidifying impact of S and N,  $(S+N)_{id}(crit)$ , according to (De Vries, 1993; UN/ECE, 1996; all fluxes in mol<sub>c</sub> ha<sup>-1</sup> a<sup>-1</sup>):

$$(S + N)_{id}(crit) = BC_{td}^* + BC_{we} - BC_{gu} + N_{gu} + N_{im} + N_{de} + Ac_{le}(crit) \quad (Eq. 4)$$

where  $BC_{id}^*$  is the chloride corrected total deposition flux of base cations,  $BC_{we}$  is a base cation weathering flux,  $BC_{gu}$  and  $N_{gu}$  are the net uptake fluxes of base cations and nitrogen needed for forest growth,  $N_{im}$  is a long-term nitrogen immobilisation flux at critical load,  $N_{de}$  is a denitrification flux at critical N load and  $Ac_{le}(crit)$  is a critical leaching flux of acidity.

A critical load of S and N is thus calculated as the sum of major processes buffering the incoming acidity (net base cation input by deposition and weathering minus growth uptake and net nitrogen removal by growth uptake, immobilisation and denitrification) and an acceptable leaching rate of acidity. The latter flux is determined by the precipitation excess and a critical concentration of acidity. Generally, the load of potential acidity is defined as the load of S and N compounds minus the sea salt corrected wet (bulk) or total deposition of base cations. Here we use the sum of S and N compounds to have a direct comparison with the input of these compounds (Posch et al., 1995a for a discussion of the advantages and disadvantages of different definitions of critical loads of acidity). Use of Eq. 4 implies that various combinations of critical S and N loads are acceptable with respect to acidification effects, as long as the sum of both loads does not give rise to acidity leaching above a critical value (De Vries, 1993; Posch et al., 1993).

In addition to acidification, N deposition may cause adverse effects due to eutrophication of an ecosystem. Critical N loads related to these effects can be

$$N_{id}(crit) = N_{gu} + N_{im} + N_{de} + N(crit) \quad (\text{Eq. 5})$$

calculated according to (De Vries, 1993; UN/ECE, 1996) :

where  $N_{id}(crit)$  is the critical N load with respect to eutrophication and  $N(crit)$  is a critical N leaching flux. Calculation of the critical N load with this simple steady-state model is based on the assumption that any N input above a net N uptake by forest growth, N immobilisation, denitrification and an acceptable rate of N leaching will finally lead to unacceptable high N contents in foliage and soil organic matter, thus causing adverse affects such as nutrient imbalances, increased sensitivity to frost, drought and diseases and vegetation changes.

Until now Eq. 5 has only been applied to calculate critical N loads related to vegetation changes and ground water pollution (e.g. De Vries, 1996b), since information on critical N leaching rates related to these effects are available. Since both effects are not clearly related to the vitality of the forest, such critical loads are less relevant for use in this correlative study between crown condition and stress factors.

In the present study, critical loads were calculated in relation to effects on (i) the understorey of forests (vegetation changes) and (ii) the sensitivity of trees to stress. In deriving critical N loads, related to vegetation changes, a natural low N leaching flux of  $100 \text{ mol}_c \text{ ha}^{-1} \text{ a}^{-1}$  has been used, since vegetation changes may already occur in that situation (Bobbink et al., 1992; 1995). Critical loads for N related to effects on forest vitality were, however, derived by relating the critical N leaching to critical N contents



in foliage (associated with nutrient imbalances and an increased sensitivity to natural stress; e.g. De Vries, 1992, 1993), using data from Tietema and Beier (1995).

The critical N leaching rate was thus set at  $1400 \text{ mol}_c \text{ ha}^{-1} \text{ a}^{-1}$  (Annex 4). Note, however, that the critical N load related to eutrophication aspects may exceed the acceptable critical load of both S and N from an acidification point of view (De Vries, 1993). Empirical data and model results related to nutrient imbalances caused by elevated N deposition indicate a range of  $15\text{-}30 \text{ kg ha}^{-1} \text{ a}^{-1}$  (De Vries, 1992; Bobbink et al. in UN/ECE, 1996), which is generally above the range for critical loads of S and N, except for calcareous soils.

### **6.2.2 Adaptations of the simple mass balance approach**

The major premise of the calculation of a critical load described above, and used in the framework of the UN/ECE, is that it assumes a steady-state situation, that may occur in the future, to derive a long-term acceptable load. In the correlative study between crown condition and stress factors, such a threshold is not very relevant. Instead, we need to know the actual threshold at the time of consideration. This implies that dynamic processes buffering the acid input at present can not be neglected. Furthermore, the rate of such processes may change due to a change in soil chemistry, such as a decrease in base saturation and C/N ratio. In turn this may cause a decrease in the buffering of incoming acidity by release of exchangeable base cations and accumulation of N. Simulation of such processes requires the use of a dynamic model, such as SMART (De Vries et al., 1989). However, since the uncertainty in the considered soil parameters, especially CEC, base saturation and C/N ratio, at each stand is likely to be much higher than the possible change in a 10 year period, we used an intermediate approach as described below. As stated before, this actual threshold was called 'critical deposition level'.

First of all, critical deposition levels were only calculated for soils with a base saturation below 25%. Above this value, all the incoming acidity was assumed to be buffered by base cations only. In fact, in this situation acid deposition causes an increase in the availability in base cation nutrients (Section 7.2). Below this value, Al release is considered to start. Since a critical  $\text{Al}/(\text{Ca} + \text{Mg} + \text{K})$  ratio is the basis for the critical deposition level calculation, only the soils with a low base saturation were thus considered. For the other soils, the critical deposition level was assumed to equal the present deposition level. The base saturation of 25% was based on model simulations (De Vries et al., 1989) and laboratory data (De Vries, 1997) indicating a significant Al release starting in a range between 10 and 25%.

Apart from inclusion of base cation exchange, as indicated above, the calculation of nearly all model inputs in this study differs from the standard application of the SMB model. Instead of using a long-term average value for the calculation of each model input, we considered the time period 1985-1995 in deriving input data, to account for the buffer processes at the time of consideration. More specifically, the differences are



indicated in Table 23. Especially for acidity, the critical deposition level is likely to be higher than the critical acid load. More information on this aspect is given in Section 6.3.2.

*Table 23 Difference in the calculation of critical deposition levels used for policy making (critical load maps in the UN/ECE framework) and those derived for the monitoring plots*

Aspect	Policy making	Level 1 monitoring plots
general	long-term critical loads for grids	actual critical deposition levels for plots (in the considered period 1985-1995)
base cation deposition <sup>1)</sup>	30 a average value	average for 1985-1995
uptake	average during rotation period	actual average uptake for 1985-1995
immobilisation	long-term acceptable value	actual immobilisation for 1985-1995
denitrification	related to critical N load	related to actual average N deposition level for 1985-1995
critical N leaching	related to vegetation changes	related to elevated foliar N contents

<sup>1)</sup> Applies also to precipitation excess, used to calculate critical leaching rates of acidity.

As with the steady-state approach, sulphate adsorption was not considered since input-output budgets for most forest soils in Europe indicate sulphate saturation (Berdén et al., 1987; Van Breemen and Verstraten, 1991; De Vries et al., 1995a). A more detailed description of the calculation of the various inputs is given in Annex 4.

## 6.3 Results and discussion

### 6.3.1 Critical concentration levels for sulphur and nitrogen compounds and ozone and calculated exceedance at the monitoring plots

#### 6.3.1.1 Sulphur and nitrogen compounds

A summary of critical levels for S and N compounds related to acute effects by short-term exposures (one day or less) and to chronic effects by long-term exposures (one year) is given in Table 24.

*Table 24 Critical levels ( $\mu\text{g}\cdot\text{m}^{-3}$ ) for short-term and long-term exposures to  $\text{SO}_2$ ,  $\text{NO}_x$  and  $\text{NH}_3$*

Exposure	$\text{SO}_2$	$\text{NO}_x$	$\text{NH}_3$
Short term <sup>1)</sup>	70	95	270
Long term	20	30	8

<sup>1)</sup> One day except for  $\text{NO}_x$  where it equals four hours

<sup>2)</sup> One year

The critical level values are based upon results of an UN/ECE Workshop on Critical Levels at Bad Hartzburg (UN/ECE, 1989) and on revisions and additions agreed upon at a similar workshop at Egham (Ashmore and Wilson, 1994). An overview is also given in the Manual on methodologies and criteria for mapping critical levels/loads (UN/ECE, 1996)

The critical values are related to adverse effects on all vegetation types, except for  $\text{SO}_2$  where the values refer to forest ecosystems and natural vegetation. Mäkelä and Schöpp (1990) suggested that the critical level for  $\text{SO}_2$  should equal  $15 \mu\text{g m}^{-3}$  in areas where

the effective temperature sum equals 1000 °C days. Note, however, that the calculated summer index is nearly always above this value (Section 4.3.2).

For NO<sub>x</sub> and NH<sub>3</sub>, separate critical levels have not been set for different vegetation classes, because of a lack of information. The sensitivity is, however, thought to decrease according to (semi)natural vegetation > forests > crops. Critical levels are related to both growth stimulation in response to the fertiliser effect of nitrogen and adverse physiological effects at toxic levels. The critical level for NO<sub>x</sub> is based on the sum of NO and NO<sub>2</sub> concentrations. The knowledge to establish separate critical levels is still lacking, even though there is evidence that NO is more phytotoxic than NO<sub>2</sub> (Morgan et al., 1992; UN-ECE, 1995, 1996).

Comparison of the calculated annual average concentrations of SO<sub>2</sub>, NO<sub>2</sub> and NH<sub>3</sub> (Section 5.2.2.1) and the long-term critical levels (Table 24) shows that these levels are only exceeded for SO<sub>2</sub>. Note, however, that the concentration levels for nitrogen oxides in Section 4.3 only refer to NO<sub>2</sub> and not to the sum of NO<sub>2</sub> and NO. In general, NO<sub>2</sub> equals, however, approximately 90% of the NO<sub>x</sub> concentration and the underestimation due to this aspect is likely to be limited. The cumulative frequency distribution of calculated annual average SO<sub>2</sub> concentrations for all the monitoring plots between 1986 and 1995 shows that the critical concentration of 20 µg m<sup>-3</sup> is exceeded in 20% of the cases (Section 5.2.2.1)

Calculated maximum annual average concentrations of NO<sub>2</sub> and NH<sub>3</sub> are near 20 and 2 µg m<sup>-3</sup>, which is lower than the critical levels of 30 and 8 µg m<sup>-3</sup>, respectively. Even though the concentration levels of NO<sub>2</sub> and NH<sub>3</sub> are underestimated (Section 5.2.2.1), it is clear that direct above-ground effects only play a role at certain local circumstances (e.g. near intensive animal husbandry in The Netherlands) but not on a European scale.

### 6.3.1.2 Ozone

Critical ozone levels for forests are based on results from UN/ECE workshops related to this topic in Bern (1993; Führer and Achermann, 1994) and in Kuopio (1996; Kärenlampi and Skärby, 1996). Critical levels for ozone have been defined by the sum of differences between the hourly ozone concentrations in ppb during daylight hours (defined as the period with a global radiation > 50 W m<sup>-2</sup>) and a threshold value of 40 ppb during a certain period (growing season). The inclusion of daylight hours is based on the observation that ozone uptake at night is negligible due to closure of the stomatal pores (Ashmore and Wilson, 1994). This accumulated ozone exposure over a threshold of 40 ppb, called AOT40, is expressed in ppb.hours or ppm.hours.

For forests, a critical AOT40 of 10 000 ppb.h (10 ppm.h) accumulated over a six-month growing season commencing at first of April has been adopted, independent of the three species considered. In this context, the following considerations should be kept in mind (Kärenlampi and Skärby, 1996):



- The value is based on data for beech, since the deciduous trees are considered more sensitive to ozone than coniferous trees, but this may not be true for Scots pine (Steingröver et al., 1995).
- The cut-off concentration of 40 ppb, which is based on a reduction in annual biomass increment, is not an absolute value and an AOT30 may be more appropriate in the Nordic countries. In this case, however, the accumulated dose might include some background ozone (UN/ECE, 1995).
- The use of a six months growing season, starting the first of April is an underestimation for the Mediterranean countries and an overestimation for the Nordic countries (Section 4.2.2, Table 20).

Calculated annual average AOT40 values for O<sub>3</sub> in 1990 (Section 5.3) exceeded the long-term critical AOT level of 10 ppm.h at more than 90% of the monitoring plots. The critical level was exceeded for all deciduous forest stands and at approximately 80% of the coniferous forest stands.

### 6.3.2 Critical deposition levels for sulphur and nitrogen compounds and calculated exceedances at the monitoring plots

#### 6.3.2.1 The eutrophying impact of nitrogen

The overall variation in critical N deposition levels related to the understorey (the possible occurrence of vegetation changes) is comparable to the range in calculated present deposition levels (Fig. 40A). Most values (ca. 90 %) ranged between 100 and 1000 mol<sub>c</sub> ha<sup>-1</sup> a<sup>-1</sup>, which is comparable to the calculated long-term critical N loads derived previously for forest soils in Europe (De Vries et al., 1994). Values are slightly lower than the empirical range of 500-1400 mol<sub>c</sub> ha<sup>-1</sup> a<sup>-1</sup> (7-20 kg ha<sup>-1</sup> a<sup>-1</sup>) reported by Bobbink et al. (1992; 1995).

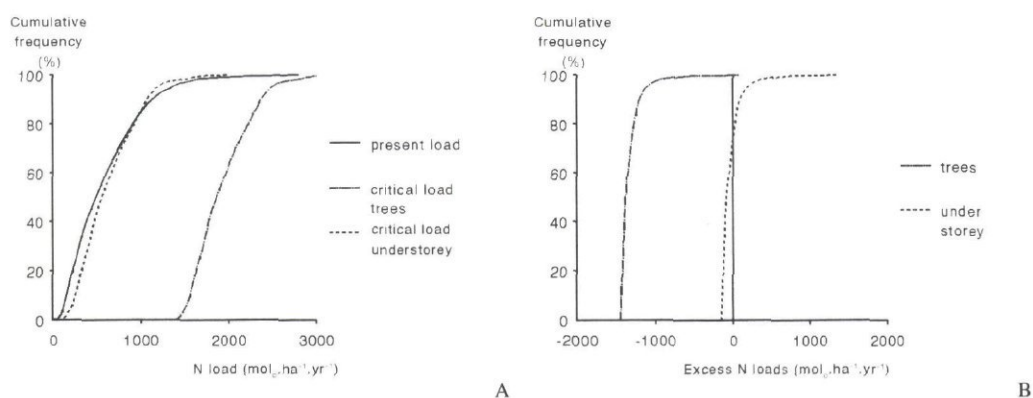


Fig. 40 Cumulative frequency distributions of critical and present nitrogen deposition levels (A) and the difference between present and critical nitrogen deposition levels (B) for all tree species included

The percentage of plots where these critical N deposition levels are exceeded equals 25% (Fig. 40B). The maximum excess equals 1370 mol<sub>c</sub> ha<sup>-1</sup> a<sup>-1</sup>. Critical deposition



levels related to effect on trees are much higher and vary mostly between 1500 and 2500 mol<sub>c</sub> ha<sup>-1</sup> a<sup>-1</sup> or 20-35 kg ha<sup>-1</sup> a<sup>-1</sup>. This coincides with the empirical range of 15-30 kg ha<sup>-1</sup> a<sup>-1</sup> reported by Bobbink et al. (1992; 1995) mentioned before (Section 6.2.1). These values are hardly ever exceeded. The calculated N deposition levels are, however, strongly underestimated in source areas (Section 5.2). Available literature indicate that elevated N deposition is a serious problem in relation to forest condition (e.g. nutrient imbalances, elevated susceptibility to natural stress factors.) in high N deposition areas, which are mainly located in Western and Central Europe (e.g. Boxman et al., 1986; De Visser, 1994).

Critical N deposition levels vary among the five major tree species. In Fig. 41A, this is illustrated for critical N deposition levels related to vegetation changes (critical deposition levels related to tree vitality increase by a constant amount of 1300 mol<sub>c</sub> ha<sup>-1</sup> a<sup>-1</sup> and have thus the same distribution). The highest values were generally calculated for the deciduous tree species, where N uptake is higher due to the higher yields and assumed higher N contents in stemwood for these tree species.

According to the model calculations, N uptake is the most important N removal process followed by denitrification and N immobilisation (Fig. 41B). The calculated N immobilisation was negligible at ca 40% of all plots. This was partly due to the occurrence of soils with a very low C/N ratio, which are assumed to be N saturated. In most cases, however, this was due to the fact that the net N input (N deposition minus N uptake and a natural N leaching rate) was negligible at these plots (Eq. A4-9: the description of N immobilisation). This is reflected by a negligible denitrification at 30% of the plots, since the rate of this process is related to the net N input corrected for net N immobilisation (Eq. A39: the description of denitrification).

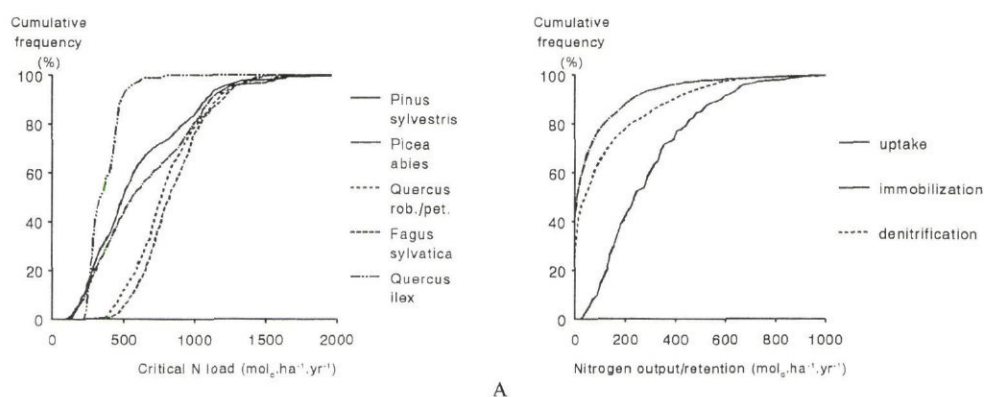


Fig. 41 Cumulative frequency distributions of critical nitrogen deposition levels of the five major tree species (A) and the N output/retention process of all considered tree species (B)

The spatial pattern of critical N deposition levels, related to the occurrence of vegetation changes (Fig. 42) is only partly correlated with the distribution of tree species over Europe. Extremely low critical N deposition levels (below 250 mol<sub>c</sub> ha<sup>-1</sup> a<sup>-1</sup>) occurred in the Northern countries, where tree growth is limited by the extreme climate, whereas high values (> 1000 mol<sub>c</sub> ha<sup>-1</sup> a<sup>-1</sup>) occurred nearly all in Central Europe.

the Northern countries, where tree growth is limited by the extreme climate, whereas high values ( $> 1000 \text{ mol}_c \text{ ha}^{-1} \text{ a}^{-1}$ ) occurred nearly all in Central Europe.

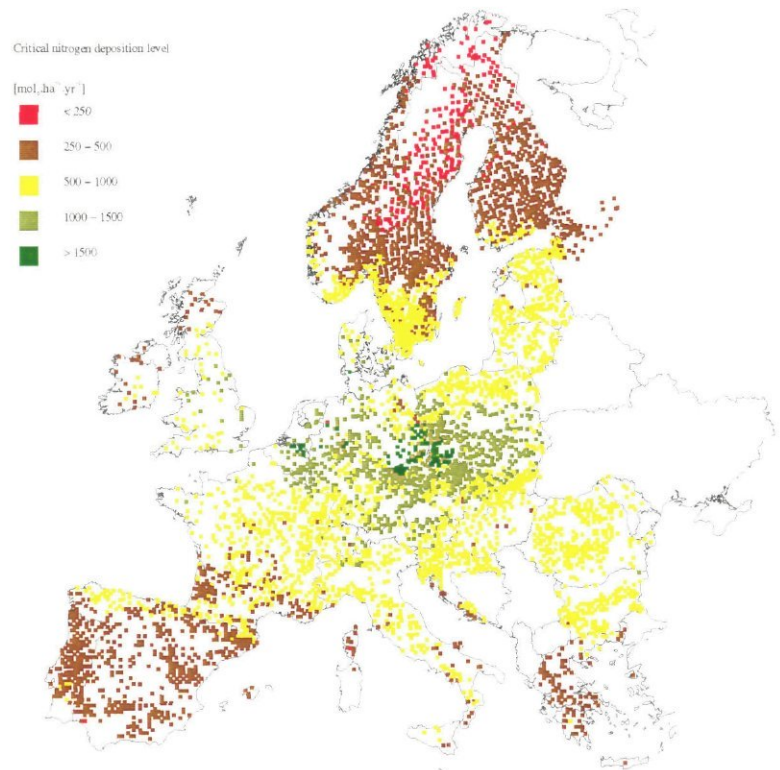
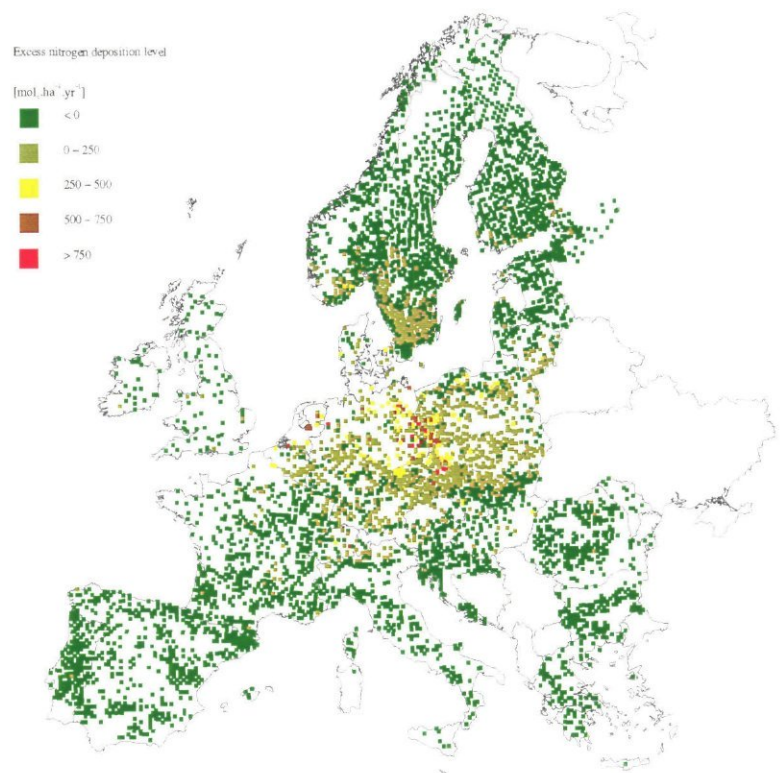


Fig. 42 The calculated 10 years average critical N deposition level related to effects on the forest understorey for all monitoring plots



In this region, N immobilisation and denitrification were enhanced because of the larger input of N from the atmosphere (Compare Fig. 29). The relatively low critical N deposition level in Southern Europe (specifically in Spain) is due to the low uptake of N in these areas by slow growing trees such as *Quercus ilex*. An excess of present N deposition levels over critical N deposition levels mainly occurs in the high N deposition areas in Central and Western Europe (Compare Fig. 43 and Fig. 29).

### 6.3.2.2 The acidifying impact of sulphur and nitrogen

Calculations of critical deposition levels for acidity were limited to stands with a base saturation of less than 25% (Section 6.2.2), covering 42% of all the monitoring plots (Section 3.3.2). The spatial variation of these plots is given in Fig. 9. The overall variation in critical acid deposition levels for all the plots included is almost as large as the variation in present deposition levels (Fig. 44)

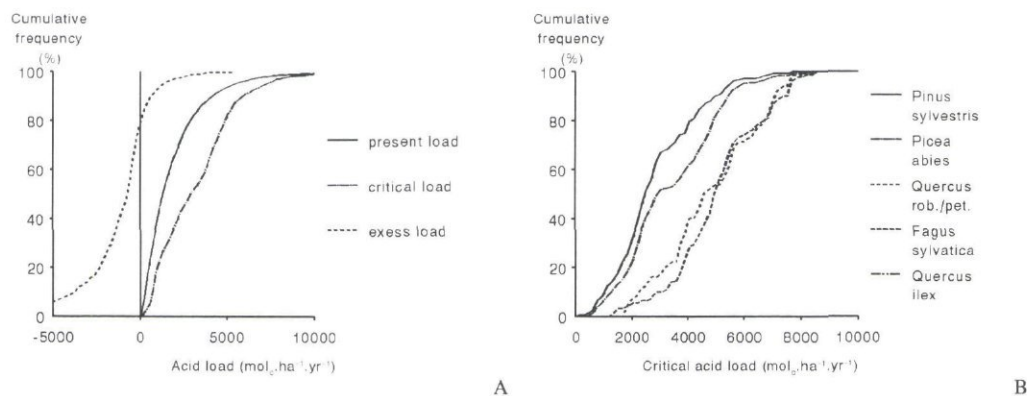


Fig. 44 Cumulative frequency distributions of critical, present and excess acid deposition levels for all tree species included (A) and critical acid deposition levels for the five major tree species (B)

Both present deposition levels and critical deposition levels vary mostly between 1000 and 8000 mol<sub>c</sub> ha<sup>-1</sup> a<sup>-1</sup> (Fig. 44). The area where actual critical deposition levels are exceeded equals only 12%. Note, however, that critical deposition levels for acidity were considered relevant for 42% of the plots. At these plots, critical deposition levels of acidity were thus exceeded in 29% of the cases. The excess of the critical deposition level at these plots varied between 0 and 5400 mol<sub>c</sub> ha<sup>-1</sup> a<sup>-1</sup> (Fig. 44A).

Critical acid deposition levels increase going from the coniferous tree species (*Pinus sylvestris*) to the deciduous tree species (*Quercus robur* + *petraea* and *Fagus sylvatica*; Fig. 44B) This is partly due to the fact that the coniferous trees mainly occur on acidic soils with a low weathering rate in areas where base cation deposition is mostly relatively low. Another important reason is the higher Al/(Ca+Mg+K) ratio used for deciduous trees (1.7) compared to coniferous trees (0.8).



The actual critical deposition levels for the considered 10 year period at the various plots are generally much higher than long-term critical loads derived previously for forest soils in Europe (De Vries et al., 1994a). In comparison to the critical loads given in the CCE reports (Hettelingh et al., 1991; Downing et al., 1993; Posch et al., 1995a) values are even much higher. Major reasons for this are that the official critical load maps (i) include values for both soils and surface waters (especially in Scandinavia), the latter being much lower, (ii) are based on the 5 percentile in a 150 x 150 km<sup>2</sup> grid, instead of the actual values presented on the map in this report, (iii) are derived by using long-term data for the various model inputs, which are generally lower than the actual inputs during the considered 10 year period in this study (especially the values for the base cation deposition are larger in our study) and (iv) are often based on criteria which do not only include a critical Al/base cation ratio, but also a critical Al mobilisation rate to avoid depletion of readily available Al compounds. In practice the critical Al mobilisation, which do not lead to an actual stress on the ecosystem at this moment, appeared to be most limiting (De Vries et al., 1994a).

The high base cation input and the correlated high acidity leaching rate, because of the use of a critical Al/(Ca+Mg+K) ratio, appeared to be the most important cause for the high critical acid deposition levels. This is illustrated in Fig. 45A. N retention processes by uptake, immobilisation and denitrification appeared to be less important. With respect to net base cation input, the deposition generally appeared to be the largest source, followed by weathering. Base cation removal by net uptake was generally much lower (Fig. 45B).

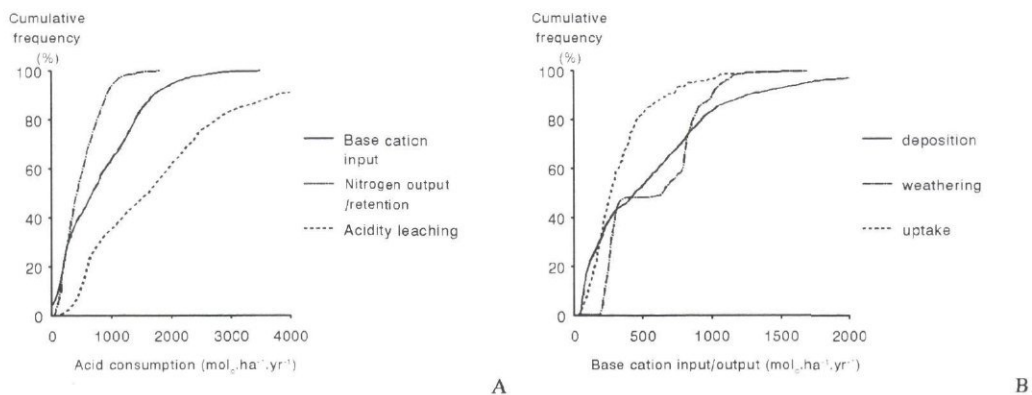


Fig. 45 Cumulative frequency distributions of acid consumption processes (A) and base cation input/output processes (B) for all tree species considered

The spatial pattern of critical acid deposition levels (Fig. 46) correlated with the soils with a low base saturation and with the spatial pattern of base cation deposition and the distribution of tree species over Europe. Extremely low critical acid deposition levels (below 1000 mol<sub>c</sub> ha<sup>-1</sup> a<sup>-1</sup>) were only calculated for Northern Europe. The uniform pattern for critical acid deposition levels in Sweden is due to a similar assignment of weathering rates to the assumed podzolic soil types on the FAO soil map of Europe 1 : 5 000 000. High critical acid deposition levels mainly occur in Southern Europe where base cation deposition is high and deciduous tree species occur more frequently.

1 : 5 000 000. High critical acid deposition levels mainly occur in Southern Europe where base cation deposition is high and deciduous tree species occur more frequently.

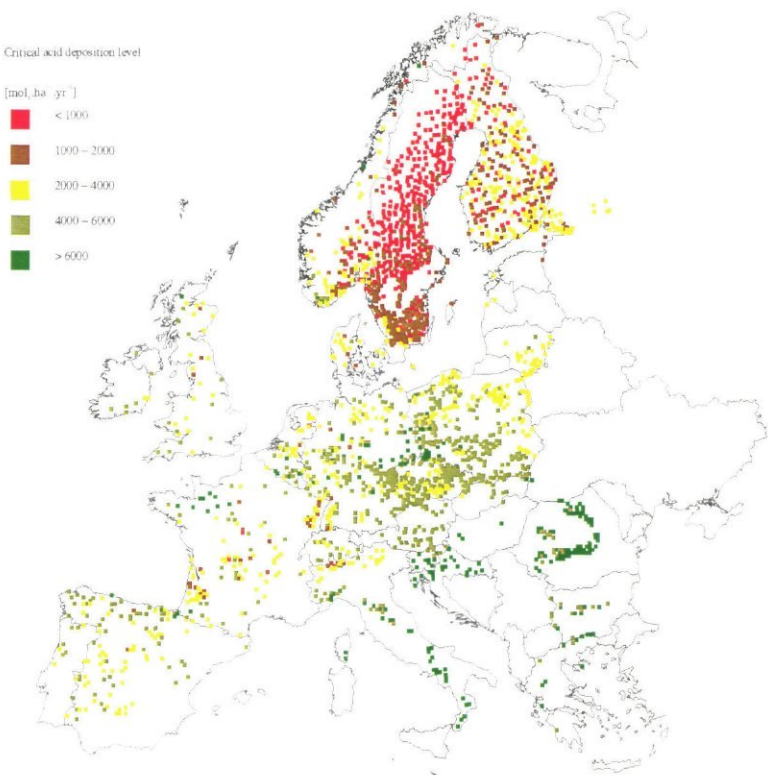
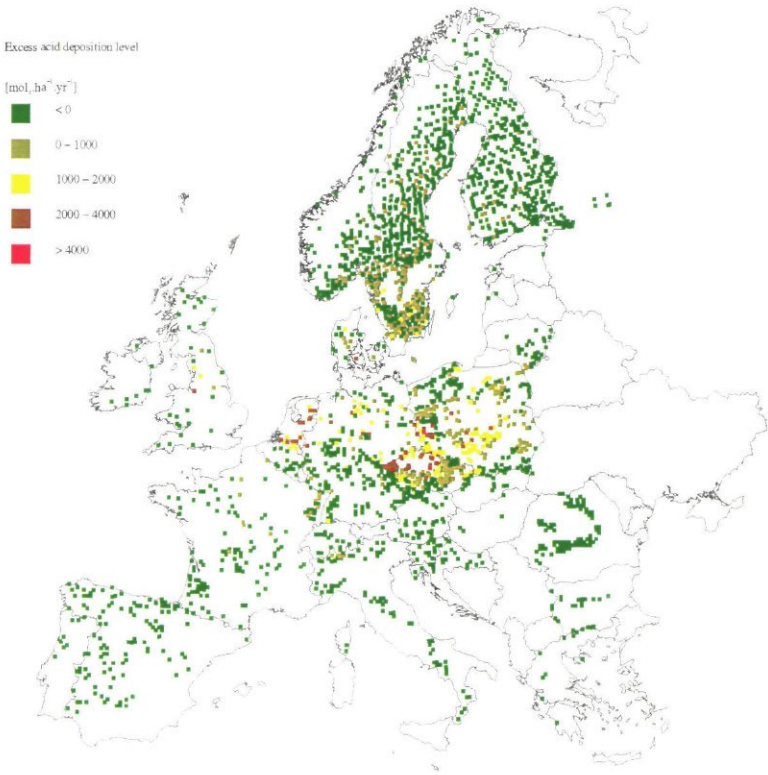


Fig. 46 The calculated 10 years average critical acid deposition level for all monitoring plots





An excess in present acid deposition levels over critical acid deposition levels mainly occurs in Central and Western Europe and the Southern part of Sweden (Fig. 47), where the present atmospheric deposition level for acidity is high (Fig. 30) and the critical acid deposition level is comparatively low (Fig. 46).

## **6.4 Uncertainties**

### **6.4.1 Derivation of critical levels**

There are several assumptions that have been made in deriving critical levels that should be considered to know their usefulness. This includes: (i) the accepted proof of a linkage between a pollutant and specific adverse effects, (ii) the differentiation between short-term and long-term exposures, (iii) the effects of pollutant combinations and (iv) the influence of environmental modification factors, such as temperature and water availability, as discussed below.

#### ***Accepted proof of a linkage***

Establishing critical levels for pollutants, based on an absolute proof of a linkage between pollutant substance and specific adverse effects, include (i) proof of a relationship between cause (pollutant substance) and effect (damage to vegetation), (ii) quantification of this relationship by means of dose-response functions, and (iii) understanding of the internal processes mediating the relationship and of the external and internal factors influencing it. The usefulness of the application of Koch's postulates (Last et al., 1984) is, however, limited to constellations where monocausal, qualitative, usually acute, effects are being investigated. This is not the case with respect to the direct effects of air pollution on forests. These values are based on, so-called, dose-response functions using statistical methods, such as regression curves, to extrapolate dose-response findings in a restricted range of concentrations.

#### ***Short-term and long-term exposures***

Optimally, critical levels should be established for the whole range of possible exposure duration, but practical considerations have made it necessary to concentrate on the two extremes: 'acute' effects of short-term exposures to high pollutant concentrations (episodes) lasting 24 hours or less, and 'chronic' effects of long-term exposures to relatively low concentrations over longer periods (a growing season or a year).

#### ***Effects of pollutant combinations***

Critical levels for one pollutant have been set in the context of the pollutant mixture. Available experimental results show that pollutant combination effects are mainly additive (sum of individual pollutant effects) or synergistic (more than additive). Synergism is specifically known to occur between  $\text{NO}_x$  and other pollutants, such as  $\text{SO}_2$  and  $\text{O}_3$  (e.g. Ashmore and Wilson, 1994). At an UN-ECE sponsored workshop on critical levels at Egham in 1992, it was for example concluded that elevated  $\text{NO}_x$  concentrations alone are generally not sufficiently toxic to affect plants. The definition



of the critical level thus assumes that SO<sub>2</sub> and O<sub>3</sub> are present at concentrations close to their critical level (Ashmore and Wilson, 1994).

#### ***Influence of environmental modification factors***

Finally, it is well known that especially climatic circumstances may effect the critical levels of air pollutants. It is suggested that critical levels for SO<sub>2</sub> should be corrected downwards when the effective temperature sum is very low (Mäkelä and Schöpp, 1990) and that critical ozone levels should be corrected for soil moisture availability and air temperature. At present, however, these effects are not considered in establishing a critical level (UN-ECE, 1996).

Regarding the calculated exceedances of critical levels, it is clear that the results are affected by the uncertainties in the calculated concentration levels for SO<sub>2</sub>, NO<sub>2</sub> and NH<sub>3</sub> (Section 5.2.3.1). The underestimation for the concentration levels for N compounds means that the negligible excess at all monitoring plots is questionable. This is specifically true for NO<sub>2</sub>, where the calculated maximum concentration nearly equals the critical level. For NH<sub>3</sub>, it is unlikely that there are stands where the critical level is exceeded, since the value is approximately four times as high as the calculated maximum concentration level.

### **6.4.2 Calculation of critical deposition levels for nitrogen**

The uncertainty in the calculated critical N deposition levels derived above can be large due to uncertainties in the assumed critical N leaching rates in relation to effects, model assumptions and input data (Sverdrup et al., 1990; De Vries, 1991).

#### ***Criteria***

The choice of the critical N leaching rate strongly affects the critical deposition levels of N. The nearly negligible N leaching rate that was taken to calculate critical N deposition levels related to vegetation changes might not be appropriate in certain situations.

Empirical data on vegetation changes in forest (e.g. Bobbink et al., 1992; 1995) show that the critical N deposition levels are slightly lower, although the results are in a similar order of magnitude. The same is the case with the critical N deposition levels related to effects on trees. Assuming an uncertainty in the critical N leaching rate of 50% , the resulting uncertainty in critical N deposition levels will be in the same order of magnitude.

#### ***Model structure***

Uncertainties related to the description of N dynamics in the SMB model (cf the assumptions and description of the model in Section 6.2.1) result from (i) neglecting N fixation which is important for trees such as red alder, (ii) neglecting NH<sub>4</sub> fixation which may play a role in clay soils, (iii) assuming that nitrification is complete, while it is likely to be inhibited at high C/N ratios, (iv) the simple description of net N

immobilisation as a function of net atmospheric N input and the C/N ratio, while the carbon pool in the soil is fixed (Annex 4, Eq. A 4-9) and (v) neglecting the interaction between net N uptake and a change in soil conditions (De Vries et al., 1994b). However, considering the uncertainty in present uptake estimates this aspect is likely to be unimportant.

Even though the dynamics of the N transformation processes is strongly simplified, the resulting fluxes for denitrification and denitrification seem plausible in view of available data on these processes for forest soils (De Vries et al., 1994a).

### ***Input data***

Assuming that the model structure is correct, the effect of the uncertainty in the input data can directly be quantified. The most important input parameter is the net uptake, which is affected by the interpolated yield values and the assumed N contents in stemwood. Comparison between model inputs used in a previous study carried out at a European scale and values derived in various individual countries indicated that the overall uncertainty in N uptake was generally less than 50%, although it can be more than 100% at specific plots (De Vries et al., 1994a). Consequently, considering the previously mentioned uncertainty in critical N leaching rates, the resulting uncertainty will also vary mostly within this range.

## **6.4.3 Calculation of critical deposition levels for acidity**

As with nitrogen, the critical acid deposition levels, that were derived by applying the SMB model, are subject to (large) uncertainties due to the uncertainties in the assumed critical  $Al/(Ca+Mg+K)$  ratios in relation to effects, model assumptions and input data.

### ***Criteria***

First of all the reliability of the calculated critical deposition levels for acidity might be questioned, because of great uncertainties in critical values for the  $Al/(Ca+Mg+K)$  ratio, related to direct toxic effects of Al. This is mainly due to a lack of knowledge about the effects of Al in the field situation. Values are mainly based on laboratory experiments and the applicability in the field situation seems often limited. The uncertainty is also partly due to a natural range in the sensitivity of various tree species for Al toxicity (Sverdrup and Warfvinge, 1993). Note also that we used critical annual average values whereas the temporal variation can be large, with peak values in the summer.

Exceedances of critical deposition levels are thus much better correlated with the occurrence of vegetation changes in forests (e.g. Van Dobben et al., 1994) than with forest damage (e.g. Hendriks et al., 1994), even though there are indications for such relationships, (Lenz and Schall, 1991 and Nelleman and Frogner, 1994 for forests in Germany and Norway, respectively). Regarding critical acid deposition levels, the  $Al/(Ca+Mg+K)$  ratio may be irrelevant for peat soils, since Al mobilisation hardly



occurs in these soils. When one wants to avoid a decrease in base saturation or pH, the critical acid deposition level is likely to be much lower.

### ***Model assumptions***

Uncertainties in the model structure relate to the assumptions made. First of all the use of a simple mass balance model, limited to abiotic effects on the soil only, is questionable. The development of multi-stress models, including interactions of desiccation, acidification and eutrophication on forests and effects of drought, pests and diseases, are necessary to support the results of such simplified models. A first comparison of critical deposition levels for a Norway spruce stand in Solling (Germany), derived with integrated forest-soil models and simple mass balance models seems promising in this context (De Vries et al., 1995b).

An important assumption in the SMB model is the assumed homogeneity of the rootzone both in a horizontal and vertical direction. Use of a one-layer model such as SMB implies that the critical  $Al/(Ca+Mg+K)$  ratio used refers to the situation at the bottom of the rootzone, whereas most roots occur in the topsoil. Values for the  $Al/(Ca+Mg+K)$  ratio generally increase with depth due to Al mobilisation, BC uptake and transpiration.

Another uncertainty related to model structure is the calculated increase in critical deposition level with an increased precipitation excess due to an increase in the calculated critical rate of H leaching. Using a semi-quantitative method, Kuylensstierna and Chadwick (1989) assumed that an increase in the precipitation excess causes a decrease in the critical acid deposition level for European forest soils. The rationale behind their approach is that the exchangeable base cation pool of soils is depleted more rapidly in areas with a high precipitation excess. The rationale behind the SMB model is that it is acceptable that an ecosystem comes in the Al buffer range as long as the  $Al/(Ca+Mg+K)$  ratio remains below a critical value. When using a critical value for the Al concentration (e.g. De Vries et al., 1994), an increased precipitation excess largely increases the critical deposition level due to dilution of the mobilised Al. When using an Al/BC ratio criterion, however, the critical Al leaching rate is not affected by the precipitation excess, since BC is diluted as well and the effect is much less pronounced.

Other assumptions in the SMB model such as (i) disregarding  $SO_4$  interactions, (ii) neglecting complexation of Al with inorganic and organic anions and (iii) a very simple hydrology are likely to be less significant. First, most European forest soils are  $SO_4$ -saturated. Second, complexation of Al with inorganic anions such as  $SO_4$  and OH only causes a small increase in the total inorganic Al concentration in the soil solution. Disregarding organic acid as a source of acidity is not likely to have a significant effect on the concentration of inorganic Al since it mainly causes formation of non-toxic organically complexed Al. Third, ignoring surface runoff and preferential flow likely has a small effect since both water and ions are removed from the soil in situations where this occurs (De Vries et al., 1994b).



### ***Input data***

Assuming that the model structure is correct, the effect of the uncertainty in the input data can directly be quantified. Comparison between model inputs used in a previous study carried out at a European scale and values derived in various individual countries indicated that the overall uncertainty of most model inputs (weathering, uptake, N retention processes and precipitation excesses) was generally less than 50%, although it can be more than 100% at specific plots (De Vries et al., 1994). At plots where the soil type has been derived by interpolation (e.g. all plots in Sweden), the uncertainty of the soil related model inputs (all inputs except the base cation deposition) is not only affected by the inherent uncertainty in the estimate itself, but also by the uncertainty (reliability) of the soil map. Assuming that a similar uncertainty is associated with the present model inputs, it is likely that the uncertainty in the calculated base cation input by deposition and weathering, combined with the uncertainty in Al/(Ca+Mg+K) ratio, which affects the associated acidity leaching, has the largest effect on the calculated critical acid deposition level. Even though the calculated precipitation excess may be too large, the effect on the critical deposition level is limited as discussed above. The overall uncertainty in critical acid deposition levels likely varies between plus or minus 50%.

## **6.5 Conclusions**

In view of the aims stated in Section 6.1. the following conclusions can be made :

1. Calculated annual average SO<sub>2</sub> concentrations between 1986 and 1995 often exceeded the critical concentration of 20 µg.m<sup>-3</sup>. Exceedances varied between years with an average of 20% of the level 1 plots during the considered 10 year period. These plots are concentrated in Central Europe, such as Germany, Poland and Czech Republic. Calculated maximum annual average concentrations of NO<sub>2</sub> and NH<sub>3</sub> were 27 and 3 µg m<sup>-3</sup>, which is lower than the critical levels of 30 and 8 µg m<sup>-3</sup>, respectively. Even though the calculated concentration levels of NO<sub>2</sub> and NH<sub>3</sub> are underestimated, it is clear that direct above-ground effects only plays a role at certain local circumstances but not on a European scale. Calculated annual average AOT40 values for O<sub>3</sub> in 1990 (Section 4.3) exceeded the long-term critical AOT level of 10 ppm.h at more than 90% of the monitoring plots. The critical level was exceeded for all deciduous forest stands and at approximately 80% of the coniferous forest stands.
2. The range in calculated critical N deposition levels related to the possible occurrence of vegetation changes in the forest understorey was comparable to the range in calculated present N deposition levels. Values varied mostly (ca. 90 %) between 100 and 1000 mol<sub>c</sub> ha<sup>-1</sup> a<sup>-1</sup>, which is slightly lower than an empirical range of 500-1400 mol<sub>c</sub> ha<sup>-1</sup> a<sup>-1</sup>. The percentage of plots where these critical N deposition levels are exceeded equals 25%. The maximum excess equals 1370 mol<sub>c</sub> ha<sup>-1</sup> a<sup>-1</sup>. Excess deposition levels mainly occur in Central and Western Europe, such as Germany, Poland, the Czech Republic and The Netherlands, where present

deposition levels are highest. It is unclear, however whether the changes in forest understorey (ground vegetation) are related to crown condition effects.

3. The range in calculated critical N deposition levels related to effects on trees, such as nutrient imbalances and increased susceptibility to drought, frost and diseases/pests was much higher than those related to vegetation changes. Values varied mostly between 1500 and 2500 mol<sub>c</sub> ha<sup>-1</sup> a<sup>-1</sup> or 20-35 kg ha<sup>-1</sup> a<sup>-1</sup>, which coincides with an empirical range of 15-30 kg ha<sup>-1</sup> a<sup>-1</sup>. These values are hardly ever exceeded. The calculated N deposition levels are, however, underestimated in some areas. In these areas, occurring mainly in Central and Western Europe, it is well known that N deposition plays an important role in affecting forest vitality.
4. Calculated critical deposition levels for acidity, which were limited to stands with a base saturation of less than 25% covering 42% of all the monitoring plots, varied in the same range as the calculated present deposition levels. Both present deposition levels and critical deposition levels varied mostly between 1000 and 8000 mol<sub>c</sub> ha<sup>-1</sup> a<sup>-1</sup>. The number of plots where critical acid deposition levels are exceeded equalled 12% of all plots and 29% of the plots where base saturation was below 25%. The critical deposition level excess at these plots, which are mainly located in Central and Western Europe varies between 0 and 5400 mol<sub>c</sub> ha<sup>-1</sup> a<sup>-1</sup>.
5. The excess of actual critical deposition levels on the level 1 plots is much lower than the excess of long-term critical deposition levels, since the official maps (i) include values for both soils and surface waters, the latter being much lower, (ii) are based on the 5 percentile in a 150 x 150 km<sup>2</sup> grid, instead of actual values, (iii) are derived by using long-term data for the various model inputs, which are generally lower than the actual inputs used in this study and (iv) are often based on criteria that avoid long-term deterioration, which lead to lower loads than criteria related to actual stress.
6. The uncertainty in the calculated critical deposition levels for nitrogen and acidity derived above can be large due to uncertainties in the assumed values for critical N leaching rates or critical Al/(Ca+Mg+K) ratios in relation to effects, model assumptions and input data. High critical N-deposition levels in central Europe, for example, may be biased by the description of N-immobilisation as a function of N-input. On average the uncertainty likely varies between plus and minus 50%.
7. The uncertainty in critical deposition level exceedances, which is affected by uncertainties in both present deposition levels and critical deposition levels, can be very high. The calculated high exceedances in central Europe are, however, quite reliable considering air pollution measurements in this area.



## 7 Relationships between crown condition and stress factors

Jaco Klap<sup>1)</sup>, Jan Oude Voshaar<sup>2)</sup>, Wim de Vries<sup>1)</sup>, Jan Willem Erisman<sup>3)</sup>

<sup>1)</sup> DLO Winand Staring Centre (SC-DLO), Wageningen, The Netherlands

<sup>2)</sup> Centre for Biometry Wageningen (CBW), Wageningen, The Netherlands

<sup>3)</sup> National Institute of Public Health and the Environment (RIVM), Bilthoven, The Netherlands

### 7.1 Introduction

#### **Statistical method**

This chapter focuses on the relationship between the observed crown condition (response variable) of five major tree species (*Pinus Sylvestris*, *Picea abies*, *Quercus robur* and *Q. petraea*, *Fagus sylvatica* and *Quercus ilex*; cf. Section 1.2), as described by defoliation, and influencing parameters (predictor variables) such as stand and site characteristics, natural meteorological stress and anthropogenic stress by air pollution (Chapter 1: short overview). This relationship was investigated using multiple regression analyses. Relatively simple statistical methods and techniques were used to explore the available crown condition monitoring data during 10 years at the Level 1 plots in relation to the available stand and site characteristics and the modelled stress factors. In a later more comprehensive study, additional tree species will be included, and information on the foliar composition will be used in the statistical analysis (both as an effect parameter and a stress factor). In that consecutive study, the statistical methods to analyse possible relationships will be extended to more advanced techniques (Section 7.2.1).

#### **Response variables: crown condition**

The crown condition is described by the degree of defoliation and discoloration (Chapter 2). In this pilot study the response variables for each of the five considered tree species were limited to three defoliation measures, namely : (i) the average current year defoliation at each plot, (ii) the change in the average defoliation compared to the observation in the previous year and (iii) the average estimated trend in defoliation during the observation period, using all observations for the same plot. The change and the trend in defoliation were added as response variables to accommodate for the effect of country on the observed defoliation due to (i) different standards for the reference trees to which defoliation is related and (ii) systematic observer variation between countries (Section 6.2.2).

#### **Predictor variables: stress factors**

The predictor variables that have been considered in this pilot study were limited to those described in the preceding chapters. The predictor variables thus include time-independent (constant) site and stand characteristics as given in Chapter 3, and time-dependent modelled data on meteorological variables (Section 4.2) and air pollution and atmospheric deposition (Sections 4.3 and 4.4). In the latter case, the exceedance of critical thresholds (critical deposition/concentration levels) were also used as predictor variables (Chapter 5). The possible impact of the time-dependent predictor variables

was extended with possible 'lagged' effects years after the occurrence of certain events. Furthermore, the annual deviation of the modelled time-dependent meteorological stress factors from the mean values in the considered 10 year period were used as predictor variables (Section 6.2.3). In this pilot study, the three response variables were correlated with various subsets of predictor variables as indicated above (Section 6.2.4).

### ***Aims and contents of Chapter 6***

Major aims of the statistical analysis were:

- The derivation of the most important predictor variables explaining the variation in observed defoliation and in defoliation changes, while neglecting correlations of repeated observations at the same site (focus on spatial patterns).
- The assessment of the most important predictor variables explaining systematic trends in the defoliation figures.
- The assessment of the relative impact of stand and site characteristics, natural meteorological stress and anthropogenic stress variables (air pollution) in each of the above-mentioned models.
- The exploration of the data base in such a way that the difference in reference trees (assessment methods) for crown condition in the different countries can be accounted for.

This chapter first gives a more detailed overview of the methodological approach (Section 7.2). More information on the statistical method that was used is given in Section 7.2.1. Detailed information on the response variables considered and their advantages/ disadvantages is given in Section 7.2.2. Section 7.2.3 gives in-depth information on the predictor variables considered, including lagged effects, correlations and interactions between and thresholds for variables. Alternative models correlating differently defined defoliation parameters with different sets of predictor variables, with their merits are given in Section 7.2.4. Section 7.3 gives an overview of the results, including an analysis of the correlation between the predictor variables (Section 7.3.1) and the results for the three main statistical models (Sections 7.3.2-7.3.5). Finally the main conclusions are summarised (Section 7.4).

## **7.2 Methodological approach**

### **7.2.1 Statistical method**

#### **7.2.1.1 Regression model**

The most direct way to investigate these relations is building regression models for the responses defoliation and discolouration that contain all predictor variables that affect this response. In this large-scale Pan-European study the effects of e.g. air pollution can only be estimated or tested properly, if all other relevant effects are taken into account. Omitting relevant predictors would decrease the precision of the estimates of the effects of the remaining predictor variables considerably, and result in a lower power of the



tests. Moreover the estimates may not be interpreted properly due to confounding of predictors (caused for example by the correlation between predictor variables).

Within the regression model the effect of each predictor variable was tested by deleting it from the model. When this deletion diminished the model explanation significantly, then the effect of the predictor variable (stress factor) was called 'significant'. Successive deletion of non significant terms (backward elimination) was a popular method of predictor selection in the last decades. Also variants like forward selection and step-wise selection of the 'best model' were popular. However, since predictor variables may be exchangeable, there may be more than one 'best' model. Therefore a more thoroughly search procedure (all possible subset selection) was used to trace alternative models.

Because the response variable defoliation varies on a limited scale (0-100%), a logit transformation (Eq. 6) was performed to make a meaningful use of linear and additive effects.

$$\text{logit}(\text{defoliation}) = \text{Ln} \left( \frac{\text{defoliation}}{1 - \text{defoliation}} \right) \quad (\text{Eq. 6})$$

where:

defoliation = the defoliation on the scale between 0 and 1 (i.e. percentage / 100)

This formula was not capable to handle the values 0 % (= not defoliated) and 100% (= dead). Therefore these values were treated as 1.0 % and 99.9 %, respectively (the value 99 % was already reserved for trees that were completely defoliated but not dead). The fitted models were of the type of Eq. 7.

$$\text{logit}(\text{defoliation in year } t) = f_1(\text{site}) + f_2(\text{stand age}) + f_3(\text{drought}) + f_4(\text{temperatures}) + f_5(\text{deposition}) + f_6(\text{air pollution}) + f_7(\text{country}) + f_8(\text{species}) \quad (\text{Eq. 7})$$

where:

site	= parent material, altitude, permanent/measured soil characteristics, etc
drought (Ret)	= moisture deficit in year t, t-1, t-2+
temperatures	= temperature stress parameters in year t, t-1, t-2+
deposition	= deposition of nitrogen and acidity in year t, t-1, t-2+
air pollution	= concentration SO <sub>2</sub> , NO <sub>2</sub> , NH <sub>3</sub> and O <sub>3</sub> in year t, t-1, t-2+
country	= country is included to accommodate for different use of reference trees (Section 7.2.2)
species	= tree species, in the case two or more species are analysed together

Apart from the average current year defoliation at each plot, the change in the average defoliation compared to the observation in the previous year and the average estimated trend in defoliation during the observation period were used as response variables (Chapter 2 and Section 7.2.2).

Regression models were fitted for each tree species separately, since the effect of many predictors may differ for species. The analysis of many species together would need the use of many interaction terms, which would contain a risk of misinterpretations. The results for *Quercus robur* and *Quercus petraea* were analysed together, using a limited number of interactions between meteorological variables and tree species as additional predictor variables (Section 1.2).

The use of the 'complete' model was only possible for sets (mostly of one species) with sufficient observations. Oude Voshaar (1994) states, as a rule of thumb, that the maximum number of degrees of freedom used by the predictor variables should not exceed  $0.25 \times$  the number of observations. This percentage should even be lower when predictors are only roughly estimated or when temporal and spatial correlations are expected. (Section 7.2.3). Sometimes, the number of predictor variables had to be limited in order to satisfy this limitation. The choice of the tree species selected for this study was also based on this limitation. The calculations were carried out with the statistical computer program GENSTAT.

#### **7.2.1.2 Temporal and spatial correlations**

Temporal and spatial correlations are an important aspect of the analysis of data from a dense gridnet with repeated observations on the same site (longitudinal data). Examples of such models are described by Baessler (1995) and Liang and Zeger (1986). These models exploit two types of information that the data contain on the effects of air pollution:

- effect of different stress factor values on different locations,
- effect of different stress factor values in different years within locations (the longitudinal aspect).

Within this pilot study, the correlations within these two types of information were not fully exploited, due to lack of time and the fact that the essential parts of the software were still under development. However, the temporal aspect of repeated observations at the same plot was preliminarily accounted for in some of the selected models (Section 7.2.4).

#### **7.2.1.3 Data set used**

In principle all available reliable observations were used, including the continuous increase in the number of plots in the monitoring programme. The total number of plots increased from about 1100 in 1987 to about 5400 in 1995. The total number of plots which have been assessed at least once is 5843, which is more than the 1995 assessment because some plots were abandoned within the considered time period, or were not assessed in 1995 for other reasons. This means that there is a large variability in the length of the time series, which may be aggravated by the occurrence of missing years within the time series for a considerable number of plots (Chapter 2). In the



applied regression model, however, the analysis of locations with unequal time series did not cause limitations in the derivation of relationships between response and explaining variables. Therefore, the stress factors were derived for all 5843 locations. Since the analyses were done per tree species, the actual number of plots in each separate analysis was much smaller than 5843. Although the number of observations on defoliation is small in the first years, the inclusion of these years is considered useful to:

- cover a wider range of combinations of stress parameters and
- have longer time series for at least part of the plots.

The first year of defoliation data included in the analysis was 1988. The data base with defoliation data contains also data for the year 1987. The data for this first year were left out from the analysis for reasons explained in Chapter 2. The model was adapted to cope with changes in the methodological approach within a country (as occurred in the UK between 1991 and 1992).

### **7.2.2 Response variables considered**

In the pilot study the response variable (effect parameter) for each of the five considered tree species was limited to three defoliation measures, namely: (i) the average actual defoliation at each plot, (ii) the change in the average defoliation compared to the observation in the previous year and (iii) the average estimated trend in defoliation during the observation period (Chapter 2). In the first two cases, the number of trees per species at each plot was used as weights in the regression analysis, whereas the number of years, minus 1, for which forest condition data were available for each plot was used as weight for the analysis of trends. The ‘observational units’ in the analysis were plot-year combinations for the analysis of current year defoliation and changes in defoliation, whereas the units were plots for the analysis of trends.

In the analyses we used, however, average values for each tree species at the plot, since no information is available on the difference between predictor variables on the individual tree level at which the data are assessed. The calculation of average values for the current defoliation and of the change and trend in defoliation was done after the logit transformation of the observed values for the individual trees (Chapter 2). The effect of using mean logit- transformed data instead of logit-mean values (by first averaging the results per plot and then transforming this figure) and the differences with the mean value of non-transformed data was investigated for one of the models. Other defoliation values that may be used in the analysis, such as median values (or other percentile values) or a percentage of trees above or below certain critical values, will be investigated in the comprehensive study.

In an analysis of the actual defoliation differences between countries should be accounted for, since different reference trees are used to determine the degree of defoliation (Chapter 2). In case of an absolute reference tree, the reference tree is constant in the whole country (or part of a country), but this reference may differ between countries. A relative (locally defined) reference tree is intended to correct the

defoliation for non-optimal values of some factors (e.g. altitude, age, parent material). This correction is, however, subjective and may differ per country. Furthermore, there may be a systematic 'observer variation' between countries (Chapter 2). A consequence of the use of different reference trees is that the response variable (defoliation) is not directly comparable between countries. A country effect was therefore included in the model to accommodate for these differences. These country differences can be regarded as shifts on the measurement scale of the (logit of the) defoliation (Section 7.2.3). Due to these country effects, in fact only the information from different locations within countries is exploited.

Models for the actual defoliation (Section 7.2.4) are successful when the within-country ranges of the predictor variables are large enough to estimate their regression coefficients. In that case the country differences can be estimated simultaneously. When the within-country ranges of the predictor variables are, however, small, they are confounded with the predictor 'Country'. In this case the effects of the relevant predictors and the country differences can not be estimated accurately. Since at least partial confounding was expected, we tried to circumvent this problem by also analysing the change in defoliation (Model B) and the trend in defoliation (Model C). In this situation the effects of different reference trees is likely to be very small (Section 2.3.2 of Part A of the 10 Years Overview Report; UN/UN-ECE, 1997). These models might be successful if besides the actual defoliation also the change or trend respond to the predictor variables. The presumed advantages and disadvantages of the use of changes and trends as response variable were already summarised in Table 1 in Chapter 2.

### **7.2.3 Predictor variables included**

Table 25 gives an overview of all predictor variables (key stress factors) included in the model with their degrees of freedom. The table also gives information on: (i) the temporal aggregation and lagged effects of stress factors, (ii) the interactions between effects of different predictor variables and (iii) the occurrence and use of threshold values of the stress factors considered. These aspects, including the possible correlations between predictor variables are discussed below.

#### **7.2.3.1 Key factors considered**

Stand and site characteristics included are stand age, water availability class, altitude and soil class, since their influence on forest condition is known to be important (Table 25). Soil classes were defined on the basis of their parent material (including their organic matter, clay and carbonate content) according to the clustering used to present soil data results (Chapter 3) and to calculate weathering rates for soils (Chapter 6). Apart from these characteristics, the country was also included as a separate (geographical) factor in the analysis when the actual defoliation is used as effect parameter (Section 7.2.2). These country differences (scale shifts in defoliation



measurements) can be estimated from the data if these differences are not confounded with other predictors in the regression model (compare Section 7.2.2).

*Table 25 Overview of predictors used in the statistical model, with their temporal aggregation, the possible use of threshold values the inclusion of lagged effects and interactions, with their degrees of freedom*

Key factor	Temporal aggregation <sup>1)</sup>	Unit	Threshold value <sup>2)</sup>	Main effect	Lagged effects	Degrees of freedom
Country	-	-	-	+	-	30 <sup>3)</sup>
Tree species <sup>10)</sup>	-	-	-	+	-	<sup>10)</sup>
Stand age	-	years	-	+	-	1 <sup>4)</sup>
Altitude	-	m	-	+	-	1 <sup>4)</sup>
Drainage status	-	[class]	-	+	-	3
Soil Class <sup>5) 6)</sup>	-	[class]	-	+	-	4
Soil C/N ratio <sup>6)</sup>	-	g g <sup>-1</sup>	-	+	-	1
Soil pH <sup>6)</sup>	-	[ ]	-	+	-	1
Base saturation <sup>6)</sup>	-	%	-	+	-	1
Rel. Transpiration	Day→Grow.Seas.	%	-	+	+	3
Winter index	6h,Day→Winter	°C days (<0)	+ <sup>7)</sup>	+	+	3
Late frost	6h,Day→Spring	°C (min<0)	+ <sup>7)</sup>	+	+	3
Heat index	6h,Day→Summer	°C day (max>35)	+ <sup>7)</sup>	+	+	3
Summer index	6h,Day→Gr.Seas.	°C day (>5)	+ <sup>7)</sup>	+	+	3
Air SO <sub>2</sub> conc.	Day→Year	mg m <sup>-3</sup>	20 mg m <sup>-3</sup>	+	+	3
Air NO <sub>2</sub> conc.	Day→Year	mg m <sup>-3</sup>	30 mg m <sup>-3</sup>	+	+	3
Air NH <sub>3</sub> conc.	Day→Year	mg m <sup>-3</sup>	8 mg m <sup>-3</sup>	+	+	3
Air O <sub>3</sub> conc.	Day→Gr.Seas./ a.	Ppb	40; 10 pmh <sup>8)</sup>	+	+	3
N deposition	Day→Year (sum)	mol <sub>c</sub> ha <sup>-1</sup> a <sup>-1</sup>	(+) <sup>9)</sup>	+	+	3
Acid deposition	Day→Year (sum)	mol <sub>c</sub> ha <sup>-1</sup> a <sup>-1</sup>	+ <sup>9)</sup>	+	+	3
<i>Interaction terms:</i>						
Rel. Transp. * O <sub>3</sub>	(yearly value)		-	+	+	3
Summer Index * O <sub>3</sub>	(yearly value)		-	+	+	3
Rel. Trans. * Acid	(yearly value)		-	+	+	3
Sum. Index * Acid	(yearly value)		-	+	+	3
Acid Dep * Bas. Sat.	(yearly value)		-	+	+	3
N dep. * Winter Index	(yearly value)		-	+	+	3
N dep * Late frost	(yearly value)		-	+	+	3
<i>Total degrees of freedom (maximum)</i>				<u>60</u>	<u>36</u>	<u>96</u>

<sup>1)</sup> When the temporal aggregation is left blank, then these data are fixed characteristics or are only measured in one year.

<sup>2)</sup> For the parameters indicated with (+), there are threshold values that could be used in the analysis, but these are considered irrelevant with respect to effects on the forest condition parameters

<sup>3)</sup> Maximum number of countries; actual number depends on the distribution of the species over the countries, and on possible clustering (or splitting up) of countries; this factor is not used when the change or trend in defoliation is used as an effect parameter.

<sup>4)</sup> One degree of freedom if the classes are set to ages/meters; else the degrees of freedom equals the number of classes minus one.

<sup>5)</sup> Parent material clusters based on peat, sand, loam, clay and calcareous soils.

<sup>6)</sup> 'Soil class' and the cluster of soil chemical characteristics are more or less exchangeable and were therefore mostly analysed in separate models.

<sup>7)</sup> The temperature indices contain are already based on implicit threshold values.

<sup>8)</sup> Threshold value for ozone equals 40 ppb while calculating AOT40; the critical value for the AOT40 equals 10 ppm.h.

<sup>9)</sup> Separate threshold values for each individual site, since critical deposition levels depend on stand and site characteristics (Chapter 5).

<sup>10)</sup> Tree species and interactions with tree species only when two species were analysed together (*Quercus robur* and *Q. petraea*)

The factor tree species was included when two or more tree species were analysed together. In this pilot study, this was the case for the *Quercus* species *Q. robur* and *Q. petraea*. The addition of the tree species resulted in a shift between the observed tree species on the observed scale of defoliation.

Soil parameters included in the model are limited to those influencing N behaviour (C/N ratio) and Al mobilisation (pH and base saturation) which in turn may affect forest condition (Chapter 3). These factors also influence the critical acid deposition level of the soil. The other key factors are equal to those described and calculated in Chapters 4 and 5.

#### **7.2.3.2 Temporal aggregation and lagged effects**

The temporal frequency considered in the stress factors is related to the question whether the effects are chronic or acute, and the prolonged or delayed effect (combined in lagged effects) of certain stress factors on the forest condition, with respect to the frequency of the available data. Temporal aggregation of data with a frequency of more than once a year was implemented in the form of aggregated values (mean values, sum values etc.) over a certain season or over the complete year. For instance, drought stress and exposure to ozone were aggregated over the growing season, whereas frost and cold parameters have been aggregated over the winter and spring period, respectively. Deposition fluxes have been aggregated over the whole year. In principle these values were aggregated in such a way, based on the literature, that the strongest relationship with forest condition could be expected (for details see Section 5.2).

Besides direct effects of stress factors in the current year, the effects of stress factors can also be revealed in the forest condition in later years. This aspect of temporal correlation can, in principle, be covered by advanced statistical techniques (by including the longitudinal aspect; Section 7.2.4). The full implementation of the temporal correlation is, however, not a part of the pilot study. Therefore, the so-called 'lagging terms' or 'lag/lagged effects' of the stress factors were introduced, which relate the forest condition in the current year to the possible impact of stress factors in preceding years. The lag effects are set up in such a way that they both cover prolonged effects of harmful episodes and the revelation of the effect of a harmful event several years after the occurrence of such an event.

Lagged effects are specifically relevant for meteorological stress factors (such as an extreme drought or frost period), but it may also hold for a severe acute event of atmospheric pollution. In order to limit the number of predictor variables, the lagged effect of a stress factor were described by two variables: the value in the preceding year ( $t-1$ ) and an aggregated number of relevant years before the preceding year ( $t-2$ ,  $t-3$ , ...). This number of years differs, depending on the tree species considered. Furthermore, even the number of years for each tree species may vary, depending on the stress considered stress factor (and depending which study the figures are retrieved from). The values presented in Table 26 are based on the maximum values regularly



found in various sources. These values were used in the implementation of this approach.

Note that the use of lag terms in the statistical analysis caused a considerable increase in the number of explaining variables and in the consumption of degrees of freedom by the statistical model (see Table 26).

Table 26 Selection of predictors from the exposure to stress factors in the current and the preceding years for the considered tree species

Tree species	Current year	Lagged effects		
		Period (years)	Preceding year	Previous years (formula)
<i>Pinus sylvestris</i>	$X_t$	2	$X_{t-1}$	$X_{t-2}$
<i>Picea abies</i>	$X_t$	6	$X_{t-1}$	$(5*X_{t-2} + 4*X_{t-3} + 3*X_{t-4} + 2*X_{t-5} + X_{t-6})/15$
<i>Q. robur + petraea</i>	$X_t$	4	$X_{t-1}$	$(3*X_{t-2} + 2*X_{t-3} + X_{t-4})/6$
<i>Fagus sylvatica</i>	$X_t$	6	$X_{t-1}$	$(5*X_{t-2} + 4*X_{t-3} + 3*X_{t-4} + 2*X_{t-5} + X_{t-6})/15$
<i>Quercus ilex</i> <sup>1)</sup>	$X_t$	4	$X_{t-1}$	$(3*X_{t-2} + 2*X_{t-3} + X_{t-4})/6$

<sup>1)</sup> *Quercus ilex* is presumed to show similar lagged effects as *Quercus robur + petraea* (no actual figures available)

### 7.2.3.3 Correlations between predictor variables

An important condition for an unambiguous interpretation of the results of the regression analysis, is that the predictor variables in the selected model are independent. When predictor variables are correlated, it is difficult to separate the effects of each individual variable (confounding). As stated before, the temporal correlations between data observed or modelled at the same site have not been explicitly included in the statistical analyses, since essential parts of the software were still under development (Section 7.2.1). The same is true for the possible spatial correlations between data at neighbouring sites, even though this effect is likely to be limited. Insight in such correlations is, however, necessary to evaluate the results of the statistical analyses.

The presence of correlations between predictor variables can be due to (i) the coincidence of large-scale patterns for the two correlating predictor variables (spatial correlations), (ii) pure mechanistic aspects related to processes by which one factor affects the other one and (iii) repeated observations or modelled data at the same site (temporal correlations). Examples of spatial correlations are the coincidence of the patterns for the SO<sub>2</sub> concentration and the deposition of acidity and the correlation of several predictor (and effect) variables with 'Country'. An example of a causal relationship could be the relation between the soil pH and atmospheric deposition, even though there is not a strong evidence for this relationship (Chapter 3). Temporal correlations can be expected between current year stress variables with the corresponding values for the preceding years (lagging terms), especially when there are large spatial differences and relatively little variation between the years. Correlations between the predictor variables that were investigated include those between:

- the annual and 10 year average values of the time-dependent predictor variables (spatial correlations);

- the time-dependent predictor variables and the predictor country (country correlations);
- the annual average values of the time-dependent predictor variables in the current year, the preceding year and the earlier years (temporal correlations).

The correlation of predictor variables with the predictor variable 'Country' hampers the accurate derivation of country coefficients, which give an estimation of the scale shifts in defoliation between the participating countries. Therefore, it is important to base the procedure of the estimation of the country coefficient on a set of predictor variables which (i) give the best explanation of the observed variance and (ii) have minimum correlation with the factor 'Country'. The set of predictor variables used for the estimation of country coefficients is further described in Section 7.2.4.

#### **7.2.3.4 Included interactions**

The inclusion of interactions between predictors in the regression model is relevant if the effects are not additive (on the logit scale). To avoid 'data fishing', only those interactions were included that were expected before hand, including those between meteorological stress factors (such as temperature and transpiration reduction) and the concentrations of O<sub>3</sub> and those between N deposition and vulnerability for frost (Table 25). Furthermore, the interaction between acid deposition and base saturation may be relevant since acid inputs cause the release of base cations at high base saturation (positive effect) and of aluminium at a low base saturation (negative effect). The interactions between tree species and late frost was included in the analysis of the two *Quercus* species, since both tree species are considered to react differently on his stress factor (see Section 1.2).

#### **7.2.3.5 Threshold values**

A final relevant aspect is the use of threshold values with respect to the stress factors, such as critical concentration levels for SO<sub>2</sub>, NO<sub>2</sub>, NH<sub>3</sub> and O<sub>3</sub> in the atmosphere. In the case of known threshold values, linear models can be used by using the exceedance of the threshold value as predictor variable. Neglecting such threshold values may lead to the conclusion that the stress factor is unimportant since the value (e.g. SO<sub>x</sub> concentration) is below the critical value at nearly all locations. If the value given in the literature is highly uncertain a non linear relationship can be used to describe the relation (broken stick model, exponential or logistic curves, etc.) and the critical values are estimated from the data.

In Table 25, a number of threshold values used for concentration and deposition levels in this study is given (Chapter 6). Some of them are, however, not directly related to the forest condition in terms of defoliation and discoloration. For example, Critical deposition levels (threshold values) for nitrogen deposition are related to vegetation changes and not so much to tree vitality (Chapter 6). The statistical model has been implemented by both including and excluding threshold values.



## 7.2.4 The investigated relationships between response and predictor variables

### 7.2.4.1 Models used

The three major models that have ultimately been applied all investigated the relationship between the three differently defined defoliation parameters (Section 7.2.2) and effects of different stress factor values on different locations (spatial differences). The effects of changes in stress factors in different years at given locations (temporal differences), was, however, accounted for in different ways.

First, an analysis was conducted using all predictor variables, in order to gain insight in which predictor variables are important for the explanation of the variation in the actual defoliation as response variable (Table 26: Model A-1). This analyses combines the information of both spatial and temporal differences. As an alternative, the deviation of the yearly value of the meteorological predictor variables compared to their mean values over the considered 10 year period and the mean values themselves were used as alternative sets of predictor variables (Table 26: Model A-2), for reasons explained below.

A comparable selection of analyses was conducted for the change and trend in defoliation (Section 7.2.2 and Table 26: Models B and C). The analyses of the change and trend in defoliation are indicated with Model B-1 and B-2 and Model C-1 and C-2, analogous with Model A-1 and A-2. In Model C ('Trends') the average values of, and the trends in the stress factors over the observed years were used as predictor variables. In Model C-2 the average meteorological values over the years with defoliation data were replaced by the deviation of these values from the mean values over all 11 years with meteorological data. Such a measure, for example, indicates whether the years with defoliation data coincide with a dry episode of several years.

Table 26 Types of models used in the statistical analysis with their temporal aspects

Model	Response variable <sup>1)</sup>	Predictor variables <sup>1)</sup>	Temporal correlation	Country effect	Weighing factor
Model A-0	$y_t$	$x_c$	neglected	included	N trees (plot; t)
Model A-1	$y_t$	$x_c, x_t$	neglected	included	N trees (plot; t)
Model A-2	$y_t$	$x_c, x_t - \bar{x}, \bar{x}$	neglected	included	N trees (plot; t)
Model B-0	$\delta y_t$	$x_c$	neglected	excluded	Min(N trees (plot; t, t-1))
Model B-1	$\delta y_t$	$x_c, x_t$	neglected	excluded	Min(N trees (plot; t, t-1))
Model B-2	$\delta y_t$	$x_c, x_t - \bar{x}, \bar{x}$	neglected	excluded	Min(N trees (plot; t, t-1))
Model C-0	$\bar{\delta y}$	$x_c$	irrelevant	excluded	N years (plot) - 1
Model C-1	$\bar{\delta y}$	$x_c, \bar{\delta x}, \bar{x}_t$	irrelevant	excluded	N years (plot) - 1
Model C-2	$\bar{\delta y}$	$x_c, \bar{\delta x}, \bar{x}_t - \bar{x}, \bar{x}$	irrelevant	excluded	N years (plot) - 1

<sup>1)</sup> Legend:  $y_t$  = response variable (defoliation);  $\delta y_t$  = change in defoliation;  $\bar{\delta y}$  = trend in defoliation;  $x_c$  = time-independent predictor variables;  $x_t$  = time-dependent predictor variable in current year (including lagging term etc.);  $\bar{x}$  = mean time-dependent predictor variable over 10 year period;  $x_t - \bar{x}$  = deviation of the time-dependent predictor variable from the long-term (10 year) average value (refers only to meteorological stress factors);  $\bar{x}_t - \bar{x}$  = deviation of the mean over the defoliation years in the time-dependent predictor variable from the long-term (10 year) average value (refers only to meteorological stress factors)  $\bar{\delta x}$  = trend over observed years

In order to gain insight in the relationship between the measured defoliation data and measured time-independent stand and site characteristics and chemical soil data (Chapter 3), an additional analysis was carried out in which the time-dependent

modelled stress factors (Chapters 4 and 5) were excluded as predictor variables (the models A-0, B-0 and C-0 in Table 26).

As stated before, the advantage of the models B and C is that it circumvents the confounding of the observed defoliation with country. In these models, country has thus not been included as a predictor variable (exceptions to this general approach are given in the next section). In the sub-models A-1 and A-2 the confounding between country, predictor variables and the response variable (actual defoliation) is large. In the latter sub-model (A-2), however, the confounding between predictor variables and country is less than in model A-1. In this model, the average of the meteorological stress factors over the whole period was used as an estimation of the climatic characteristics for each separate site, whereas the deviation of the yearly values from the long-term mean were used as alternative predictor variables. The use of these predictor variables has the following advantages:

- they are not (or less) confounded with countries; therefore the country coefficients were estimated using these alternatives of the meteorological stress factors;
- the confounding of the values for current year and previous years can be avoided;
- this approach accommodates for the adaptation of individual trees and stands to local conditions, due to provenance selection or by adaptation after so many years of presence at the same location under more or less the same conditions;
- the deviation of the current year figures compared to the long-year means provides better estimates of the actual stress.

Besides the use of the values from previous years as predictor variables of the defoliation in the current year, no other temporal (nor spatial) correlations were included explicitly in the statistical model. However, the analysis of changes and trends may give a first insight in the temporal aspect of the relationship between defoliation and the stress factors.

#### **7.2.4.2 Sets of predictor variables used in the various models**

##### ***Model A***

The explanation of the variation in the actual (logit transformed) defoliation data (Model A) was sought using different combinations of predictor variables (Table 27), grouped in the main models that were described in the preceding section. For each separate sub-model a selection was made of relevant predictor variables. A first coarse selection was based on the most significant and most plausible predictor variables. The final model was selected by step-wise regression techniques, using the pre-selected set of predictor variables.

First, the importance of a standard set of site and stand characteristics as predictor variables was investigated, using both measured and interpolated data (sub-model A-0.0). In three alternative sub-models the contents of the predictor variable was limited to the data that were actually assessed (sub-model A-0.1), additional site characteristics were included (sub-model A-0.2) and the impact of adding average meteorological data



over the 10 years as site characteristics was tested (sub-model A-0.3). The impact of the factor 'Country' was tested by using 'Country' as sole predictor variable (sub-model A-0.4) and by omitting it from the standard model (sub-model A-0.5).

Table 27 Sets of predictor variables tested in Model A (and Model B<sup>1)</sup>)

Model code <sup>1)</sup>	Country	Stand and site			Meteo stress	Air pollution		Temporal aspects				Inter- actions
		Av. <sup>2)</sup>	Std. <sup>3)</sup>	Ext. <sup>4)</sup>		Absol.	CLE's <sup>5)</sup>	t	t-1	lag	avg.	
Model A-1 (site & stand, no time-dependency)												
A-0.0	X	-	X	-	-	-	-	-	-	-	-	-
A-0.1	X	X		X	-	-	-	-	-	-	-	-
A-0.2	X	-		X	-	-	-	-	-	-	-	-
A-0.3	X	-	X	-	X	-	-	-	-	-	X	-
A-0.4	X	-	-	-	-	-	-	-	-	-	-	-
A-0.5	-	-	X	-	-	-	-	-	-	-	-	-
Model A-1 (Full model; absolute meteo)												
A-1.0	X	-	X	-	X	X	X	X	X	X	X	-
A-1.1	X	-	X	-	X	X	X	X	-	-	-	X
A-1.2	X	-	X	-	X	X	-	X	X	X	X	-
A-1.3	X	-	X	-	X	X	-	X	-	-	-	X
A-1.4	X	-	X	-	X	-	X	X	X	X	X	-
A-1.5	X	-	X	-	X	-	X	X	-	-	-	X
A-1.6	-	-	X	-	X	X	X	X	X	X	X	-
A-1.7	-	-	X	-	X	X	X	X	-	-	-	X
Model A-2 (Full model; relative meteo)												
A-2.0	X	-	X	-	X	X	X	X	X	X	-	-
A-2.1	X	-	X	-	X	X	X	X	-	-	-	X
A-2.2	X	-	X	-	X	X	X	X	X	X	X	-
A-2.3	X	-	X	-	X	X	-	X	X	X	-	-
A-2.4	X	-	X	-	X	X	-	X	-	-	-	X
A-2.5	X	-	X	-	X	-	X	X	X	X	-	-
A-2.6	X	-	X	-	X	-	X	X	-	-	-	X
A-2.7	-	-	X	-	X	X	X	X	X	X	-	-
A-2.8	-	-	X	-	X	X	X	X	-	-	-	X

<sup>1)</sup> With a few modifications the same sets of predictor variables apply for the B Models with the same number (see preceding text).

<sup>2)</sup> Available = available data from real assessments on age, altitude, soil type, water availability class, soil chemical composition.

<sup>3)</sup> Standard = available and extrapolated stand & site characteristics: altitude, age, pH, C/N ratio and base saturation.

<sup>4)</sup> Extended = Standard + soil cluster, water availability class, bio-geographic (climatic) region

<sup>5)</sup> Exceedance of critical concentration of deposition levels for air pollutants (Chapter 5).

The sub-models within the A-1 group analyse the relationships using both measured and interpolated stand and site characteristics and modelled stress factors for meteorological condition and air pollution. Sub-model A-1.0 is the basic model for this analysis, using all available data. In sub-model A-1.2 the exceedances of the critical values for the anthropogenic stress factors were excluded, whereas in sub-model A-1.4 the absolute values were excluded instead. In sub-model A-1.6 the effect of omitting country as a predictor variable was tested. Although country should always be in the model because of the difference in standards in the different countries, these models can reveal relationships of the defoliation with predictor variables which are strongly confounded with the factor country (so that they will never show up when Country is in

the explanatory model). The sub-models A-1.1, A-1.3, A-1.5 and A-1.7 were based on a limitation of the variables in the preceding sub-model by neglecting lagged effects, while including interactions between different predictor variables (Table 27).

The contents of the sub-models of the A-2 group is comparable with those of the A-1 Models. The main difference is, that the absolute values for the meteorological data (current year, previous years en earlier years) are replaced by the differences of these values with the mean values over the 10 year period. The mean values were treated as an optional addition (sub-model A-2.2).

### ***Model B***

The tested sets of predictor variables for Model B are similar to those tested for Model A, with a few changes. The factor 'Country' was omitted in almost all sub-models of Model B. However, in sub-model B-0.4 the effect of the factor 'Country' as a single predictor was still tested. Furthermore, in the sub-models B-1.6, B-1.7, B-2.7 and B-2.8 the factor 'Country' was added to the standard model. The average values over 10 year for the time-dependent predictor variables were excluded from the standard for Models B-1 and B-2. Only in sub-models B-0.3 and B-2.1, this group of predictors was optionally included instead of excluded.

### ***Model C***

The sets of predictor variable used in the various tests for Model C are presented in Table 28. In principle the same groups of sub-models are distinguished as for Models A and B. The contents of the sub-models for C-0 was equal of the ones of Model B-0. In Model C-1 the mean values over the observed years per plot and the trend over these year were applied as predictor variables. The mean values and trend figures were calculated over the years for which defoliation data were available. In Model C-2 the mean values were replaced by the deviation of these mean value compared to the mean over the 10 year period. The sub-models C-1.0 and C-2.0 are the basic models the respective groups. The sub-models C-1.1 and C-2.1 only consider the absolute values for the anthropogenic stress factors, whereas the sub-models C-1.2 and C-2.2 only consider the exceedances of critical values for these factors. The sub-models C-1.3 and C-2.3 test the effect of the addition of Country.

#### **7.2.4.3 Strategy of model selection**

Each sub-model was first tested with all predictor variables included. The results of these analyses were used to make a selection of predictor variables that were tested more thoroughly, based on the significance in the complete sub-model and the plausibility of the relationship. This selection of predictor variables was included in a step-wise regression model, which added (and sometimes dropped) the elements of the set of predictor variables. Elements were added as long as the addition was significant and the addition added at least 0.5 % to the explained variance ( $R^2_{adj}$ ). The elements of the final models were marked according to the magnitude of the addition to the explained variance: > 2 %, 1-2 % and 0.5-1 %. Furthermore, the elements were



marked in italics if the found relationship had an unexpected sign (Table 29), although these assumed signs could be arbitrary and depend sometimes on the range of the stress factor.

Table 28 Sets of predictor variables tested in Model C

Model code	Country	Stand and site			Meteo stress	Anthrop. stress		Temporal aspects		Inter- actions
		Av. <sup>1)</sup>	Std. <sup>2)</sup>	Ext. <sup>3)</sup>		Absol.	CLE's	mean <sup>4)</sup>	trend	
Model C-1 (site & stand, no time-dependency)										
C-0.0	X	-	X	-	-	-	-	-	-	-
C-0.1	X	X		X	-	-	-	-	-	-
C-0.2	X	-		X	-	-	-	-	-	-
C-0.3	X	-	X	-	X	-	-	<sup>4)</sup>	-	-
C-0.4	X	-	X	-	-	-	-	-	-	-
C-0.5	-	-	X	-	-	-	-	-	-	-
Model C-1 (Full model; absolute meteo)										
C-1.0	X	-	X	-	X	X	X	X	X	-
C-1.1	X	-	X	-	X	X	-	X	X	X
C-1.2	X	-	X	-	X	-	X	X	X	X
C-1.3	-	-	X	-	X	X	X	X	X	-
Model C-2 (Full model; relative meteo)										
C-2.0	X	-	X	-	X	X	X	X	X	-
C-2.1	X	-	X	-	X	X	X	X, <sup>4)</sup>	X	-
C-2.2	X	-	X	-	X	X	-	X	X	X
C-2.3	X	-	X	-	X	-	X	X	X	X
C-2.4	-	-	X	-	X	X	X	X	X	-

<sup>1)</sup> Available = available data from real assessments on soil type, water availability class, soil chemical composition, age, altitude.

<sup>2)</sup> Standard = available and extrapolated stand & site characteristics: altitude, age, pH, C/N ratio and base saturation.

<sup>3)</sup> Extended = Standard + soil cluster, water availability class, bio-geographic (climatic) region

<sup>4)</sup> Mean (X) = mean over years with defoliation data available; extended mean () mean over all 10 years

Table 29 Expected signs of the relationships between defoliation and the predictor variables

Predictor variable	Expected relation with defoliation <sup>1)</sup>	Remarks
Age	pos	
Altitude	pos	optimum in Mediterranean areas possibly not at sea level
pH	neg	above a certain pH a further increase may increase defoliation
C/N	pos/neg	effect is unclear
Base Saturation	neg	no effect is expected until a threshold value where BC deficiency may occur
Winter Index	pos	
Late Frost	pos	
Heat Index	pos	
Summer Index	neg	optimum curve per species would be better
Rel. Transpiration	neg	higher Rel.Trans. (less drought) gives less defoliation
[SO <sub>2</sub> ]	pos	
[NO <sub>2</sub> ]	pos	reverse effect possible, due to fertilising effect of N
[NH <sub>3</sub> ]	pos	reverse effect possible, due to fertilising effect of N
Acid Deposition	pos	reverse effect possible, due to additional release of base cations
N Deposition	pos	reverse effect possible, due to fertilising effect of N
[O <sub>3</sub> ]	pos	
AOT40	pos	

<sup>1)</sup> Assumed equal for the actual defoliation and for the change and trends in defoliation.

The same selection procedure was also applied on certain subsets of the data base, in order to reveal relationship that might be hidden in the noise of the complete data base. Several relationships were for example tested on data from separate countries with many plots for most tree species and a large variation in stress factors (e.g. France, Germany and Poland), on combinations of these countries and for plots where the critical deposition level for acidity was exceeded. Furthermore, alternative models were tested using non-linear relationships, using so-called spline relationships. These splines were tested for predictors for which a non-linear optimum curve was expected (e.g. pH and altitude) or for which the effects only occur above a certain, not exactly identified threshold value (e.g. relative transpiration). In the latter case, the threshold values were estimated from the available data. These additional tests were only carried out for model A (actual defoliation). No additional tests were done for model B and C (resp. changes and trends), because of lack of time and the less promising results from the standard sub-models. Each additional predictor was tested whether it had an 'expected' sign or not. If not, an explanation was sought. If no suitable explanation could be found, the results of the correlation tests between predictor variables (Section 7.3.1) were used in the selection of 'second-best' predictor variables, which had a more expected relationship with the defoliation and added almost the same to the explained variance.

## 7.3 Results

### 7.3.1 Correlation between predictor variables

A selection of the results of the investigated correlations is given in Annex 5 (Section A5.1). The results of this investigation were used in the model selection in the consecutive sections, since strong correlations may lead to the selection of incorrect models and to mis-interpretations.

The correlations between the various time-dependent predictor variables (an example for *Pinus sylvestris* is given in Annex 5, Table A17), show that strong correlations occur between (i) air pollution and deposition variables, (ii) certain meteorological stress variables (e.g. late frost and winter index) and (iii) between ozone concentration and most meteorological stress variables. The correlations between the mean values over the 10 year period are generally stronger than between the annual values. The use of exceedances of critical deposition/concentration levels instead of the actual levels/loads resulted in considerably lower correlations (not presented). Furthermore, the correlation between the annual meteorological predictors was considerably less, when these values were replaced by the deviation from the mean value over 10 years (as applied in Models A-2, B-2 and C-2).

The 'correlation' between the predictor 'Country' and the mean values over the 10 year period for the time-dependent variables varied between 13 and 84%, depending on the parameter and the tree species (Table A18). The values for the current year variables were generally slightly lower (not presented).



The correlation between different temporal alternatives of the same variable appeared to be very strong for the air pollution and deposition parameters (Table A19). This indicates that these parameters vary only slightly between the years and that they are susceptible of confounding. The use of exceedances of critical deposition/concentration levels instead of the actual levels/loads caused a decrease in these correlations (not presented). The correlations between the different temporal alternatives for the meteorological parameters was less than for the air pollution parameters (Table A19). These correlations almost disappeared when the values were replaced by the deviations from the 10 year mean values (not presented).

### 7.3.2 Analysis of actual defoliation data (Model A)

#### 7.3.2.1 Reference models

This section gives a short overview of the relationship between the yearly observed defoliation data and the measured and modelled site and stand characteristics and stress factors (Model A). We focus here on the results of sub-model A-1, in which all predictor variables are used (see before). More detailed information on the outcome of the various statistical models and sub-models can be found in Annex 5 (Section A5.2).

The actual defoliation of the five major tree species is mainly determined by differences between countries. The explained variance by the predictor 'Country' variable varied between 33 and 39 % for most species except for *Quercus ilex* (Table 30). The smaller amount of explained variance for this species by country (9 %) is probably due to the limited number of countries where this tree species occurs. For all species the predictor 'Age' was an important secondary predictor, except for *Q. ilex*, because for many stands where this species occurred there was not sufficient information on age (for a considerable number of stand age class was missing or recorded as 'irregular'). It is, however, expected that a similar relationship with age would also apply for this species. The sub-models based on available data only (A-0.1) could not be tested properly, because for many plots the information was not complete.

Table 30 The explained variance in the reference Model A-1.0 by the predictor 'Country', the combination 'Country' and 'Age' and the selected best fit model for the five considered tree species

Tree species	Observ.	Country	+ Age	Selected predictors from Model A-1.0	R <sup>2</sup> <sub>adj</sub>
<i>Pinus sylvestris</i>	9164	38.7	42.6	<u>Country</u> , <u>Age</u> , ( <i>[NH<sub>3</sub>]</i> <sub>t-1</sub> )	43.1
<i>Picea abies</i>	7362	38.0	52.2	<u>Country</u> , <u>Age</u>	52.2
<i>Quercus robur+petraea</i>	4563	38.0 <sup>1)</sup>	39.9 <sup>1)</sup>	<u>Country</u> , <u>Age</u> , ( <i>RelTrans</i> <sub>t-1</sub> ), ( <i>Spec</i> )	40.7
<i>Fagus sylvatica</i>	3945	32.5	34.2	<u>Country</u> , <u>Age</u> , AOT60, ( <i>[NO<sub>2</sub>]</i> )	35.8
<i>Quercus ilex</i>	1481	9.3	- <sup>2)</sup>	<u>Country</u> , <i>[NO<sub>2</sub>]</i> <sub>lag</sub> , <i>AcidDep</i> <sub>t-1</sub> , <i>NitDep</i> <sub>lag</sub> + ( <i>RelTrans</i> <sub>t</sub> ), <i>RelTrans</i> , ( <i>[SO<sub>2</sub>]</i> <sub>t</sub> )	22.1

Legend: Underlined = contribution > 2%; Normal = contribution 1-2%; (Between brackets) = contribution 0.5-1 %;

*Italics* = unexpected sign

<sup>1)</sup> Including 'Species' for the tree species cluster '*Quercus robur* & *Quercus petraea*'

<sup>2)</sup> Age is not a significant predictor variable for *Q. ilex* (see text)

Further analysis of the various sub-models showed that all other predictor variables (stand and site characteristics and time-dependent stress factors) do contribute marginally to a larger explained variance. Using the criterion of a minimum increase of 0.5 % of explained variance by an additional predictor, no other variable could be selected for *Picea abies* besides Country and Age. For *Pinus sylvestris*, the  $\text{NH}_3$  concentration of the previous year added 0.5-1.0% to the explained variance. For *Quercus robur* + *Q. petraea* the difference between the two species ('Spec') and the relative transpiration (in either the current or the previous year; compare Annex 5; Table A 22) added 2 % to the explained variance (Table 30). For *Fagus sylvatica* the additional explained variance was mostly due to the (average) concentrations of  $\text{NO}_2$  and  $\text{O}_3$ . The increase of explained variance for *Quercus ilex* after the addition of 'Country' in the showed model was due to various natural and anthropogenic stress factors. Several predictors, however, showed up with unexpected signs (Annex 5; Table A 22), indicating that the model is not very stable. Since age appeared to be an important factor for the other species, it is likely that the lack of more detailed information on age is a serious limitation of a more reliable analysis for this species.

For most of the examined species there was little variation in the outcome of the various alternative sub-models A-1.0 - A-1.5 and A-2.0 - A-2.5 (Annex 5; Tables A 20 - A 24). For *Quercus robur* + *Q. petraea* there are indications that also late frost could be relevant. For *Quercus ilex* the relative transpiration and the  $\text{NO}_2$  concentration were frequently present in the selected model. In both cases, however, the signs of the regression coefficients are contrary to the expectations (e.g. a lower defoliation at an increased  $\text{NO}_2$  concentration level). As stated in Table 29, this may be the case in low N deposition areas where trees are N deficient. The various sub-models within the time-independent stand and site characteristics (A-0) did not give much additional information. For most species 'Climatic Zone' offered a reasonable alternative for the analysis including the meteorological and air pollution parameters.

Models without the predictor 'Country' all had a lower explained variance than the models with Country. The large number of predictors with an unexpected sign indicates that the omission of country could easily result in unstable models. The highly significant predictors with the 'right' sign in these models, however, can give a good indication of relevant additional predictors. The effect of these predictor variables was either hidden behind or confounded with the effect of country. Predictors that are revealed by these sub-models are acid deposition for *Pinus sylvestris* and the  $\text{SO}_2$  concentration for all other examined species. The presence (with an unexpected sign) of acid deposition in the models for *Quercus ilex* is probably related to the strong (negative) correlation between the acid deposition and relative transpiration (drought). The highest acid deposition probably occurred in the areas with the highest precipitation, which thus had the highest relative transpiration. A significant correlation of the defoliation with the acid deposition was not expected, since net acid deposition (acid deposition minus base deposition) is around zero in the Mediterranean area (Section 3.2).



### 7.3.2.2 Additional tests

The results of the additional tests on the complete data set and on a limitation of the observed data (plots where the critical deposition level for acidity was exceeded and on separate countries and combinations of a few countries, to avoid the large impact of the country as predicting variable; Section 6.2.4) revealed that more predictors are relevant than in the standard models (Table 30 and Annex 5, Table A 20). The addition of these predictors mostly caused a small increase of the explained variance. The limitation of the data set to locations with an exceedance of the critical deposition level for acidity resulted only in marginal shifts compared to the models presented. The limitation of the analysis to separate countries reduced the explained variance to the level of the original models without country. The main predictor in the within-country analysis was mostly age. After age only one or two more predictors gave the impression of a stable model. Furthermore, the regression coefficients for the same predictor variable varied, depending on which country was analysed. Only the inclusion of several non-linear relationships (using splines) really increased the explained variance in the actual defoliation by an improved precision for the predictor age, relative transpiration and the ozone variables for most species.

A 'best' set of predictor variables selected, based on both the standard analysis and the additional analyses, is given in Table 31. These set of predictor variables were used in the subsequent analyses, which give an overview of the effect of the variation on the predictor 'Country' and the variation in the other predictor variables.

Table 31 Selected statistical models based on the standard and supplementary statistical analysis

Species	Selected predictive model <sup>1)</sup>	R <sup>2</sup> <sub>adj</sub> (%)
<i>Pinus sylvestris</i>	Country + S3(Age) + AcidDep + S2(RelTrans <sub>i</sub> )	43.9
<i>Picea abies</i>	Country + S3(Age)	54.5
<i>Quercus robur</i> + <i>Q. petraea</i>	Country + Spec + S3(Age) + S2(RelTrans <sub>i-1</sub> ) + [NO <sub>2</sub> ] <sub>i</sub>	41.7
<i>Fagus sylvatica</i>	Country + S3(Age) + S2(AOT60) + D(RelTrans <sub>iag</sub> ) + [SO <sub>2</sub> ] <sub>i</sub> + [NO <sub>2</sub> ] <sub>i</sub>	36.6
<i>Quercus ilex</i>	Country + S3(Alt) + S2(RelTrans <sub>i</sub> ) + [NO <sub>2</sub> ] <sub>i</sub> + S2(AOT60)	15.2

<sup>1)</sup> Formulas containing 'spline' effects: S2 = spline with two degrees of freedom, S3 = spline with three degrees of freedom; D( ) means that for this meteorological variable the deviation from the 10 year average value was used.

### 7.3.2.3 Separation of country effects and stress factors

An estimation of the scale shifts between the various countries was made using the models described in Table 31. It was assumed that (i) cause-effect relationships with the stress factors are the same in all countries, (ii) the countries account in a similar way for the various site conditions in their reference (but on a different level; which in statistical terms means that no interaction is expected between country and the site characteristics) and (iii) the definition of the reference tree remained the same through the complete period of monitoring. However, the possible interactions between 'Country' and other time-independent predictors and possible changes in the reference tree were not extensively investigated.

Table 32 gives an overview of the regression coefficients of the predictor 'Country' indicated as 'Country Coefficients' for the observed tree species based on the selected

regression models. Negative values indicate that lower values are obtained than the European mean estimation under the same environmental conditions and positive values mean that the supplied values are higher than the European mean estimation.

Table 32 Preliminary country coefficients (on the logit scale) for the different tree species, based on the regression models of Table 31 (the values represent the deviation of the national values from the mean over all countries)

Country	<i>Pinus sylvestris</i>	<i>Picea abies</i>	<i>Q. robur+petraea</i>	<i>Fagus sylvatica</i>	<i>Quercus ilex</i>
FR	-0.880	-1.653	-1.205	-0.921	-0.445
BE	0.320	-0.228	-1.042	-0.747	
NL	-1.158		-0.645		
DL	-0.045	0.036	0.186	0.382	
IT	-0.272	-1.725	-0.463	-1.110	-1.289
UK-1 <sup>1)</sup>	0.746	0.607	0.295	1.038	
UK-2 <sup>1)</sup>	0.176	0.183	-0.183	0.434	
IR		0.584			
DK	0.295	0.248	0.595	1.085	
EL	-0.375		0.407	-0.557	1.377
PO	-0.583		-1.840		
ES	-0.504	0.289	-0.383	-0.456	0.208
LX	0.269	-0.203	-0.283	0.041	
SW	-0.488	-0.004	-0.191	0.552	
AU	-0.908	-1.661	-2.150	-0.773	
FI	-0.799	-0.112			
RO	1.111	-0.090	0.466	-0.017	
PL	0.626	0.799	0.435	0.863	
SR	1.070	0.889	0.669	0.478	
NO	-0.674	-0.669			
CH	-0.283	-0.185	0.440	0.274	
HU	-0.497	-1.030	0.397	-1.014	
LI	0.534	0.983	0.237		
CR		-0.689	-0.139	-0.834	-0.156
CZ	0.868	0.746	1.443	0.687	
EE	0.014	-0.762			
SL	0.071	0.092	0.243	0.024	0.304
MO			0.986		
BY	-0.079	3.532			
BU	0.859	-0.515	1.566	0.571	
LA	0.587	0.538	0.159		

<sup>1)</sup> UK-1 = UK till 1991; UK-2 = UK from 1992 onwards

These coefficients were also used to construct tables by which the defoliation figures supplied by the various countries can be translated to the level of a 'Mean European Country'. For the countries with a negative Country Coefficient the supplied values by the country increase when they are transformed to the European level. For the countries with a positive Country Coefficient the supplied values by the country decrease when they are transformed to the European level. Annex 5 (Section A5.3) gives an overview of how the values supplied on the national levels would transform into values on a European level. The first column of these tables give the values in the way they were supplied by the countries and the other columns give per country the adjusted values.



The differences in the calculated country coefficients are generally in line with the results found in the intercalibration exercises performed for some tree species in some distinct regions. There are, however, differences, which can be attributed to (i) the preliminary status of the statistical model, (ii) the preliminary status of the adjustment coefficients from the intercalibration exercises (Chapter 2 of Part A of the Overview Report; Müller-Edzards et al., 1997) and (iii) possible gradual changes in the national reference trees.

The effect of the use of these country coefficients is shown in Fig. 48 and 49. The first (top) figure (Fig. 48) shows the spatial distribution of the originally submitted defoliation data for the year 1995 for the six tree species considered in this study. Several sharp boundaries between the various countries can be recognised on this map, e.g. between Germany, Poland and the Czech republic. The occurrence of such (unnatural) contrasts between countries can at least partly be countered by the inclusion of the Country as an additional predictor variable. The result of the adjustment of the original values (Fig. 49), using the estimated country coefficients, reveals a spatial distribution which is in some areas considerably different from the original view.

In the 'new' map, most contrasts at state borders that could not be substantiated by natural processes, have disappeared, e.g. between Germany, Poland and the Czech republic. There are, however, distinct areas revealed now, that show a better or worse forest condition than the European average, e.g. the Mid-Scandinavia and north-eastern France. The demarcation of these areas does not coincide state boundaries. The area in Mid Scandinavia, for example, contrasts clearly with a much better area in Southern Sweden and the area in North Eastern France (drought?) contrasts clearly with much better areas in Central and West France and a narrow strip close to the German border. This 'better' area continues across the German border.

The map with adjusted values (Fig. 49) gives only a preliminary view of the possibilities of what might become possible in the future, when a more thorough analysis of the data will be conducted in the comprehensive study. The presented figures should therefore only be considered as an example and not as 'true' adjusted values.

The models in Table 31, which were used to estimate the country coefficients, were also used to determine estimations of the relationships between the separate predictor variables and the defoliation. Fig. 50-54 shows graphs for the relationship for the most important predictors for the six considered tree species. The separate lines for the individual countries show that there are considerable differences between the countries.

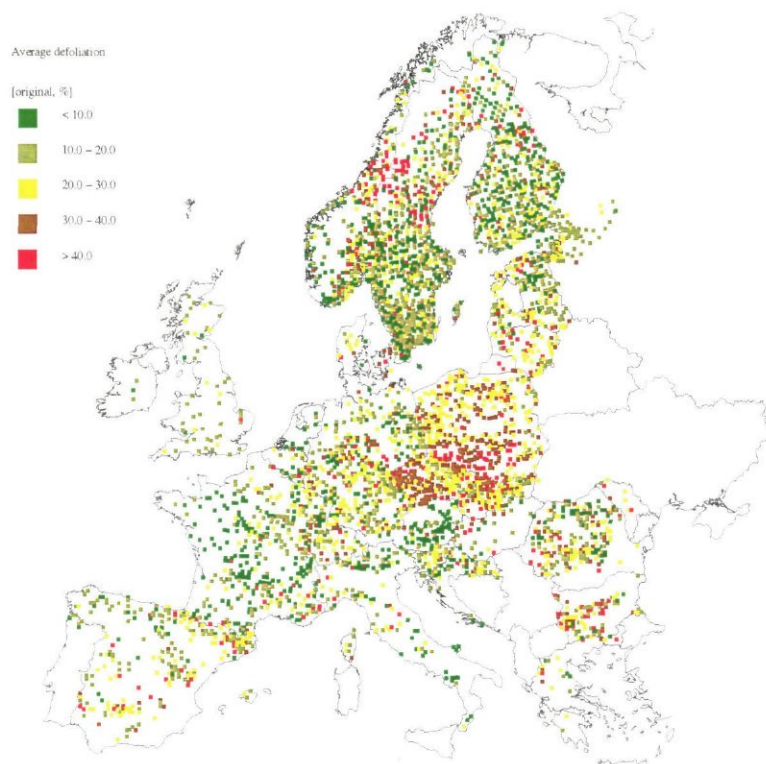


Fig. 48 Average defoliation per plot based on the 1995 results for the six investigated species

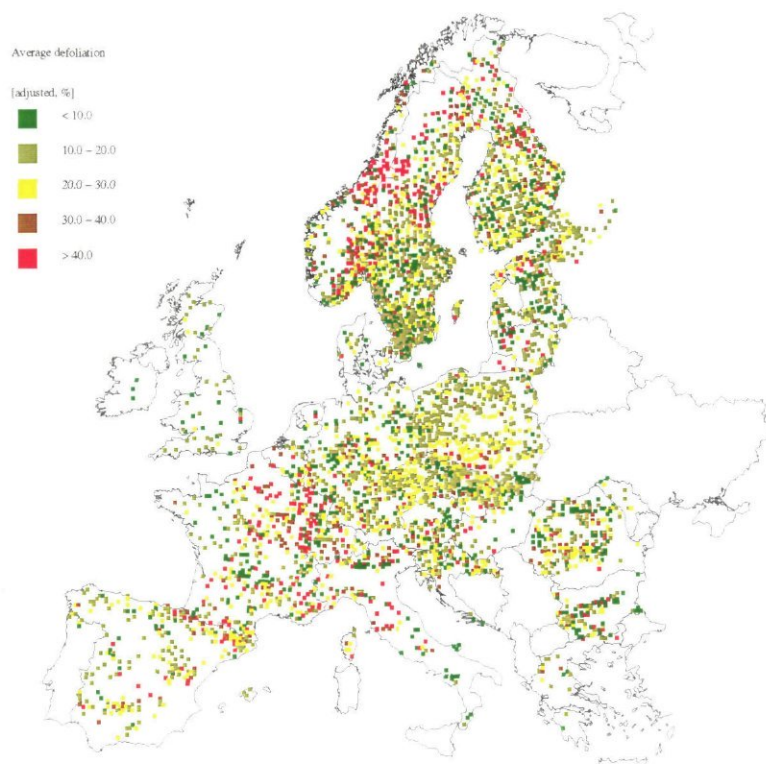


Fig. 49 Average defoliation per plot based on the (preliminarily) adjusted values for the 1995 results for the six investigated species. Note that the adjustments are based on a preliminary analysis of the data



For all species except *Quercus ilex* a clear increase with age was found for the defoliation. The strongest increase occurred in the younger age classes. The increase flattens after 60 years for *Pinus sylvestris* and *Quercus robur+petraea* (Fig. 50 and 52) and after 80 years for *Picea abies* and *Fagus sylvatica* (Fig. 51 and 53). For *Picea abies* no other relationships were found.

The relationship with relative transpiration (drought) were almost linear for *Quercus robur + petraea* and *Quercus ilex* (Fig. 52 and 54). For *Pinus sylvestris* the relationship with the relative transpiration showed a range of no effect (100-70%). Below a relative transpiration of 70%, the correlation between drought and defoliation was almost linear (Fig. 50). Significant relationships with only a weak 'slope' were found for *Pinus sylvestris* with acid deposition (Fig. 50), for *Quercus robur + petraea* with the NO<sub>2</sub> concentrations (Fig. 52), for *Fagus sylvatica* with the NO<sub>2</sub> and SO<sub>2</sub> concentrations (Fig. 53) and for *Quercus ilex* with the AOT60 (Fig. 54). Very strong relationships were found for *Fagus sylvatica* with the AOT60 (Fig. 53) and for *Quercus ilex* with the NO<sub>2</sub> concentrations (Fig. 54).

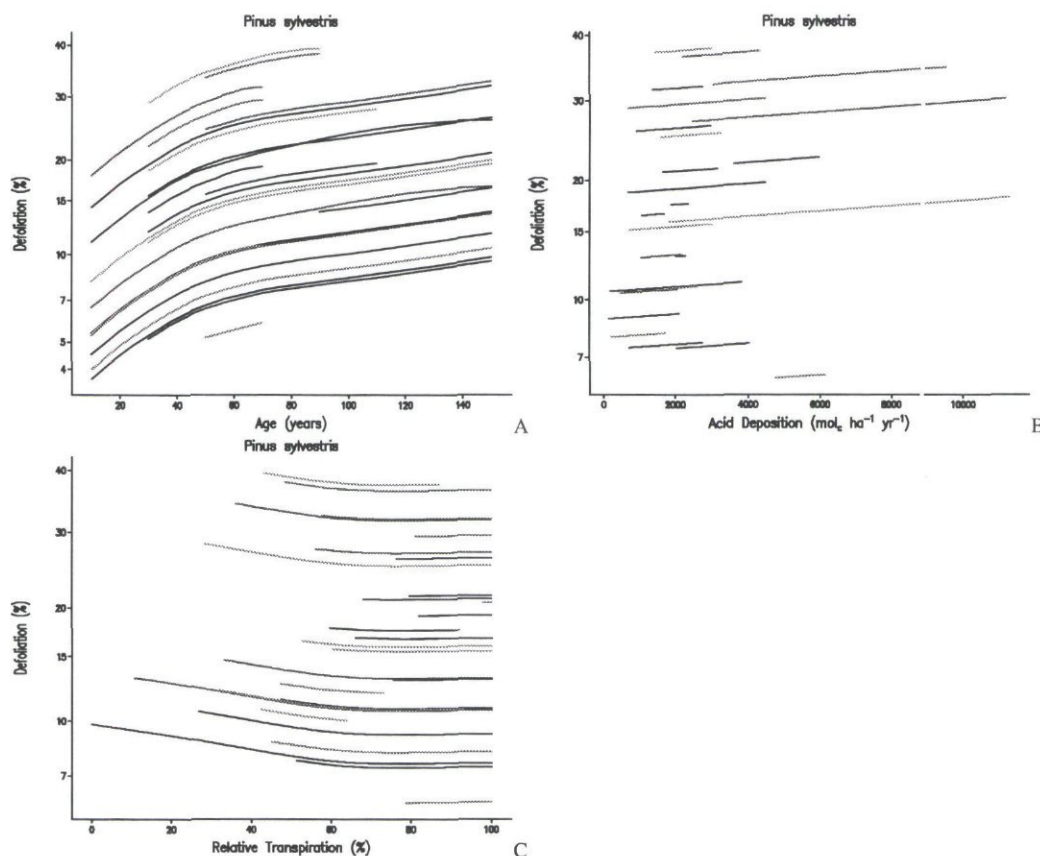


Fig. 50 Illustration of the relation between the included predictor variables (A: age, B: acid deposition and C: current year relative transpiration) and the defoliation for *Pinus sylvestris*. The values for each separate predictor are corrected for the variation in the other predictors. Each line represents a different country.

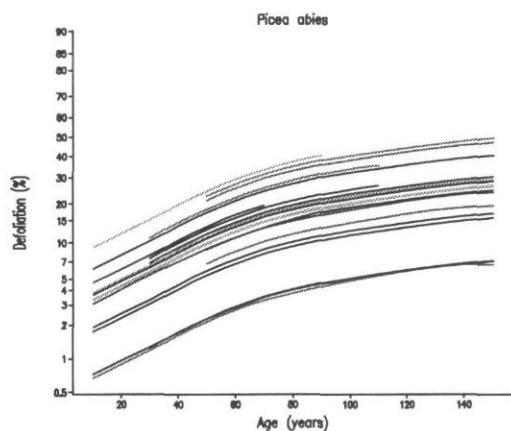


Fig. 51 Illustration of the relation between the included predictor variables (age) and the defoliation for *Picea abies*; each line represents a different country

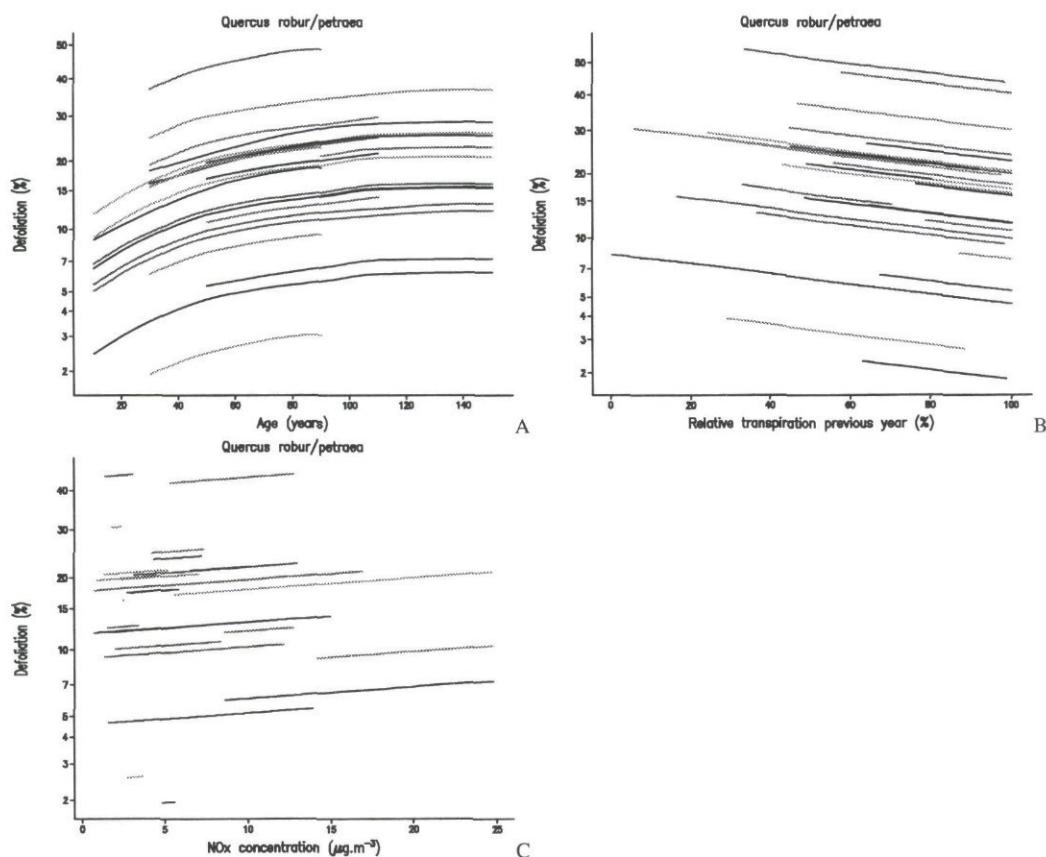


Fig. 52 Illustration of the relation between the included predictor variables (A: age, B: previous year relative transpiration and C: current year  $\text{NO}_x$  concentration) and the defoliation for *Quercus robur* and *Quercus petraea*. The values for each separate predictor are corrected for the variation in the other predictors. Each line represents a different country.



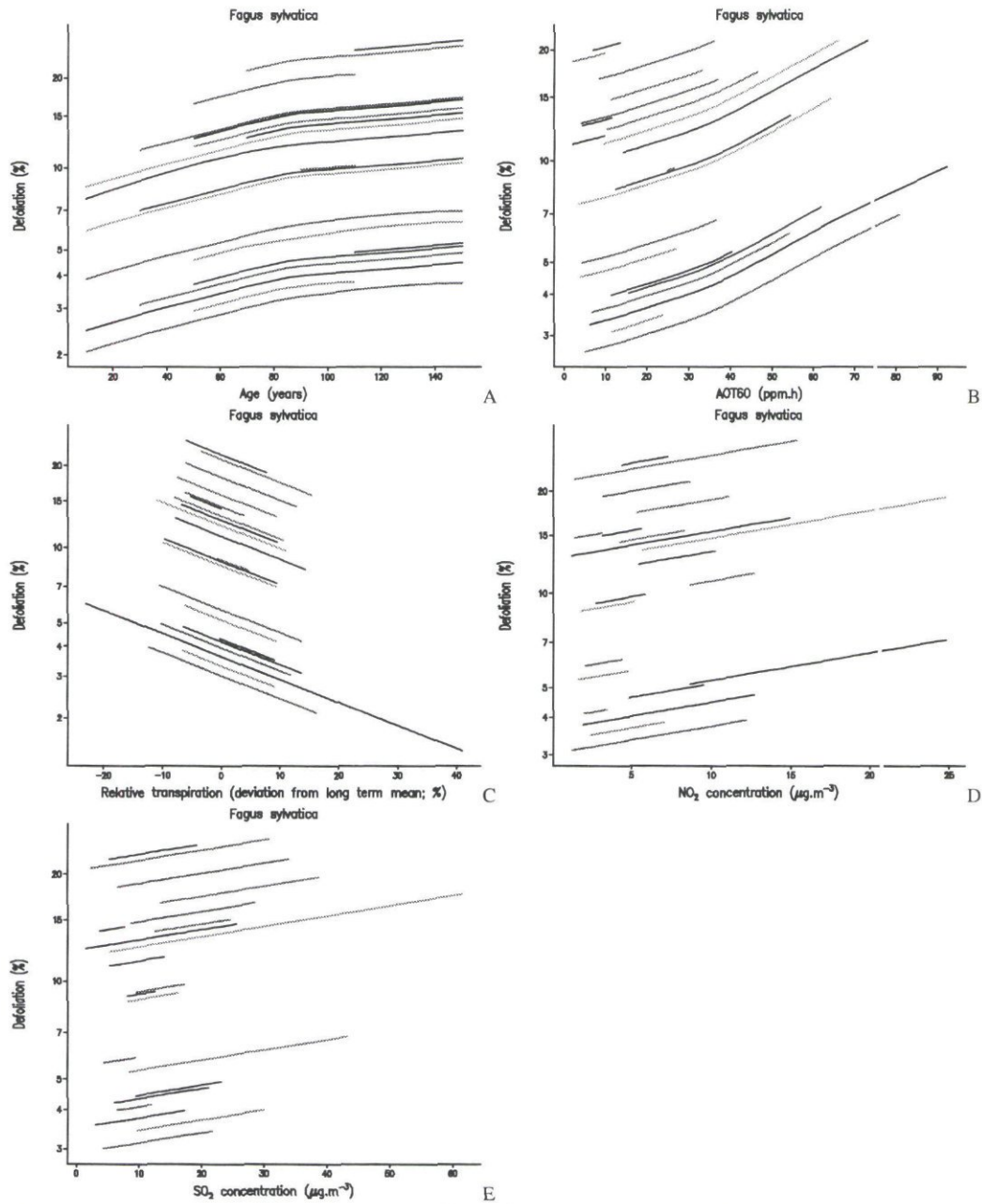


Fig. 53 Illustration of the relation between the included predictor variables (A: age, B: AOT60, C: the lagged effect of relative transpiration and the current year concentrations of SO<sub>2</sub> (D) and NO<sub>x</sub> (E)) and the defoliation for *Fagus sylvatica*. The values for each separate predictor are corrected for the variation in the other predictors. Each line represents a different country.

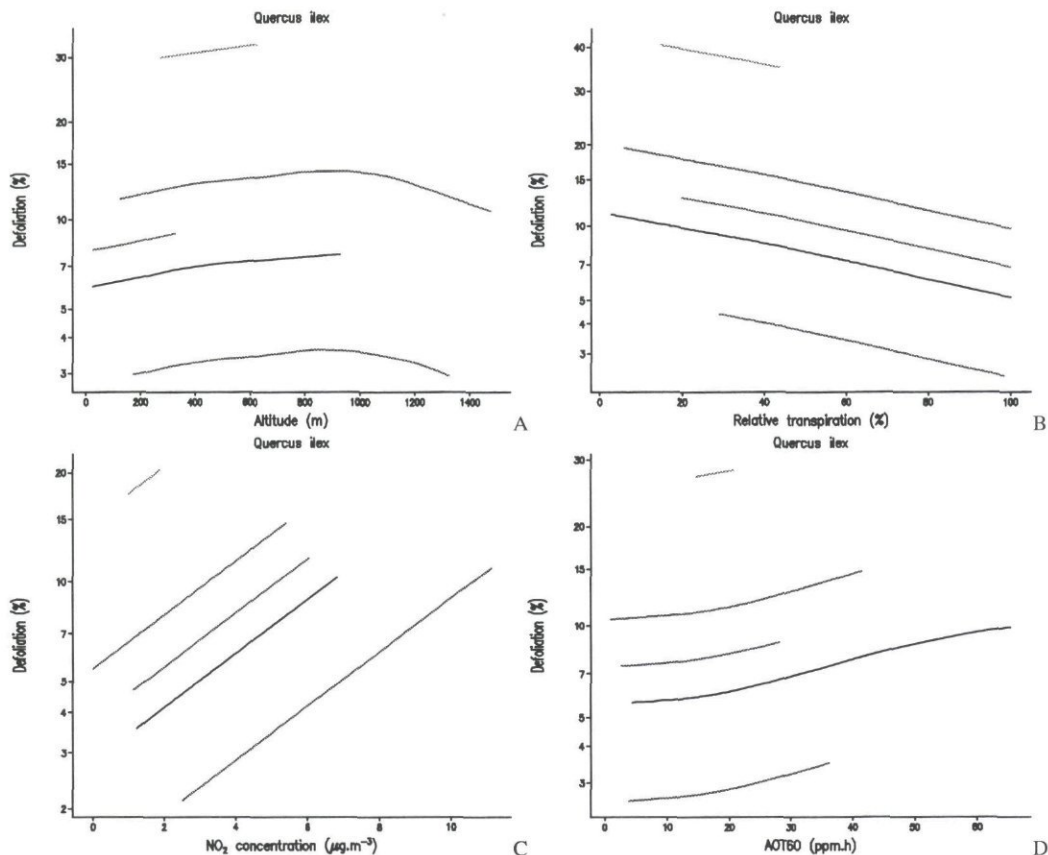


Fig. 54. Illustration of the relation between the included predictor variables (A: altitude, B: current year relative transpiration, C: NO<sub>x</sub> concentration and D: AOT60) and the defoliation for *Quercus ilex*. The values for each separate predictor are corrected for the variation in the other predictors. Each line represents a different country.

Graphs, like the ones given above, offer good possibilities for the further analysis of the data. Furthermore such figures may help in making selections of the data base on which certain relationships can be investigated in more detail. For example, the data can be limited to either the flat part or the steep part of the line in the two left hand figures.

### 7.3.3 Analysis of the changes in defoliation (Model B)

This section gives a short overview of the relationship between the yearly change in the observed crown condition data and the measured and modelled site and stand characteristics and stress factors (Model B). More detailed information on the outcome of the various statistical models and sub-models can be found in Annex 5 (Section A5.3).

The results of the standard model (B-1.0) by which the change in defoliation was correlated with all predictor variables shows that hardly any significant plausible correlations were found (Table 33). Where-ever any relationships were found, the explained variance was considerably less than for the relationships with actual



defoliation. The explained variance was even worse than for Model A without country. Only for *Picea abies* and *Fagus sylvatica* relationships were found that pointed in the expected direction. For these species there was an increase in defoliation after the occurrence of extreme heat and of drought (respectively) in the years before the defoliation assessment. For the other species only unexpected relationships were found or even no relationships at all (e.g. *Quercus ilex*). Unexpected relationships with stress in preceding years can, however, be explained by recovery of the tree in the current year, instead of the lagged effect itself.

Country appeared still to be an important predictor for the change in defoliation for *Pinus sylvestris* and *Pinus sylvestris*. This was not expected, since this model was introduced to exclude country effects. The results, however, showed that for these species the predictor country is even more important than any other combination of predictors. For the other species the predictor country is also better than any other single predictor variable.

Table 33 Composition and explained variance of the best fit of reference Model B-1.0

Tree species	Observations	Selected predictors from Model B-1.0	R <sup>2</sup> <sub>adj</sub> (%)
<i>Pinus sylvestris</i>	6471	( <i>SumX<sub>del</sub></i> ), ( [NO <sub>2</sub> ] )	2.9
<i>Picea abies</i>	4745	( Heat <sub>lag</sub> )	0.7
<i>Quercus robur+petraea</i>	3555	( <i>SumX<sub>t</sub></i> )	0.5
<i>Fagus sylvatica</i>	2933	( RelTrans <sub>del</sub> )	0.6
<i>Quercus ilex</i>	1263	-	0.0

Legend: Underlined = contribution > 2%; Normal = contribution 1-2%; (Between brackets) = contribution 0.5-1%;

*Italics* = unexpected sign

#### 7.3.4 Analysis of trends in defoliation (Model C)

This section gives a short overview of the relationships between the trend in the crown condition data over the observed years and the measured and modelled site and stand characteristics and the mean values of and the trends in the modelled stress factors (Model C). More detailed information on the outcome of the various statistical models and sub-models can be found in Annex 5 (Section B5.4).

The explanation of the variability in the trend in defoliation is better explained by the available predictor variables than the changes in defoliation, although the explained variance is still very low (Table 33; compare with Table 32). The resulting explanatory models contain several elements with 'unexpected' signs. Contrary to the analysis of changes, the signs can not easily be explained.

For *Pinus sylvestris* the variation in the trends could only be related to the climatic region and the occurrence of late frost, if only the expected signs are taken into account (Table 33 and Annex 5, Table A30). This means that the increase in defoliation is larger when there is more late frost. For *Picea abies* and *Fagus sylvatica*, the increase in defoliation is stronger when the heat index is high. For *Picea abies* this increase is also correlated with continuous drought (xRelTrans). For *Quercus robur* + *Q. Petraea* the trend in defoliation seems to be correlated with the C/N ratio and with an increasing

winter index. For *Quercus ilex* no clear relationships of the trend in defoliation with the stress factors could be distinguished.

As with the changes in defoliation, the trends in defoliation are also correlated with the predictor 'Country', with an explained variance of 5 to 15%, depending on the tree species. This means that this measure did also not completely fulfil one of the objectives for which it was introduced. The relatively strong correlation with country indicates that there is either (i) a clear regional spatial pattern in the trends in defoliation or (ii) a gradual change in the standard for the reference tree in several countries.

Table 33 Composition and explained variance of the best fit of reference Model C-1.0

Tree species	Observations	Selected predictors from Model C-1.0	R <sup>2</sup> <sub>adj</sub> (%)
<i>Pinus sylvestris</i>	1825	<u>xSumX</u> , <u>x[NO<sub>2</sub>]</u> , ( <u>d[NH<sub>3</sub>]</u> )	3.8
<i>Picea abies</i>	1576	( <u>xHeat</u> ), ( <u>xSumX</u> ), ( <u>dWinX</u> ), ( <u>xL-Frost</u> ), ( <u>dRelTrans</u> )	3.4
<i>Quercus robur+petraea</i>	823	( <u>dWinX</u> ), ( <u>C/N</u> ), ( <u>d[NH<sub>3</sub>]</u> ), <u>dSumX</u>	3.4
<i>Fagus sylvatica</i>	765	<u>dHeat</u>	0.7
<i>Quercus ilex</i>	206	<u>xWinX</u>	1.4

Legend: x\_\_ = mean value of stress factor; d\_\_ = trend in stress factor; Underlined = contribution > 2%; Normal = contribution 1-2%; (Between brackets) = contribution 0.5-1%; *Italics* = unexpected sign

## 7.4 Discussion and recommendations

As stated earlier, the statistical analysis presented in this chapter forms a pilot study within a broader analysis of the data. The results show (i) that it is worthwhile to make further investigations of the relationships, since there are indications that various stress factors have significant impact on the observed crown condition and (ii) that improvement may still be achieved in the following fields:

- other response variables based upon the same defoliation data;
- improvement of both the defoliation data and the predictor variables;
- the use of additional data that are not yet included in the analysis;
- improvement of the statistical techniques, including the full incorporation of temporal and spatial correlations and the separate analysis of more homogeneous subsets;
- a better link with the information collected at the Intensive Monitoring network and the Integrated Monitoring network.

The various aspects, which are foreseen in a more comprehensive study on this topic, are discussed in detail below.

### *Alternative response and predictor variables*

In this study the analysis was completely based on the mean value per plot (per tree species per year) as response variable. Also the changes and trends were calculated on the basis of this variable. It is, however, still possible to calculate alternative response variables from the same defoliation data. In this context, an analysis was already carried out using the share of trees at the plot that had a defoliation above 10% or above 25%. The results for *Pinus sylvestris* for the year 1995 were in line with the results already found for the actual mean defoliation. Other possible response variables are the 10 and



90 percentiles of the defoliation per plot, the width of the range of defoliation values per plot, etcetera. Furthermore, an analysis of (the trend in) the defoliation of (a selection of) individual trees may offer additional perspectives. Similarly alternative predictor variables, which indicate the same stress (meteorological stress or air pollution) in a different way, can also be assessed.

#### ***Improvement of available data***

The defoliation data were collected by different countries using different standards. In the current study, the systematic differences between the countries were estimated from the available data, by including country as a predictor variable. It would, however, be better if the results from inter-calibration exercises could be used instead. It is, therefore, strongly advised that the inter-calibration exercises (which are described in Chapter 2 of Part A of the Overview Report; Müller-Edzards et al., 1997) will be continued. This procedure should eventually lead to a key by which the data from the separate countries could be made comparable. On the other hand, it is very important that the individual countries stick to their own methods and do not gradually or abruptly change their reference trees, since such a change may seriously hamper the analysis of the trend in defoliation data and may also hamper the derivation of a solid key between the various standards.

Further improvement is possible in the predictor variables, both the ones that are actually assessed at the plots and the ones that are interpolated, extrapolated or model-derived (Chapters 8 and 9). An example of the first category is the completion of missing data on the age or an indication of the dominant age class at the plots with age class 'irregular'. Insufficient information on this issue appeared to be an important problem for the analysis of *Quercus ilex* in the current study. It is recommended that this information can be completed at the next forest condition assessment for the plots that are still in the programme.

Improvement of the preciseness of the model-derived predictor variables might also contribute to a better estimation of the relationship between stress factors and defoliation, especially as long as the predictor 'country' has to remain in the model, since this hampers the transnational comparability of the data set. Furthermore, the use of ozone data for only one year might have hindered a proper analysis of the relationship between defoliation and this important factor. The derivation of ozone data for all other years with defoliation data is therefore strongly advised.

#### ***Use of additional data***

Unsuccessful fits may be caused by factors that strongly affect the response but that are not available or only partly available (e.g. data on pests and diseases) for inclusion in the analysis. If the values of such factors can easily be made available for all sites it is preferred to include it as a predictor in the analysis. Reliable site-specific information on biotic stress factors, such as pests and diseases, might well be the most important information that was lacking in this analysis. It is recommended that the recording of these features (which is done at the forest condition assessment) will be improved. Possibilities to use existing data bases on forest sanity should be explored. Furthermore, it is important to obtain information on the forest structure, with relationship to

competition and management, and the provenance of the trees planted. Whenever this information is available in the separate countries, it would be worthwhile to include this information in the analysis.

Furthermore, it is expected that information on the foliar content may improve the possibilities for a better correlation between the various stress factors and forest condition (defoliation, possibly also discoloration). The foliar composition is considered an important intermediate factor between soil conditions and air pollution on the one hand and the crown condition parameters on the other hand.

#### ***Improvement of statistical techniques and models***

The statistical models applied in this pilot study had a relatively simple structure by excluding temporal and spatial correlations. The techniques to implement these correlations in the statistical model were still under development during the execution of this preliminary analysis. It is, however, expected that these techniques will be available in a later stage. Additional techniques may offer possibilities for a better understanding of already found relationships or may reveal relationships that were not found in the current models. In the consecutive phase more appropriate models can be accomplished.

In the consecutive phase the temporal and spatial correlations will be included fully by using more advanced statistical techniques, including the longitudinal aspect of the data. This is necessary, because not including these correlations would cause a considerable overestimation of the significance of the explaining models which could lead to an incorrect selection of relevant predictor variables. However, the prosperity of the analysis including these correlations depends highly on the results of this pilot study. The exploration of this 'systematic part of the analysis' in this pilot study is an important tool for the selection of a more limited set of predictor variables which can be used in the consecutive phase, in which the significance of the pre-selected relationships can be tested more properly (the so-called 'stochastic aspect' of these models).

The statistical analysis had been carried out in a very short time. It was not possible to analyse all relationships or to perform in-depth studies of the found relationships. A further analysis of the data is, therefore, strongly recommended. Graphs, like the ones shown in Fig. 47-51, offer a good opportunity to have a quick view on the impact of the relationships that were found in the statistical analysis. Furthermore, such graphs may help in the selection of a homogeneous subset which may offer better possibilities for the investigation of certain relationships. In previous studies (e.g. Nellemann & Frogner, 1994) a stratification of the data set to more homogeneous subsets reduced the number of factors that affect the defoliation, which facilitated the interpretation of the results.

#### ***Link with the information of Intensive Monitoring and Integrated Monitoring***

The monitoring at the Level 1 is based on the yearly assessment of the defoliation and discoloration only, with only few additional variables. The current study links these variables with site-specific estimates of various predictor variables. At the plots of the Intensive Monitoring and Integrated Monitoring Programmes, many of these variables



are actually measured (UN/ECE and EC, 1997b; De Vries et al., 1997). The results of this study may be used as a basis for the evaluation of the far more precise data gathered at the two other levels of monitoring. On the other hand, the data of these two monitoring networks might be useful for the validation of the estimations of the variables for the current study.

## 7.5 Conclusions

1. The statistical analysis of the relationship between crown condition (defoliation; the response variable) and site and stand characteristics and meteorological and anthropogenic stress factors (predictor variables) was carried out, using multiple regression analysis. This analysis was preceded by an analysis of the correlations between various predictor variable, in order get better insight in possible confounding. Whenever it was expected that unexpected predictors were selected due to confounding, the explaining model was 'improved' by testing which 'better'(more expected) factors could replace the unexpected one, without losing significance.
2. The correlative exercise between the predictor variables showed that there are rather strong correlations between (i) the time-dependent air pollution variables, (ii) the predictor 'Country' and most meteorological and air pollution variables, especially when the mean values over the 10 year period are considered and (iii) the various temporal alternatives of the same meteorological or air pollution variables. For the meteorological variables this could be counteracted by using the deviation from the long-year average values. Especially the strong correlation with country can cause confounding or mis-interpretations, as shown by the subsequent regression analyses, e.g. for the correlation between acid deposition and crown condition for *Pinus sylvestris*.
3. The analysis of a large number of alternative statistical models and the subsequent in-depth analysis of the data resulted in the following selection of additionally relevant predictors: average acid deposition and current year's relative transpiration for *Pinus sylvestris*, current year's SO<sub>2</sub> concentration for *Picea abies*, current year's relative transpiration and SO<sub>2</sub> concentration for *Quercus robur* + *Q. petraea*, the AOT60, the current year's SO<sub>2</sub> concentration and the lagging term of the relative transpiration for *Fagus sylvatica* and the current year's relative transpiration, SO<sub>2</sub> concentration and NO<sub>2</sub> concentration for *Quercus ilex*.
4. The results using the current year data as response variable showed a strong relationship with 'Country' with an explained variance between 35 and 39%. Age additionally explained 2-14% depending upon tree species. This exception is probably due to the 'irregular' age at many of the plots with *Q. ilex* combined with some missing values for age.

5. Omitting country can facilitate the selection of relevant predictor variables but also easily lead to the selection of irrelevant predictors and to an incorrect estimation of the regression coefficients, although the resulting models contained more meteorological and air pollution variables than models with country. The within-country variation in the most important stress factors was only weakly correlated with crown condition. It is not clear whether this is the reality or whether it is due to the rough derivation of the stress factors. The visual resemblance between maps with forest condition data and stress factors could therefore also be related to the different reference levels in the individual countries.
6. A further exploration of the analysis of subsets could probably reveal the investigated relationships more precisely, since many 'irrelevant' observations (but with a lot of noise) can be excluded. Also the selection of alternative response variables, based on the observed defoliation data, might offer additional opportunities to reveal more relationships or to optimise already found relationships. Finally, the outcome of the analysis can be further improved by (i) the addition of data that are presently not available (e.g. on pests and diseases and on foliar composition), (ii) the implementation of temporal and spatial correlations and (iii) the improvement of various variables.



## 8 Discussion

*Jan Willem Erisman<sup>1)</sup>, Wim de Vries<sup>2)</sup>, Erik de Jong<sup>1)</sup>, Erik van Leeuwen<sup>1)</sup>, Jaco Klap<sup>2)</sup>, Kees Hendriks<sup>2)</sup>, Christian Müller-Edzards<sup>3)</sup>*

<sup>1)</sup> National Institute of Public Health and the Environment (RIVM), Bilthoven, The Netherlands

<sup>2)</sup> DLO Winand Staring Centre (SC-DLO), Wageningen, The Netherlands

<sup>3)</sup> Programme Coordinating Centre-West (PCC West), BFH, Hamburg, Germany

### 8.1 Introduction

It is generally accepted that there is a relation between forest damage and natural and anthropogenic stress. Trees have a limited capability of adapting to the change in environmental conditions as a result of anthropogenic activities and show less resistance to natural stress. Through the introduction of tall stacks in the sixties, atmospheric pollution has changed from severe local problems to a large-scale phenomenon. Pollution is, however, much diluted and the relation between forest damage and anthropogenic stress has become less obvious. It has become difficult to determine direct causal relationships between causes and the effects.

The strength of the available crown condition dataset is its temporal and spatial coverage which should make it possible to derive empirical relations. It was expected that within the data base crown condition, stress factors and combinations of the two vary so much, that unique situations could be distinguished. An important drawback of the data set is, however, the limited transnational comparability of the crown condition data (response variables) and availability and quality of natural and anthropogenic stress data (predictor variables). It is the first time that site specific meteorological stress data and air pollution data are estimated for all EU ICP Forest Level 1 plots. The data bases and models developed for this purpose became only recently available and have not all been tested with measurements so far. This might form a serious limitation to the study on relationships between crown condition and stress. We will focus this discussion strongly on the quality aspect of the data.

The quality and comparability of the crown condition data is discussed in Chapter 2 of Part A of the Overview Report (Müller-Edzards et al., 1997). In that section it is concluded that the agreement for the four damage classes is generally high, but that it is low for the 5% defoliation classes used in the correlative study. Furthermore, the transnational comparability is limited. In this context a correction factor for countries, which can be derived from inter-calibration exercises, is needed for a comparison of the data on an European scale. Information on such factors is however limited to a few tree species and countries (Section 2.3 of Part A of the Overview Report; Müller-Edzards et al., 1997). The limited comparability of the defoliation data hampered the statistical analyses of empirical cause-effect relationships between defoliation and environmental stress factors. It led to the need to include 'country' as a predictor variable, which means that the effect of the within country variation in stress factors on defoliation was investigated.

The first part of this section will deal with the uncertainty and the availability of stress data in relation to their use in deriving relationships with crown condition. In the second part the derived relationships between crown condition and stress will be discussed.

## **8.2 Quality of stress data**

### **8.2.1 Introduction**

The availability and the quality of stress data determines to a large extent the significance of the relation between stress and defoliation. As stated before, this is especially the case since the use of 'country' as a predictor implies that only the variability in stress factors within countries is included in the statistical relationships (Chapter 7). The factors influencing defoliation are listed in Table 1. The stress factors are usually derived from measurements or model input data. The accuracy of the measurements determine the accuracy of the stress factors used in the study to a large extent. Extra uncertainty is added through the use of interpolation techniques and process based models. In this section the uncertainty in site characteristics, meteorological data and meteorological stress factors, and air pollution stress (concentration and deposition data of SO<sub>2</sub>, NO<sub>2</sub>, NH<sub>3</sub> and O<sub>3</sub>) will be discussed, all in relation to its use in deriving relationships with crown condition.

### **8.2.2 Site characteristics**

Stand and site characteristics that influence crown condition are tree species, tree age, local climate, altitude, soil type and water availability (UN ECE, EC, 1995, 1996). The variation in these factors is very large, and the data can be grouped in several ways providing common factors in relation to variation in stress factors. This improves the statistical analysis. Most of these factors are available from the observations at the plots. The uncertainty arising from grouping or averaging of site data is largest for plots with mixed species. The averaging of e.g. the Leaf Area Index or tree height for these sites leads to large uncertainty, especially for the relative transpiration rate. For the calculation of deposition, tree heights form an important input parameter. Tree heights were derived from the age, species and soil type using yield tables. The uncertainty of the obtained results is relatively high. Furthermore, extrapolation of pH, base saturation and C/N ratios to sites where no measurements were taken leads to large uncertainty in certain areas (e.g. Sweden, Poland, etc.). Systematic errors might be introduced in these areas, because the soil maps used for interpolation in these areas are of a low quality. These factors affected the spatial pattern of calculated critical acid deposition levels in these areas.

The extrapolation of pH, base saturation and C/N ratios to plots where no measurements were taken is hampered when the interpolation of soil types is based on the FAO soil map of Europe 1:5 000 000 (e.g. countries in Northern and Eastern



Europe). This will affect the spatial pattern of calculated critical acid deposition levels in these areas.

Soil type and climate determine the pH and base saturation to a very large extent. An impact of acid deposition levels on the actual values of soil parameters could therefore not be substantiated on a European scale in a correlative study. Use of threshold values for pH or acid inputs did not improve the correlation. A similar correlation study between the total N deposition and the C/N ratio, also including several thresholds, did not result in high correlations. These results were similar for the humus layer as well as the mineral soil layer. It is not so remarkable, however, that the calculated correlation coefficient between the calculated site specific annual average acid deposition over the considered 10 year period and measured pH values in the mineral layer is negligible. This can be expected when absolute values of soil chemical data are used, since their order of magnitude is soil type and climate determined. When data on changes in soil chemical properties in time (such as decrease in pH) come available through repeated soil surveys, a relationship with acid deposition is much more probable.

### **8.2.3 Meteorological stress**

The data set of the meteorological stress factors is formed by interpolation of measured meteorological observations. Several data bases had to be combined in order to cover the complete period of 1980 - 1995. The uncertainty in the final interpolated data is large, especially for precipitation. For this component only invalidated measurements were available. Regional precipitation is overestimated in large parts of Europe and underestimated in some other regions, e.g. France. Cross validation showed that the uncertainty in meteorological data is lowest for temperature, wind speed and relative humidity and highest for precipitation. Uncertainty determined with cross validation is on the average 100%. This large uncertainty has a large impact on the uncertainty in the relative transpiration rate and in the critical deposition level estimates. In areas where the precipitation amount is overestimated, the transpiration reduction is underestimated. In addition to this, long-term averaged regional data were used as input for the model to calculate the relative transpiration, because of lack of actual local data. Together with uncertainty in model parameters this forms an extra uncertainty. As this is the most important drought stress indicator, an effect of drought stress on defoliation is hampered. The relative transpiration estimates are not evaluated using measurements. Encouraging is the fact that the spatial and temporal variation are as expected from expert knowledge. The temperature indicators are more accurate, as the uncertainty in the interpolated temperature values is lower.

### **8.2.4 Air pollution**

An effect of exceedances of critical concentration levels of NO<sub>2</sub> and NH<sub>3</sub> on defoliation is not expected because critical levels are not exceeded in accordance with the procedure used. This result might be biased, however, since the spatial and temporal

resolution of the modelled concentration is too poor and the concentrations, especially of  $\text{NH}_3$ , are underestimated to a large extent. This is mainly the case in or near source regions, i.e. for  $\text{NH}_3$  in areas with intensive livestock breeding and for  $\text{NO}_2$  and  $\text{SO}_2$  in industrial areas. In The Netherlands, parts of France and Denmark the  $\text{NH}_3$  concentrations are clearly underestimated. Regional concentrations up to  $2 \mu\text{g m}^{-3}$  are modelled, whereas local observations show annual averages of up to  $20 \mu\text{g m}^{-3}$  (e.g. Erisman, 1995).  $\text{SO}_2$  concentrations are also underestimated in or near to source areas, though to a lesser extent.

The deposition estimates are subject to many uncertainty sources. It was one of the aims of this project to compare site specific deposition estimates with throughfall measurements. The comparison shows that the average modelled values for the 296 sites are significantly different from the deposition values derived from throughfall measurements. Site specific values for total potential acid or total nitrogen deposition can differ up to a factor of two from those derived from throughfall. Despite this, the correlation between modelled deposition and measured throughfall values is high for nearly all components. Deposition estimates from throughfall data have uncertainty because of canopy exchange processes. The uncertainty is larger for components with much canopy exchanges, such as nitrogen components and base cations, than for components with very little exchange, such as sulphur and sodium.

The uncertainty in regional scale estimates of deposition, estimated by error propagation, is large and varied between 90 and 140% depending on the compound and the region. A comparison between plot specific modelled deposition and deposition derived from throughfall data, collected for as many sites in Europe and as many years as possible, showed that absolute values differed significantly for almost all compounds. There was however a significant correlation between the modelled deposition and throughfall for most. Apart from the stochastic uncertainty in the calculated air pollution, the concentration and deposition levels for N, especially for  $\text{NH}_3$ , compounds were systematically underestimated for plots located in or near to source areas.

Ozone concentrations and AOT40 levels were derived for the forest sites in a very late stage of the project. The methods to derive small scale estimates in Europe are only developed recently. A thorough validation of the model results have not yet been performed. A first look at the distribution of ozone concentrations looked acceptable. Furthermore, a comparison between the growing season average modelled data and those measured at seven stations agreed very well. The uncertainty in data is, however, not quantified. Furthermore, only for one year calculations could be done, because of lack of emission and modelled concentration data which serve as input for the EDEOS model.

The uncertainties in the calculated critical deposition levels for nitrogen and acidity are large due to uncertainties in the assumed values for critical N leaching rates or critical  $\text{Al}/(\text{Ca}+\text{Mg}+\text{K})$  ratios in relation to effects, model assumptions and input data. High critical N-deposition levels in Central Europe, for example, may be biased by the description of N-immobilisation as a function of N-input. On average the uncertainty



likely varies between plus and minus 50%. The uncertainty in critical deposition level exceedances, which is affected by uncertainties in both present loads and critical deposition levels is very high. The calculated high exceedances in Central Europe are, however, quite reliable considering air pollution measurements in this area.

### **8.3 Relationships between crown condition data and stress**

This section first discusses the results of the correlative study in the current study, followed by a comparison with existing theories about forest decline and some final remarks are made.

#### **8.3.1 Correlative studies with European data**

It was expected that the large temporal and spatial variation in crown condition, together with the large variation in stress factors would enable the identification of empirical relations between crown condition and stress factors. The low transboundary comparability of the defoliation data and the uncertainty in the stress factor estimates seriously hampered the clear revelation of the relevant stress factors. However, several clear relationships were revealed on top of the 'country' parameter as a source of variation, including relative transpiration and concentrations of SO<sub>2</sub>, NO<sub>x</sub> and NH<sub>3</sub>. When using the actual defoliation data, country is the predictor variable explaining most of the variation in crown condition. When using the changes and trends in defoliation for each plot as the effect parameter, the country effect, is much less and other predictor variables become important, such as age and relative transpiration, but the variance accounted for is very low (below 10%).

There are several reasons for explaining these results. One obvious reason is the time frame in which this pilot study was executed. This was too limited to develop more accurate methods and/or to test several statistical methods and use e.g. stratification of the data. Furthermore, the problem itself is not straightforward. If the relations between crown condition and stress factors were so obvious, this study would have been done several years ago and definite answers would be found then. Also, although the best available methods and models were used to determine stress factors, the uncertainty on the local scale is too high to distinguish the local phenomena which are actually taking place. Uncertainty in both the response variables as well as in the predictor variables is not explicitly taken into account. Uncertainty is important, because statistical relationships might 'drown' in large local noise. Furthermore, if a stress factor is poorly estimated, it will not come out as an important factor, leading to mis-interpretations. Finally, several factors influencing crown condition data were not taken into account: trees showing mechanical damage (e.g. windbreak, snowbreak, etc.) are excluded from the samples; stress due to diseases, insects, plagues, etc., and other factors influencing crown condition, such as action of man, fire, grazing, etc. were not taken into account.

There are some other limitations which hampered the correlative study. First of all, the vitality indicator is non-specific. It is questionable if the crown condition data provide good insight in the tree (or stand) vitality. Other effect parameters, such as myccorhiza depletion, changes the ground vegetation effects on roots, etc. may be more indicative for pollution effects. Secondly, air pollution interacts with natural stress, but also with e.g. age, and other tree characteristics. The stress factors are mixtures of static and dynamic stress. Finally, local conditions and variation in conditions including biotic stress strongly affects crown condition. These local factors must be quantified accurately enough. The possibilities for future studies are limited by the accuracy of the data. The crown condition data must be corrected for country effects, or other systematic differences between observers when used for studies deriving cause effect relations. The monitoring period is still not long enough to eliminate natural variability and to detect significant trends due to anthropogenic stress factors without grouping the data. The uncertainty in stress factors must be reduced, e.g. by incorporating local concentration variations due to nearby sources or source areas and to more accurately incorporate local factors influencing deposition, water stress and exposure to pollutants. The statistical methods are only explored to a limited extent. It should be determined whether stratification of the data would improve the outcome, or selection of only the most accurate data would help. Also inclusion of biotic factors and using non-linear relationships might improve results.

### **8.3.2 Evaluation of relationships and comparison with existing hypothesis on forest decline**

The aim of this section is to integrate the results on the degree of the actual defoliation and defoliation trends reported in Chapter 2 of this study with information on major stand and site characteristics and stress factor reported in Chapters 3-6 for the six selected tree species. The interesting question is what the major stress factors are for the considered tree species and whether these stress factors were found to be significant in the correlative study performed (Chapter 7). If for example the exposure of a stress factors is much stronger for species A than for species B, it should be expected that this stress factor would be significant for species A.

The table below shows an overview of the major natural and anthropogenic stress factors and the response variables (actual defoliation and defoliation trends) for the considered tree species in the correlative study. Stress factors explaining the variation in defoliation in the correlative study are shaded. Stress factors are reported as being high, intermediate or low, by comparing them between the various tree species. The country effect, which dominates the variance accounted for in the different models is not included, because this is mainly ascribed to methodological differences in the crown condition assessments. Age is considered as a natural stress factor, although it is very likely that the effect of age is enhanced by anthropogenic stress factors reducing tree resistance.



The table shows that in general defoliation is mainly affected by tree age and drought as natural stress factors, and SO<sub>2</sub> and NO<sub>x</sub> as anthropogenic stress factors. The results are in line, but do not support one general hypothesis on the increase in defoliation. *Quercus petraea* and *Fagus sylvatica* show relatively high trends in defoliation. These species are exposed to high air pollution levels, combined with medium meteorological stress. High defoliation trends are also shown for *Quercus ilex*. The air pollution stress is relatively low for this species, whereas meteorological stress is high. *Pinus sylvestris* shows a small trend in defoliation, and air pollution and meteorological stress is low to medium. However, soil pH is low and exceedance of critical deposition levels are high (poorly buffered soils). Acid deposition is found as a predictor variable for defoliation for this species. *Picea abies* does not show a trend in defoliation. Even though the exceedance of the critical deposition level is high and soil pH is low, as with *Pinus sylvestris*, the meteorological stress is relatively low.

Table 34 Natural and anthropogenic stress factors affecting the individual tree species

Species	Predictor variables													Response variables		
	Stand and site characteristics	Soil		Meteorology					Air pollution				Deposition	Defoliation		
		pH	C/N	Winter index	Late frost	Summer index	Heat index	Relative transpiration	SO <sub>2</sub>	NO <sub>x</sub>	NH <sub>3</sub>	O <sub>3</sub>	Acidity	Nitrogen <sup>1)</sup>	Actual value	Negative trend
<i>Pinus sylvestris</i>	age	-	+	+	+	0	0	+	0	0	-	-l	0/h	0	+	0
<i>Picea abies</i>	age	-	+	+	0	-	-	+	0	0	-	-l	0/h	0	+	-
<i>Quercus robur</i>	age	0	0	0	+	0	0	0	+	+	+	+h	+l	+	0	+
<i>Quercus petraea</i>	age	0	0	0	+	0	0	0	+	+	+	0/h	+l	+	0	+
<i>Fagus sylvatica</i>	age	0	0	0	-	0	0	0	+	+	+	+h	+l	+	0	0
<i>Quercus ilex</i>	altitude	-	-	-	+	+	+	-	-n	-n	0	0/h	=l	-	-	+

Legend: +=high, -=low, 0=intermediate; signature behind slash: h=high, l=low, n=no exceedance of critical threshold; shaded fields indicate factors that in this study significantly affected the condition of this species

<sup>1)</sup> Exceedances of nitrogen calculated in this study are related to understorey and ground vegetation, and therefore effects on crown condition are not reliable.

It is clear from the results of this report that there are spatial and temporal trends in crown conditions, generally showing an increase in defoliation. The extent of the increase is different in parts of Europe and for the different tree species. From the studies performed by the NFC's, the comparison of exceedances of critical levels with trends in defoliation and from the correlative study a clear effect of natural stress, site characteristics and air pollution is shown. More specific, an effect of tree age, drought and ozone critical level and acid critical deposition level exceedance was demonstrated. The effects are, however, strongly dependent on site factors and no uniform relations could be obtained. These results are generally in line with other correlative studies, such as those by Mather (1994), Nellesmann et al. (1994), Hendriks et al. (1997) etc. It is generally also in line with the different hypotheses given in the introduction of this report (Section 1.3), i.e. not one single factor is responsible for the deterioration forest condition in Europe. Many processes play a role, with all different contributions to the

forest condition in different areas. Furthermore, many single hypotheses were related to the condition of the forest *ecosystem* and not on the forest trees.

### 8.3.3 Final remarks

One of the conclusions is that limited transnational comparability and the uncertainties in the derived site and stand characteristics, air pollution and meteorological stress hampered the analysis of the variation in crown condition data. It is difficult to quantify the uncertainty in the assessment of individual observations. This is necessary to be included in the regression analysis in order to judge the results. It has never been the aim of the ICP on forest to derive cause-effect relations using the Level 1 data. The Level 2 plots were extended with measurements which should provide more insight in such relations. However, the large data base covering large parts of Europe and, for some countries, ten years of crown condition data provides a unique opportunity to derive empirical cause-effect relations. Such studies will, however, always be dependent on external data bases, to provide estimates of the natural and anthropogenic stress data which are not measured at the Level 1 plots.

It is the first time that external data bases were used to study the relation between crown condition and stress factors on the European scale. This study, which was executed under much time pressure, has provided some very important insights. It is concluded that the uncertainty in site specific stress estimates need to be reduced, but also the systematic country differences in application of the crown condition assessments need further attention. For the improvement of site specific stress estimates Level 2 will provide data which might serve for validation, or calibration of models. It is in this respect important to safeguard the quality and comparability of the measurements. Furthermore, because the measurements are limited, continuity is needed to become long-term data, reflecting variability and trends. It is in this respect also important to seek connections with other monitoring activities in Europe and on the national level.

The selected stress factors need further refinement. One possibility for this is to work-out hypothesis on forest decline and its causes. Again Level 2 data are suitable for this, next to existing literature and studies where intensive monitoring was performed. When more or improved results are obtained for the five tree species which are used in this study, the empirical relations might be tested on the other tree species.



## 9 Conclusions

Wim De Vries<sup>1)</sup>, Jan Willem Erisman<sup>2)</sup>

<sup>1)</sup> DLO Winand Staring Centre (SC-DLO), Wageningen, The Netherlands

<sup>2)</sup> National Institute of Public Health and the Environment (RIVM), Bilthoven, The Netherlands

In this chapter we draw conclusions from the results presented in the previous chapters. This is the first time that the ICP crown condition data have been used in a pilot study to relate them to estimates of stress factors using external data bases. Note that the term pilot study was used, since it has never been the aim of the Level 1 assessments to determine empirical cause-effect relationships. The aim of this pilot study was to correlate the crown condition data with natural and anthropogenic stress factors using 10 years of crown condition assessments at the Level 1 plots. The crown condition surveys at Level I were related to measured and interpolated data on the chemical soil composition, calculated meteorological stress factors and concentration and deposition levels for sulphur and nitrogen compounds, and ozone. Furthermore, critical level values for the air pollutants under consideration were calculated.

### 9.1 Stand and site characteristics

With respect to the distribution of tree species over major stand and site characteristics can conclude that: (i) stand ages between 20 and 100 years are evenly distributed over the various tree species, except for *Quercus ilex*, where most stands are relatively young (ii) coniferous tree species (*Pinus sylvestris* and *Picea abies*) and the *Quercus* species (*Q. robur* and *Q. petraea*) mainly occur in the lowlands below 500 m (approximately 70-90 % of the sites), whereas *Fagus sylvatica* and *Quercus ilex* are quite evenly distributed over the altitudes between < 250 m up to 1500 m and (iii) coniferous tree species occur mainly on coarse textured poorly buffered sandy soils, whereas the deciduous tree species occur more frequently on fine textured well buffered clay soils and on calcareous soils. Negative impacts of higher altitudes on the crown condition and of high acid loads may thus be larger for coniferous tree species.

### 9.2 Chemical soil composition

Measured values of the pH(CaCl<sub>2</sub>) in the humus layer are generally 0.5 pH unit lower than in the mineral topsoil. Inversely, the base saturation is generally much higher in the humus layer compared to the mineral soil. Acid topsoil conditions, i.e. a pH(CaCl<sub>2</sub>) below 3.5 in the humus layer and below 4.0 in the mineral topsoil, and a base saturation below 25% in the mineral soil, occurs at approximately 40-50% of the sites. It is likely that acid inputs to these soils is buffered by the release of toxic aluminium. Extremely acid topsoil conditions, namely a pH(CaCl<sub>2</sub>) below 3.5 and a base saturation below 10% occurs at less than 10% of the sites. At those sites, acidic deposition will certainly be buffered by the mobilisation of toxic Al. C/N ratios are mostly lower in the humus

layer compared to the mineral soil. C/N ratios in the humus layer below 20, which might indicate enhanced N accumulation, occurred at 10% of the sites.

The FAO soil type explained 68% of the variation in pH and 49% of the variation in base saturation. Using soil clusters, the explanation decreased to 50% and 37%, respectively. The spatial pattern of pH and base saturation and C/N ratio over Europe is thus strongly correlated with soil type (parent material class). To a lesser extent, this is also true for the C/N ratio, where soil type explained 11% of the variation. Fine textured (clay) soils and calcareous soil with a high pH and base saturation and a low C/N ratio mainly occur in Southern Europe. Considering the overwhelming effect of soil type and climate on actual pH and base saturation values, an impact of acid deposition levels could not be substantiated, neither be expected on a European scale. The same holds for C/N ratios in relation to N deposition levels. When data on changes in soil chemical properties, such as pH, in time become available through repeated soil surveys, a relationship with atmospheric deposition is much more probable.

### **9.3 Meteorological stress**

The spatial pattern of temperature indices trends are north-south orientated, both in summer and in winter, going from colder northern regions where mainly coniferous species occur to warmer southern regions with mainly deciduous species. The temperature stress indices do not show much variation in time for the period 1985 to 1995. Relative transpiration is lower for deciduous trees in the South of Europe than for the coniferous trees in the North. More than 50% of the deciduous stands experience a relative transpiration rate below 80%. The relative transpiration shows a clear, but complex pattern, coinciding for a large extent with patterns of rainfall and temperature. The absolute values, however, deviate from long-term mean values as used in other pan-European studies. This holds especially for precipitation, which is generally high as compared to other meteorological data sets.

The meteorological stress is overall most severe at higher altitudes, in the north (winter index, spring frost) and south (summer index, heat and spring frost) of Europe. Not all mountainous regions, such as the Alps, are identified in the meteorological stress maps. The reason for this is the absence of meteorological stations in these areas and by interpolation the extreme meteorological values cannot be obtained. The meteorological stress factors are above average in Central Europe (land climate) and are most optimal in coastal areas. Extreme temperatures are rare here because of the influence of the sea. Furthermore, drought stress is generally no problem because precipitation is above average.



## 9.4 Air pollution

Calculated annual average  $\text{SO}_2$  concentrations for all the monitoring sites between 1986 and 1995 varied mainly between 2 and  $50 \mu\text{g m}^{-3}$ . The critical concentration of  $20 \mu\text{g m}^{-3}$  was exceeded at 20% of the monitoring sites. Sites are concentrated in Central Europe, such as Germany, Poland and Czech Republic. A clear reduction in exposure of  $\text{SO}_2$  concentration is shown between 1986 to 1995. During the last three years the concentration remained constant.

Calculated maximum annual average concentrations of  $\text{NO}_2$  and  $\text{NH}_3$  were 27 and  $3 \mu\text{g m}^{-3}$ , which are lower than the critical levels of 30 and  $8 \mu\text{g m}^{-3}$ , respectively. Even though the calculated concentration levels of N compounds ( $\text{NO}_2$  and  $\text{NH}_3$ ) are underestimated, it is clear that direct above-ground effects only play a role at certain local circumstances but not on a European scale.  $\text{NH}_3$  concentrations show no clear trend during the ten years, whereas  $\text{NO}_2$  concentrations decreased very little. As a result, nitrogen deposition decreased somewhat between the ten years. The range in calculated critical N deposition levels related to effects on trees, such as nutrient imbalances and increased susceptibility to drought, frost and diseases/pests was much higher than those related to vegetation changes. (Note that the critical deposition levels as used in this study differ from the critical loads used in the abatement strategies: more detailed information on the differences is given in Section 6.3.2.) Values varied mostly between 1500 and  $2500 \text{ mol}_\text{c} \text{ ha}^{-1} \text{ a}^{-1}$ . These values are hardly exceeded. The calculated deposition levels of N compounds are, however, underestimated.

Available data for high N deposition areas, mainly in Central Europe, indicate that elevated N-deposition is a serious problem in relation to crown condition (nutrient imbalances, elevated susceptibility to natural stress factors etc.) Unlike effects on trees, impacts on the forest understorey can be expected at a much larger scale. The percentage of sites where these critical N deposition levels are exceeded equals 25%, mainly occurring in Central and Western Europe, such as Germany, Poland, the Czech Republic and The Netherlands, where present loads are highest. It is unclear, however, whether the changes in forest understorey are related to crown condition effects. This analysis is valid only for the 10 year period considered. The possible long-term effects due to nitrogen deposition and exposure cannot be eliminated from these results.

The spatial distribution of the acid (S and N) deposition largely resembles the source area distribution. As with the concentration levels of  $\text{SO}_2$ ,  $\text{NO}_2$  and  $\text{NH}_3$ , highest deposition levels are observed in Central and Western Europe. Base cation deposition is largest in coastal areas and in southern Europe. This is mainly due to the main sources, i.e. soil dust, Sahara dust and sea salt. Base cation deposition can compensate almost entirely for the potential acid inputs in the south of Europe, whereas in central Europe it equals about 25% of the potential acid input. Potential acid deposition decreased between 1986 and 1992, but remained fairly constant after 1992. The strong decrease is mainly the result of the decrease in  $\text{SO}_x$  deposition, and to a small decrease in  $\text{NO}_y$  deposition. Calculated critical deposition levels for acidity, which were limited to stands with a base saturation of less than 25% covering 42% of all the monitoring sites, varied in the same range as the calculated present loads. The number of sites where critical

acid deposition levels are exceeded equalled 12% of all sites and 29% of the sites where base saturation was below 25%.

Calculated annual average AOT40 values for O<sub>3</sub> exceeded the long-term critical AOT level of 10 ppm.h at more than 90% of the monitoring sites. The critical level was exceeded for all deciduous forest stands and at approximately 80% of the coniferous forest stands. Even a five fold excess (50 ppm.hr) was calculated for 29% of the plots. The spatial pattern of ozone concentrations show relatively low concentrations in the northern part of Europe, with mostly coniferous forests and relatively high concentrations in the south where *Quercus robur* + *Quercus petraea* and *Quercus ilex* mostly occur. In central Europe, ozone concentrations are highest, specifically in mountainous regions.

## 9.5 Relationships between crown condition and environmental stress factors

*great effect?*  
A first comparison of the observed 10 year average crown condition and the calculated stress factors for air pollution shows a clear coincidence of high defoliation/discoloration and high exceedances of critical levels and deposition levels for sulphur and nitrogen compounds in central Europe.

Results using country as predictor variable showed a strong relationship between defoliation and countries (an explanation of 33- 39 % of defoliation) and age (an increase in explanation between 2 and 13%). Other stress factors that sometimes appeared to be significant, were relative transpiration (*Pinus sylvestris*, *Quercus robur* + *Quercus petraea*, *Fagus sylvatica* and *Quercus ilex*), the concentration of NO<sub>2</sub> (*Quercus robur* + *Quercus petraea*, *Fagus sylvatica* and *Quercus ilex*), the SO<sub>2</sub> concentration (*Fagus sylvatica*) and the ozone concentration (*Quercus ilex*). When using changes and trends in defoliation, the effect of country appeared to be much less significant explaining sometimes up to 10% of the defoliation, however. This implies that different defoliation standards may still have an effect on changes and trends in defoliation. Excluding country as an explaining variable, altitude, various meteorological stress parameters (relative transpiration, late frost, summer index and winter index), and air pollution stress factors (NO<sub>2</sub> and NH<sub>3</sub> concentrations, AOT30 and acid deposition) explained mostly less than 10% of the changes and trends in defoliation. Note that it is not suggested here that the AOT30 or AOT60 values should be used, instead of the AOT40 as critical levels for ozone.

Even though the variability in defoliation on the Level 1 plots is hardly explained by measured and modelled stress factors, this does not mean that there is no such relationship, since (i) the derivation of environmental stress factors was subject to large uncertainties at the local scale, (ii) the transnational comparability of crown condition data is limited induced by the use of different reference trees and (iii) the impact of biotic stress on the defoliation (insect attacks, fungi diseases, game and grazing, action of man) was not included into this study, due to limited data availability.



## 9.6 Overall conclusions

When actual defoliation data were used, there was a strong relationship with countries and age. Other stress factors that sometimes appeared to be significant, were altitude, relative transpiration, AOT60, concentrations of SO<sub>2</sub> and NO<sub>2</sub> and deposition levels of acidity. Using changes and trends in defoliation, country and stress parameters such as climatic zone, altitude, late frost, summer index and ammonia concentrations appeared to explain in most cases less than 10% of the changes and trends in defoliation. This outcome, however, has to be interpreted with care. The derivation of environmental stress factors was subject to high uncertainty on the local scale. Research undertaken during the last decade give evidence that a mixture of environmental stress factors has an impact on crown condition. The combination of different stress factors varies on the local and on the regional scale. Furthermore, the quality of crown condition data resulted in large differences on the spatial scale. Due to limited data availability, the impact of biotic stress on the defoliation (insect attacks, fungi diseases, game and grazing, action of man) was not included into this study.

It is generally accepted that the impact of air pollution on crown condition is not straight forward. The lack of significant correlation between crown condition and air pollution in this study may be a product of uncertainty of the methods and data used.

## 10 Uncertainties and recommendations

Wim De Vries<sup>1)</sup>, Jan Willem Erisman<sup>2)</sup>, Jaco Klap<sup>1)</sup>

<sup>1)</sup> DLO Winand Staring Centre (SC-DLO), Wageningen, The Netherlands

<sup>2)</sup> National Institute of Public Health and the Environment (RIVM), Bilthoven, The Netherlands

In this chapter we present recommendations for future activities with regard to the correlative studies on the Level 1 forest condition data base. Research in the relation between defoliation and stress factors is presently limited by the uncertainties in the deposition model results, in the derivation of site and stand characteristics, and of meteorological stress as well as the quality of the crown condition data.

The derivation of environmental stress factors may lead to large uncertainties especially on the local scale. Several parameters for the analysis of cause-effect relationships between the crown condition at Level I and anthropogenic stress factors, were derived with the help of interpolation procedures or models.

Measured soil data (pH, base saturation and C/N ratio) were only available for one half of the crown condition plots, and for the remaining plots soil data were derived from the available soil type or, if even the soil type was lacking from the FAO-soil map. This procedure also affects the spatial pattern of the calculated critical acid deposition levels in areas where these data have to be estimated.

Meteorological stress was interpolated from data of unknown accuracy. The uncertainty of the obtained results is highly variable, which also affected the calculation of the relative transpiration (drought stress). Air pollution data were obtained from two recently established models, which use EMEP-modelled air pollution data on a 150 x 150 km<sup>2</sup> resolution. The uncertainty in the calculated concentration and deposition levels for N compounds is large because the concentrations are underestimated to a large extent for sites located in or near to source areas. The underestimation is largest for NH<sub>3</sub> because of the many scattered low level sources and by using 50 m height model results. The underestimation can be an order of magnitude. The total acid deposition is also underestimated in or near to source areas, but it is usually overestimated in background areas.

The uncertainty in the calculated critical deposition levels for nitrogen and acidity derived above can be large due to uncertainties in the assumed values for critical N leaching rates or critical Al/(Ca+Mg+K) ratios in relation to effects, model assumptions and input data. The uncertainty in critical deposition level exceedances, which is affected by uncertainties in both present loads and critical deposition levels, can be very high. The calculated high exceedances in central Europe are, however, quite reliable considering air pollution measurements in this area.

In this respect is recommended that:

1. Monitoring is extended. This will result in larger time series than actually available for analyses of the temporal and spatial development of crown condition in Europe.



Larger data bases also would allow to include more tree species and to analyse longer time series in the investigation of cause-effect relationships.

2. For the assessment of long-term trends in defoliation larger data sets of intercalibration exercises will result in a higher reliability and comparability of the results. Continuation of training courses on the national level will further improve the quality of the assessment in the countries. The international training courses will contribute to deeper insights in existing differences of the application of the methods in the participating countries.
3. Quality of present data is improved, e.g. by (i) further improvement and validation of the extrapolation procedure of chemical soil data, (ii) improvement of meteorological data bases and small scale source estimates (emission of air pollutants) and (iii) validation of several parameters used in the calculation of the relative transpiration using rainfall data collected by bulk deposition and throughfall.
4. Additional data are included in the assessment, e.g. (i) assessment of additional stand characteristics (e.g. mean stand heights, stand density, homogeneity of the stand and the nearest distance to nearest forest edge, sources, roads etc in certain classes) at the plots for further improvements of deposition estimates and (ii) (improvement of) the assessment of the occurrence of biotic stress (pest, disease, fungi, insect attacks, etc.).
5. A link should be established with the Intensive Monitoring Programme at the so-called Level II (Intensive Monitoring) plots.
6. The statistical analysis should be further developed by e.g. improved stratification of the data with respect to altitude, age, climatic zone, etc. in order to improve statistical relations.

## References

- Ågren, G.I. and E. Bosatta, 1988. Nitrogen saturation of terrestrial ecosystems. *Environmental Pollution* 54: 185-198.
- Alemdag, S., 1967. *Türkiyedeki sarıçam ormanlarının kuruluşu, verim gücü ve bu Ormanların işletilmesinde takip edilecek esaslar* [Structure and yield potential of Scotch pine (*Pinus sylvestris* L.) forest in Turkey and the principles to be followed in managing these forests]. Teknik bülten serisi. Ormancılık araştırma enstitüsü yayınları; no 20. 160 pp.
- Andersson, L. and R.J. Harding, 1991. Soil-moisture deficit simulations with models of varying complexity for forest and grassland sites in Sweden and the U.K. *Water Resources Management* 5: 25-46.
- Aneja V.P. and Z. Li, 1992. Characterization of ozone at high elevation in the eastern United States: trends, seasonal variations and Exposure. *Journal of Geophysical research* 97: 9873.
- Aronsson, A., 1980. Frost hardiness in Scots pine. II Hardiness during winter and spring in young trees of different mineral status. *Studia Forest Suecica* 155: 1-27.
- Ashmore, M.R. and R.B. Wilson (Eds), 1994. *Critical levels of Air Pollutants for Europe*. Background Papers prepared for ECE Workshop on Critical levels. Egham, U.K. 23-26 March 1992, UK department of the environment.
- Asman, W.A.H. and J.A. Van Jaarsveld, 1992. A variable-resolution transport model applied for NH<sub>x</sub> for Europe. *Atmospheric Environment* 26A:445-464.
- Auclair, A.N.D., R.C. Worrest, D. Lachance and H.C. Martin, 1992. Climatic perturbation as a general mechanism of forest dieback. In: P.D. Manion, D. Lachance, (Eds) *Forest decline concepts*. St. Paul, Minnesota. pp.38 - 58
- Baeumler, A., 1995. *Marginal regression models for spatial or temporal correlated forest damage data*. In: R.W. Payne (Ed.): Spatial and temporal modelling in agricultural research. Rothamsted, IACR-Rothamsted, Proceedings of Fourth HARMA Workshop. p. 32-42.
- Baldocchi, D.D., B.B. Hicks and P. Camara, 1987. A canopy stomatal resistance model for gaseous deposition to vegetated surfaces. *Atmospheric Environment* 21: 91-101.
- Barrie L.A., 1985. Scavenging ratios, wet deposition and in-cloud oxidation: an application to the oxides of sulphur and nitrogen. *Journal of Geophysical research*, 90: 5789-5799.



- Barrie L.A., 1992. Scavenging ratios: black magic or a useful scientific tool. In: S.E. Schwarz and W.G.N. Slinn (Eds), *Precipitation scavenging and atmosphere-surface exchange, Hemisphere*. New York, 403-420.
- Bates, T.E., 1993. Soil handling and preparation. In : M.R. Carter (Ed.). *Soil sampling and methods of analyses*: 19-24.
- Beljaars, A.C.M. and A.A.M. Holtslag, 1990. A Software library for the calculation of surface fluxes over land and sea. *Environmental Software* 5 (2): 60-68.
- Berdén, M., S.I. Nilsson, K. Rosén and G. Tyler, 1987. *Soil acidification extent, causes and consequences*. National Swedish Environment Protection Board, Report 3292, 164 pp.
- Berg, B. and H. Staaf, 1981. Leaching, accumulation and release of nitrogen in decomposing forest litter. In: F.E. Clark and T. Rosswall (Eds.). *Terrestrial Nitrogen Cycles*. Ecology Bulletin 33: 163-178.
- Billet, M.F., E.A. FitzPatrick and M.S. Cresser, 1988. Long-term changes in the acidity of forest soils in North-East Scotland. *Soil Use and Management* 4: 102-107.
- Black, T.A., W.P. Gardner and G.W. Thurtell, 1969. The prediction of evaporation, drainage and soil water storage for a bare soil. *Soil Science Society of America Proceedings* 33: 655-660.
- Bobbink, R., M. Hornung and J.G.M. Roelofs, 1995. The effects of air-borne nitrogen pollution on vegetation-critical loads. In: WHO Europe. *Updating and revision of air quality guidelines for Europe*.
- Bobbink, R., D. Boxman, E. Fremstad, G. Heil, A. Houdijk and J. Roelofs, 1992. Critical loads for nitrogen eutrophication of terrestrial and wetland ecosystems based upon changes in vegetation and fauna. In: P. Grennfelt and E. Thornelof (Eds.): *Critical Loads for Nitrogen. Report from a workshop held at Lökeberg, Sweden, 6-10 April 1992*. Nordic Council of Ministers, Report 1992, 41: 111-161.
- Bosch, C., E. Pfannkuch, U. Baum and K.E. Rehfuess, 1983. Über die Erkrankung der Fichte (*Picea abies* Karst.) in den Hochlagen des Bayerischen Waldes. *Forstwissenschaftliches Centralblatt* 102: 167-181
- Boughton, W.C., 1984. A simple model for estimating the water yield of ungauged catchments. *Civ. Eng. Trans., I.E. Aust.*, report CE26: 83-88.
- Boxman, A.W. en H.F.G. Van Dijk, 1988. *Het effect van landbouw ammonium deposities op bos- en heidevegetaties*. Katholieke Universiteit Nijmegen, 96 pp.

Boxman, A.W., R.J. Sinke and J.G. Roelofs, 1986. Effects of ammonium on the growth and kalium (<sup>86</sup>Rb) uptake of various ectomycorrhizal fungi in pure culture. *Water Air and Soil Pollution* 32: 517-522.

Breeuwsma, A., J.P. Chardon, J.F. Kragt and W. De Vries, 1991. Pedotransfer functions for denitrification. In: ECE, 1991. *Soil and Groundwater Research Report II "Nitrate in Soils"*. Commission of the European Community, Luxembourg: 207-215.

Bruck, R.I., 1985. Boreal montane ecosystem decline in the southern Appalachian Mountains: potential role of anthropogenic pollution. In: H.S. Stubbs (Ed.) *Air pollution effects on forest ecosystems*. St. Paul, Minnesota. p.137-155

Buat Menard, P. R.A. Duce, 1986. Precipitation scavenging of aerosol particles over remote marine regions. *Nature*, 321: 508-510.

Burton, K.W., E. Morgan and A. Roig, 1983. The influence of heavy metals upon the growth of Sitka spruce in South Wales forests. 1. Upper critical and foliar concentrations. *Plant and Soil* 73: 327-336

Butzke, H., 1988. Zur zeitlichen und kleinräumigen Variabilität des pH-Wertes im Waldböden Nordrhein-Westfalens. *Forst und Holzwirt* 43 (4): 81-85.

Calder, I., 1986. A stochastic model of rainfall interception. *Journal of Hydrology* 89: 65-71.

Carbonnier, C., 1971. Bokens produktion i soedra Sverige [Yield of beech in Southern Sweden]. Stockholm, Skogshoegskolan. *Studia forestalia suecica*, 91: 89 pp.

Chamberlain A.C., 1966. Transport of gases from grass and grass-like surfaces, *Proc. R. Soc. Lond.* A290, 236-265.

Cronan, C.S. and D.F. Grugal, 1995. The ues of Calcium/ Aluminium ratios as indicators of stress in forest ecosystems. *Journal of Environmental Quality* 24: 209-226

Davenport, A.G., 1960. Rationale for determining design wind velocities. *J. Struct. Div. Am. Soc. Civ. Eng.*, 86:39-68.

De Leeuw F.A.A.M. and E.D.G. Van Zandvoort, 1995. *Mapping of exceedances of ozone critical levels for crops and forests in The Netherlands, preliminary results*. RIVM Report no. 722401011, Bilthoven, The Netherlands.

De Visser, P.H.B., 1994. *Growth and nutrition of Douglas-fir, Scots pine and pedunculate oak in relation to soil acidification*. Wageningen, Doctoral thesis, Wageningen Agricultural university, The Netherlands, 185 pp.



De Vries, W., 1991. *Methodologies for the assessment and mapping of critical loads and the impact of abatement strategies on forest soils*. Wageningen, The Netherlands, DLO Winand Staring Centre for Integrated Land, Soil and Water Research, Report 46, 109 pp.

De Vries, W., 1992. Empirical data and model results for critical nitrogen loads in The Netherlands. In: P. Grennfelt and E. Thörnelöf (Eds): *Critical loads for Nitrogen. Report from a workshop held at Lökeberg, Sweden 6-10 April, 1992*. Nordic Council of Ministers, Report 1992, 41: 383-402.

De Vries, W., 1993. Average critical loads for nitrogen and sulphur and its use in acidification abatement policy in The Netherlands. *Water, Air and Soil Pollution* 68: 399-434.

De Vries, W., 1994. *Soil response to acid deposition at different regional scales. Field and laboratory data, critical loads and model predictions*. Wageningen, The Netherlands, Agricultural University, Ph.D. Thesis, 487 pp.

De Vries, W., 1996a. *Proposed clustering of soil types for the presentation of soil data at two monitoring levels*. Wageningen, DLO Winand Staring Centre for Integrated Land, Soil and Water Research, Internal note.

De Vries, W., 1996b. *Critical loads for acidity and nitrogen for Dutch forests on a 1 km x 1 km grid*. Wageningen, The Netherlands, DLO Winand Staring Centre for Integrated Land, Soil and Water Research, Report 113, 46 pp.

De Vries, W., 1997. Rates and mechanisms of aluminium, base cation and silica release in sandy soils at pH 3.0. *Geoderma* (submitted).

De Vries, W. and E.E.J.M. Leeters, 1996. *Effects of acid deposition on 150 forest stands in The Netherlands. 1. Chemical composition of the humus layer, mineral soil and soil solution*. Wageningen, The Netherlands, DLO Winand Staring Centre for Integrated Land, Soil and Water Research, Report 69.1.

De Vries, W., M. Posch and J. Kämäri 1989. Simulation of the long-term soil response to acid deposition in various buffer ranges. *Water, Air and Soil Pollution* 48: 349-390.

De Vries, W., A. Hol, S. Tjalma en J.C. Voogd, 1990. *Voorraden en verblijftijden van elementen in een boscosysteem: een literatuurstudie*. Wageningen, DLO-Staring Centrum, Rapport 94, 205 pp.

De Vries, W., G.J. Reinds and M. Posch, 1994a. Assessment of critical loads and their exceedance on European forests using a one-layer steady-state model. *Water Air and Soil Pollution* 72: 357-394.

De Vries, W., M. Posch, G.J. Reinds and J. Kämäri, 1994b. Simulation of soil response to acidic deposition scenarios in Europe. *Water Air and Soil Pollution* 78: 215 -246.

De Vries, W., J.J.M. Van Grinsven, N. Van Breemen, E.E.J.M. Leeters and P.C. Jansen, 1995a. Impacts of acid atmospheric deposition on concentrations and fluxes of solutes in Dutch forest soils. *Geoderma* 67: 17-43.

De Vries, W., M. Posch, T. Oja, H. Van Oene, J. Kros, P. Warfvinge and P.A. Arp, 1995b. Modelling critical loads for the Solling spruce site. *Ecological Modelling*: 283-293.

De Vries, W., G.J. Reinds, E.M. Vel and H.D. Deelstra, 1997. *Intensive Monitoring of Forest Ecosystems in Europe*. Technical report 1997. UN/ECE, EC, Forest Intensive Monitoring Coordinating Institute, Report (in press).

Derrick M.R., J.L. Moyers, K.A. Yarborough and M. Warren (1984) Aerosol and precipitation chemistry relationships at Big Bend National Park, *Water, Air and Soil Pollution* 21: 171-181.

Dolman, A.J. and E.J. Moors, 1994. *Hydrologie en waterhuishouding van bosgebieden in Nederland*. Wageningen, SC-DLO, rapport 333, 76 pp.

Doorenbos, J. and A.H. Kassam, 1979. *Yield response to water*. Rome, FAO, Irrigation and Drainage paper 33, 193 pp.

Downing, R.J., J.P. Hettelingh and P.A.M. de Smet (Eds), 1993. *Calculation and mapping of critical loads in Europe*. Bilthoven, The Netherlands, Coordination Centre for effects, Status Report 1993, 163 pp.

Draaijers, G.P.J. and J.W. Erisman, 1995. A canopy budget model to assess atmospheric deposition from throughfall measurements. *Water, Air and Soil Pollution* 85: 2253-2258.

Draaijers, G.P.J., R. Van Eck and R. Meijers, 1992. Measuring and modelling dry deposition in complex forest terrain. In: T. Schneider (Ed.), *Acidification Research Evaluation and Policy Applications*, Studies in Environmental Science 50, Elsevier Science Publishers, Amsterdam, The Netherlands: 285-294.

Draaijers G.P.J., E.P van Leeuwen, P.G.H. de Jong and J.W. Erisman, 1996a. *Base cation deposition in Europe: acid neutralisation capacity and contribution to forest nutrition*. RIVM report no. 722108017, Bilthoven, The Netherlands.

Draaijers, G.P.J., J.W. Erisman, T. Spranger and G.P. Wyers, 1996b. The application of throughfall measurements for atmospheric deposition monitoring. *Atmospheric Environment* 30: 3349-3361.

Driessen, P.M., 1986. *The water balance of the soil*. In : H. van Keulen and J. Wolf (Eds). Modelling of agricultural production weather, soils and crops. Wageningen, PUDOC: 76-116.



Eder B.K. and R.L. Dennis, 1990. On the use of scavenging ratios for the inference of surface-level concentrations and subsequent dry deposition of  $\text{Ca}^{2+}$ ,  $\text{Mg}^{2+}$ ,  $\text{Na}^+$  and  $\text{K}^+$ , *Water, Air and Soil Pollution* 52: 197-215.

Eleveld H., E. Kirchner, J. Beck, F. de Leeuw and A. van Pul (in prep). *European deposition and Exposure to ozone on a small scale: the EDEOS model*. RIVM report no. 722401xxx, Bilthoven, The Netherlands.

Ellenberg, H. (Jr.), 1983. Gefährdung wildlebender Pflanzenarten in der Bundesrepublik Deutschland - Versuch einer ökologischen Betrachtung. *Forstarchiv* 54: 127-133

Ellenberg, H. (Jr.), 1985. Veränderungen der Flora Mitteleuropas unter dem Einfluss von Düngung und Immissionen. *Schweiz Zeitschrift für das Forstwesen* 136: 19-39

Ellenberg, H. Jr., 1991. Ökologische Veränderungen in Biozönosen durch Stickstoffeintrag. In: K. Henle and G. Kaule (Eds) *Arten- und Biotopschutzforschung für Deutschland. Berichte aus der ökologischen Forschung*. 4: 75-90

Ellenberg, H. (Sen.), 1995. Allgemeines Waldsterben - ein Konstrukt? *Naturwissenschaftliche Rundschau* 38: 93-96.

Erisman J.W., 1992. *Atmospheric deposition of acidifying compounds in The Netherlands*. Ph.D. thesis, University of Utrecht, The Netherlands.

Erisman, J.W., 1993. Acid deposition onto nature areas in The Netherlands; Part I. Methods and results. *Water Soil Air Pollution* 71:51-80.

Erisman, J.W., 1995. *Thematic report no. IV; Dutch Priority Programme on Acidification, Phase 3*. RIVM report 722108007.

Erisman J.W. and D.D. Baldocchi, 1994. Modelling dry deposition of  $\text{SO}_2$ . *Tellus* 46B: 159-171.

Erisman, J.W. and G.P.J. Draaijers 1995. *Atmospheric deposition in relation to acidification and eutrophication*, Studies in Environmental Science, 63, Elsevier, Amsterdam, The Netherlands.

Erisman J.W. and G.P. Wyers, 1993. Continuous measurements of surface exchange of  $\text{SO}_2$  and  $\text{NH}_3$  implications for their possible interaction in the deposition process, *Atmospheric Environment* 27A: 1937-1949.

Erisman J.W., W.A.J. Van Pul and G.P. Wyers, 1994a. Parameterization of surface resistance for the quantification of atmospheric deposition of acidifying pollutants and ozone. *Atmospheric Environment* 28, no.16: 2595-2607.

Erisman, J.W., C. Beier, G.P.J. Draaijers and S.E. Lindberg, 1994b. Review of deposition monitoring methods. *Tellus* 46B, 79-93

Erisman, J.W., G.P.J. Draaijers, J.H. Duyzer, P. Hofschreuder, N. van Leeuwen, F.G. Römer, W. Ruijgrok and G.P. Wyers, 1994c. *Contribution of aerosol deposition to atmospheric deposition and soil loads onto forests*. RIVM report no. 722108005.

Erisman J.W., C. Potma, W.A.J. Van Pul, E.P. Van Leeuwen and G.P.J. Draaijers, 1995. A generalized description of the deposition of acidifying pollutants and base cations on a small scale in Europe. In: M. Posch, P.A.M. De Smet, J.P. Hettelingh, R.J. Downing (Eds). *Calculation and mapping of critical thresholds in Europe*. RIVM report no. 259101004, RIVM, Bilthoven, The Netherlands.

Erisman, J.W., C. Potma, G.P.J. Draaijers and E.P. Van Leeuwen, 1996a. A generalised description of the deposition of acidifying pollutants on a small scale in Europe. *Water, Air and Soil Pollution* 85, 2101-2106.

Erisman, J.W., M.G. Mennen, D. Fowler, G. Spindler, J.H. Duyzer, W. Ruigrok and G.P. Wyers, 1996b. *Towards development of a deposition monitoring network for air pollution of Europe*. Report no. 722108015. National institute of Public Health and the Environment, Bilthoven, The Netherlands.

European Environmental Agency (EEA), 1995. *Review of CORINAIR 90, Proposals for air emissions 94*. Report to the European Environmental Agency from the European Topic Centre on Air Emissions, Copenhagen, Denmark.

Evans, L.S., 1984. Botanical aspects of precipitation. *Botanica Review* 50: 449-489

Falkengren-Grerup, U., N. Linnermark and G. Tyler, 1987. Changes in acidity and cation pools of south Swedish soils between 1949 and 1985. *Chemosphere* 16: 2239-2248.

FAO, 1981. *FAO - Unesco soil map of the world, 1 500 000. Volume V Europe*. Unesco Paris 1981, 199 pp.

FAO, 1988. *Soil map of the World, revised legend*. World soil resources report 60, FAO, Rome, 138 pp.

FAO, 1990. Guidelines for soil description. 3<sup>rd</sup> edition (revised). FAO, Rome. *FWB (Forschungsbeirat Waldschäden/ Luftverunreinigungen (Ed.) (1989). Dritter Bericht. KfA Jülich. Karlsruhe. 70 pp.*

Federer, C.A., 1982. Transpirational supply and demand: plant, soil and atmospheric effects evaluated by simulation. *Water Resource Research* 18: 355-362.

Fitzgerald J.W., 1975. Approximations formulas for the equilibrium size of an aerosol particle as a function of its size and composition and the ambient relative humidity, *Journal of Applied Meteorology*, 14: 1044-1049.



Fowler D., 1978. Dry deposition of SO<sub>2</sub> on agricultural crops, *Atmospheric Environment* 12: 369-373.

FSSC, 1997. *Forest Soil Condition Report*. UN-ECE: ICP Forests, EC, pp.

Fürher, J. and B. Achermann (eds.), 1994. *Critical levels for ozone*. A UN-ECE workshop report; Schriftenreihe der FAC No16. Berne-Liebefeld, 329 pp

Führer J., 1996. *The critical levels for ozone on crops and the transfer to mapping. Workshop on Critical Levels for Ozone in Europe: Testing and Finalising the concepts*. 15-17 april 1996, Kuopio, Finland.

Galloway, J.N., D.L. Savoie, W.C. Keene and J.M. Prospero, 1993. *Atmospheric Environment*, 27A: 235-250.

Garcia Abejon, J.L. and J.A. Gomez Loranca, 1984. *Tablas de produccion de densidad variable para Pinus sylvestris L. en el sistema central*. Com. I.N.I.A. Serie: Recursos nat.; no 29. 36 pp.

Garland, J.A., 1978. Dry and wet removal of sulfur from the atmosphere. *Atmospheric Environment*, 12: 349.

Gash, J.H.C., C.R. Lloyd and G. Lachaud, 1995. Estimating sparse rainfall interception with an analytical model. *Journal of Hydrology* 170: 79-86.

Glatzel, G. and M. Kazda, 1985. Wachstum und mineralstoffennährung van buche (*Fagus sylvatica*) und spitzahorn (*Acer platanoides*) auf versauertem und schwermetallbelastetem bodenmaterial aus dem einsicherungsbereich. *Zeitschrift für Pflanzenernährung und Bodenkunde* 148: 429-438.

Guerzoni S., A. Cristini, R. Caboi, O. Le Bolloch, I. Marras, and L. Rundeddu, 1995. Ionic composition of rain water and atmospheric aerosols in Sardinia, southern Mediterranean, *Water, Air and Soil Pollution* 85: 2077-2082.

Halbäcken, L. and C.O. Tamm, 1986. Changes in soil acidity from 1927 to 1982-1984 in a forest area of south-west Sweden. *Scandinavian Journal of Forest Research* 1: 219-232.

Hamilton, G.J. and J.M. Christie, 1971. *Forest magement tables (metric)* - rev. ed. London, HMSO. Forestry Commission Booklet; no 34. 201 pp.

Harding, R.J., R.L. Hall and P.T.W. Rosier, in prep. Measurement and modelling of the water use of beech and ash plantations in southern Britain. *Journal of Hydrology*, submitted.

Harrison, L.P., 1963. Fundamental concepts and definitions relating to humidity. In: A. Wexler (Ed.). *Humidity and moisture*. New York, Reinhold Publishing Co.: 3-80.

Harrison R.M. and C.A. Pio (1983) A comparative study of the ionic composition of rainwater and atmospheric aerosols: implications for the mechanism of acidification of rainwater, *Atmospheric Environment* 17: 2539-2543.

Hartmann, G., 1996. Ursachanalyse des Eichensterbens in Deutschland - Versuch einer Synthese bisheriger Befunde. In: A. Wulf and R. Kehr (Eds) *Eichensterben in Deutschland*. Berlin, Parey Buchverlag: 125-151.

Heij, G.J. and F. Schneider (Eds), 1995. *Eind rapport Additioneel Programma Verzurings onderzoek, derde fase (1991-1994)*. Rapport 100-05, 160 pp.

Heij, G.J., W. De Vries, A.C. Posthumus and G.M.J. Mohren, 1991. Effects of air pollution and acid deposition on forests and forest soils. In: T. Schneider and G.J. Heij (Eds). *Acidification research in The Netherlands. Final report of the Dutch Priority Programme on Acidification*. Studies in Environmental Science 46, Elsevier Science Publishers, Amsterdam, The Netherlands: 97-137.

Hellinga, G., 1983. *Bosbescherming*. Wageningen, PUDOC, 385 pp.

Hendriks, C.M.A., W. De Vries and J. Van den Burg, 1994. *Effects of acid deposition on 150 forest stands in The Netherlands. 2. Relationship between forest vitality and the chemical composition of the foliage, humus layer and the soil solution*. Wageningen, The Netherlands, DLO Winand Staring Centre for Integrated Land, Soil and Water Research, Report 69.2, 55 pp.

Hendriks, C.M.A., W. De Vries, J.H. Oude Voshaar, E.P. Van Leeuwen and J.M. Klap, 1997. *Assessment of the possibilities to derive relationships between stress factors and forest condition for The Netherlands*. DLO Winand Staring Centre for Integrated Land, Soil and Water Research, Report 147.

Hettelingh, J.P., R.J. Downing and P.A.M. De Smedt, 1991. *Mapping critical loads for Europe*. National Institute of Public Health and Environmental Protection. Coordination Centre for Effects, Bilthoven, The Netherlands, Technical report no. 1, 183 pp.

Hicks B.B., D.D. Baldocchi, T.P. Meyers, R.P. Hosker (Jr.) and D.R. Matt, 1987. A preliminary multiple resistance routine for deriving dry deposition velocities from measured quantities, *Water Air Soil Pollution* 36: 311-330.

Hicks, B.B., R.R. Draxler, D.L. Albritton, F.C. Fehsenfeld, J.M. Hales, T.P. Meyers, R.L. Vong, M. Dodge, S.E. Schwartz, R.L. Tanner, C.I. Davidson, S.E. Lindberg and M.L. Wesely, 1989. *Atmospheric processes research and process model development*. State of Science/Technology, Report No. 2. National Acid Precipitation Assessment Program.

Hommel, P.W.F.M., E.E.J.M. Leeters, P. Mekking and J.G. Vrieling, 1990. *Vegetation changes in the Speulderbos (The Netherlands) during the period 1958-1988*.



Wageningen, The Netherlands, DLO Winand Staring Centre for Integrated Land, Soil and Water Research, Report 23, 9 pp.

Houdijk, A.L.M.F., 1994. *De invloed van verhoogde aluminium-calcium verhoudingen in aanwezigheid van humuszuur en van de uitputting van de aluminiumvoorraad in de bodem op de vitaliteit van de Corsicaanse den*. Katholieke Universiteit Nijmegen, 51 pp.

Houston, D.R., 1992. A host-stress-saprogen model for forest dieback-decline diseases. In: P.D. Manion and D. Lachance (Eds). *Forest decline concepts*. St. Paul, Minnesota. pp. 3 - 25

Hutchinson, T.C., L. Bozic and G. Munoz-Vega, 1986. Responses to five species of conifer seedlings to aluminum stress. *Water, Air and Soil Pollution* 31: 283-294

Innes, J.L., 1993. *Forest health: Its assessment and status*. Oxon, CAB International, 677 pp.

Ivens, W.P.M.F., 1990. *Atmospheric deposition onto forests*. Ph.D. thesis, University of Utrecht, The Netherlands.

Jaffrezo J.L. and J.L. Colin, 1988. Rain-aerosol coupling in urban area: scavenging ratio measurement and identification of some transfer processes, *Atmospheric Environment* 22: 929-935.

James, B.R. and S.J. Riha, 1986. pH buffering in forest soil organic horizons: relevance to acid precipitation. *Journal of Environmental Quality* 13: 229-234.

Jansen, J.J., J. Sevenster and P.J. Faber, 1996. *Opbrengsttabellen voor belangrijke boomsoorten in Nederland*. Wageningen, IBN-DLO / LUW vakgroep Bosbouw. IBN-rapport 221, Hinkeloord Report 17. 202 pp.

Jansson, P.-E., 1991. *Simulation model for soil water and heath conditions. Description of the SOIL model*. Uppsala, Swedish University of Agricultural Sciences, Report 165.

Kabat, P., B.J. Van den Broek and R.A. Feddes, 1992. SWACROP: a water management and crop production simulation model. *ICID bulletin* 41(2): 61-83.

Kalma, J.D., B.C. Bates and R.A. Woods, 1995. Predicting catchment-scale soil moisture status with limited field measurements. In: J.D. Kalma and M. Sivapalan. *Scale issues in hydrological modelling*. Chichester, John Wiley and Sons: 203-225.

Kandler, O., 1992. The German forest decline situation: a complex disease or a complex of diseases? In: P.D. Manion, P.D. and D. Lachance (Eds) *Forest decline concepts*. St. Paul, Minnesota. pp 59-84

Kandler, O., 1994. Vierzehn Jahre Waldschadensdiskussion. *Naturwissenschaftliche Rundschau* 47: 419-430.

Kane M.M., A.R. Rendell and T.D. Jickells, 1994. Atmospheric scavenging processes over the North Sea, *Atmospheric Environment* 28: 2523-2530.

Kärenlampi, L. and L. Skärby (eds.), 1994 *Proceedings of the Workshop on Critical levels for Ozone in Europe; Testing and Finalising the Concepts* Kuopio, Finland, 15-17 April 1996. Published by the University of Kuopio, Dept. of Ecology and Environmental Science.

Kimmins, J.P., D. Binkley, L. Chatarpaul and J. De Catanzaro, 1985. *Biogeochemistry of temperate forest ecosystems Literature on inventories and dynamics of biomass and nutrients*. Petawawa National Forestry Institute, Canada, Information Report PI-X-47E/F, 227 pp.

Klap, J.M., W. de Vries and E.E.J.M. Leeters, 1996. *Effects of acid atmospheric deposition on the chemical composition of loess, clay and peat soils under forest in The Netherlands. 1. Actual assessments*. Wageningen, The Netherlands, DLO Winand Staring Centre for Integrated Land, Soil and Water Research, Report 97.1, pp.

Klap, J.M., W. De Vries, C.M.A. Hendriks, J.H. Oude Voshaar, G.J. Reinds, E.P. Van Leeuwen and J.W. Erisman, 1997. *Assessment of the possibilities to derive relationships between stress factors and forest condition for Europe*. DLO Winand Staring Centre for Integrated Land, Soil and Water Research, Report 149.

Krüger, O., 1993. *The applicability of the EMEP-code to estimate budgets for airborne acidifying components in Europe*. In: proceedings CEC/BIATEX Workshop 4-7 May 1993, Aveiro, Portugal.

Landmann, G., 1995. Forest decline and air pollution effects in the French mountains: a synthesis. In: G. Landmann and M. Bonneau (Eds). *Forest decline and atmospheric deposition effects in the French mountains*. Berlin, Springer-Verlag, 461 pp.

Landmann, G. and M. Bonneau (Eds), 1995. *Forest decline and atmospheric deposition effects in the French mountains*. Berlin, Springer-Verlag, 461 pp.

Last, F.T., D. Fowler, and P.H. Freer Smith, 1984. Die postulate von Koch und die Luftverschmutzung. *Forstwissenschaftliches Zentralblatt* 103: 28-48.

Leenmans, R. and W.P. Cramer, 1990. *The IIASA data base for mean monthly values of temperature, precipitation and cloudiness on a global terrestrial grid*. Laxenburg, Austria, IIASA, Working paper WP-90-45, 64 pp.

Legates D.R. and C.J. Willmott, 1990. Mean seasonal and spatial variability in gauge-corrected, global precipitation, *International Journal of Climatology*, 10: 111-123.



- Lenz, R. and P. Schall, 1991. Belastungen in fichtendominierten Waldökosysteme. Risikokarten zu Schlüsselprozessen der neu-artigen Waldschäden. *Allgemeine Forst-Zeitschrift* 46: 756-761.
- Liang, K.Y. and S.L. Zeger, 1986. Longitudinal data analysis using generalized linear models. *Biometrika* 73:13-22.
- Lövblad G., J.W. Erisman and D. Fowler, 1993. *Models and methods for the quantification of atmospheric input to ecosystems*. Proceedings Nordic Council/EMEP/BIATEX workshop in Göteborg 3-6 November 1992.
- Lovett G.M. and J.D. Kinsman, 1990. Atmospheric pollutant deposition to high-elevation ecosystems, *Atmospheric Environment* 24A: 2767.
- Mäkelä, A. and W. Schöpp, 1990. Regional-scale SO<sub>2</sub> Forest-Impact Calculations. In: Alcamo, J., R.Shaw and L. Hordijk (Eds), *1990 The Rains model of Acidification, Science and Strategies in Europe*. Kluwer Academic Publishers, Dordrecht: 263-269
- Marschner, H., 1990. *Mineral Nutrition of Higher Plants*. London, San Diego, New York, Boston, Sydney, Tokyo.
- Matyssek, R., T. Keller, and M.S. Günthardt-Goerg, 1990. Ozonwirkungen auf den verschiedenen Organisationsebenen in Holzpflanzen. *Schweizerische Zeitschrift für das Forstwesen* 141: 631-651
- Mengel, K., 1991. *Ernährung und Stoffwechsel der Pflanze*. 7<sup>th</sup> revised edition. Jena.
- Milford J.B. and C.I. Davidson, 1985. The sizes of particulate trace elements in the atmosphere - a review, *Journal for Air Pollution Control and Assessment* 35: 1249-1260.
- Monteith, J.L., 1965. *Evaporation and environment*. In: G.E. Fogg (Ed.). *The state and movement of water in living organisms*. New York, Academic press, Symp. Soc. Exper. Biol., Vol. 19: 205-234.
- Moors, E.J., W. Bouten, A.J. Dolman and A.W.L. Veen, 1996. De verdamping van bossen. *H<sub>2</sub>O* 29 (16): 462-466.
- Morgan, S.M., J.A. Lee and T.W. Ashenden, 1992. Effects of Nitrogen Oxides on Nitrate Assimilation in Bryophytes. *New Phytologist* 120: 89-97
- Müller-Edzards, C., W. De Vries and J.W. Erisman (Eds), 1997. *Ten years of monitoring forest condition in Europe - Studies on temporal development, spatial distribution and impacts of natural and anthropogenic stress factors. Technical Background Report*. UN/ECE and EC. Geneva, Brussels.

- Neftel A., 1995. *High NO<sub>x</sub> and low NO<sub>x</sub> chemistry of ozone formation: Evaluation for small-scale episodes in Switzerland*. Proceedings of the EMEP Workshop on the Control of Photochemical Oxidants over Europe, 24-27 October 1995, St. Gallen, Switzerland.
- Nelleman, C. and T. Frogner, 1994. Spatial patterns of spruce defoliation seen in relation to acid deposition, critical loads and natural growth conditions in Norway. *Ambio* 23: .
- Nihlgård, B., 1985. The ammonium hypothesis - an additional explanation for the forest dieback in Europe. *Ambio* 14: 2-8
- Nilsson, J., 1986. *Critical loads for nitrogen and sulphur*. Report 1986: 11, Nordic Council of Ministers, Copenhagen, Denmark: 183 pp.
- Nilsson, J. and P. Grennfelt (Eds.), 1988. *Critical loads for sulphur and nitrogen*. Report from a Workshop held at Skokloster, Sweden, March 19-24, 1988. Miljø rapport 1988: 15. Nordic Council of Ministers, Copenhagen, Denmark, 418 pp.
- Nilsen, P. and J. Larsson, 1992. *Bonitering av skog ved hjelp av vegetasjonstype og egenskaper ved voksestedet* [Site index estimation from vegetation type and site properties]. Cs, Norsk Institutt for Skogsforskning. Rapport Skogsforskning 22/92. 43 pp.
- Nys, C., 1989. Fertilisation, dépérissement et production de l'épicéa commun (*Picea abies*) dans les Ardennes. *Revue forestière française* 41: 336-347
- Oude Voshaar, J.H., 1994. *Statistiek voor onderzoekers: met voorbeelden uit de landbouw- en milieuwetenschappen*. Wageningen, Wageningen Pers. 253 pp.
- Posch, M., J.P. Hettelingh, H.U. Sverdrup, K. Bull and W. de Vries, 1993. Guidelines for the computation and mapping of critical loads and exceedances of sulphur and nitrogen in Europe. In: R.J. Downing, J.P. Hettelingh and P.A.M. de Smet (Eds). *Calculation and mapping of critical loads in Europe*. Bilthoven, The Netherlands, Coordination Centre for effects, Status Report 1993: 21-37.
- Posch, M., W. de Vries and J.P. Hetteling, 1995a. Critical loads of sulfur and nitrogen. In: M. Posch, P.A.M. De Smet, J.P. Hettelingh and R.J. Downing (Eds): *Calculation and mapping of critical thresholds in Europe*. Bilthoven, The Netherlands, Coordination Centre for effects, Status Report 1995: 31-41.
- Posch, M., P.A.M. De Smet, J.P. Hettelingh and R.J. Downing (Eds), 1995b. *Calculation and mapping of critical thresholds in Europe*. Bilthoven, The Netherlands, Coordination Centre for effects, Status Report 1995, 198 pp.
- Pratt G.C. and S.V. Krupa (1985) Aerosol chemistry in Minnesota and Wisconsin and its relation to rainfall chemistry, *Atmospheric Environment* 19: 961-971.



- Pritchett, W.L and R.F. Fischer, 1987. *Properties and management of forest soils*. 2<sup>nd</sup> edition, Wiley and sons, 469 pp.
- RIVM, 1993. *Data obtained from the National Air Quality Monitoring Network*, The Netherlands (unpublished).
- Roberts, T.M., R.A. Skeffington and L.W. Blank, 1989. Causes of type 1 spruce decline. *Forestry* 62 (3): 179-222.
- Roelofs, J.G.M., A.J. Kempers, A.L.F.M. Houdijk and J. Jansen, 1985. The effect of airborne ammonium sulphate on *Pinus nigra* var. *maritima* in The Netherlands. *Plant and Soil* 84: 45-56.
- Römer F.G. and B.W. te Winkel, 1994. *Dry deposition of aerosols on vegetation: acidifying components and basic cations*. KEMA report no. 63591-KES/MLU 93-3243, Arnhem, The Netherlands.
- Rosén, K., 1990. *The critical load of nitrogen to Swedish forest ecosystems*. Uppsala, Sweden, Swedish University of Agriculture Science, Department of forest soils. Internal Report, 15 pp.
- Ruijgrok W., H. Tieben and P. Eisinga, 1994. *The dry deposition of acidifying and alkaline particles to Douglas fir: a comparison of measurements and model results*. KEMA report no. 20159-KES/MLU 94-3216, Arnhem, The Netherlands.
- Rutter, A.J., 1968. *Water consumption by forests*. In: T. Kozlowski (Ed.). *Water deficits and plant growth*. Volume 2. London, Academic press: 23-84.
- Rutter, A.J., A.J. Morton and P.C. Robins, 1975. A predictive model of rainfall interception in forests. 1 Generalization of the model comparison with observations in some coniferous and hardwood stands. *Journal of Applied Ecology* 12: 367-380.
- Sandnes H., 1993. *Calculated budgets for airborne acidifying components in Europe, 1985, 1987, 1988, 1989, 1990, 1991 and 1992*. EMEP report 1/93. MSC-West, Oslo, Norway.
- Sandroni S., P. Bacci, G. Boffa, U. Pellegrini and A. Ventura, 1993. Tropospheric ozone in the Pre-Alpine and Alpine regions. In: *Physico-chemical behaviour of atmospheric pollutants*. Proceedings of the sixth European symposium, Varese 18-22 October 1993, Report EUR 15609/1 EN, p.513.
- Savoie D.L., J.M. Prospero and R.T. Nees, 1987. Washout ratios of nitrate, non-sea-salt sulfate and sea-salt on Virginia Key, Florida and on Mamerican Samoa, *Atmospheric Environment* 21: 103-112.

Schaug, J., U. Pedersen and J.E. Skjelmoen, 1991. *Data report 1989, part 2: monthly summaries*. EMEP Co-operative programme for monitoring and evaluation of the long-range transmission of air pollutants in Europe, Norwegian Institute for Air Research, EMEP/CCC-Report 2/91.

Schober, R., 1975. *Ertragstafeln wichtiger Baumarten bei verschiedener Durchforstung*. Frankfurt a. M., Sauerländer. 154 pp.

Schulze, E.D. and O.L. Lange, 1990. Die Wirkungen von Luftverunreinigungen auf Waldökosysteme. *Chemie in unserer Zeit* 24: 117-130.

Scott, B.C., 1981. Sulfate washout ratios in winter storms, *Journal of Applied Meteorology* 20: 619-625.

Simpson D., 1992. Long period modelling of photochemical oxidants in Europe. Model calculations for July 1985, *Atmospheric Environment* 26A: 1609.

Simpson D., 1993. Photochemical model calculations over Europe for two extended summer periods: 1985 and 1989, model results and comparison with observations, *Atmospheric Environment* 27A: 921.

Simpson D., Y. Andersson-Sköld and M.E. Jenkin, 1993. *Updating the chemical scheme for the EMEP MSC-W oxidant model: Current status*. Norwegian Meteorological Institute EMEP MSC-W Note 2/93.

Slinn W.G.N., 1977. Some approximations for the wet and dry removal of particles and gases from the atmosphere, *Water, Air and Soil Pollution* 7: 513-543.

Slinn W.G.N., L. Hasse, B.B. Hicks, A.W. Hogan, D. Lal, P.S. Liss, K.O. Munnich, G.A. Sehmel and O. Vittori, 1978. Some aspects of the transfer of atmospheric trace constituents past the air-sea interface, *Atmospheric Environment* 12: 2055-2087.

Slinn W.G.N., 1982. Predictions for particle deposition to vegetative surfaces., *Atmospheric Environment* 16: 1785-1794.

Smith, W.H., 1981. *Air Pollution and Forests. Interactions between Air Contaminants and Forest Ecosystems*. New York, Heidelberg, Berlin.

Speight, M.R. and D. Wainhouse, 1989. *Ecology and Management of Forest Insects*. Oxford.

Stevens, P., 1987. Throughfall chemistry beneath Sitka spruce of four ages at Beddgelert Forest, North Wales. *Plant and Soil* 101: 291-294.

Stevenson C.M., 1967. An analysis of the chemical composition of rain-water and air over the British Isles and Eire for the years 1959-1964, *Tellus* 19: 56-70



Stull R.B., 1988. *An introduction to boundary layer meteorology*, Kluwer Academic Publishers.

Sverdrup, H.U., W. de Vries and A. Henriksen, 1990. *Mapping critical loads. A guidance to the criteria, calculations, data collection and mapping of critical loads*. Miljö rapport 1990: 14. Nordic Council of Ministers, Copenhagen, Denmark, 124 pp.

Sverdrup, H.U., 1990. The kinetics of base cation release due to chemical weathering. Lund University Press, Sweden, 246 pp.

Sverdrup, H.U. and P.G. Warfvinge, 1992. Calculating field weathering rates using a mechanistic geochemical model - PROFILE. *Journal of Applied Geochemistry* 27: 273-283.

Sverdrup, H. and W. de Vries, 1994. Calculating critical loads for acidity with a mass balance model. *Water, Air and Soil Pollution* 72 :143-162.

Sverdrup, H.U. and P.G. Warfvinge, 1993. *The effect of soil acidification on the growth of trees, grass and herbs as expressed by the (Ca+Mg+K)/Al ratio*. Reports in Ecology and Environmental Engineering 1993: 2, Lund University, Department of Chemical Engineering II, 108 pp.

Sverdrup, H.U., W. de Vries and A. Henriksen, 1990. *Mapping critical loads. A guidance to the criteria, calculations, data collection and mapping of critical loads*. Miljø rapport 1990: 14. Nordic Council of Ministers, Copenhagen, Denmark, 124 pp.

Tamm, C.O., 1991. *Nitrogen in terrestrial ecosystems. Questions of productivity, vegetational changes and ecosystem stability*. Ecological Studies 81. Berlin, Heidelberg, New York, London, Paris, Tokyo, Hong Kong, Barcelona.

Tamm, C.O. and L. Hallbäcken, 1986. Changes in Soil pH over a 50-year period under different forest canopies in SW Sweden. *Water, Air, and Soil Pollution* 31: 337-341.

Thom A.S., 1975. *Momentum, mass and heat exchange of plant communities*. In: J.L. Monteith (Ed.). *Vegetation and Atmosphere*. Academic Press, London. p. 58-109.

Tietema, A., 1992. *Nitrogen cycling and soil acidification in forest ecosystems in The Netherlands*. Ph.D. thesis, University of Amsterdam, The Netherlands, 139 pp.

Tietema, A. and C. Beier, 1995. A correlative evaluation of nitrogen cycling in the forest ecosystems of the EC projects NITREX and EXMAN. *Forest Ecology and Management* 71: 143-151.

Tiktak, A. and W. Bouten, 1992. Modelling soil water dynamics in a forested ecosystem. III: Model description and discretization. *Hydrological Proceedings* 6: 455-465.

Tuovinen J.P., K. Barrett and H. Styve, 1994. *Transboundary acidifying pollution in Europe: Calculated fields and budgets 1985-1993*. EMEP/MSC-W, report 1/94, Norwegian Meteorological Institute, Oslo.

Tiktak, A., J.J.M. Van Grisven, J.E. Groenenberg, C. Van Heerden, P.H.M. Janssen, J. Kros, G.M.J. Mohren, C. Van der Salm, J.R. Van de Veen and W. De Vries, 1995. *Application of three Forest-Soil-Atmospheric models to the Speuld experimental forest*. Bilthoven, RIVM, Report 733001003.

Ulrich, B., R. Mayer and P.K. Khanna, 1979. *Die Deposition von Luftverunreinigungen und ihre Auswirkungen in Waldökosystemen im Solling*. Schriften der Forstwissenschaftlichen Fakultät der Universität Göttingen 58.

Ulrich, B., R. Mayer and P.K. Khanna, 1980. Chemical changes due to acid precipitation in a loess-derived soil in Central Europe. *Soil science* 130: 193-199.

Ulrich, B., 1983. *Interaction of forest canopies with atmospheric constituents: SO<sub>2</sub>, alkali and earth alkali cations and chloride*. In: B. Ulrich and J. Pankrath (Eds). *Effects of accumulation of air pollutants in forest ecosystems*, Reidel, Dordrecht, The Netherlands, 33-45; 127-146.

UBA (Federal Environmental Agency) (Ed.), 1994. *IMA-Querschnittsseminar Wirkungskomplex Stickstoff und Wald*. UBA-Texte 28-95. Berlin.

UN/ECE, 1979. *Convention on Long-range Transboundary Air Pollution*. Geneva

UN-ECE, 1989. *Report of the Critical Levels Workshop, Bad Harzburg, Germany, 14-18 March 1988*; Federal Environment Agency Berlin, Germany

UN/ECE, 1991. *Interim Report on Cause-Effect Relationships in Forest Decline*.

UN/ECE, 1994. *Manual on methodologies and criteria for harmonised sampling, assessment, monitoring and analyses of the effects of air pollution on forests*. Hamburg/Geneva: Programme-Coordinating Centres, UN/ECE: ICP Forests, 177pp.

UN-ECE, 1995. *Effects of Nitrogen and Ozone*. Report of the International Cooperative Programmes and the Mapping Program of the Working Group on Effects. EVB. AIR/WF.1/R.110, 77p p

UN-ECE, 1996. *Manual on methodologies and criteria for mapping critical levels/loads and geographical areas where they are exceeded*. Berlin, Germany. Umwelt Bundes Amt, Texte 71/96, 144 pp.

UN/ECE and EC, 1996. *Forest condition in Europe. Report on the 1995 survey*. Geneva, Brussels: UN/ECE, CEC, 156 pp.



UN/ECE and EC, 1997a. C. Müller Edzards, J.W. Erisman, W. de Vries, M. Dobbertin and S. Gosh. *Ten years of forest condition monitoring in Europe: Studies on temporal development, spatial distribution and impacts of natural and anthropogenic stress factors. Overview Report.* EC and UN/ECE. Brussels, Geneva.

UN/ECE and EC, 1997b. *Forest condition in Europe. 1997 Executive Report.* Geneva, Brussels: UN/ECE, CEC, 41 pp.

Van Breemen, N., C.T. Driscoll and J. Mulder, 1984. Acidic deposition and internal proton sources in acidification of soils and waters. *Nature* 307: 599-604.

Van Breemen, N. and J.M. Verstraten, 1991. Soil acidification and N cycling. In: T. Schneider and G.J. Heij (Eds). *Acidification research in The Netherlands. Final report of the Dutch Priority Programme on Acidification.* Studies in Environmental Science 46, Elsevier Science Publishers, Amsterdam, The Netherlands: 289-352.

Van Dam, O., J.W.M. Van der Drift and C.A. Van Diepen, 1994. *Estimation of available soil moisture capacity for the soil units of the EC soil map.* DLO Winand Staring Centre, Wageningen, Technical document 20, 87 p.

Van Dobben, H.F., M.J.M.R. Vocks, E. Jansen en G.M. Dirkse, 1994. *Veranderingen in de ondergroei van het Nederlandse dennenbos over de periode 1985-1993.* IBN Rapport 085. 37 pp.

Van den Broek, B.J. and P. Kabat, 1996. SWACROP: dynamic simulation model of soil water and crop yield applied to potatoes. In: P. Kabat, B. Marshall, B.J. Van den Broek, J. Vos and H. Van Keulen (Eds). *Modelling and parametrization of the soil-plant-atmosphere system.* Wageningen, Wageningen pers: 299-333.

Van den Burg, J., P.W. Evers, G.F.P. Martakis, J.P.M. Relou en D.C. Van der Werf, 1988. *De conditie en de minerale-voedingstoestand van opstanden van grove den (Pinus sylvestris) en Corsicaanse den (Pinus nigra var. Maritima) in de Peel en op de zuidoostelijke Veluwe najaar 1986.* Wageningen, Instituut voor Bosbouw en Groenbeheer, "De Dorschkamp", Rapport nr. 519, 66 pp.

Van den Burg, J. en H.P. Kiewiet, 1989. *Veebezetting en de naaldsamenstelling van grove den, Douglas en Corsicaanse den in het Peelgebied in de periode 1956 t/m 1988. Een onderzoek naar de betekenis van de veebezetting voor het optreden van bosschade.* Wageningen, Instituut voor Bosbouw en Groenbeheer, "De Dorschkamp", Rapport nr. 559, 76 pp.

Van Goor, C.P. (1985). The impact of tree species on soil productivity. *Netherlands Journal of Agricultural Science* 33: 133-140

Van Keulen, H., 1986. A simple model of water-limited production. In : H. van Keulen and J. Wolf (Eds). *Modelling of agricultural production weather, soils and crops.* Wageningen, PUDOC: 130-152.

Van Leeuwen E.P., C.J.M. Potma, G.P.J. Draaijers, J.W. Erisman and W.A.J. Van Pul, 1995. *European wet deposition maps based on measurements*. RIVM report no. 722108006, Bilthoven, The Netherlands.

Van Leeuwen, E.P., G.P.J. Draaijers and J.W. Erisman, 1996. Mapping wet deposition of acidifying components and base cations over Europe using measurements, *Atmospheric Environment* 30: 2495-2511.

Van Leeuwen E.P., P.G.H. de Jong, G.P.J. Draaijers and J.W. Erisman (in prep) *Mapping deposition of acidifying components and base cations on a small scale in Europe: results for 1993 and model evaluation*. RIVM report no. 722108xxx, Bilthoven, The Netherlands.

Van Pul W.A.J., J.W. Erisman, J.A. Van Jaarsveld and F.A.A.M. De Leeuw, 1992. High resolution assessment of acid deposition fluxes. In: T. Schneider (Ed.). *Acidification Research: Evaluation and policy applications*. Studies in Environmental Science, Elsevier, Amsterdam.

Van Pul W.A.J., C.J.M. Potma, E.P. van Leeuwen, G.P.J. Draaijers and J.W. Erisman, 1995. *EDACS: European Deposition maps of Acidifying Components on a Small scale. Model description and results*. RIVM report no. 722401005, Bilthoven, The Netherlands.

Van Roestel, J., 1984. *Transpiratie en interceptie van bos: een literatuurstudie*. Utrecht, SWNBL, Rapport 7b

Van der Voet, P., C.A. Van Diepen and J.H. Oude Voshaar, 1994. *Spatial interpolation of daily meteorological data. A knowledge-based procedure for the regions of the European Communities*. Wageningen, DLO Winand Staring Centre for Integrated Land, Soil, and Water Research, Report 53.3, 117p.

Wieringa, J., 1992. Updating the Davenport roughness classification. *Journal of Wind Engineering and Industrial Aerodynamics* 41.

Wood, J.A., 1989. *Peatland acidity budgets and the effect of acid deposition*. Environment Canada, Discussion Paper no. 5, 34 pp.

Wunderli S. and R. Gehrig, 1990. Surface ozone in rural, urban and Alpine regions of Switzerland, *Atmospheric Environment* 24A: 2641.

Zaveri R.A., R.D. Saylor, L.K. Peters, R. McNider and A. Song, 1993 A model investigation of summertime diurnal ozone behavior in rural mountaineous locations, *Atmospheric Environment* 29: 1043.

Zech, W. and E. Popp, 1983. Magnesiummangel, einer der Gründe für das Fichten- und Tannensterben in NO-Bayern. *Forstwissenschaftliches Centralblatt* 102: 50-55.



Zöttl, H.W. and E. Mies, 1983. Nährelementversorgung und Schadstoffbelastung von Fichtenökosystemen im Südschwarzwald unter Immissionseinfluß. *Mitteilungen der Deutschen Botanischen Gesellschaft* 38: 429-434

**Annexes: Technical details on assessment methods and additional results**



## Annex 1 Interpolation of meteorological data

*Erik van Leeuwen, Erik de Jong, Jan Willem Erisman*

*National Institute of Public Health and the Environment (RIVM), Bilthoven, The Netherlands*

### A 1.1 The interpolation procedure

Interpolation of meteorological data to each Level I site is performed using a simple inverse distance weighting procedure from a maximum of four meteorological stations. Most emphasis in the method is put on selecting the most representative stations in the vicinity of the site under consideration to be used for the interpolation to that site. First, data are interpolated to grids with a resolution of  $0.5^\circ \times 1.0^\circ$  lat/lon. Subsequently data at each site are extracted from these grids. For each corner of a grid cell the method starts by selecting the ten best suitable stations to be used to interpolate the meteorological data, following the approach described by Van der Voet et al. (1994). The selection procedure is primarily based on the smallest geographical distance between the co-ordinates of the grid corner and the surrounding meteorological stations. The similarity between both is expressed by the so-called difference score (in km). The lower this score, the larger the similarity. Besides by geographical distance, the difference score is determined by difference in altitude and difference in the distance to the coast between the grid corner and the surrounding meteorological stations. Furthermore, a penalty is added to the score if the grid corner and the station are located on different sides of a climatic barrier, such as the Alps and the Pyrenees. This way, a station located on one side of the barrier will not be used to interpolate to a grid corner located on the other side of the barrier. If altitude for a specific site was not archived, it was obtained using the EPA altitude grid on a  $1/6^\circ \times 1/6^\circ$  lat./lon. resolution.

All ten selected stations are first checked on availability of precipitation data. If at a station precipitation for a certain time step is not recorded, it is calculated using the precipitation data recorded for the preceding or following time steps, as in the ECMWF and DWD data bases the time period for which precipitation is specified is either 6 or 12 hours. If in a certain 6-hr interval the precipitation observation time period is specified as 12 hours, it is valid for the previous 6-hr interval as well. Also, while for a current 6-hr interval precipitation might be invalid, the precipitation observation time in the next 6-hr interval could be 12 hours, indicating that this value is valid for the current interval as well. If precipitation data for both the current and the preceding or following time steps are not recorded, the precipitation value at the station is set to 'non valid'. After this, all selected stations are checked on availability of data on temperature, dew point temperature and wind speed. Stations missing data of one of these parameters are deleted from the selected station set. Then all stations in the obtained 'subset' are assigned to their respective quadrants (N,E,S,W) and sorted, in each quadrant, according to an increasing difference score. Now, a maximum of four best stations is selected (ideally, one station from each quadrant). If no stations remain from the selection procedure, interpolation to the concerning grid corner can not be performed and the parameter values are assigned 'non valid' there. If only one station remains from the selection procedure, the parameter values from this station are

assigned to the concerning grid corner. If two or more stations remain, if located in different quadrants, from each quadrant the nearest station is selected. Only one station can be selected from each quadrant. If, for example all selected stations are located in one quadrant, the program just selects one (nearest) station to be used for interpolation. In the last step in the selection procedure, stations which are separated from the grid corner by more than two times the average distance of all stations in the subset are deleted from this set. For example, if four stations are selected, the programme calculates the average distance of the three nearest stations and subsequently determines whether the fourth station is separated from the grid corner by more than two times this average distance. If necessary, this step is repeated for the three remaining stations, and subsequently the possibly two remaining stations in the example. Finally before interpolation, for each station in the subset the relative humidity is calculated using temperature and dew point temperature at the station together with a temperature/vapour pressure table.

After the selection procedure, the stations from the remaining subset for each 6-hr interval are used in the interpolation procedure. Interpolation is performed to all four corners of each grid cell. Temperature, dew point temperature, wind speed and relative humidity are interpolated from a maximum of four best stations using a simple inverse distance weighting procedure in which instead of distance the difference score (as described above) is used. For precipitation amount and cloud cover the values from the nearest station are assigned to the corner of the grid cell. Grid values are obtained by averaging the values from the four corners. Finally, to derive site-specific estimates, point data are obtained by extraction from these grids.

## **A 1.2      Uncertainties in the meteorological estimates**

The interpolation procedure was evaluated on the basis of the prediction error, i.e. the difference between observed and interpolated values at a given station (cross validation). For 1989 and 1993 this statistic was obtained via cross validation for each station with a data coverage larger than 75%. Cross validation involves estimating values at each station by interpolation from the neighbouring stations, excluding the value of the point being estimated. The mean root of the squared values of the prediction errors was used to quantify the precision of the interpolation method. For 1989 and 1993, for every 6-hr block  $j$  the difference between the predicted value  $x_{\text{pred } j}$  and the observed value  $x_{\text{obs } j}$  is calculated for each meteorological variable for each station. For the whole period of  $M$  6-hr blocks, these differences between predicted and observed values are evaluated by calculation of the *Root Mean Squared Error* (RMSE), defined as:



$$RMSE = \sqrt{\frac{1}{M} \sum_{j=1}^M (X_{obsj} - X_{predj})^2} \quad (\text{Eq. A 1})$$

where:

RMSE : Root Mean Squared Error  
M : total number of 6-hr blocks with valid data  
 $x_{obs j}$  : observed value X at 6-hr block j  
 $x_{pred j}$  : predicted value at 6-hr block j  
j : number of 6-hr block

Subsequently, at each station the RMSE is divided by the mean value over  $M$  6-hr blocks of the parameter concerned, giving the relative interpolation error. Smaller values for this statistic indicate better prediction of the meteorological variable. A relative RMSE of e.g. 1.00 indicates a prediction error of 100%.

This exercise gives unrealistic results if the mean value over  $M$  6-hr blocks of the parameter concerned lies somewhere in between -1 and 1, because dividing by such a number results in extremely large relative errors. This is especially the case for the precipitation amounts, which are smaller than one in most 6-hr periods, but may also be the case for air and dew point temperatures in northern Europe. Large errors might furthermore be found where station density is low, and where a large gradient in the meteorological parameter concerned is present. To some extent measurement errors are also incorporated in the numbers presented here, although it can not be detected where 'bad stations' are located. If at a certain station values of a certain parameter are systematically measured too high due to, for example, badly calibrated equipment, the back calculated value using cross validation differs from the measured value to a large extent.

Despite the exercise reported here, it is very hard to quantify the total uncertainty in each interpolated meteorological parameter accurately. This is because uncertainty arises from several sources: (i) errors in the selection procedure (interpolation errors), (ii) errors in the meteorological measurements, and (iii) the use of (three different) invalidated data sets from ECMWF, NCAR and DWD (meaning that they are not screened for errors and unrealistic values or outliers) in which moreover many missing data values are archived. In general uncertainty can be considerable, especially for parameters showing strong regional differences, such as precipitation amount. Air temperature and relative humidity perform good in large parts of Europe (average uncertainty about 25%), but for individual plots uncertainty can be as large as 100%. Wind speed, cloud cover and dew point temperature perform fairly good (average uncertainty about 50%), but for individual plots uncertainty can amount 200%. Largest uncertainty is associated with the interpolated precipitation amounts (average uncertainty about 100%), though locally uncertainty can be much higher. The uncertainty numbers are presented in Table A1. Considering the meteorological databases available on a European scale, better estimates than the values obtained in this study are not available.

*Table A1 Estimated average and maximum uncertainty numbers for the meteorological parameters.*

Meteorological parameter	Average uncertainty (%)	Maximum uncertainty (%)
Precipitation amount	100	-
Air Temperature	25	100
Dew point temperature	50	200
Relative humidity	25	100
Wind speed	50	200
Cloud cover	50	200



## Annex 2 Calculation of evapotranspiration, transpiration, interception and soil evaporation

**Kees Hendriks**

*DLO Winand Staring Centre (SC-DLO), Wageningen, The Netherlands*

In this annex the calculation of the parameters required for the calculation of the relative transpiration ( $RE_T$ ) is discussed. The set-up of the annex follows the sequence of the calculations. At the beginning the Penman-Monteith equation is given showing the parameters to be calculated.

### A 2.1 Calculation of potential evapotranspiration $ET_p$

The potential evapotranspiration ( $ET_p$ ) is calculated using the Penman-Monteith equation (Monteith, 1965). The equation is given as:

$$\lambda E_{Penman-Monteith} = \frac{sA + R_a c_p (q_s - q_a) / R_a}{s + g(1 + R_c / R_a)} \quad (\text{W m}^{-2}) \quad (\text{Eq. A 2})$$

in which:

- $\lambda$  = latent heat of vaporisation ( $\text{J kg}^{-1}$ )
- $E$  = evaporation rate ( $\text{kg m}^{-2} \text{s}^{-1}$ )
- $A$  = available energy ( $\text{W m}^{-2}$ )
- $s$  = slope of the saturation vapour pressure-temperature curve ( $\text{mbar } ^\circ\text{C}^{-1}$ )
- $\gamma$  = psychrometer coefficient ( $\text{mbar } ^\circ\text{C}^{-1}$ )
- $D_a$  = density of dry air ( $\text{kg m}^{-3}$ )
- $c_p$  = specific heat at constant pressure ( $\text{J kg}^{-1} ^\circ\text{C}^{-1}$ )
- $e_s$  = saturated vapour pressure (mbar)
- $e_a$  = vapour pressure at temperature  $T_a$  (mbar)
- $R_a$  = aerodynamic resistance ( $\text{s m}^{-1}$ )
- $R_c$  = crop canopy resistance ( $\text{s m}^{-1}$ )

Where  $\gamma$  equals  $0.67 \text{ mbar } ^\circ\text{C}^{-1}$ ,  $D_a$  is  $1.2047 \text{ kg m}^{-3}$  and  $c_p$  equals  $1004 \text{ J kg}^{-1} ^\circ\text{C}^{-1}$ , and  $\lambda$  can be calculated following Harrison (1963) as:

$$\lambda = 2501 - 2.3601 * T \quad (\text{kJ kg}^{-1}) \quad (\text{Eq. A 3})$$

where  $T$  is the average daily air temperature in  $^\circ\text{C}$ .

The other parameters have to be calculated following more complex series of equations, which are presented in the following sections.

### A 2.1.1 Calculation of available energy

The available amount of energy,  $A$ , can be calculated as:

$$A = R_n - D - G - M - \mu A \quad (\text{W m}^{-2}), \quad (\text{Eq. A 4a})$$

where (all in  $\text{W m}^{-2}$ ):

$R_n$  = net radiation

$D$  = advection

$G$  = soil heat flux

$M$  = energy storage in the forest

$\mu A$  = energy absorbed for photosynthesis

Following Dolman and Moors (1994)  $\mu A$ ,  $M$  and  $G$  are small in relation to  $R_n$  and therefore can be neglected. Also following Dolman and Moors (1994) it is supposed that no advection takes place by which  $D$  can be taken zero.  $A$  can be approximated as

$$A = R_n \quad (\text{W m}^{-2}) \quad (\text{Eq. A 4b})$$

$R_n$  is calculated according to Beljaars and Holtslag (1990) in the EDACS model (Annex 3). Major parameters needed to calculate  $R_n$  are cloud cover, albedo, latitude, day number and relative humidity. From these parameters net short-wave radiation and net long-wave radiation can be estimated, from which, adjusted with the albedo,  $R_n$  is calculated.

### A 2.1.2 Calculation of the slope of the saturation vapour pressure deficit-temperature curve ( $s$ ), saturated vapour pressure $e_s$ , and ambient pressure $e_a$

The Penman-Monteith equation contains the term for the slope of the saturation vapour pressure-temperature curve,  $s$ , which can be calculated as:

$$s = e_s(T) \left[ \frac{7.5 * 237.3}{(T + 237.3)^2} \ln 10 \right] \quad (\text{mbar}^\circ\text{C}^{-2}) \quad (\text{Eq. A 5})$$

where:

$e_s$  = saturated vapour pressure (mbar)

$T$  = air temperature ( $^\circ\text{C}$ )

$e_s$  can be calculated according to:

$$e_s = e_s(0) 10^{\frac{7.5}{T + 273.3}} \quad (\text{mbar}) \quad (\text{Eq. A 6})$$

where  $e_s(0)$  is 6,107 mbar.



The actual vapour pressure  $e_a$  can be simply calculated according to:

$$e_a = e_s * \frac{RH}{100} \quad (\text{mbar}) \quad (\text{Eq. A 7})$$

where  $RH$  is the relative air humidity (%), which is obtained from the meteorological data base.

### A 2.1.3 Aerodynamic resistance, $R_a$ and crop resistance, $R_c$

In EDACS the aerodynamic resistance  $R_a$  is calculated following the procedure used by Garland (1978). The crop resistance or stomatal resistance  $R_c$  is calculated following the procedure used by Baldocchi et al. (1987). Both procedures are extensively discussed in Annex 3, Section A3.2.1.

### A 2.2 Interception evaporation, $E_i$

Moors et al. (1996) showed that  $E_i$  can be estimated satisfactory only for time periods of one day or shorter, and only when using process orientated models. When interception is calculated as a percentage of gross precipitation, the uncertainty may become more than 100% (Moors et al., 1996). Therefore, we calculated the interception on a daily basis using the interception model of Gash (1995). In this model at first the amount of precipitation  $P'$ , which is needed to saturate the crown, has to be calculated according to:

$$P' = -R_{avg} \frac{S}{E_{avg}} \ln[1 - \frac{E_{avg}}{R_{avg}}] \quad (\text{mm d}^{-1}) \quad (\text{Eq. A 8})$$

where:

- $R_{avg}$  = mean rainfall rate ( $\text{mm hr}^{-1}$ )
- $E_{avg}$  = mean evaporation rate during rainfall ( $\text{mm hr}^{-1}$ )
- $S$  = canopy storage capacity (mm)

For small rain-showers when  $P < P'$  interception,  $E_i$ , can be calculated as:

$$E_i = (1 - p - p_{tr}) P \quad (\text{mm d}^{-1}) \quad (\text{Eq. A 9})$$

where:

- $P$  = daily precipitation ( $\text{mm d}^{-1}$ )
- $p$  = free throughfall coefficient (-)
- $p_{tr}$  = stem flow coefficient (-)

For showers of rain when  $P > P'$ , interception is calculated as:

$$E_i = (1 - p - p_{tr}) P' + \frac{E_{avg}}{R_{avg}} (P - P') \quad (\text{mm d}^{-1}) \quad (\text{Eq. A 10})$$

Interception of the trunk is often small and therefore frequently neglected (hence  $p_{tr} = 0$ ). In the adapted form for sparse forest, the storage capacity of the canopy  $S$  is

calculated per unit area of cover as  $S_c=S/c$  where  $c$  is the canopy cover, which is assumed to be 0.8 for all plots.

Mean rainfall ( $R_{avg}$ ) and evaporation rates ( $E_{avg}$ ) for the period the crown was saturated, are calculated per climatic region using the meteorological data. For each region,  $R_{avg}$  en  $E_{avg}$  are calculated for about 5 to 10 meteorological stations scattered throughout the regions.  $R_{avg}$  (mm hr<sup>-1</sup>) was calculated as the amount of precipitation (mm) divided by the time rain was recorded (hr).  $E_{avg}$  (mm hr<sup>-1</sup>) was calculated using the Penman-Monteith equation (Eq. A 2) in which  $R_c$  is set to 0 for the hours rain was recorded. Average values for  $R_{avg}$  and  $E_{avg}$  per region were used for all plots in the interception procedure.

The storage capacity of the forest depends on tree species. Dolman and Moors (1994) give values for  $S$  for several tree species which are shown in Table A 2. The storage capacity in Table A 2 are average values for 'normally' managed forest with a relative high canopy coverage. Because we do not know the crown coverage of the sample plots we assume that these criteria are met by the actual crown coverages of the plots.

Table A 2 Storage capacity of the crown ( $S$ ) and free throughfall coefficient ( $p$ ) for several tree species (modified after Dolman and Moors, 1994)

Tree species	$S$ (mm)			$p$ (-)		
	summer	winter	whole year	summer	winter	whole year
<i>Quercus robur</i>	0.9	0.3		0.3	0.8	
<i>Quercus ilex</i>			0.9			0.3
<i>Fagus sylvatica</i>	1.0	0.3		0.1	0.8	
<i>Pinus sylvestris</i>			1.0			0.15
<i>Picea abies</i>			2.8			0.05

Table A 2 shows that differences between deciduous species are relative small. Therefore we use  $S=1.0$  mm during summer time and  $S= 0.3$  mm during winter time for all deciduous tree species. Values for  $p$  differ considerable per tree species, and therefore combining tree species was not possible. The summer  $S$ -value (0.9) and summer  $p$ -value (0.3) for *Quercus robur* were assumed to be appropriate values for *Quercus ilex* for the whole year.  $S$  and  $p$  values are calculated as an average, proportional to the tree species per Level 1 plot.

## A 2.3 Soil evaporation

According to Van den Broek and Kabat (1996) potential soil evaporation  $E_{s,p}$  can be calculated based on Beer's Law for the absorption of the radiation flux by the canopy:

$$E_{s,p} = e^{(6 \cdot LAI)} E_{Tp} \quad (\text{mm d}^{-1}) \quad (\text{Eq. A 11})$$

where:

$6$  = extinction coefficient for net radiation

$LAI$  = leaf area index (-)



The *LAI* is calculated depending on a maximum *LAI*, differing for each tree species, and the defoliation class *DC*, given in 5% classes:

$$LAI = (1-DC) * LAI_{max} \quad (\text{Eq. A 12})$$

Since *LAI* is not recorded in the monitoring programme, a maximum *LAI* is derived from literature (adapted from Dolman and Moors, 1994) (Table A3). For *Quercus ilex*, the same *LAI* was assumed as for *Quercus robur* in summer. In the calculation of the interception a tree species proportional *LAI* was used.

Table A 3 Maximum leaf area index (*LAI*) for several tree species during summer and winter

Tree species	Summer	Winter
<i>Pinus sylvestris</i>	3.0	2.5
<i>Picea abies</i>	12.0	10.0
<i>Quercus robur</i> + <i>Q. petraea</i>	4.0	0.5
<i>Quercus ilex</i>	4.0	4.0
<i>Fagus sylvatica</i>	6.0	0.5

Actual soil evaporation,  $E_{s,a}$ , can be calculated as a function of time since the last rainfall event, following Black *et al.* (1969):

$$E_{s,a} = w(\sqrt{t_d + 1} - \sqrt{t_d}) E_{s,p} \quad (\text{Eq. A 13})$$

in which:

$t_d$  = time since last rainfall (d)

$w$  = an empirical parameter ( $d^{-1/2}$ ), taken 0.33 according to Tiktak *et al.* (1995).

## A 2.4 Actual transpiration, $E_{Ta}$

Actual transpiration,  $E_{Ta}$ , equals the potential level,  $E_{Tp}$ , when the soil moisture supply is unlimited. Because on most forest plots a soil moisture deficit is more common than a surplus, actual transpiration will be reduced. Actual transpiration can be calculated using the forest water balance as explained in Section 4.2.3.

$E_{Ta}$  can be calculated as a function of the available soil moisture. Based on literature, Rutter (1968) showed that actual transpiration will reduce when the soil moisture content will become less than 0.40 of the maximum capacity. This relation, however, does not take into account any differences between soil types and atmospheric demand. Van Keulen (1986) developed a simple model, based on soil moisture contents and transpiration rate, that overcomes these limitations. In this model a critical soil moisture content is used below which water uptake by plant roots is hampered. As long as the critical soil moisture content is not exceeded,  $E_{Ta}$  equals  $E_{Tp}$ .

The critical soil moisture content is calculated on the basis of a depletion fraction of the soil moisture content. Van Keulen (1986) takes this depletion fraction the same for all

soil types. Instead of the use of a critical soil moisture content, a critical pressure head ( $h_{cr}$ ) can be used. Van Roestel (1984) suggests a pressure head ( $h$ ) of -1000 cm above which actual transpiration is reduced. With the model of Van Keulen (1986) it is calculated that for a  $h_{cr}$  of -1000 cm the soil water depletion fraction for the texture classes fine sand, loam, light clay and peat is 0.60, 0.52, 0.44 and 0.46 respectively. These depletion fractions can be used to calculate critical soil moisture contents by multiplication of the depletion fraction and the available soil water capacity (AWC). When the critical soil moisture content ( $SMC_{cr}$ ) is exceeded, actual transpiration is assumed to decrease from 1, at  $SMC_{cr}$ , to 0 at the wilting point ( $h = -16000$ ) (Van Keulen, 1986). Thus  $E_{Ta}$  now can be calculated as:

$$E_{Ta} = E_{Tp} \text{ for } SMC_i \geq SMC_{cr} \quad (\text{Eq. A 14a})$$

and

$$E_{Ta} = E_{Tp} (SMC_i / SMC_{cr}) \quad \text{for } SMC_i < SMC_{cr} \quad (\text{Eq. A 14b})$$

where:

$SMC_i$  = soil moisture content at day  $i$  (mm)

$SMC_{cr}$  = critical soil moisture content

$SMC_{cr}$  can be calculated as:

$$SMC_{cr} = (1-p) AWC \quad (\text{Eq. A 15})$$

where:

$AWC$  = available water content (mm)

$p$  = soil water depletion fraction (-)

The soil water depletion factor can be considered as a function of the maximum transpiration rate ( $E_{Tp}$ ). Doorenbos and Kassam (1979) give indicative  $p$ -values for different groups. On the average, the  $p$ -values decrease 66% going from  $E_{Tp} = 2 \text{ mm d}^{-1}$  to  $E_{Tp} = 10 \text{ mm d}^{-1}$ . We also applied this reduction of  $p$  in our model. With the model of Van Keulen (1986) we calculated a basic  $p$ -value ( $p_b$ ) for the different soil types for  $h = -1000 \text{ cm}$  and  $E_{Tp} = 2 \text{ mm}$  (Table A 4).  $p$  is calculated as:

$$p = p_b - \frac{p_b - 0.33p_b}{8} (E_{Tp} - 2) \quad (-) \quad (\text{Eq. A 16})$$

Table A 4 Soil water depletion fraction ( $p$ ) above which actual transpiration is reduced

Soil texture class	Depletion fraction $p$
sand	0.63
loam	0.49
clay	0.42
peat	0.46

## **Annex 3      Calculation of concentration and deposition levels of acidifying compounds, base cations and ozone**

*Erik van Leeuwen, Erik de Jong, Jan Willem Erisman*

*National Institute of Public Health and the Environment (RIVM), Bilthoven, The Netherlands*

In this annex, first the models used to obtain site-specific dry deposition estimates of acidifying compounds and base cations is described, followed by the methods used to derive wet deposition estimates. Then a brief description of the uncertainty in the resulting numbers is given. Finally, the (preliminary) model used to estimate the ozone concentrations at the plots is described and an indication of the resulting uncertainty is given.

### **A 3.1 General description of EDACS**

Dry deposition estimates of acidifying compounds and base cations are obtained using the EDACS model. The components considered in EDACS are  $\text{SO}_2$  and  $\text{SO}_4^{2-}$ -aerosol ( $\text{SO}_x$ );  $\text{NO}$ ,  $\text{NO}_2$  ( $\text{NO}_x$ );  $\text{HNO}_3$  and  $\text{NO}_3^-$ -aerosol,  $\text{NH}_3$  and  $\text{NH}_4^+$ -aerosol ( $\text{NH}_x$ ), and  $\text{Na}^+$ ,  $\text{Ca}^{2+}$ ,  $\text{K}^+$  and  $\text{Mg}^{2+}$ -aerosol. In the EDACS-model dry deposition is estimated with the inference method, i.e. deposition at the surface is inferred from the concentration and deposition velocity at the same height (Erisman, 1992; Erisman and Baldocchi, 1994; Van Pul et al., 1992,1995). In the inference method it is assumed that a constant flux layer between the reference height and the surface (i.e. the atmospheric surface layer) is present. This assumption implies that (i) there is no significant advection in the layer, (ii) the air flow is well-adapted to the surface properties, and (iii) chemical reactions form a negligible source or sink. In that case the deposition flux at the reference height equals the deposition flux at the surface. The adaptation of the air flow to the surface strongly depends on the surface roughness and the stability of the air. The reference height must fulfil following criteria: (i) it must be high enough so that the concentration is not severely affected by local deposition and (ii) it must be below the surface layer height. In EDACS the reference height is taken at 50 m above ground level, which is considered as an optimum (Erisman, 1992).

The deposition velocity is calculated using a resistance model in which for each component transport to the surface and absorption or uptake by the surface are described. The parametrisations depend on surface characteristics and other environmental and meteorological conditions (Erisman et al., 1994). Meteorological data are used to describe among others the transport of the components to the surface and the surface condition. Which meteorological data were used and how they were processed is described in Section 4.2.2.1 and Annex 1, respectively. Dry deposition velocity fields for every 6 hour period are calculated using the parametrisations together with forest specific characteristics, the roughness lengths derived for each site and the meteorological information. Subsequently, the 6-hourly deposition velocity fields are averaged to daily values. For the acidifying components these fields are combined with the daily concentration data ( $150 \times 150 \text{ km}^2$ ) calculated by the EMEP/LRT to obtain



dry deposition fluxes. Using calculated concentration fields, the relation between emissions and deposition is maintained and assessments or scenario studies can be carried out. Daily fluxes were subsequently summed to annual totals. For base cations 6-hourly dry deposition velocity fields were averaged to annual means before they were combined with annual mean air concentration fields.

Wet deposition estimates were obtained using (i) results from the EMEP-LRT model, (ii) maps compiled by Van Leeuwen et al. (1996), and (iii) measurements from the EMEP network. Details on the methods and data used can be found in Section A 3.3.

### A 3.2 Methods to derive dry deposition fluxes

The dry deposition flux of gases and particles from the atmosphere to a receptor surface is governed by (i) the concentration in air, (ii) turbulent transport processes in the boundary layer, (iii) the chemical and physical nature of the depositing species, and (iv) the efficiency of the surface to capture or absorb gases and particles (e.g. Hicks et al., 1987). The flux of a trace gas is given as:

$$F = V_d(z) c(z) \quad (\text{Eq. A 17})$$

where:

$c(z)$  = the concentration at height  $z$ ;

$V_d(z)$  = the dry deposition velocity at height  $z$  (Chamberlain, 1966).

In Eq. A 17,  $z$  is the reference height above the surface, here taken as 50 m. If the surface is covered with vegetation, a zero-plane displacement ( $d$ ) is included:  $z=z-d$ .  $d$  is usually taken as 0.6-0.8 times the vegetation height (Thom, 1973).

#### A 3.2.1 Dry deposition velocity

##### *Gases*

The parametrisation of the dry deposition velocity is based on a description with a resistance analogy or Big Leaf Model (e.g. Thom, 1975, Hicks et al., 1987, Fowler, 1978, Erisman et al., 1994a). In this resistance model the most important deposition pathways by which the component is transported to and subsequently taken up at the surface are parametrised. The resistances used in the  $V_d$  parametrisation in EDACS are presented in Fig. A1 and described in Erisman et al. (1994a).

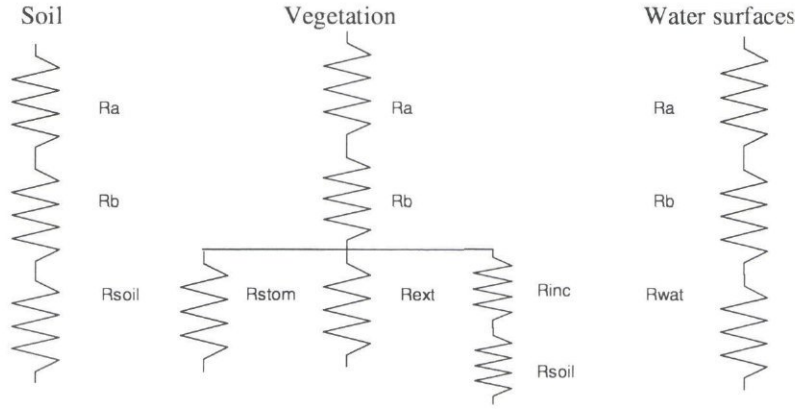


Fig. A 1 Resistances used in EDACS. For explanation of the symbols see text.

$V_d$  is represented by the inverse of three resistances:

$$V_d(z) = (R_a(z-d) + R_b + R_c)^{-1} \quad (\text{Eq. A 18})$$

These three resistances represent the three stages of transport. The aerodynamic resistance ( $R_a$ ) represents the resistance against turbulent transport of the component close to the surface, the quasi-laminar sub-layer resistance ( $R_b$ ) accounts for the transport of the component by molecular diffusion through a laminar layer adjacent to the surface, and the surface resistance ( $R_c$ ) accounts for the uptake at the surface. The atmospheric resistance to transport of gases across the constant flux layer is assumed to be similar to that of heat (e.g. Hicks et al., 1989).  $R_a$  is approximated following the procedures by Garland (1978):

$$R_a(z-d) = \frac{1}{\kappa u_*} \left[ \ln\left(\frac{z-d}{z_0}\right) - y_h\left(\frac{z-d}{L}\right) + y_h\left(\frac{z_0}{L}\right) \right] \quad (\text{Eq. A 19})$$

in which  $\kappa$  is the Von Karman constant (0.4),  $u_*$  the friction velocity,  $L$  the Monin Obukhov length and  $z_0$  the roughness length.  $z_0$  values can be obtained from look-up tables, e.g. those proposed by Davenport (1960), revised by Wieringa (1992), or Voldner et al. (1986).  $y_h[(z-d)/L]$  is the integrated stability function for heat. These can be estimated using procedures described by Beljaars and Holtslag (1990).  $R_b$  is approximated by the procedure presented by Hicks et al. (1987):

$$R_b = \frac{2}{\kappa u_*} \left( \frac{Sc}{Pr} \right)^{\frac{2}{3}} \quad (\text{Eq. A 20})$$

where  $Sc$  and  $Pr$  are the Schmidt and Prandtl numbers, respectively.  $Pr$  is 0.72 and  $Sc$  is defined as:  $Sc = \nu/Di$ , with  $\nu$  being the kinematic viscosity of air ( $0.15 \text{ cm}^2 \text{ s}^{-1}$ ) and  $Di$  the molecular diffusivity of pollutant  $i$  which is thus component specific.

The surface resistance ( $R_c$ ) is composed of the resistances of the various uptake processes at the surface. For a surface covered with vegetation this is:

- stomatal resistance ( $R_{stom}$ ): the resistance to transport through stomata of leaves and needles;
- mesophyll resistance ( $R_m$ ): the resistance of internal plant tissues against uptake (in a chemical way). For the components considered  $R_m$  is assumed 0;
- cuticle resistance ( $R_{cut}$ ) or external surface resistance ( $R_{ext}$ ): the resistance of the exterior plant parts against uptake of the component;
- in-canopy aerodynamic resistance ( $R_{inc}$ ): the resistance accounting for transport of air above the vegetation towards the soil and lower plant parts;
- soil resistance ( $R_{soil}$ ): the resistance against absorption at the soil surface.

These resistances, which act in parallel or in series, are summed to yield a (total) surface resistance ( $R_c$ ):

$$R_c = [(R_{inc} + R_{soil})^{-1} + R_{ext}^{-1} + (R_m + R_{stom})^{-1}]^{-1} \quad (\text{Eq. A 21})$$

$R_c$  is affected by meteorology, leaf area, stomatal physiology, soil and external leaf surface pH, and presence and chemistry of water drops and films. Especially the state of the leaf and soil surface (i.e. the presence of water films and snow) is an important variable governing the deposition of soluble gases like  $\text{SO}_2$  and  $\text{NH}_3$ .

The scheme to derive the surface resistances for  $\text{SO}_2$ ,  $\text{NO}_2$ ,  $\text{NO}$ ,  $\text{HNO}_3$ ,  $\text{NH}_3$  used in EDACS is described in Erisman et al. (1994a). This scheme is based among others on Wesely (1989) and Lövblad et al. (1993), and dry deposition measurements (e.g. performed within the framework of the BIATEX project).

### Particles

Deposition velocities of particles composed of  $\text{SO}_4$ ,  $\text{NO}_3$ ,  $\text{NH}_4$  and base cations are calculated using two different parametrisations. The particle dry deposition velocity for low vegetation and other areas with a roughness length ( $z_0$ ) less than 0.5m is calculated using a parametrisation by Wesely et al. (1985), and for forests and other areas with a  $z_0$  above 0.5 m using a parametrisation based on the model of Slinn (1982) which was recently extended and tested with micro-meteorological measurements performed at the Speulder forest in The Netherlands (Ruijgrok et al., 1996; Erisman et al., 1994c). It includes both turbulent exchange and sedimentation of coarse particles.

Here only the parametrisation for rough surfaces (forests) is given. The general form for  $V_d$  at a height of 50 m equals:

$$V_d = (V_{da}^{-1} + V_{ds}^{-1})^{-1} + V_s \quad (\text{Eq. A 22})$$

where following Slinn's (1982) approach, turbulent exchange is split in an aerodynamic and a surface deposition velocity ( $V_{da}$  and  $V_{ds}$ , respectively). Deposition as a result of sedimentation due to the earth's gravitational force is represented by  $V_s$ . The aerodynamic deposition velocity equals the inverse of the aerodynamic resistance ( $R_a$ ):



$$V_{da} = 1/R_a(z=50) \quad (\text{Eq. A 23})$$

The surface deposition velocity depends on the collection efficiency of the surface which, in turn, is determined by the various deposition processes, the size of the depositing aerosol, atmospheric conditions and surface properties. Ruijgrok et al. (1996) showed from theoretical considerations that  $V_{ds}$  has the following limiting form:

$$V_{ds} = E \frac{u_*^2}{u_h} \quad (\text{Eq. A 24})$$

in which  $E$  represents an overall collection efficiency,  $u_*$  the friction velocity and  $u_h$  the wind speed at canopy height. The collection efficiency depends on atmospheric and surface conditions. Ruijgrok et al. (1996) showed that values of  $V_{ds}$  show a different response to the driving force  $u_*^2/u_h$  for different wetness conditions of the surface and ambient relative humidity ( $rh$ ). Their parametrisations of the collection efficiency under different conditions are presented in Table A 5.

The sedimentation velocity of particles can be computed using Stoke's Law and equals  $0.0067 \text{ m s}^{-1}$  when assuming a mean particle density of  $1700 \text{ kg m}^{-3}$ . At relative humidities larger than 80%, the effect of hygroscopic particle growth has to be taken into account. Ruijgrok et al. (1994) parametrised this effects based on work of Fitzgerald (1975):

$$V_s = 0.0067 * 1.89 e^{\frac{0.00066 rh}{1.058-0.01 rh}} \quad (\text{Eq. A 25})$$

Table A 5 Parametrisations of the collection efficiency under different conditions (after Ruijgrok et al., 1996). The surface is considered wet during and a few hours after precipitation.

E	Condition
$0.679 * u_*^{0.56}$	wet surface, $rh \leq 80$
$0.679 * u_*^{0.56} * [1 + 0.37 * e^{(rh-80)/20}]$	wet surface, $rh > 80$
$0.140 * u_*^{0.12}$	dry surface, $rh \leq 80$
$0.140 * u_*^{0.12} * [1 + 0.09 * e^{(rh-80)/20}]$	dry surface, $rh > 80$

The  $V_d$  calculated with the parametrisation described above (Eq. A 3-9) holds for  $\text{Na}^+$ ,  $\text{Mg}^{2+}$  and  $\text{Ca}^{2+}$  containing particles with MMD's representative for the Speulder forest. For  $\text{K}^+$  containing particles the outcome should be halved, because of the smaller MMD of such particles (Ruijgrok et al., 1994). The parametrisation is assumed to be representative for other areas in Europe.

Input to the deposition module of EDACS is information on component type, roughness length and meteorology (Table A6). Also information on the 'pollution climate' of the surface is taken into account by expressing the ratio between the ammonia and sulphur concentration (denoted N/S) as low or high. With this ratio the interaction of ammonia and sulphur in the deposition process of ammonia and sulphur is modelled (Erisman and Wyers, 1993; Erisman et al., 1994a). An extensive description of all databases used in the EDACS model is given in van Pul et al. (1995).

For each site, 6-hourly meteorological information was used to calculate the friction velocity, surface heat fluxes (sensible and latent heat) and short-wave incoming radiation. These meteorological parameters are calculated using the scheme described by Beljaars and Holtslag (1990). In this scheme the land-use specific  $z_0$  values were used. In EDACS the *LAI* (Leaf Area Index) of the vegetation is needed to calculate the effective stomatal resistance of the 'big leaf' layer. A simple seasonal variation of the *LAI* in agricultural area was assumed. The *LAI* linearly increases from zero in April to 5 in July and August, and linearly decreases from the August-value to zero in November.

Surface wetness, as a result of rainfall, was taken from the synoptic data. If rain was reported, the surface was assumed wet during the time period of 6 hours. Drying of the surface or information on surface wetness of the previous time period were not taken into account because only 6 hr average meteorological data are used and it is assumed that these processes take place on time scales smaller than 6 hours.

Table A 6 Parameters used in EDACS

Input	Description	Spatial resolution	Temporal resolution
General	latitude, longitude	site	6 hr
	time (month, day, hour)		
	pollution climate (N/S ratio): 1 = low, 2 = high, 3 = very low	150 x 150 km <sup>2</sup>	24 hr
Concentrations	Acidifying components: SO <sub>2</sub> , NH <sub>3</sub> , NO <sub>2</sub> , NO, HNO <sub>3</sub> , particles: SO <sub>4</sub> <sup>2-</sup> , NO <sub>3</sub> <sup>-</sup> , NH <sub>4</sub> <sup>+</sup>	150 x 150 km <sup>2</sup>	24 hr
	Base cations: Na <sup>+</sup> , Mg <sup>2+</sup> , Ca <sup>2+</sup> , K <sup>+</sup>	50 x 50 km <sup>2</sup>	annual mean
Land use type (roughness length)	coniferous forest deciduous forest mixed forest	site	-
Meteorology	short wave radiation (W m <sup>-2</sup> )	1.0° x 0.5°	6 hr
	temperature at 1.5 m (°C)		
	relative humidity at 1.5m (%)		
	wind speed at 50 m (m s <sup>-1</sup> )		
	friction velocity (m s <sup>-1</sup> )		
	Obukhov length (m)		
	surface wetness: 0 = dry, 1 = wet, 9 = snow		

### A 3.2.2 Air concentrations

Concerning the acidifying compounds, concentration data calculated by the EMEP Lagrangian long-range transport model (hence EMEP-LRT) on a 150 x 150 km<sup>2</sup> scale (Sandnes, 1993) were used to obtain concentration fields of acidifying components over Europe for 1985-1995. The EMEP model uses annual mean emission maps of SO<sub>2</sub>, NO<sub>x</sub> and NH<sub>3</sub> on a 50 x 50 km<sup>2</sup> grid as input. The concentration at 50m height is taken to be representative for an EMEP-LRT grid cell of 150 x 150 km<sup>2</sup>, and is consequently used to estimate the deposition to surfaces within this area. Daily averaged values of



the concentrations of SO<sub>2</sub>, NH<sub>3</sub>, NO, NO<sub>2</sub>, HNO<sub>3</sub>, and SO<sub>4</sub><sup>-</sup>, NO<sub>3</sub><sup>-</sup> and NH<sub>4</sub><sup>-</sup> particles were calculated and used as input for EDACS.

Air concentrations of base cations were estimated from precipitation concentrations using scavenging ratios. The latter were derived from simultaneous measurements of base-cation concentrations in precipitation and surface-level air, using a relatively simple scavenging process model (see below). This approach to estimate air concentrations is based on the premise that cloud droplets and precipitation efficiently scavenge particles resulting in a strong correlation between concentrations in precipitation and the surface-level air (Eder and Dennis, 1990). This assumption will only be valid for well-mixed conditions at sufficient distance from sources. Particles will be scavenged when they serve as cloud condensation nuclei (in-cloud scavenging) or when they are intercepted by falling hydrometeors (below-cloud scavenging). Experiments of Jaffrezo and Colin (1988) indicate in-cloud processes to be the dominant scavenging pathway for Na<sup>+</sup>, whereas for Mg<sup>2+</sup>, Ca<sup>2+</sup> and K<sup>+</sup> both in-cloud and below-cloud scavenging is important.

Factors that will influence the magnitude and variability of scavenging ratios include particle size distribution (Kane et al., 1994; Jaffrezo and Colin, 1988; Buat-Menard and Duce, 1986) and to a lesser extent particle solubility (e.g. Slinn et al., 1978; Jaffrezo and Colin, 1988), precipitation amount (Barrie, 1985; Savoie et al., 1987), precipitation rate (Slinn, 1977; Scott, 1981), droplet accretion process (Scott, 1981) and storm type (Barrie, 1992). Event scavenging ratios can range between several orders of magnitude even for single species at a single location. However, scavenging ratios have been found reasonably consistent when averaged over one year or longer (Galloway et al., 1993). For this reason, and because other data are not available, annual mean precipitation concentrations were used to infer annual mean air concentrations of Na<sup>+</sup>, Mg<sup>2+</sup>, Ca<sup>2+</sup> and K<sup>+</sup>. Precipitation concentration data were taken from Van Leeuwen et al. (1995). They compiled measurement results from about 600 sites scattered over Europe (Section 3.3). Ambient air concentrations derived this way will reflect the large scale background situation.

The scavenging ratio (SR) is defined as:

$$SR = [C]_{rain} * \rho / [C]_{air} \quad (\text{Eq. A 25})$$

where  $[C]_{rain}$  denotes the concentration in precipitation (mg/l),  $[C]_{air}$  the concentration in ambient air (in  $\mu\text{g}/\text{m}^3$ ) and  $\rho$  the density of air, taken as  $1200 \text{ g m}^{-3}$ . For the size range alkaline particles usually occur in, the following relationship between the scavenging ratio and the mass median diameter ( $MMD$ , in  $\mu\text{m}$ ) can be derived from data of Kane et al. (1994):

$$SR = 188 * e^{(0.227 * MMD)} \quad (\text{Eq. A 26})$$

Rearranging Eq. A 25 and A 26 gives a simple empirical model describing the relationship between air concentration on the one hand and precipitation concentration and mass median diameter on the other hand:



$$[C]_{air} = ([C]_{rain} * 1200) / (188 * e^{0.227 * MMD}) \quad (\text{Eq. A 27})$$

The *MMD* of particles will depend, among others, on the distance to sources. More efficient removal by dry and wet deposition of the larger particles results in decreasing *MMD*'s with source distance. As no information was available on the distribution of *MMD* of alkaline particles over Europe, it was assumed to cover the variation in precipitation concentration. Both *MMD* and  $[C]_{rain}$  will increase with decreasing distance to source areas. Linear relationships between *MMD* and  $[C]_{rain}$  were derived assuming coinciding 'means', 'means  $\pm \sigma_g$ ' and 'means  $\pm 2\sigma_g$ ' in which  $\sigma_g$  represents the geometric standard deviation (Table A 7). Mean and  $\sigma_g$  of *MMD* were assumed equal to the ones reported by Milford and Davidson (1985), and mean and  $\sigma_g$  of  $[C]_{rain}$  in Europe were taken from Van Leeuwen et al. (1995). Model results were tested with simultaneous measurements of base-cation concentrations in precipitation and surface-level air made by Stevenson (1967), Harrison and Pio (1983), Derrick et al. (1984), Pratt and Krupa (1985), Savoie et al. (1987), Jaffrezo and Colin (1988), Eder and Dennis (1990), RIVM (1993), Galloway et al. (1993), Kane et al. (1994), Römer and Te Winkel (1994) and Guerzoni et al. (1995). Model predictions fitted the measurement results very well (Draaijers et al., 1996). The impact of relative humidity on the *MMD* of particles is not taken into account. This will result in a slight overestimation of air concentrations in areas with above-average relative humidities and vice versa.

Table A 7 Relationships between mass median diameters of alkaline aerosols (*MMD*, in  $\mu\text{m}$ ) and precipitation concentrations ( $[C]_{rain}$ , in  $\text{mg l}^{-1}$ ) in Europe

Component	Relationship between <i>MMD</i> and $[C]_{rain}$
Na <sup>+</sup>	$MMD = 0.574 * [C]_{rain} + 6.082$
Mg <sup>2+</sup>	$MMD = 2.778 * [C]_{rain} + 5.694$
Ca <sup>2+</sup>	$MMD = 1.520 * [C]_{rain} + 6.316$
K <sup>+</sup>	$MMD = 2.740 * [C]_{rain} + 4.096$

### A 3.3 Methods to derive wet deposition estimates of acidifying components and base cations

To obtain wet deposition estimates for each year in the period 1986-1995, several data sources were used. Van Leeuwen et al. (1996) compiled wet deposition maps of acidifying components and base cations for 1989 (Van Leeuwen et al., 1996) and 1993 (Van Leeuwen et al., in prep) using measurements made at about 750 and 600 sites scattered over Europe, respectively (number differing per component and per year). Information on precipitation concentrations for both years was obtained from the EMEP database (Schaug et al., 1991) and, via questionnaires, from organisations responsible for wet deposition monitoring in their countries. Concentrations measured with bulk samplers were corrected for the contribution of dry deposition onto the funnels of these samplers (Van Leeuwen et al., 1996). Point observations were interpolated to a 50 x 50 km<sup>2</sup> field covering the whole of Europe using kriging interpolation. Wet deposition

fluxes were obtained by multiplying the annual mean concentrations by long-term mean precipitation amounts (Legates and Willmott, 1990).

As the detailed wet deposition maps were only available for 1989 and 1993, additional data bases were required to obtain data for the years 1986 to 1995. For this purpose two data bases containing information for the whole period were considered. First, the precipitation concentrations daily measured within the EMEP network (ca 70 sites) can be used for interpolation over Europe for each year. Second, the wet deposition estimates of acidifying components generated by the EMEP-LRT model, available on a  $150 \times 150 \text{ km}^2$  resolution, can be used. However, both sources only provide low spatial resolution estimates which are not very accurate to estimate the deposition on the site-level. Therefore it was investigated whether the detailed maps could be used to apply a correction to the values obtained from both data sources mentioned above for all missing years. It was investigated whether the ratios between the concentration fields obtained from both sources and the detailed interpolated concentration fields obtained by Van Leeuwen et al. (1996) for 1989 equalled the ratios for 1993. If the ratios are constant over these two years, they can be assumed to be constant for other years as well, and hence be used for correction.

This exercise was first performed for the EMEP measurements. The values measured at the EMEP sites were compared with the accompanying values extracted from the interpolated maps from Van Leeuwen et al. (1996). Ratios found were not constant over the years. Comparison of the modelled EMEP-LRT fields with the maps from Van Leeuwen et al. (1996) on an EMEP grid cell basis ( $150 \times 150 \text{ km}^2$ ) revealed better results, though for each component some serious outliers were detected, and the scatter in the plots was considerable. Largely, the outliers found were located in particular parts of Europe, mostly in Russia and Spain. For these reasons it was decided to use EMEP-LRT fields to determine wet deposition of acidifying components at the plots.

Deposition of base cations is not calculated by the EMEP-LRT model. However, precipitation concentrations of base cations are measured within the EMEP network. These measurements were used to investigate trends in precipitation concentrations for each component separately. Annual mean EMEP measurement data were available for the period 1986 to 1994 at 77, 67, 76 and 67 sites for  $\text{Na}^+$ ,  $\text{Mg}^{2+}$ ,  $\text{Ca}^{2+}$  and  $\text{K}^+$  respectively. Available time series ranged from 5 to 9 years. For all sites a regression analysis was carried out, and the Pearson correlation coefficient was calculated. The trends were considered significant if the correlation coefficient ( $R^2$ ) was larger than 0.25 (arbitrarily chosen). Applying this criterion resulted in 32, 21, 32 and 26 sites with significant trends for  $\text{Na}^+$ ,  $\text{Mg}^{2+}$ ,  $\text{Ca}^{2+}$  and  $\text{K}^+$  respectively.

The trends found were assumed to hold for the whole period 1986 to 1995, though at some sites they may be calculated using information from, for example, the period 1986 to 1990 only. The slopes of the regression lines at these sites were interpolated to a grid with a resolution of  $50 \times 50 \text{ km}^2$  using an inverse distance weighting procedure. In order to obtain a grid covering the whole of Europe, an interpolation radius of 1500 km was used. Though the sites used were reasonably well distributed over Europe, using



information available on only such a small number of sites results in extrapolation rather than interpolation in large areas.

The detailed precipitation concentration maps for 1989 (Van Leeuwen et al., 1996) and 1993 (Van Leeuwen et al., in prep), also available on a resolution of 50 x 50 km<sup>2</sup>, were used as references. For each component separately, for the period 1986 to 1991 the values from the detailed 1989 maps were corrected by adding (when calculating for the period 1990 to 1991) or subtracting (when calculating for the period 1986 to 1988) *x* times the slope of the regression line (in which *x* refers to the number of years deviating from 1989). For 1992 to 1995 the same procedure was applied using the detailed maps for 1993. Using this procedure precipitation concentration maps for all years were obtained, in which large scale temporal patterns are to some extent corrected for the general trend in emissions per component. The maps thus obtained were also used to derive air concentration maps used to calculate dry deposition of base cations following the procedure described in Section A 3.2.2.

### A 3.4 Model validation procedures

Deposition estimates derived from throughfall and bulk precipitation measurements were compared to modelled deposition estimates for all measurement sites. For this purpose, the model was run using stand-specific roughness lengths. Table A8 gives the relationships between tree height (*h*) and roughness length (*z*<sub>0</sub>) were used (Erisman, 1992), assuming an open canopy forest (crown coverage < 60%).

Table A8 Relationships between tree height (*h*) and roughness length (*z*<sub>0</sub>), assuming an open canopy forest (crown coverage < 60%; Erisman, 1992).

Season	Forest type	Relationship
Summer	deciduous	$z_0 = 0.090 * h$
	coniferous/mixed	$z_0 = 0.085 * h$
Winter	deciduous	$z_0 = 0.060 * h$
	coniferous/mixed	$z_0 = 0.085 * h$

The impact of canopy closure on the roughness length could not be taken into account due to lack of data.

A canopy budget model initially developed by Ulrich (1983) was used to estimate the impact of canopy leaching on throughfall and stemflow fluxes of Mg<sup>2+</sup>, Ca<sup>2+</sup> and K<sup>+</sup>. An extensive description and uncertainty analysis of the model used is presented by Draaijers and Erisman (1995). In the model, Na<sup>+</sup> is assumed not to be influenced by canopy exchange through which dry deposition of Na<sup>+</sup> can be calculated by subtracting wet deposition from the throughfall+stemflow flux. Particles containing Mg<sup>2+</sup>, Ca<sup>2+</sup> and K<sup>+</sup> are assumed to have the same mass median diameter as Na<sup>+</sup> containing particles. Dry deposition of Mg<sup>2+</sup>, Ca<sup>2+</sup> and K<sup>+</sup> can subsequently be calculated according to:

$$DD_x = (TF_{Na}+SF_{Na}-BP_{Na})/BP_{Na} * BP_x \tag{Eq. A 28}$$



where *DD*, *TF*, *SF*, and *BP* represent dry deposition, throughfall, stemflow and bulk-precipitation flux, respectively and *x* denotes  $\text{Mg}^{2+}$ ,  $\text{Ca}^{2+}$  or  $\text{K}^+$ . In Eq. A 28  $(TF_{\text{Na}} + SF_{\text{Na}} - BP_{\text{Na}}) / BP_{\text{Na}}$  represents the so-called 'dry deposition factor'. In this study annual mean throughfall, stemflow and bulk precipitation fluxes are used through which differences in dry deposition factor caused by seasonal changes in pollution climate and canopy characteristics are neglected. Additional error will arise by using bulk precipitation data instead of wet-only deposition though a correction for the dry deposition on the funnels of the samplers was applied. The assumption that  $\text{Mg}^{2+}$ ,  $\text{Ca}^{2+}$  and  $\text{K}^+$  containing particles are deposited with equal efficiency as  $\text{Na}^+$  containing particles introduces an error as the particle size distribution of these constituents is not necessarily the same (Milford and Davidson, 1985).

### A 3.5 Uncertainty in deposition and concentration estimates

In the first part of this Annex, uncertainty sources in wet, dry and total deposition will be described. The uncertainty in EDACS results is derived from several publications, i.e. Draaijers et al. (1996a) concerning dry deposition of base cations, Erisman (1993) and Van Pul et al. (1995) concerning dry deposition of acidifying compounds, and Van Leeuwen et al. (1995) concerning wet deposition of acidifying compounds and base cations. The reader is referred to these publications for a more elaborate description of the uncertainty estimates. At the end of this section, the comparison of modelled deposition with throughfall measurements will be presented.

#### A 3.5.1 Wet deposition

The wet deposition estimates are subject to several sources of uncertainty. These are divided into three main categories: (i) uncertainty associated with the measurements, (ii) uncertainty associated with assumptions and simplifications in the methods used, and (iii) uncertainty caused by the interpolation procedure. Van Leeuwen et al. (1995) give an extensive description of these uncertainties. The main source of uncertainty is found to differ per region. Three type of regions were distinguished, i.e. A: West, Northwest and Central Europe where data quality is assumed to be good and sufficient (representative) data are present, B: East, Southeast and Southwest Europe, where less data are available of which the representativeness and quality can be questionable and C: mountainous areas (e.g. the Alps) and upland areas, areas with complex terrain. On the average, the overall uncertainty for a 50 x 50 km<sup>2</sup> grid cell is estimated to be 50% in area A, 60% in B and 70% in C

### A 3.5.2 Dry deposition

Uncertainty in the dry deposition estimates is determined by uncertainty in dry deposition velocities and in ambient air concentrations. Below, a distinction is made between sulphur and nitrogen compounds on the one hand, and base cations on the other hand. For both, first uncertainty in the deposition velocity is described briefly followed by uncertainty in the ambient air concentrations.

#### *Sulphur and nitrogen compounds*

The uncertainty in the dry deposition velocities is mainly the result of using the simple resistance formulation for a highly complex process, and, more specifically, the surface resistance ( $R_c$ ) parametrisations. Accurate  $R_c$  parametrisations are not available for all vegetation species, surface types and conditions. The influence of surface wetness is e.g. parametrised only very roughly. It is found to be one of the major factors influencing the deposition process of soluble gases. The overall uncertainty in the surface resistance parametrisation due to above mentioned factors varies between 20% and 100%, and depends on component and surface type (Van Pul et al., 1995).

The concentration at 50m above ground level is taken to be representative for an EMEP LRT gridcell of  $150 \times 150 \text{ km}^2$ , and is consequently used to estimate the deposition to surfaces within this area. Uncertainty in the air concentrations derived from the EMEP-LRT model is not yet quantified accurately. Krüger (1993) estimates uncertainty in the air concentrations modelled by the EMEP-LRT to be 40-70% using a statistical analysis with EMEP measurements. Furthermore it is assumed that the concentration distribution within a grid cell of  $150 \times 150 \text{ km}^2$  is homogeneous. This is not the case, especially in grid cells containing industrialised areas or many scattered sources such as intensive animal husbandry farms and/or roads. The uncertainty in the deposition in a  $1/6^\circ \times 1/6^\circ$  grid cell due to these concentration gradients is assumed to be 25% on the average (Van Pul et al., 1995). In addition, the EMEP model takes local deposition into account to a limited extent.

#### *Base cations*

Ruijgrok et al. (1994) assessed the uncertainty of the model on which the parametrisation of the deposition velocity of base cations is based. The overall uncertainty in modelled deposition velocities integrated over the size distribution representative for alkaline particles at the Speulder forest was found to equal 60%. For other plots additional uncertainty will arise due to limited availability and accuracy of relevant meteorological parameters. The uncertainty in deposition velocity caused by variation in size distribution of alkaline particles amounts 30-50% per  $50 \times 50 \text{ km}^2$  grid cell, assuming a  $MMD$  of  $5 \mu\text{m}$  and taking a  $\sigma_g$  of 2-3 to represent the variation (Ruijgrok et al., 1994). Draaijers et al. (1996) give an extensive description of the uncertainty associated with dry deposition of base cations.

Uncertainty in the base cation air concentrations is introduced by uncertainties in the scavenging ratios and precipitation concentration maps used to estimate the air concentrations. The uncertainty in average precipitation concentration per  $50 \times 50 \text{ km}^2$  grid cell was estimated 30-50% (Van Leeuwen et al., 1995). Theoretical models (Slinn,



1982) and field measurements (Kane et al., 1994) suggest that the scavenging efficiency increases with particle diameter. Using the relationship between particle mass median diameter and scavenging efficiency presented by Kane et al. (1994), the uncertainty in estimated ambient air concentrations caused by variation in size distribution was estimated to amount 50-100% per 50 x 50 km<sup>2</sup> grid cell, assuming an average mass median diameter (*MMD*) of 5 µm and taking a geometric standard deviation ( $\sigma_g$ ) of 2-3. Large sub-grid concentration gradients are likely to exist, especially when point sources and/or many scattered sources such as agricultural fields and unpaved roads are present. In emission areas, surface-level air concentrations will be larger than concentrations at 50 m height, whereas in (more) background situations surface-level concentrations will be lower as a result of dry deposition. Besides in areas very close to or far away from major sources, large potential errors may arise in areas where sufficient mixing has not occurred and/or areas with a strongly deviating precipitation climatology. In the scavenging model the impact of particle solubility, precipitation amount, precipitation rate, droplet accretion process and storm type is not taken into account (Draaijers et al., 1996a).

### **A 3.5.3 Total deposition**

The uncertainty in regional scale deposition estimates strongly depends on the pollution climate and on landscape complexity of the area under study. Deposition estimates yield higher uncertainty in areas built up by complex terrain (fog and cloud deposition is neglected and seeder-feeder effects are not taken into account) and with strong horizontal concentration gradients. The uncertainty in total deposition is determined by the uncertainty in wet and dry deposition. Using error propagation methods and assuming presented uncertainties in deposition velocities and air concentrations represent random errors, the total uncertainty in dry deposition for a grid cell was estimated to amount 80-120% on average (Draaijers et al., 1996a). Van Leeuwen et al. (1995) estimated the uncertainty in wet deposition at 50-70% on average. The uncertainty in total deposition can be calculated to amount 90-140% (Draaijers et al., 1996a). Relatively large uncertainty in total deposition will be found in mountainous and upland areas, areas close to sources, 'background' areas, and areas with extremely high or low average ambient relative humidity. Additional errors in mountainous areas may arise due to ignoring the contribution of fog and cloud water deposition to the total deposition.

Table A9 presents the correlation coefficients of linear regression equations between modelled and measured dry, wet and total deposition. Also given in this table are the results of a 'paired two sample for means' t-test from which it can be determined if the averages of modelled and throughfall data are significantly different. Besides, in this table the relative standard error is presented. This is the predicted y-value (model estimates) for each x-value (throughfall estimates) in the regression, divided by the average of the x-values, giving a measure of the relative uncertainty.



Fig. A2A-G, Fig. A3A-G and Table A9 show that although there is usually a high correlation and significant regression equations ( $p < 0.05$ ) were found (wet deposition of  $\text{SO}_4^{2-}$  being the only exception), averages are different on the  $p < 0.05$  level (except for  $\text{NH}_x$  dry and  $\text{Mg}^{2+}$  dry and wet deposition) and there is considerable scatter. This means that on the average the model performs well, but for individual plots the deviation from the measured level can be large, given the uncertainty in the throughfall measurements. To a large extent this can be attributed to the large uncertainty in air concentrations. Air concentrations of acidifying components are based on the EMEP model which has a poor spatial resolution ( $150 \times 150 \text{ km}^2$ ) and only accounts for the long-range transported fraction, whereas air concentrations of base cations are based on a simple scavenging model. The scatter in the results can also be attributed to uncertainty in the throughfall measurements (Draaijers et al., 1996a). The uncertainty in atmospheric deposition estimated from throughfall, stemflow and precipitation measurements is estimated to be 30% for sulphur and 40% for nitrogen and base cations, provided that state-of-the-art measurements and analytical techniques are used in combination with a sufficiently large number of replicate samplers (Draaijers et al., 1996b).

Generally, for  $\text{SO}_x$ ,  $\text{NO}_y$  and  $\text{NH}_x$  the dry deposition constitutes a large fraction of the total deposition at the measurement sites. For  $\text{Na}^+$  and  $\text{Mg}^{2+}$  the opposite is the case, whereas for  $\text{Ca}^{2+}$  and  $\text{K}^+$  dry and wet deposition are about the same.  $\text{Na}^+$  and  $\text{Mg}^{2+}$ , being mostly of marine origin, are mainly deposited in coastal areas where precipitation amounts, and hence wet deposition fluxes are high.

Table A 9 Pearson correlation coefficients of linear regression equations between modelled and measured wet, dry and total deposition, respectively. Moreover results of a 'paired two sample for means' t-test to see whether both estimates are equal on the average or not, and the relative standard error (relSE) are presented. \* denotes both estimates differ not significantly ( $p < 0.05$ ). n denotes the number of measurements used in the comparison.

		$\text{SO}_x$	$\text{NO}_y$	$\text{NH}_x$	$\text{Na}^+$	$\text{Mg}^{2+}$	$\text{Ca}^{2+}$	$\text{K}^+$	Acid	Tot_N
Dry deposition	r	0.46	0.31	0.65	0.72	0.50	0.59	0.30	0.55	0.62
	t-test	-	-	*	-	*	-	-	-	-
	RelSE	98%	67%	71%	69%	84%	58%	51%	79%	63%
	n	292	292	296	236	236	236	236	292	292
Wet deposition	r	0.02	0.24	0.63	0.83	0.51	0.72	0.24	0.42	0.50
	t-test	-	-	-	-	*	-	-	-	-
	RelSE	73%	78%	47%	89%	117%	62%	51%	60%	57%
	n	292	292	296	236	236	236	236	292	292
Total deposition	r	0.49	0.13	0.72	0.79	0.54	0.69	0.28	0.63	0.68
	t-test	-	-	-	-	-	-	-	-	-
	RelSE	82%	67%	49%	109%	90%	56%	49%	64%	51%
	n	292	292	296	236	236	236	236	292	292

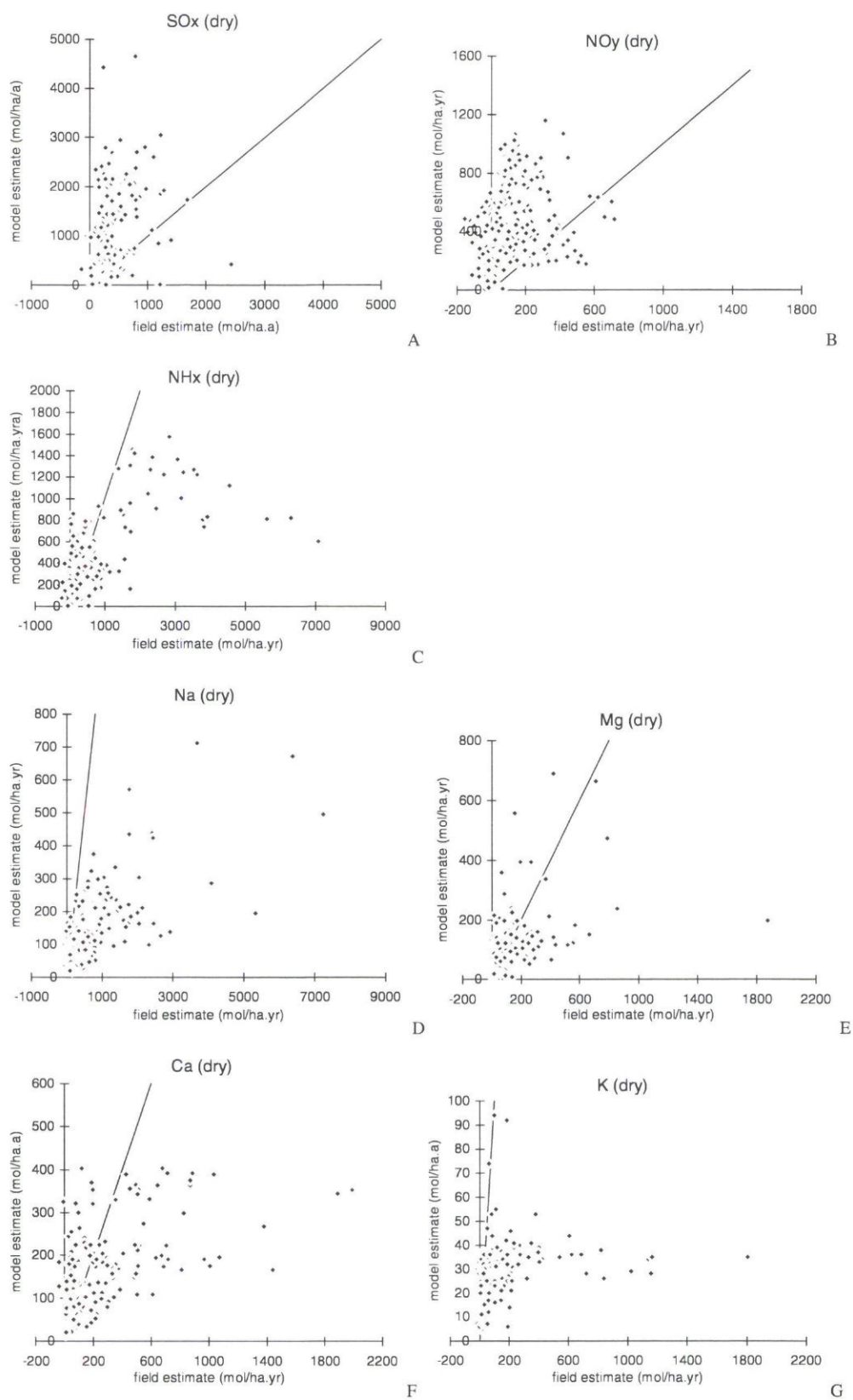


Fig. A 2 Relationship between modelled dry deposition and dry deposition estimated from throughfall and bulk precipitation measurements. The line  $y = x$  is also presented.

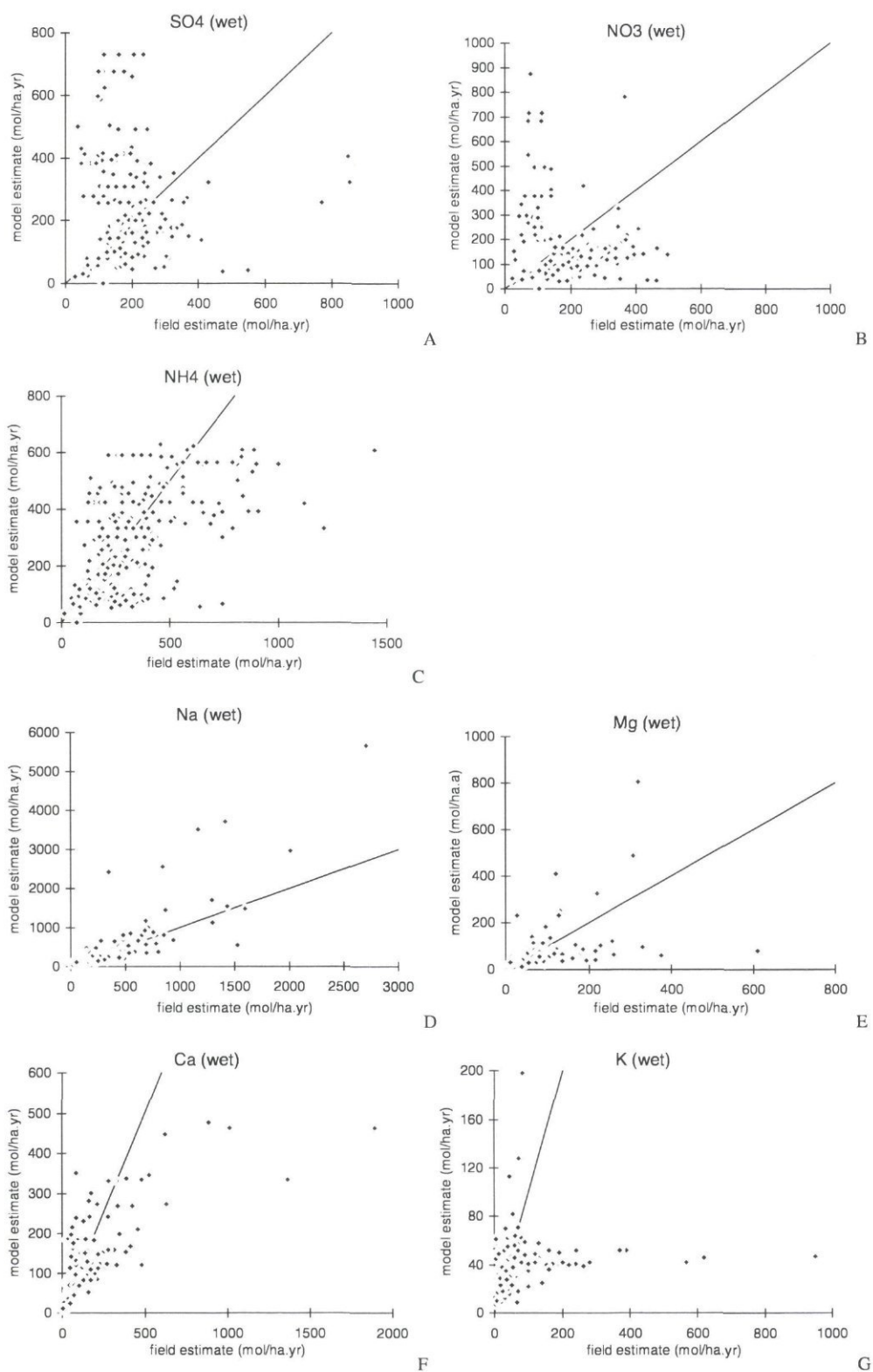


Fig. A 3A-G Relationship between modelled wet deposition and wet deposition estimated from throughfall and bulk precipitation measurements. The line  $y = x$  is also presented.



Modelled dry and wet deposition of potential acid and total nitrogen compare fairly good to throughfall estimates, with correlation coefficients ranging from 0.42 to 0.62 (Table A 9 and Fig. A 4A-D), though in general the modelled dry and wet deposition estimates are larger. In the wet deposition estimates the large scale EMEP deposition fields show up clearly, as many dots in the scatter plots are situated exactly next to each other. Two groups of plots can be distinguished; one group scattering around the 1:1 line, where both model and measured estimates are low, and another group where modelled values are high, whereas measured data are much lower. For total nitrogen this might be explained by canopy uptake. For potential acid, this has probably also to do with the use of  $\text{SO}_2$  surface resistance parametrisations which were derived from measurements at plots with high  $\text{NH}_3$  concentrations, promoting  $\text{SO}_2$  deposition (Erisman et al., 1994a). By using these parametrisations in areas with low  $\text{NH}_3$  concentrations this leads to overestimates of the  $\text{SO}_2$  deposition, and hence to large modelled potential acid deposition estimates.

The relative standard error, as listed in Table A 9 can be considered as an average difference between modelled dry, wet and total deposition values and those derived from throughfall measurements. For dry deposition the average difference ranges from 51% for  $\text{K}^+$  to 98% for  $\text{SO}_x$ , whereas for wet deposition the average difference ranges from 47% for  $\text{NH}_x$  to 117% for  $\text{Mg}^{2+}$ . For total deposition the average difference ranges from 49% for  $\text{NH}_x$  and  $\text{K}^+$  to 109% for  $\text{Na}^+$ . These values are within the range of the uncertainty estimates determined by error propagation.

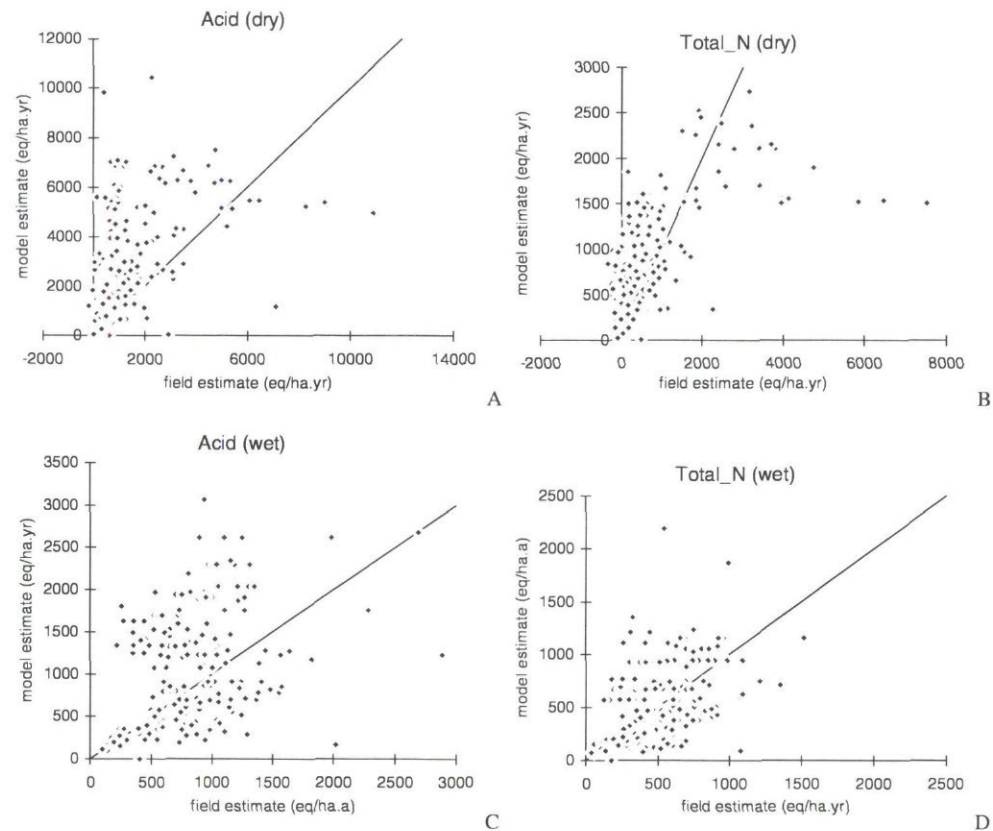


Fig. A 4A-D Relationship between modelled dry and wet deposition of potential acid and total nitrogen and dry and wet deposition estimated from throughfall and bulk precipitation measurements. The line  $y = x$  is also presented.

### *A 3.6 General description of EDEOS*

Ozone concentration estimates are made using the EDEOS model (European Deposition and Exposure of Ozone on a Small scale). This model, based on the EDACS model, aims at mapping the ozone exposure in Europe on a resolution of  $1/6^\circ \times 1/6^\circ$  lat/lon (ca  $12 \times 20 \text{ km}^2$ ) (Eleveld et al., 1997 in prep). Small-scale estimates are obtained by downscaling modelled EMEP concentration fields on a  $150 \times 150 \text{ km}^2$  grid. Long-range transport of ozone is fully described by the EMEP Lagrangian Long Range Transport Model (Simpson, 1992; Simpson, 1993). The ozone and  $\text{NO}_x$  concentrations calculated by EMEP are assumed to be representative for 50 m altitude and must therefore be translated to values at vegetation height. The small-scale ozone concentration estimates are constructed by accounting for deposition, for chemical interactions between ozone and NO (calculated by the EMEP model) and for elevation effects. The design of the EDEOS calculation procedure enables evaluation of abatement strategies, since emission data for nitrogen oxides ( $\text{NO}_x$ ) and volatile organic compounds (VOC) are used as input parameters in the large scale EMEP model. It must be noted that the EDEOS model is still under development and generated results are therefore preliminary.

For finding the ozone concentration at ground level at a particular place and time, in EDEOS corrections are made for:

- deposition, depending on land use type (roughness length) and meteorological situation;
- chemical interactions with NO, i.e. the photostationary state between NO,  $\text{NO}_2$  and  $\text{O}_3$ ;
- the elevation of the site above sea level;
- the diurnal cycle of the ozone concentration, as modelled EMEP concentration data are only provided at 6-h intervals: 00:00 h, 06:00 h, 12:00 h and 1800 h;

The input to the model consists of the following items:

- concentrations of  $\text{O}_3$ , NO and  $\text{NO}_2$  at 50 m reference height taken from EMEP model calculations on a  $150 \times 150 \text{ km}^2$  resolution at 6-h intervals;
- for the deposition calculation:
  - land use and roughness length;
- meteorological data from ECMWF and NCAR interpolated to a  $0.5^\circ \times 1.0^\circ$  lat/lon grid;
- emissions of NO and  $\text{NO}_2$  from CORINAIR on a  $0.5^\circ \times 1.0^\circ$  lat/lon resolution;
- elevation data on a  $1/6^\circ \times 1/6^\circ$  lat/lon resolution from EPA.

The resulting output of the model consists of hourly mean ozone concentrations. For technical details on the methods the reader is referred to Eleveld et al. (1997, in prep).



## **A 3.7 Corrections of the ozone concentrations**

### **A 3.7.1 Deposition correction**

At ground level, ozone concentrations are lower than at 50m height, mainly as a result of deposition of ozone to the ground and by depletion of ozone through reaction with NO. For the deposition correction, first the deposition velocity ( $V_d$ ) has to be determined. This parameter, depending both on the land use (roughness length) and on meteorological parameters, is calculated following the procedure developed within the EDACS framework (Section A 3.2.1). Some additions were added to this procedure to include the ozone parametrisation and to calculate deposition velocities for variable heights. The deposition velocity  $V_d$  at height  $z$  is calculated using the resistance analogy described in Erisman et al. (1994) and in Section A 3.2.1.

### **A 3.7.2 Chemical interactions of ozone with NO**

Near the ground surface a vertical concentration gradient can be found caused by the chemical reactions of ozone with locally emitted gases (Neftel, 1995). From both EMEP O<sub>3</sub>, NO and NO<sub>2</sub> concentration data at 50 m height and emission data from CORINAIR (EEA, 1995) the effect of chemical interactions of O<sub>3</sub> by NO is calculated in EDEOS. CORINAIR combines contributions from different source categories, i.e. combustion and industries, process emitting industries, refineries, transport and domestic emissions into total NO<sub>x</sub> emissions. Moreover, point sources are accounted for separately. For the use in EDEOS, these emission data are transformed into effective concentrations using a box model (Eleveld et al., 1997, in prep.). This model also demands meteorological data to be included in EDEOS. The boundary layer height is computed by a parametrisation from the Royal Dutch Meteorological Institute using the same meteorological data.

When photostationary equilibrium holds, the formation and depletion of ozone are in equilibrium. The photostationary equilibrium ratio  $K$  is assumed to be constant over a height up to 50 m. This assumption is rather crude, as  $K$  can vary over several orders of magnitude from 50 m to 1.5 m, with an average of a factor 10. Following the procedure described by Eleveld et al. (1997, in prep.) the concentrations of O<sub>3</sub>, NO and NO<sub>2</sub> at a variable height are calculated using the concentrations of these components at a height of 50 m calculated by the EMEP model, the constant photostationary equilibrium ratio  $K$  and local NO<sub>x</sub> emissions.

### **A 3.7.3 Elevation dependence**

The elevation of a site has a strong influence both on the mean ozone concentration and on its diurnal cycle. From monitoring data it can be concluded that at higher elevations ozone concentrations are generally higher and the diurnal cycle is less pronounced



(Zaveri, 1993). Therefore the parametrisation of the ozone concentration depending on the elevation and the time  $t$  of day are closely related. An explicit parametrisation of the elevation dependence, applicable for the whole of Europe has not yet been published in literature. In EDEOS the elevation dependence is modelled using a number of experimental studies in which ozone concentrations were monitored on a number of plots which were close to each other (assuring similar local emission and meteorological conditions) but at different altitudes (Aneja and Li, 1992; Lovett and Kinsman, 1990; Sandroni et al., 1993; Wunderli and Gehrig, 1990). Calculating a least squares fit of the results obtained from these studies results in an explicit altitude dependence of ozone concentration (equation A3-14). All data were first normalised with respect to the ozone concentration measured at an elevation of 1000 m. Clearly a trend towards higher ozone concentrations with increasing altitude was identified (Eleveld et al., 1997, in prep.).

$$C(z) = \log([1.88 \pm 0.04] + [6.5 \pm 1.3] \times 10^{-4} z) \times C(z=0) / \log(1.88) \quad (\text{Eq. A 29})$$

The formula is already re-normalised to sea level ( $z=0$ ).

#### **A 3.7.4 Diurnal cycle in ozone concentration**

As the original EMEP concentrations and the meteorological data used in the EDEOS model have a temporal resolution of 6 hours, the model will calculate ground concentrations of ozone also only four times a day. These pre-calculated concentrations at 00:00, 06:00, 12:00 and 18:00 hours have to be used to describe the variation in ozone concentration from hour to hour. This is necessary because for determining AOT40 values peak values must be known. By using 6-hr values, the AOT40 is underestimated. A discrete Fourier transform is applied over the pre-calculated ozone concentrations (Eleveld et al., 1997, in prep.). It is assumed that the hourly ozone concentrations can be approximated by a truncated Fourier series (De Leeuw and Van Zandvoort, 1995).

## Annex 4     Calculation of model inputs to derive critical deposition levels

*Wim de Vries, Gert Jan Reinds, Jaco Klap and Kees Hendriks*  
*DLO Winand Staring Centre (SC-DLO), Wageningen, The Netherlands*

### A 4.1 Assessment of model input data

Input data for the SMB model used in this study are chloride corrected base cation deposition, base cation weathering, growth uptake of base cations and nitrogen, N immobilisation, denitrification and precipitation excess (precipitation minus evapo-transpiration), which affects the critical acidity leaching rate. To obtain these data for all forest stands, we used or derived transfer functions (relationships) with available data on basic land characteristics, such as tree species and soil type and geographic site characteristics such as elevation and temperature. Below we give a short summary of the derivation of the various input data. Detailed information is given in separate sections.

*Table A 10   Influence of location, tree species and soil type accounted for in the assessment of input data for the SMB model*

Data related to	Location	Tree species	Soil type
Base cation deposition	x	x	x
Weathering	x	-	x
Growth uptake	x	x	x
N immobilisation	x	-	x
Denitrification	x	-	x
Precipitation excess	x	x	x

As with S and N, base cation deposition data for each stand for the period 1985-1995 were derived with the atmospheric deposition model EDACS (Section 5.3). Cl deposition, which was subtracted from the sum of Ca, Mg, K and Na deposition, was based on the modelled Na deposition multiplied by a Cl/Na ration in sea salt of 1.16. Base cation weathering rates for the root zone were derived by a relationship with parent material class and texture class (either available or derived from soil type information), and annual average temperature in the considered 10 year period.

Growth uptake was calculated at each site by multiplying the annual average growth rate of stems and branches with the density and the element content in stems and branches. As with tree height (Section 3.2), the annual average growth rate of stems (the yield) was derived as a function of tree species, tree age, climatic zone and site quality characteristics, related to soil type and meteorology (Annex 2). The annual growth rate of branches was calculated from literature derived branch to stem ratios of mature tree species, while assuming that branch growth decreases linearly from a maximum at the time of planting till zero at the time that the annual stem growth rate is at its maximum. Densities and element contents of stems and branches were derived

from the literature. Above a certain threshold value, a linear relationship between N contents in stems and branches and N deposition was assumed.

N immobilisation and denitrification were both described as a fraction of the net N input to the soil over the considered 10 year period. The immobilisation and denitrification factors were calculated as a function of the C/N ratio of the soil and the soil type, respectively. Finally, the precipitation excess was calculated with the water balance model described in Section 4.2, using interpolated meteorological data for each site, and averaging the result over the considered 10 year period.

### A 4.2 Base cation weathering

Base cation weathering rates for each site were estimated from an assumed parent material class (5 classes; Chapter 3) and texture class for each FAO soil type (FAO, 1988) encountered at the various plots (Table A 4-2). For those plots, where soil type information was not available, an assignment was made by an overlay with the FAO soil map of Europe (FAO, 1981), taking the dominant soil unit within each mapping unit. The assumed parent material class for each soil type on the FAO soil map of Europe below forests has been given by De Vries (1991). A similar relationship for the soil types using the updated FAO classification used at present is given in De Vries (1996).

The precipitation rate was considered irrelevant for the weathering rate, which might lead to an underestimate in areas with a large precipitation excess. The assumption that texture class has a dominating influence on the weathering rate was based on a linear relationship between weathering rate and clay content (Sverdrup et al., 1990). However, there is a strong correlation between parent material and texture. Parent material class 1 is mainly associated with texture class 1 and 1/2 while parent material class 2 is mainly correlated with texture class 2 and 2/3.

Table A 11 Weathering rates ( $\text{mol}_c \text{ ha}^{-1} \text{ a}^{-1} \text{ m}^{-1}$ ) used for the various combinations of parent material class and texture class that occur below forests

Parent material	Coarse			Medium		Fine
	1	1/2	1/3	2	2/3	3
Acidic <sup>1)</sup>	500	1000	-	1500	2000	2500
Intermediate <sup>2)</sup>	1000	1500	1500	2000	2500	3000
Basic <sup>3)</sup>	1500	2000	-	2500	3000	-

<sup>1)</sup> Acidic : Sand (stone), gravel, granite, quartzite, gneiss, schist, shale (greywacke, glacial till), Greywacke and glacial till are put in brackets since soil types containing these parent materials can be converted to the acidic or intermediate parent material class, depending on the other parent materials available

<sup>2)</sup> Intermediate : Granodiorite, Gabbro, loess, fluvial and marine sediment (greywacke, glacial till)

<sup>3)</sup> Basic : Basalt, dolomite, volcanic deposits

The weathering rates in Table A 11 were derived from results of the weathering model PROFILE that has been developed to estimate field weathering rates based on the soil mineralogy (Sverdrup and Warfvinge, 1992). Values for the rootzone were derived by



multiplying the weathering rate in Table A 11 with an assumed standard soil depth of 0.5 m, except for Lithosols, where a depth of 0.1 m was used. For peat soils (parent material class 0) a constant weathering rate of 200 mol<sub>c</sub> ha<sup>-1</sup> a<sup>-1</sup> was used based on literature information (Van Breemen et al., 1984). For calcareous soils (parent material class 4) an arbitrary high weathering rate of 10 000 mol<sub>c</sub> ha<sup>-1</sup> a<sup>-1</sup> was used to avoid any exceedance of critical acid deposition levels on these soils. Note, however, that direct effects of SO<sub>2</sub> can not be neglected at these loads (De Vries et al., 1994).

The weathering rates thus assigned were corrected for the effect of temperature according to (Sverdrup, 1990):

$$BC_{we}(T) = BC_{we}(T_o) * e^{(A/T_o - A/T)} \quad (\text{Eq. A 30})$$

where  $BC_{we}(T)$  is the weathering rate at the local mean annual temperature  $T$  (K),  $BC_{we}(T_o)$  is the average weathering rate defined in Table A 11 for each combination of parent material class and texture class at a reference temperature  $T_o$  (K) and  $A$  is a pre-exponential temperature factor (K). For  $A$  a value of 3600 K has been taken (Sverdrup, 1990). The reference temperature was calculated for each weathering rate (class) as the average of the mean annual air temperatures of all soil types in a given weathering rate (class).

### A 4.3 Growth uptake

The average annual element uptake in stems and branches has been derived by multiplying the annual increase in biomass with the element contents in both compartments according to:

$$X_{gu} = k_{gr,st} * D_{st} * ctX_{st} + k_{gr,br} * \rho_{br} * ctX_{br} \quad (\text{Eq. A 31})$$

where  $X_{gu}$  is the net uptake flux of element  $X$  (mol<sub>c</sub> ha<sup>-1</sup> a<sup>-1</sup>),  $k_{gr,st}$  and  $k_{gr,br}$  are the annual average growth rate constants of stem wood and branch wood (m<sup>3</sup> ha<sup>-1</sup> a<sup>-1</sup>) respectively,  $\rho_{st}$  and  $\rho_{br}$  are the densities of stem wood and branch wood (kg m<sup>-3</sup>) respectively, and  $ctX_{st}$  and  $ctX_{br}$  are the contents of element  $X$  in stems and branches, respectively (mol<sub>c</sub> kg<sup>-1</sup>).

The average annual growth rate of stems (yield) was calculated as a function of site quality, climatic zone, tree species and tree age as summarised in Figure A 5.

First, site quality was assessed from information on available and derived qualitative data on water availability, drainage status and nutrient availability. Each site quality characteristic was derived in three classes, i.e. good, medium and poor. The water availability class was either recorded (ca 4500 plots; Section 3.1) or derived from an assigned available water capacity (Annex 2) and a calculated precipitation deficit. The drainage status class was derived from soil type. The nutrient availability class was derived from the average C/N ratio in the upper 20 cm of the mineral soil (good for

C/N < 21, medium for 21 < C/N < 33 and poor for C/N > 33). Finally, the indices for water availability, drainage status and nutrient availability were combined to a site quality index, i.e. good, medium and poor (Klap et al., 1997). The qualitative information on site quality index was then for each site combined with information on the climatic region and the tree species to give a quantitative average yield class (in  $\text{m}^3 \text{ha}^{-1} \text{a}^{-1}$ ) according to Table A 12.

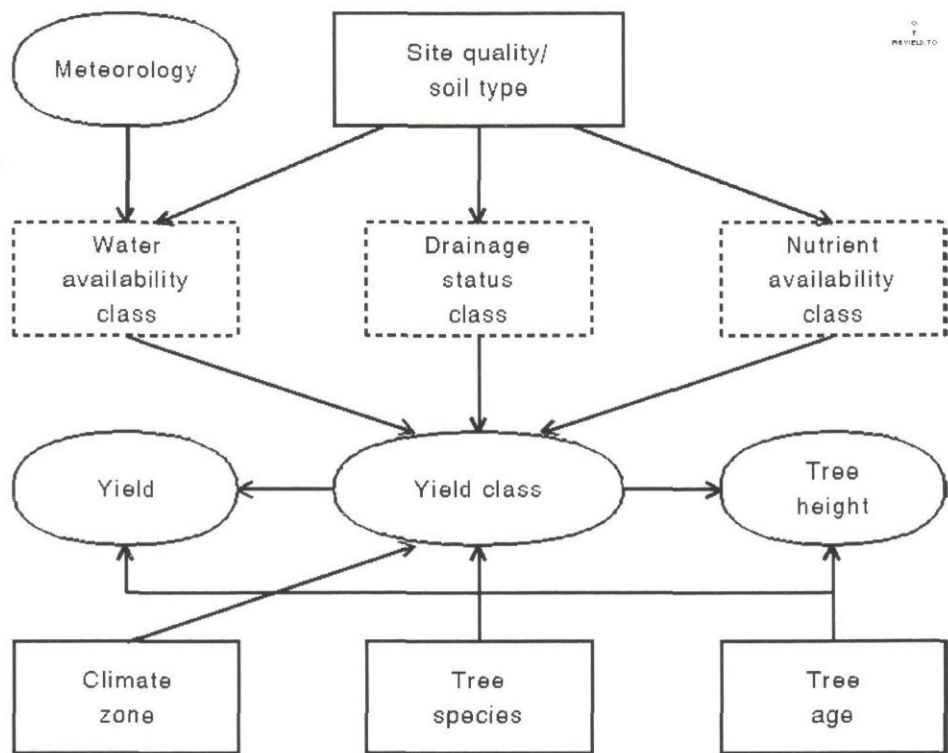


Fig. A 5 Procedure illustrating the derivation of yield and tree height as a function of site and stand characteristics.

Table A 12 is based on a compilation of a selection of European yield tables (amongst others: Jansen, et al., 1996; Hamilton and Christie, 1971; Schober, 1974; Carbonnier, 1971; Garcia Abejon, 1984; 1986; Alemdag, 1967; Nilsen and Larsson, 1992). The rounded values in Table A 12 refer to the maximum values of the curve of the average yield since the time of planting or germination. The current yield at a certain age has been derived from yield tables for the considered tree species and the different average yields. A similar approach was used to derive the tree height at each plot (Klap et al., 1997).

The annual growth rate of branches was calculated form literature derived branch to stem ratios of mature tree species, while assuming that branch growth decreases linearly from a maximum at the time of planting till zero at the time that the annual stem growth rate is at its maximum. Data for the density of stem wood and branch wood have been assumed to be equal. Average values used were 500 kg m<sup>-3</sup> for the coniferous forest stands (*Pinus sylvestris* and *Picea abies*) and 700 kg m<sup>-3</sup> for the deciduous forest stands (*Quercus robur*, *Fagus sylvatica* and *Quercus ilex*). Data used

for the branch to stem ratios of mature tree species were 0.15 kg kg<sup>-1</sup> for *Pinus sylvestris*, 0.10 for *Picea abies*, 0.30 for *Quercus ilex* and 0.25 for *Fagus sylvatica*. Data are based on Kimmins et al., 1985 and De Vries et al., 1990.

Table A 12 Estimated yield classes (m<sup>3</sup> ha<sup>-1</sup> a<sup>-1</sup>) for the five considered tree species in the correlative study as a function of climatic region and site quality (G = good, M = medium, P = poor)

Bio-geographic region <sup>1)</sup>	<i>P.sylvestris</i>			<i>P.abies</i>			<i>Q.robur</i> <sup>2)</sup>			<i>F.sylvatica</i>			<i>Q.ilex</i>		
	P	M	G	P	M	G	P	M	G	P	M	G	P	M	G
Boreal (L > 65N)	1	2	4	2	4	6	*	*	*	*	*	*	*	*	*
Boreal (not so)	2	4	6	2	6	10	*	*	*	*	*	*	*	*	*
Boreal Temperate	4	6	10	4	6	12	2	4	8	2	2	4	*	*	*
Mountainous North (L > 65N or A > 500m)	2	4	6	2	4	8	2	2	4	*	*	*	*	*	*
Mountainous North (L < 65N and A < 500m)	4	6	8	4	6	12	2	2	4	*	*	*	*	*	*
Atlantic North	4	8	12	6	10	20	4	6	8	4	6	10	*	*	*
Atlantic South	4	8	12	6	10	16	4	6	8	4	8	12	2	4	4
Sub-Atlantic	4	8	12	6	8	12	4	6	8	4	8	12	*	*	*
Continental	4	8	12	6	8	12	4	6	8	4	6	10	2	4	4
Mountainous South (A > 1500 m)	4	6	8	4	6	10	4	4	6	4	6	8	*	*	*
Mountainous South (A < 1500 m)	4	8	12	6	8	12	4	6	8	4	6	12	2	4	6
Mediterranean Higher	2	6	12	4	6	10	2	4	6	4	6	12	2	4	6
Mediterranean Lower	4	8	12	4	8	12	4	6	8	4	6	10	2	4	8

<sup>1)</sup> L stands for latitude and A for altitude

<sup>2)</sup> Also *Quercus petraea*

Data for the element contents in stems and branches were computed, according to:

$$ctX = ctX_{min} + \beta * (ctX_{max} - ctX_{min}) \tag{Eq. A 32}$$

where  $ctX_{min}$  and  $ctX_{max}$  are the minimum and maximum contents (mol<sub>c</sub> kg<sup>-1</sup>) of element X in stems or branches and  $\beta$  is a fraction (0≤β≤1), varying linearly with the latitude between 55°N and 65°N, based on data given in Rosén (1990). For X = N, Mg and K, β was set to 0 for latitude ≥ 65° and to 1 for latitude ≤ 55°. For X=Ca, β was set to 1 for latitude ≥65° and 0 for latitude ≤ 55°. Element contents of N, Mg and K in stems and branches of boreal forests (above latitude 55°) were thus taken lower than in Central and Southern European forests (below latitude 55°) whereas the opposite was done for Ca. Values used for the minimum and maximum element contents show that latitude mainly affects the element content in branch wood (Table A 13).

Table A 13 Minimum and maximum values of base cation contents in stems and branches of coniferous and deciduous forests in Europe.

Tree species	Compartment	Minimum contents (%)			Maximum contents (%)		
		Ca	Mg	K	Ca	Mg	K
Coniferous <sup>1)</sup>	Stems	0.08	0.02	0.05	0.16	0.02	0.05
	Branches	0.30	0.03	0.10	0.60	0.05	0.25
Deciduous <sup>2)</sup>	Stems	0.13	0.04	0.10	0.21	0.04	0.10
	Branches	0.45	0.03	0.05	0.75	0.05	0.20

<sup>1)</sup> *Pinus sylvestris* and *Picea abies*

<sup>2)</sup> *Quercus robur*, *Fagus sylvatica* and *Quercus ilex*.



The minimum values for Ca and the maximum values of Mg and K were assumed to apply to all forests below latitude 55°. Constant values below this latitude does not imply that there is no influence of latitude, but that there are no readily available data to derive a relationship.

The nitrogen contents in stems and branches were calculated as a function of the N deposition according to:

$$ctN = ctN_{min} + \alpha * (ctN_{max} - ctN_{min}) \tag{Eq. A 33}$$

where  $ctN_{min}$  and  $ctN_{max}$  are the minimum and maximum N content in leaves and fine roots ( $\text{mol}_c \text{ kg}^{-1}$ ).

The value of  $\alpha$  was calculated according to:

$$\alpha = \frac{N_{dt} - N_{dt,min}}{N_{dt,max} - N_{dt,min}} \quad \text{for } N_{dt,min} < N_{dt} < N_{dt,max} \tag{Eq. A 34}$$

$$\alpha = 0 \quad \text{for } N_{dt} < N_{dt,min} \tag{Eq. A 35}$$

$$\alpha = 1 \quad \text{for } N_{dt} > N_{dt,max} \tag{Eq. A 36}$$

where  $N_{dt,min}$  and  $N_{dt,max}$  are the minimum and maximum values between which the N deposition influences the N content of leaves.

Values used for  $N_{dt,min}$  and  $N_{dt,max}$  were 1500 and 7000  $\text{mol ha}^{-1} \text{ a}^{-1}$  respectively, based on data given by Van den Burg et al. (1988) and Van den Burg and Kiewiet (1989). Values used for the minimum and maximum N content in stems and branches, are given in Table A 14. Data are based on the literature compilations by Kimmins et al. (1985) and De Vries et al. (1990).

Table A 14 Values use for the minimum and maximum N content in stems and branches of the considered tree species.

Tree species	N content in stems (%)		N content in branches (%)	
	min.	max.	min.	max.
<i>Pinus sylvestris</i>	0.08	0.20	0.20	0.50
<i>Picea abies</i>	0.08	0.20	0.35	0.75
Deciduous <sup>1)</sup>	0.15	0.25	0.35	0.75

<sup>1)</sup> *Quercus robur*, *Q. petraea*, *Fagus sylvatica* and *Quercus ilex*

#### A 4.4 N immobilisation

In deriving critical loads related to a steady-state situation, a long-term acceptable rate of net immobilisation of stable organic N compounds in the soil (stable forms of humus) is calculated (De Vries, 1993). The actual accumulated amount at each stand may however be much higher since the system is not yet at steady state. In this study, N immobilisation was thus described as a fraction of the net N input (N deposition minus net N uptake and a natural N leaching rate) to the soil. The immobilisation fraction was described as a linear fraction of the C/N ratio of the soil, according to:

$$N_{im} = (N_{td} - N_{gu} - N_{le,min}) * \left( \frac{C/N_{om} - C/N_{min}}{C/N_{cr} - C/N_{min}} \right) \quad \text{for } C/N_{cr} > C/N_{om} > C/N_{min} \quad (\text{Eq. A 37})$$

Where  $C/N_{om}$  is the C/N ratio of the soil,  $C/N_{cr}$  is the critical C/N ratio above which all excess nitrogen ( $N_{td} - N_{gu} - N_{le,min}$ ) is assumed to immobilise and  $C/N_{min}$  is the minimum C/N ratio where N immobilisation is negligible.

The minimum N leaching rate ( $N_{le,min}$ ) is calculated by multiplying the precipitation excess by a natural background  $\text{NO}_3$  concentration in drainage water of  $0.02 \text{ mol}_e \text{ m}^{-3}$  (Rosén, 1990). Critical and minimum values used for the C/N ratio of the five major soil clusters distinguished in calculating critical deposition levels (Chapter 3) are shown in Table A 15.

Table A 15 Minimum and maximum C/N ratios ( $\text{g g}^{-1}$ ) used in the calculation of the N immobilisation

Soil type	Minimum	Critical
Peat <sup>1)</sup>	15	40
Coarse textured soils (sand/loam) <sup>2)</sup>	15	35
Fine textured soils (clay) <sup>3)</sup>	10	25
Volcanic soils <sup>4)</sup>	10	20
Calcareous soils <sup>5)</sup>	10	20

<sup>1)</sup> Values are based on light textured (sandy) soils. For clay soils similar values were assumed

The minimum C/N ratios were based on 5 percentile values of ca 2500 values of C/N ratios reported in a European Forest Soil Data Base (Reinds, 1995) and reported for Dutch forest soils (De Vries and Leeters, 1996; Klap et al., 1996). Critical C/N ratios reported in literature for coarse textured soil are generally close to 25 (Ågren and Bosatta, 1988; Tietema, 1992), although values near 40 have been reported as well (Berg and Staaf, 1981). These ratios, however, refer to the situation that net N mineralisation starts to occur, whereas the use of this critical ratio in Eq. (A 4-9) refers to a situation where the external N input ceases to be completely immobilised. The latter value is likely to be somewhat higher. Critical values given in Table A 4-6 were based on 75 percentile values of circa 2500 data reported for European forest soils (see above).

## A 4.5 Denitrification

Denitrification is described as a fraction of the net input to the soil according to (De Vries, 1993):

$$N_{de} = fr_{de} * (N_{id} - N_{gu} - N_{im}) \quad (\text{Eq. A 38})$$

where  $fr_{de}$  is a denitrification fraction. Using this sequence of descriptions for N transformations, it is implicitly assumed that N immobilisation is a faster process than denitrification.

Denitrification fractions were related to soil clusters based on data given in Breeuwsma (1991) for agricultural sand, clay and peat soils in The Netherlands. Data were corrected for the more acid circumstances in forest soils. Values used are given in Table A 16.

Table A 16 Denitrification fractions used for the considered soil types

Soil type	Denitrification fraction
Peat	0.8
Sand, loess <sup>1)</sup>	0.1-0.5
Clay	0.7

<sup>1)</sup> Values used are 0.1 for soils without gleyic features and 0.5 for soils with gleyic features

## A 4.6 Critical acidity leaching

The critical acidity leaching flux,  $Ac_{le}(crit)$ , was calculated as the sum of Al leaching and H leaching  $H_{le}(crit)$  (both in  $\text{mol}_c \text{ ha}^{-1} \text{ a}^{-1}$ ). The critical Al leaching flux,  $Al_{le}(crit)$ , was calculated as (De Vries, 1993):

$$Al_{le}(crit) = 3 \text{ RAlBC}(crit) (BC_{ld} + BC_{we} - BC_{gu}) \quad (\text{Eq. A 39})$$

where  $\text{RAlBC}(crit)$  is a critical molar Al/(Ca+Mg+K) ratio in the soil solution. In various studies (De Vries, 1993), a critical Al concentration was calculated by also requiring that depletion of secondary Al compounds does not occur to avoid a strong decrease in pH (Section 5.1). This does, however, not cause an actual risk to the forests and has thus not been included in this study.

The critical H leaching flux,  $H_{le}(crit)$ , was calculated as:

$$H_{le}(crit) = PE [H](crit) \quad (\text{Eq. A 40})$$

where  $PE$  is the precipitation excess leaving the root zone ( $\text{m}^3 \text{ ha}^{-1} \text{ a}^{-1}$ ) and  $[H](crit)$  is a critical H concentration ( $\text{mol}_c \text{ m}^{-3}$ ), which is related to the critical Al concentration according to:



$$[H](crit) = ([Al](crit) / KAl_{ox})^{0.33} \quad (\text{Eq. A 41})$$

where  $KAl_{ox}$  is the Al hydroxide equilibrium constant.  $KAl_{ox}$ , was set at  $10^8 \text{ mol}^{-2} \text{ l}^2$  for mineral soils (based on Heij et al., 1991) and at  $10^6 \text{ mol}^{-2} \text{ l}^2$  for peat soils (based on Wood, 1989). Since  $KAl_{ox}$  is defined in  $\text{mol}^{-2} \text{ l}^2$ , the Al and H concentration which are given in  $\text{mol}_c \text{ m}^{-3}$  are recalculated to  $\text{mol l}^{-1}$ . The value of the critical Al concentration is determined by the critical Al leaching flux divided by the water flux (precipitation excess).

The critical Al/(Ca+Mg+K) ratio has been assigned as a function of tree species based on an extensive literature review of numerous pot experiments with seedlings or young trees, either in hydroponic, sand or soil culture. (Sverdrup and Warfvinge, 1993). These authors plotted biomass growth (in most cases root elongation or root weight increment) as a function of the molar ratio of Ca+Mg+K to Al. The relationship obtained was fitted by using several cation exchange equations (e.g. Vanselow, Gapon and Gaines-Thomas) assuming that ion exchange at the root surface is the step preceding uptake. The best relationship was obtained by minimising the sum of squares of deviations between model results and experimental data. The critical ratio was set at a model predicted reduction of 20 % in biomass (root) growth compared to the control. Using this approach a standard procedure was used to evaluate the data and to determine the critical Al/(Ca+Mg+K) ratio. Results obtained indicated a critical molar Al/(Ca+Mg+K) ratio of 0.8 for coniferous tree species (*Pinus sylvestris* and *Picea abies*) and of 1.7 for deciduous tree species (*Quercus robur*, *Quercus petraea*, *Fagus sylvatica* and *Quercus ilex*).

#### A 4.7 Critical nitrogen leaching

There is no direct link between forest damage and N leaching. Recently, however, Tietema and Beier (1995) found a relationship between N contents in foliage and N leaching for a number of intensively monitored plots where nitrogen experiments have been carried out (NITREX sites). This is relevant since the sensitivity of forests for frost and fungal diseases is correlated with the N content in foliage.

In a fertilisation experiment in Sweden, it was found that frost damage to the needles of Scots pine strongly increased above an N content of 1.8% (Aronsson, 1980). At this N level, the occurrence of fungal diseases such as *Sphaeropsis sapinea* and *Brunchorstia pinea* also appears to increase. This can be derived from correlative field research in The Netherlands about the N content in needles of Corsican pine and Scots pine and the occurrence of these fungal diseases (Roelofs et al., 1985; Boxman and Van Dijk, 1988; Van den Burg et al., 1988). In this context, Van den Burg et al. (1988) suggested critical levels of 1.6 and 1.8% for Corsican pine and Scots pine, respectively. Based on these results, an N content of 1.8% in needles was considered to be critical.

Using the relationship by Tietema and Beier (1995) according to:

$$N_{le} = -48.5 + 38.2 C_f N_{fo} \quad (R^2 = 0.79) \quad (\text{Eq. A 42})$$

where  $C_f/N_{fo}$  is the N content in foliage (%), and a critical N content of 1.8% leads to a critical N leaching rate of ca 20 kg N ha<sup>-1</sup> a<sup>-1</sup> or 1450 mol ha<sup>-1</sup> a<sup>-1</sup>. The considered relationship and critical N content on foliage only refers to coniferous trees. In this study, however, a similar value was used for deciduous trees.

Annex 5 Detailed results of the statistical analyses

Jaco Klap<sup>1)</sup>, Jan Oude Voshaar<sup>2)</sup>

<sup>1)</sup> DLO Winand Staring Centre (SC-DLO), Wageningen, The Netherlands

<sup>2)</sup> Centre for Biometry Wageningen (CBW), Wageningen, The Netherlands

This Annex contains tables with the detailed results of (i) Correlations between predictor variables (Section A 5.1), (ii) the selected ‘best fitting’ models for the various sub-models (Section A 5.2 for Model A, Section A 5.3 for Model B and Section A 5.4 for Model C) and (iii) an overview of the standardised values of the national defoliation figures, by which they are made comparable to the European standard (Section A 5.5). The results in the Sections A 5.2-A 5.3 are presented per tree species: *Pinus sylvestris*, *Picea abies*, *Quercus robur* + *petraea*, *Fagus sylvatica* and *Quercus ilex*. Comments on these Tables are given in the Sections 6.3.1-6.3.4 of the main report.

A 5.1 Correlation between predictor variables

Table A 17 Correlation coefficients (%) between the time-dependent predictor variables for Pinus sylvestris

Mean values over 10 year period													
	WinX	LFros	SumX	Heat	RTrn	[SO <sub>2</sub> ]	[NO <sub>2</sub> ]	[NH <sub>3</sub> ]	AcDep	NDep	[O <sub>3</sub> ]	Aot40	
WinX		77	60	0	-38	33	45	58	36	44	59	59	WinX
LFrost	44		52	8	-60	41	42	63	36	38	72	72	Lfrost
SumX	68	51		4	-23	8	11	24	7	9	28	29	SumX
Heat	3	4	4		4	20	1	1	16	11	-7	-8	Heat
RelTrans	-27	-23	-52	2		4	3	-28	15	13	-60	-59	RelTrans
[SO <sub>2</sub> ]	37	16	44	14	4		77	34	91	87	27	29	[SO <sub>2</sub> ]
[NO <sub>2</sub> ]	45	20	45	4	2	75		65	80	90	35	39	[NO <sub>2</sub> ]
[NH <sub>3</sub> ]	54	32	65	-1	-25	36	66		45	60	58	59	[NH <sub>3</sub> ]
AcDep	42	17	40	11	12	89	78	47		94	25	26	AcDep
NDep	49	20	44	7	10	84	89	62	94		31	33	Ndep
[O <sub>3</sub> ]	54	37	74	0	-51	30	36	58	28	34		99	[O <sub>3</sub> ]
AOT40	53	36	73	-1	-50	31	40	59	30	36	99		AOT40
Actual values for the separate observations													
	WinX	LFrost	SumX	Heat	RTran	[SO <sub>2</sub> ]	[NO <sub>2</sub> ]	[NH <sub>3</sub> ]	AcDep	NDep	[O <sub>3</sub> ]	Aot40	



Table A 18 Explained variance of the mean values over 10 years of the time-dependent predictor variables by the factor 'Country' for the considered tree species

Variable	<i>Pinus sylvestris</i>	<i>Picea abies</i>	<i>Q. robur + Q. petraea</i>	<i>Fagus sylvatica</i>	<i>Quercus ilex</i>
Winter Index	52	56	44	40	44
Late Frost	84	81	75	73	75
Summer Index	30	13	50	13	50
Heat Index	18	39	53	42	53
Rel. Transpiration	66	51	57	54	57
[SO <sub>2</sub> ]	64	66	53	51	53
[NO <sub>2</sub> ]	81	79	67	67	67
[NH <sub>3</sub> ]	80	84	54	40	54
Acid deposition	74	73	62	61	62
N deposition	81	80	65	70	65
[O <sub>3</sub> ]	75	81	26	25	26
AOT 40	75	80	29	29	29

Table A 19 Correlation coefficients (%) between the current year values of the time-dependent predictor variables and the corresponding previous year, memory year and long year mean values for the observed tree species (clusters)

	<i>P. sylvestris</i>			<i>Picea abies</i>			<i>Q. robur/petr</i>			<i>F. sylvatica</i>			<i>Quercus ilex</i>		
	Prev.	Del.	Avg.	Prev.	Del.	Avg.	Prev.	Del.	Avg.	Prev.	Del.	Avg.	Prev.	Del.	Avg.
Winter Index	56	54	71	54	61	72	79	69	73	81	68	71	79	69	73
Late Frost	27	40	44	37	38	30	52	53	-16	28	46	3	52	53	-16
Summer Index	88	89	40	84	40	18	86	92	-22	89	93	9	86	92	-22
Heat Index	10	4	27	6	2	30	23	8	40	26	11	45	8	23	40
Rel. Transp.	74	81	86	60	78	82	82	74	78	78	77	84	82	74	78
[SO <sub>2</sub> ]	98	98	98	97	98	97	95	96	94	92	95	91	95	96	94
[NO <sub>2</sub> ]	98	99	99	97	98	98	96	97	97	96	97	97	96	97	97
[NH <sub>3</sub> ]	98	97	98	98	96	98	91	89	94	91	84	92	91	89	94
Acid Deposition	98	96	96	97	95	96	96	95	95	96	93	93	96	95	95
Nit. Deposition	97	96	97	97	95	96	96	95	90	95	93	95	96	95	96
[O <sub>3</sub> ] <sup>1)</sup>	-	-	-	-	-	-	-	-	-	-	-	-	-	-	-
AOT 40 <sup>1)</sup>	-	-	-	-	-	-	-	-	-	-	-	-	-	-	-

<sup>1)</sup> All correlation coefficients for [O<sub>3</sub>] and AOT40 are 100%, since the same values were used for the different years.

## A 5.2 Analysis of actual defoliation data (Model A)

Table A 20 Best explaining models for *Pinus sylvestris* in Model A

Model	Observations	Selected model	% R <sup>2</sup> <sub>adj</sub>
<i>Model A-0 Site &amp; Stand; no time dependency</i>			
A-0.0	9164	<u>Country</u> , <u>Age</u>	42.6
A-0.1	3766	<u>Country</u> , <u>Age</u> , <u>ClimZone</u>	40.6
A-0.2	9164	<u>Country</u> , <u>Age</u> , ClimZone	43.4
A-0.3	9164	<u>Country</u> , <u>Age</u>	42.6
A-0.4	9164	<u>Country</u>	38.7
A-0.5	9164	<u>Age</u> , <u>Alt</u> , (C/N)	8.0
<i>Model A-1 Absolute meteo</i>			
A-1.0	9120	<u>Country</u> , <u>Age</u> , ( <u>[NH<sub>3</sub>]</u> )	43.1
A-1.1	9120	<u>Country</u> , <u>Age</u>	42.6
A-1.2	9164	<u>Country</u> , <u>Age</u> , ( <u>[NH<sub>3</sub>]</u> )	43.1
A-1.3	9164	<u>Country</u> , <u>Age</u>	42.6
A-1.4	9120	<u>Country</u> , <u>Age</u>	42.6
A-1.5	9120	<u>Country</u> , <u>Age</u>	42.6
A-1.6	9120	<u>AcidDep</u> , <u>X[SO<sub>2</sub>]<sub>t</sub></u> , <u>[NO<sub>2</sub>]<sub>t</sub></u> , [SO <sub>2</sub> ], <u>Age</u> , <u>RelTrans</u>	29.7
A-1.7	9120	<u>AcidDep</u> , <u>Age</u> , <u>XAcidDep<sub>t</sub></u> , <u>X[SO<sub>2</sub>]<sub>t</sub></u> , [SO <sub>2</sub> ] <sub>t</sub> , <u>[NO<sub>2</sub>]<sub>t</sub></u> , <u>Alt</u>	26.3
<i>Model A-2 Relative meteo</i>			
A-2.0	9120	<u>Country</u> , <u>Age</u> , ( <u>[NH<sub>3</sub>]<sub>t-1</sub></u> )	43.1
A-2.1	9120	<u>Country</u> , <u>Age</u>	42.6
A-2.2	9120	<u>Country</u> , <u>Age</u> , ( <u>[NH<sub>3</sub>]<sub>t-1</sub></u> )	43.1
A-2.3	9164	<u>Country</u> , <u>Age</u>	42.6
A-2.4	9164	<u>Country</u> , <u>Age</u>	42.6
A-2.5	9120	<u>Country</u> , <u>Age</u>	42.6
A-2.6	9120	<u>Country</u> , <u>Age</u>	42.6
A-2.7	9120	<u>AcidDep</u> , <u>Age</u> , <u>XAcidDep<sub>t</sub></u> , <u>X[SO<sub>2</sub>]<sub>t</sub></u> , [SO <sub>2</sub> ] <sub>t-1</sub> , ( <u>[NO<sub>2</sub>]<sub>t-1</sub></u> ), <u>Alt</u>	26.5
A-2.8	9120	<u>AcidDep</u> , <u>Age</u> , <u>XAcidDep<sub>t</sub></u> , <u>X[SO<sub>2</sub>]<sub>t</sub></u> , [SO <sub>2</sub> ] <sub>t</sub> , ( <u>[NO<sub>2</sub>]<sub>t</sub></u> ), <u>Alt</u>	26.3

Legend: Underlined = contribution > 2%; Normal = contribution 1-2%; (Between brackets) = contribution 0.5-1%;  
*Italics* = unexpected sign

Table A 21 Best explaining models for *Picea abies* in Model A

Model	Observations	Selected model	% R <sup>2</sup> <sub>adj</sub>
<i>Model A-0 Site &amp; Stand; no time dependency</i>			
A-0.0	7362	<u>Country</u> , <u>Age</u>	52.2
A-0.1	3591	<u>Country</u> , <u>Age</u>	58.9
A-0.2	7362	<u>Country</u> , <u>Age</u> , ( <u>SoilClus</u> )	52.2
A-0.3	7362	<u>Country</u> , <u>Age</u>	52.2
A-0.4	7362	<u>Country</u>	38.0
A-0.5	7362	<u>Age</u> , <u>Alt</u> , <u>pH</u> , <u>C/N</u>	16.9
<i>Model A-1 Absolute meteo</i>			
A-1.0	7336	<u>Country</u> , <u>Age</u>	52.2
A-1.1	7336	<u>Country</u> , <u>Age</u>	52.2
A-1.2	7362	<u>Country</u> , <u>Age</u>	52.2
A-1.3	7362	<u>Country</u> , <u>Age</u>	52.2
A-1.4	7336	<u>Country</u> , <u>Age</u>	52.2
A-1.5	7336	<u>Country</u> , <u>Age</u>	52.2
A-1.6	7336	<u>Age</u> , [SO <sub>2</sub> ], <u>AOT30</u> , <u>X[SO<sub>2</sub>]<sub>t</sub></u> , ( <u>[NO<sub>2</sub>]</u> )	33.3
A-1.7	7336	<u>Age</u> , [SO <sub>2</sub> ] <sub>t</sub> , <u>AOT30<sub>t</sub></u> , <u>X[SO<sub>2</sub>]<sub>t</sub></u>	29.6
<i>Model A-2 Relative meteo</i>			
A-2.0	7336	<u>Country</u> , <u>Age</u>	52.2
A-2.1	7336	<u>Country</u> , <u>Age</u>	52.2
A-2.2	7336	<u>Country</u> , <u>Age</u>	52.2
A-2.3	7362	<u>Country</u> , <u>Age</u>	52.2
A-2.4	7362	<u>Country</u> , <u>Age</u>	52.2
A-2.5	7336	<u>Country</u> , <u>Age</u>	52.2
A-2.6	7336	<u>Country</u> , <u>Age</u>	52.2
A-2.7	7336	<u>Age</u> , [SO <sub>2</sub> ] <sub>del</sub> , <u>AOT30<sub>del</sub></u> , <u>X[SO<sub>2</sub>]<sub>t</sub></u>	31.9
A-2.8	7336	<u>Age</u> , [SO <sub>2</sub> ] <sub>t</sub> , <u>AOT30<sub>t</sub></u> , <u>X[SO<sub>2</sub>]<sub>t</sub></u>	29.6

Legend: Underlined = contribution > 2%; Normal = contribution 1-2%; (Between brackets) = contribution 0.5-1%;  
*Italics* = unexpected sign

Table A 22 Best explaining models for Quercus robur and Quercus petraea in Model A

Model	Observations	Selected model	% R <sup>2</sup> <sub>adj</sub>
<i>Model A-0 Site &amp; Stand; no time dependency</i>			
A-0.0	4563	<u>Country</u> , Age, ( Spec )	39.9
A-0.1	2244	<u>Country</u> , Age, SoilClus, ( <i>BaseSat</i> )	43.4
A-0.2	4563	<u>Country</u> , Age, ClimZone, ( Spec ), ( SoilClus )	41.3
A-0.3	4563	<u>Country</u> , Age, L-Frost, ( pH )	40.9
A-0.4	4563	<u>Country</u> , ( Spec )	38.0
A-0.5	4563	<i>BaseSat</i> , Spec	2.7
<i>Model A-1 Absolute meteo</i>			
A-1.0	4563	<u>Country</u> , Age, ( RelTrans <sub>t-1</sub> ), ( Spec )	40.7
A-1.1	4563	<u>Country</u> , Age, ( Spec )	39.9
A-1.2	4563	<u>Country</u> , Age, L-Frost, <u>SumX<sub>mem</sub></u> , ( RelTrans <sub>t-1</sub> ), ( pH )	43.6
A-1.3	4563	<u>Country</u> , Age, ( Spec )	39.9
A-1.4	4563	<u>Country</u> , Age, L-Frost, <u>SumX<sub>mem</sub></u> , ( RelTrans <sub>t-1</sub> ), ( pH )	43.6
A-1.5	4563	<u>Country</u> , Age, ( Spec )	39.9
A-1.6	4563	<u>WinX</u> , <u>RelTrans</u> , <u>L-Frost</u> , <u>[NH<sub>3</sub>]</u> , <i>BaseSat</i> , ( X[SO <sub>2</sub> ] ), ( Spec ), ( Age ), ( [NO <sub>2</sub> ] )	23.7
A-1.7	4563	[SO <sub>2</sub> ] <sub>t</sub> , <u>WinX<sub>t</sub></u> , <u>X[SO<sub>2</sub>]<sub>t</sub></u> , ( <i>BaseSat</i> ), ( [NH <sub>3</sub> ] <sub>t</sub> ), Age, ( <u>SumX<sub>t</sub></u> ), ( Spec ), ( RelTrans <sub>t</sub> )	22.8
<i>Model A-2 Relative meteo</i>			
A-2.0	4563	<u>Country</u> , RelTrans <sub>mem</sub> , Age, <u>L-Frost</u> , ( <u>SumX</u> ), ( pH )	44.1
A-2.1	4563	<u>Country</u> , Age, <u>L-Frost<sub>t</sub></u> , RelTrans <sub>t</sub> , ( pH )	41.9
A-2.2	4563	<u>Country</u> , RelTrans <sub>mem</sub> , Age, <u>L-Frost</u> , ( <u>SumX</u> ), ( pH )	44.1
A-2.3	4563	<u>Country</u> , RelTrans <sub>mem</sub> , Age, <u>L-Frost</u> , ( <u>SumX</u> ), ( pH )	44.1
A-2.4	4563	<u>Country</u> , Age, <u>L-Frost<sub>t</sub></u> , RelTrans <sub>t</sub> , ( pH )	41.9
A-2.5	4563	<u>Country</u> , RelTrans <sub>mem</sub> , Age, <u>L-Frost</u> , ( <u>SumX</u> ), ( pH )	44.1
A-2.6	4563	<u>Country</u> , Age, <u>L-Frost<sub>t</sub></u> , RelTrans <sub>t</sub> , ( pH )	41.9
A-2.7	4563	[SO <sub>2</sub> ] <sub>t</sub> , RelTrans <sub>mem</sub> , <u>X[SO<sub>2</sub>]<sub>t</sub></u> , <i>BaseSat</i> , ( <u>WinX<sub>mem</sub></u> )	23.5
A-2.8	4563	[SO <sub>2</sub> ] <sub>t</sub> , <u>X[SO<sub>2</sub>]<sub>t</sub></u> , <u>[NO<sub>2</sub>]<sub>t</sub></u> , Age, ( <u>AcidDep<sub>t</sub></u> ), ( <i>BaseSat</i> )	19.2
Legend: <u>Underlined</u> = contribution > 2%; Normal = contribution 1-2%; (Between brackets) = contribution 0.5-1%; <i>Italics</i> = unexpected sign			

Table A 23 Best explaining models for Fagus sylvatica in Model A

Model	Observations	Selected model	% R <sup>2</sup> <sub>adj</sub>
<i>Model A-0 Site &amp; Stand; no time dependency</i>			
A-0.0	3945	<u>Country</u> , Age, ( pH )	34.2
A-0.1	1870	<u>Country</u> , Age, ClimZone, Alt	44.2
A-0.2	3945	<u>Country</u> , ClimZone, Age	36.1
A-0.3	3945	<u>Country</u> , Age	34.2
A-0.4	3945	<u>Country</u>	32.5
A-0.5	3945	<u>Alt</u> , Age	6.0
<i>Model A-1 Absolute meteo</i>			
A-1.0	3938	<u>Country</u> , Age, AOT60, ( [NO <sub>2</sub> ] )	35.8
A-1.1	3938	<u>Country</u> , Age, AOT60 <sub>t</sub> , ( [O <sub>3</sub> ] <sub>t</sub> )	35.7
A-1.2	3945	<u>Country</u> , Age, AOT60, ( [NO <sub>2</sub> ] )	35.8
A-1.3	3945	<u>Country</u> , Age, AOT60 <sub>t</sub> , ( [O <sub>3</sub> ] <sub>t</sub> )	35.8
A-1.4	3938	<u>Country</u> , Age, ( AOT40 )	34.9
A-1.5	3938	<u>Country</u> , Age, ( AOT40 <sub>t</sub> )	34.9
A-1.6	3938	[SO <sub>2</sub> ] <sub>t</sub> , <u>L-Frost<sub>t</sub></u> , <u>X[SO<sub>2</sub>]<sub>t</sub></u> , Age	24.9
A-1.7	3938	<u>SumX<sub>t</sub></u> , [SO <sub>2</sub> ] <sub>t</sub> , Age, ( RelTrans <sub>t</sub> )	18.3
<i>Model A-2 Relative meteo</i>			
A-2.0	3938	<u>Country</u> , Age, AOT60 <sub>t</sub> , ( RelTrans <sub>mem</sub> )	36.2
A-2.1	3938	<u>Country</u> , Age, AOT60 <sub>t</sub> , ( [O <sub>3</sub> ] <sub>t</sub> )	35.7
A-2.2	3938	<u>Country</u> , Age, AOT60 <sub>t</sub> , ( RelTrans <sub>mem</sub> )	36.2
A-2.3	3945	<u>Country</u> , Age, AOT60 <sub>t</sub> , ( RelTrans <sub>mem</sub> )	36.2
A-2.4	3945	<u>Country</u> , Age, AOT60 <sub>t</sub> , ( [O <sub>3</sub> ] <sub>t</sub> )	35.7
A-2.5	3938	<u>Country</u> , Age, ( RelTrans <sub>mem</sub> ), ( AOT40 <sub>t</sub> )	35.8
A-2.6	3938	<u>Country</u> , Age, ( AOT40 <sub>t</sub> )	34.9
A-2.7	3938	<u>L-Frost<sub>t</sub></u> , [SO <sub>2</sub> ] <sub>t</sub> , RelTrans <sub>mem</sub> , Age	22.9
A-2.8	3938	<u>L-Frost<sub>t</sub></u> , [SO <sub>2</sub> ] <sub>t</sub> , Age	19.1
Legend: <u>Underlined</u> = contribution > 2%; Normal = contribution 1-2%; (Between brackets) = contribution 0.5-1%; <i>Italics</i> = unexpected sign.			



Table A 24 Best explaining models for Quercus ilex in Model A

Model	Observations	Selected model	% R <sup>2</sup> <sub>adj</sub>
<i>Model A-0 Site &amp; Stand; no time dependency</i>			
A-0.0	1481	<u>Country</u>	9.3
A-0.1	208	<u>ClimZone</u> , <u>Age</u> , <u>SoilClus</u>	14.6
A-0.2	1481	<u>Country</u> , <u>ClimZone</u>	11.1
A-0.3	1481	<u>Country</u>	9.3
A-0.4	1481	<u>Country</u>	9.3
A-0.5	1481	<i>pH</i> , <u>BaseSat</u>	3.7
<i>Model A-1 Absolute meteo</i>			
A-1.0	1480	<u>Country</u> , [ <u>NO<sub>2</sub></u> ] <sub>mem</sub> , <u>AcidDep<sub>t-1</sub></u> , NitDep <sub>mem</sub> , ( <u>RelTrans<sub>t</sub></u> ), <u>RelTrans</u> , ( [ <u>SO<sub>2</sub></u> ] <sub>t</sub> )	22.1
A-1.1	1480	<u>Country</u> , [ <u>NO<sub>2</sub></u> ] <sub>t</sub> , <u>RelTrans<sub>t</sub></u> , ( <u>AcidDep<sub>t</sub></u> )	14.5
A-1.2	1481	<u>Country</u> , [ <u>NO<sub>2</sub></u> ] <sub>mem</sub> , <u>AcidDep<sub>t-1</sub></u> , NitDep <sub>mem</sub> , ( <u>RelTrans<sub>t</sub></u> ), <u>RelTrans</u> , ( [ <u>SO<sub>2</sub></u> ] <sub>t</sub> )	22.1
A-1.3	1481	<u>Country</u> , [ <u>NO<sub>2</sub></u> ] <sub>t</sub> , <u>RelTrans<sub>t</sub></u> , ( <u>AcidDep<sub>t</sub></u> )	14.5
A-1.4	1480	<u>Country</u> , <u>RelTrans<sub>t</sub></u> , <u>RelTrans</u> , <u>RelTrans<sub>t-1</sub></u> , ( <u>WinX</u> ), <u>WinX<sub>t-1</sub></u>	18.1
A-1.5	1480	<u>Country</u> , <u>RelTrans<sub>t</sub></u> , <u>L-Frost<sub>t</sub></u>	12.0
A-1.6	1480	<u>RelTrans<sub>t</sub></u> , <u>AcidDep<sub>t-1</sub></u> , [ <u>SO<sub>2</sub></u> ], ( [ <u>NH<sub>3</sub></u> ] ), ( <u>BaseSat</u> ), ( <u>NitDep<sub>mem</sub></u> )	11.1
A-1.7	1480	<u>RelTrans<sub>t</sub></u> , <u>Alt</u> , ( [ <u>NH<sub>3</sub></u> ] )	6.7
<i>Model A-2 Relative meteo</i>			
A-2.0	1480	<u>Country</u> , <u>RelTrans<sub>t</sub></u> , [ <u>NO<sub>2</sub></u> ] <sub>t</sub> , <u>AcidDep<sub>t</sub></u> , ( <u>WinX<sub>t-1</sub></u> )	18.8
A-2.1	1480	<u>Country</u> , <u>RelTrans<sub>t</sub></u> , [ <u>NO<sub>2</sub></u> ] <sub>t</sub> , <u>AcidDep<sub>t</sub></u>	17.6
A-2.2	1480	<u>Country</u> , <u>RelTrans<sub>t</sub></u> , <u>RelTrans<sub>t-1</sub></u> , [ <u>NO<sub>2</sub></u> ] <sub>t</sub> , [ <u>NO<sub>2</sub></u> ], ( <u>AcidDep<sub>t</sub></u> )	22.1
A-2.3	1481	<u>Country</u> , <u>RelTrans<sub>t</sub></u> , [ <u>NO<sub>2</sub></u> ] <sub>t</sub> , <u>AcidDep<sub>t</sub></u> , ( <u>WinX<sub>t-1</sub></u> )	18.8
A-2.4	1481	<u>Country</u> , <u>RelTrans<sub>t</sub></u> , [ <u>NO<sub>2</sub></u> ] <sub>t</sub> , <u>AcidDep<sub>t</sub></u>	17.6
A-2.5	1480	<u>Country</u> , <u>RelTrans<sub>t</sub></u> , <u>RelTrans<sub>t-1</sub></u> , ( <u>WinX<sub>t-1</sub></u> )	17.4
A-2.6	1480	<u>Country</u> , <u>RelTrans<sub>t</sub></u> , <u>L-Frost<sub>t</sub></u> , ( <u>SumX<sub>t</sub></u> )	15.9
A-2.7	1480	<u>RelTrans<sub>t</sub></u> , <u>AcidDep<sub>t</sub></u> , [ <u>SO<sub>2</sub></u> ] <sub>t</sub> , [ <u>NH<sub>3</sub></u> ] <sub>t-1</sub> , <u>WinX<sub>t-1</sub></u> , <u>Alt</u>	14.1
A-2.8	1480	<u>RelTrans<sub>t</sub></u> , <u>AcidDep<sub>t</sub></u> , <u>Alt</u> , ( [ <u>NH<sub>3</sub></u> ] <sub>t</sub> )	9.4

Legend: Underlined = contribution > 2%; Normal = contribution 1-2%; (Between brackets) = contribution 0.5-1%;  
*Italics* = unexpected sign

### A 5.3 Analysis of change in defoliation data (Model B)

Table A 25 Best explaining models for *Pinus sylvestris* in Model B

Model	Observations	Selected model	% R <sup>2</sup> <sub>adj</sub>
<i>Model B-0 Site &amp; Stand; no time dependency</i>			
B-0.0	6471	Alt	1.9
B-0.1	2910	ClimZone	1.2
B-0.2	6471	<u>ClimZone</u>	2.3
B-0.3	6471	Alt	1.9
B-0.4	6471	<u>Country</u>	5.8
B-0.5	6471	<u>Country</u>	5.8
<i>Model B-1 Absolute meteo</i>			
B-1.0	6444	Alt , ( <i>SumX<sub>mem</sub></i> ) , ( [NO <sub>2</sub> ] )	2.9
B-1.1	6471	Alt	1.9
B-1.2	6471	Alt , ( <i>SumX<sub>mem</sub></i> ) , ( [NO <sub>2</sub> ] )	2.9
B-1.3	6444	Alt	1.9
B-1.4	6444	Alt , ( <i>SumX<sub>mem</sub></i> )	2.7
B-1.5	6444	Alt	1.9
B-1.6	6444	<u>Country</u>	5.8
B-1.7	6444	<u>Country</u>	5.8
<i>Model B-2 Relative meteo</i>			
B-2.0	6444	Alt , ( <i>RelTrans<sub>t-1</sub></i> )	2.6
B-2.1	6444	Alt	1.9
B-2.2	6444	Alt , ( <i>RelTrans<sub>t-1</sub></i> )	2.6
B-2.3	6471	Alt , ( <i>RelTrans<sub>t-1</sub></i> )	2.6
B-2.4	6471	Alt	1.9
B-2.5	6444	Alt , ( <i>RelTrans<sub>t-1</sub></i> )	2.6
B-2.6	6444	Alt	1.9
B-2.7	6444	<u>Country</u> , ( <i>RelTrans<sub>t-1</sub></i> )	6.3
B-2.8	6444	<u>Country</u>	5.8

Legend: Underlined = contribution > 2%; Normal = contribution 1-2%; (Between brackets) = contribution 0.5-1%;  
*Italics* = unexpected sign.

Table A 26 Best explaining models for *Picea abies* in Model B

Model	Observations	Selected model	% R <sup>2</sup> <sub>adj</sub>
<i>Model B-0 Site &amp; Stand; no time dependency</i>			
B-0.0	4745	-	0.0
B-0.1	2721	-	0.0
B-0.2	4745	-	0.0
B-0.3	4745	-	0.0
B-0.4	4745	<u>Country</u>	4.1
B-0.5	4745	<u>Country</u>	4.1
<i>Model B-1 Absolute meteo</i>			
B-1.0	4728	( <i>Heat<sub>mcm</sub></i> )	0.7
B-1.1	4728	-	0.0
B-1.2	4745	( <i>Heat<sub>mcm</sub></i> )	0.7
B-1.3	4745	-	0.0
B-1.4	4728	( <i>Heat<sub>mcm</sub></i> )	0.7
B-1.5	4728	-	0.0
B-1.6	4728	<u>Country</u>	4.1
B-1.7	4728	<u>Country</u>	4.1
<i>Model B-2 Relative meteo</i>			
B-2.0	4728	( <i>Heat<sub>mcm</sub></i> )	0.9
B-2.1	4728	-	0.0
B-2.2	4728	( <i>Heat<sub>mcm</sub></i> )	0.9
B-2.3	4745	( <i>Heat<sub>mcm</sub></i> )	0.9
B-2.4	4745	-	0.0
B-2.5	4728	( <i>Heat<sub>mcm</sub></i> )	0.9
B-2.6	4728	-	0.0
B-2.7	4728	<u>Country</u> , ( <i>Heat<sub>mcm</sub></i> )	4.7
B-2.8	4728	<u>Country</u>	4.1

Legend: Underlined = contribution > 2%; Normal = contribution 1-2%; (Between brackets) = contribution 0.5-1%;  
*Italics* = unexpected sign.

Table A 27 Best explaining models for *Quercus robur* and *Quercus petraea* in Model B

Model	Observations	Selected model	% R <sup>2</sup> <sub>adj</sub>
<i>Model B-0 Site &amp; Stand; no time dependency</i>			
B-0.0	3555	-	0.0
B-0.1	1832	-	0.0
B-0.2	3555	-	0.0
B-0.3	3555	-	0.0
B-0.4	3555	<u>Country</u>	2.1
B-0.5	3555	<u>Country</u>	2.1
<i>Model B-1 Absolute meteo</i>			
B-1.0	3555	( SumX <sub>t</sub> )	0.5
B-1.1	3555	( SumX <sub>t</sub> )	0.5
B-1.2	3555	( SumX <sub>t</sub> )	0.5
B-1.3	3555	( SumX <sub>t</sub> )	0.5
B-1.4	3555	( SumX <sub>t</sub> )	0.5
B-1.5	3555	( SumX <sub>t</sub> )	0.5
B-1.6	3555	<u>Country</u>	2.1
B-1.7	3555	<u>Country</u>	2.1
<i>Model B-2 Relative meteo</i>			
B-2.0	3555	( SumX <sub>t</sub> )	0.5
B-2.1	3555	( SumX <sub>t</sub> )	0.5
B-2.2	3555	( SumX <sub>t</sub> )	0.5
B-2.3	3555	( SumX <sub>t</sub> )	0.5
B-2.4	3555	( SumX <sub>t</sub> )	0.5
B-2.5	3555	( SumX <sub>t</sub> )	0.5
B-2.6	3555	( SumX <sub>t</sub> )	0.5
B-2.7	3555	<u>Country</u>	2.1
B-2.8	3555	<u>Country</u>	2.1

Legend: Underlined = contribution > 2%; Normal = contribution 1-2%; (Between brackets) = contribution 0.5-1%;  
*Italics* = unexpected sign.

Table A 28 Best explaining models for *Fagus sylvatica* in Model B

Model	Observations	Selected model	% R <sup>2</sup> <sub>adj</sub>
<i>Model B-0 Site &amp; Stand; no time dependency</i>			
B-0.0	2933	-	0.0
B-0.1	1456	-	0.0
B-0.2	2933	-	0.0
B-0.3	2933	-	0.0
B-0.4	2933	<u>Country</u>	2.2
B-0.5	2933	<u>Country</u>	2.2
<i>Model B-1 Absolute meteo</i>			
B-1.0	2927	( RelTrans <sub>t-1</sub> )	0.6
B-1.1	2927	( RelTrans <sub>t</sub> )	0.5
B-1.2	2933	( RelTrans <sub>t-1</sub> )	0.6
B-1.3	2933	( RelTrans <sub>t</sub> )	0.5
B-1.4	2927	( RelTrans <sub>t-1</sub> )	0.6
B-1.5	2927	( RelTrans <sub>t</sub> )	0.5
B-1.6	2927	<u>Country</u>	2.2
B-1.7	2927	<u>Country</u>	2.2
<i>Model B-2 Relative meteo</i>			
B-2.0	2927	( RelTrans <sub>t-1</sub> )	0.6
B-2.1	2927	-	0.0
B-2.2	2927	( RelTrans <sub>t-1</sub> )	0.6
B-2.3	2933	( RelTrans <sub>t-1</sub> )	0.6
B-2.4	2933	-	0.0
B-2.5	2927	( RelTrans <sub>t-1</sub> )	0.6
B-2.6	2927	-	0.0
B-2.7	2927	<u>Country</u> , ( RelTrans <sub>t-1</sub> )	2.7
B-2.8	2927	<u>Country</u>	2.2

Legend: Underlined = contribution > 2%; Normal = contribution 1-2%; (Between brackets) = contribution 0.5-1%;  
*Italics* = unexpected sign.



Table A 29 Best explaining models for *Quercus ilex* in Model B

Model	Observations	Selected model	% $R^2_{adj}$
<i>Model B-0 Site &amp; Stand; no time dependency</i>			
B-0.0	1263	-	0.0
B-0.1	175	-	0.0
B-0.2	1263	-	0.0
B-0.3	1263	-	0.0
B-0.4	1263	( Country )	0.5
B-0.5	1263	( Country )	0.5
<i>Model B-1 Absolute meteo</i>			
B-1.0	1263	-	0.0
B-1.1	1263	-	0.0
B-1.2	1263	-	0.0
B-1.3	1263	-	0.0
B-1.4	1263	-	0.0
B-1.5	1263	-	0.0
B-1.6	1263	-	0.0
B-1.7	1263	-	0.0
<i>Model B-2 Relative meteo</i>			
B-2.0	1263	( <i>Heat<sub>mem</sub></i> )	0.5
B-2.1	1263	-	0.0
B-2.2	1263	( <i>Heat<sub>mem</sub></i> )	0.5
B-2.3	1263	( <i>Heat<sub>mem</sub></i> )	0.5
B-2.4	1263	-	0.0
B-2.5	1263	( <i>Heat<sub>mem</sub></i> )	0.5
B-2.6	1263	-	0.0
B-2.7	1263	-	0.0
B-2.8	1263	-	0.0

Legend: Underlined = contribution > 2%; Normal = contribution 1-2%; (Between brackets) = contribution 0.5-1%;  
*Italics* = unexpected sign.

**A 5.4      Analysis of the trend in defoliation data (Model C)**

**Table A 30    Best explaining models for *Pinus sylvestris* in Model C**

Model	Observations	Selected model	% R <sup>2</sup> <sub>adj</sub>
<i>Model C-0 Site &amp; Stand; no time dependency</i>			
C-0.0	1825	<u>pH</u> , ( Alt )	2.6
C-0.1	744	<u>ClimZone</u>	4.9
C-0.2	1825	<u>ClimZone</u>	3.8
C-0.3	1825	<u>L Frost</u> , ( pH )	3.5
C-0.4	1825	<u>Country</u>	14.7
C-0.5	1825	<u>Country</u>	14.7
<i>Model C-1 Absolute meteo</i>			
C-1.0	1815	<u>xSumX</u> , x[NO <sub>2</sub> ] , ( d[NH <sub>3</sub> ] )	3.8
C-1.1	1825	<u>xSumX</u> , x[NO <sub>2</sub> ] , ( d[NH <sub>3</sub> ] )	3.8
C-1.2	1815	<u>xSumX</u> , ( pH )	3.0
C-1.3	1815	<u>Country</u>	14.7
<i>Model C-2 Relative meteo</i>			
C-2.0	1815	<u>xL Frost</u> , ( x[NO <sub>2</sub> ] ) , d[NH <sub>3</sub> ]	4.3
C-2.1	1815	<u>xL Frost</u> , ( x[NO <sub>2</sub> ] ) , d[NH <sub>3</sub> ]	4.3
C-2.2	1825	<u>xL Frost</u> , ( x[NO <sub>2</sub> ] ) , d[NH <sub>3</sub> ]	4.3
C-2.3	1815	<u>xL Frost</u> , ( pH )	3.5
C-2.4	1815	<u>Country</u>	14.7

Legend: Underlined = contribution > 2%; Normal = contribution 1-2%; (Between brackets) = contribution 0.5-1 %;  
*Italics* = unexpected sign.

**Table A 31    Best explaining models for *Picea abies* in Model C**

Model	Observations	Selected model	% R <sup>2</sup> <sub>adj</sub>
<i>Model C-0 Site &amp; Stand; no time dependency</i>			
C-0.0	1576	-	0.0
C-0.1	720	-	0.0
C-0.2	1576	-	0.0
C-0.3	1576	( RelTrans )	0.4
C-0.4	1576	<u>Country</u>	11.1
C-0.5	1576	<u>Country</u>	11.1
<i>Model C-1 Absolute meteo</i>			
C-1.0	1571	( xHeat ) , ( xSumX ) , ( dWinX ) , ( xL-Frost ) , ( dRelTrans )	3.4
C-1.1	1576	( xHeat ) , ( xSumX ) , ( dWinX ) , ( xL-Frost ) , ( dRelTrans )	3.4
C-1.2	1571	( xHeat ) , ( xSumX ) , ( dWinX ) , ( xL-Frost ) , ( dRelTrans )	3.4
C-1.3	1571	<u>Country</u>	11.1
<i>Model C-2 Relative meteo</i>			
C-2.0	1571	xRelTans , ( dHeat ) , ( dRelTrans ) , ( x[NH <sub>3</sub> ] ) , ( dWinX )	3.7
C-2.1	1571	xRelTans , ( dHeat ) , ( dRelTrans ) , ( x[NH <sub>3</sub> ] ) , ( dWinX )	3.7
C-2.2	1576	xRelTans , ( dHeat ) , ( dRelTrans ) , ( x[NH <sub>3</sub> ] ) , ( dWinX )	3.7
C-2.3	1571	xRelTans , ( dHeat ) , ( dRelTrans )	2.4
C-2.4	1571	<u>Country</u>	8.5

Legend: Underlined = contribution > 2%; Normal = contribution 1-2%; (Between brackets) = contribution 0.5-1 %;  
*Italics* = unexpected sign

Table A 32 Best explaining models for *Quercus robur* and *Q. petraea* in Model C

Model	Observations	Selected model	% R <sup>2</sup> <sub>adj</sub>
<i>Model C-0 Site &amp; Stand; no time dependency</i>			
C-0.0	823	( C/N )	0.7
C-0.1	369	-	0.0
C-0.2	823	( C/N )	0.7
C-0.3	823	( C/N )	0.7
C-0.4	823	<u>Country</u>	7.9
C-0.5	823	-	0.0
<i>Model C-1 Absolute meteo</i>			
C-1.0	823	( dWinX ), ( C/N ), ( d[NH <sub>3</sub> ] ), dSumX	3.4
C-1.1	823	( dWinX ), ( C/N ), ( d[NH <sub>3</sub> ] ), dSumX	3.4
C-1.2	823	( C/N ), ( Alt ), ( dRelTrans )	1.6
C-1.3	823	-	0.0
<i>Model C-2 Relative meteo</i>			
C-2.0	823	( dWinX ), ( C/N ), ( d[NH <sub>3</sub> ] ), dSumX	3.4
C-2.1	823	( dWinX ), ( C/N ), ( d[NH <sub>3</sub> ] ), dSumX	3.4
C-2.2	823	( dWinX ), ( C/N ), ( d[NH <sub>3</sub> ] ), dSumX	3.4
C-2.3	823	( dWinX ), ( C/N )	1.7
C-2.4	823	-	0.0

Legend: Underlined = contribution > 2%; Normal = contribution 1-2%; (Between brackets) = contribution 0.5-1%;  
*Italics* = unexpected sign.

Table A 33 Best explaining models for *Fagus sylvatica* in Model C

Model	Observations	Selected model	% R <sup>2</sup> <sub>adj</sub>
<i>Model C-0 Site &amp; Stand; no time dependency</i>			
C-0.0	765	-	0.0
C-0.1	335	-	0.0
C-0.2	765	-	0.0
C-0.3	765	-	0.0
C-0.4	765	<u>Country</u>	5.2
C-0.5	765	-	0.0
<i>Model C-1 Absolute meteo</i>			
C-1.0	764	<i>dHeat</i>	0.7
C-1.1	765	<i>dHeat</i>	0.7
C-1.2	764	<i>dHeat</i>	0.7
C-1.3	764	-	0.0
<i>Model C-2 Relative meteo</i>			
C-2.0	764	( xHeat )	0.6
C-2.1	764	( xHeat )	0.6
C-2.2	764	( xHeat )	0.6
C-2.3	764	( xHeat )	0.6
C-2.4	764	-	0.0

Legend: Underlined = contribution > 2%; Normal = contribution 1-2%; (Between brackets) = contribution 0.5-1%;  
*Italics* = unexpected sign.

Table A 34 Best explaining models for *Quercus ilex* in Model C

Model	Observations	Selected model	% R <sup>2</sup> <sub>adj</sub>
<i>Model C-0 Site &amp; Stand; no time dependency</i>			
C-0.0	206	-	1.9
C-0.1	30	-	24.2
C-0.2	206	-	1.9
C-0.3	206	-	1.9
C-0.4	206	<u>Country</u>	6.1
C-0.5	206	-	6.1
<i>Model C-1 Absolute meteo</i>			
C-1.0	206	<i>xWinX</i>	1.4
C-1.1	206	<i>xWinX</i>	1.4
C-1.2	206	<i>xWinX</i>	1.4
C-1.3	206	-	0.0
<i>Model C-2 Relative meteo</i>			
C-2.0	206	-	0.0
C-2.1	206	-	0.0
C-2.2	206	-	0.0
C-2.3	206	-	0.0
C-2.4	206	-	0.0

Legend: Underlined = contribution > 2%; Normal = contribution 1-2%; (Between brackets) = contribution 0.5-1%;  
*Italics* = unexpected sign.



**A 5.5 Adjusted defoliation values based on the country coefficients.**

*Table A 35 Adjusted values according to the European standard of the defoliation values for Pinus sylvestris supplied by the separate countries (based on results of regression analysis)*

Supplied value	FR	BE	NL	DL	IT	UK-1 <sup>1)</sup>	UK-2 <sup>1)</sup>	DK	EL	PO	ES	LX	SW	AU
0	0	0	0	0	0	0	0	0	0	0	0	0	0	0
1	2	1	3	1	1	0	1	1	1	2	2	1	2	2
5	11	4	14	5	6	2	4	4	7	9	8	4	8	12
10	21	7	26	10	13	5	9	8	14	17	16	8	15	22
15	30	11	36	16	19	8	13	12	20	24	23	12	22	30
20	38	15	44	21	25	11	17	16	27	31	29	16	29	38
25	45	19	51	26	30	14	22	20	33	37	36	20	35	45
30	51	24	58	31	36	17	26	24	38	43	42	25	41	52
35	56	28	63	36	41	20	31	29	44	49	47	29	47	57
40	62	33	68	41	47	24	36	33	49	54	52	34	52	62
45	66	37	72	46	52	28	41	38	54	59	58	38	57	67
50	71	42	76	51	57	32	46	43	59	64	62	43	62	71
55	75	47	80	56	62	37	51	48	64	69	67	48	67	75
60	78	52	83	61	66	42	56	53	69	73	71	53	71	79
65	82	57	86	66	71	47	61	58	73	77	75	59	75	82
70	85	63	88	71	75	53	66	63	77	81	79	64	79	85
75	88	69	91	76	80	59	72	69	81	84	83	70	83	88
80	91	74	93	81	84	65	77	75	85	88	87	75	87	91
85	93	80	95	86	88	73	83	81	89	91	90	81	90	93
90	96	87	97	90	92	81	88	87	93	94	94	87	94	96
95	98	93	98	95	96	90	94	93	97	97	97	94	97	98
99	100	99	100	99	99	98	99	99	99	99	99	99	99	100
100	100	100	100	100	100	100	100	100	100	100	100	100	100	100

<sup>1)</sup> UK-1 = UK till 1991; UK-2 = UK from 1992 onwards

*Table A 35 (continued)*

Supplied value	FI	RO	PL	SR	NO	CH	HU	LI	CZ	EE	SL	BY	BU	LA
0	0	0	0	0	0	0	0	0	0	0	0	0	0	0
1	2	0	1	0	2	1	2	1	0	1	1	1	0	1
5	10	2	3	2	9	7	8	3	2	5	5	5	2	3
10	20	4	6	4	18	13	15	6	4	10	9	11	4	6
15	28	5	9	6	26	19	22	9	7	15	14	16	7	9
20	36	8	12	8	33	25	29	13	9	20	19	21	10	12
25	43	10	15	10	40	31	35	16	12	25	24	27	12	16
30	49	12	19	13	46	36	41	20	15	30	29	32	15	19
35	54	15	22	16	51	42	47	24	18	35	33	37	19	23
40	60	18	26	19	57	47	52	28	22	40	38	42	22	27
45	65	21	30	22	62	52	57	32	26	45	43	47	26	31
50	69	25	35	26	66	57	62	37	30	50	48	52	30	36
55	73	29	40	30	71	62	67	42	34	55	53	57	34	40
60	77	33	45	34	75	67	71	47	39	60	58	62	39	45
65	80	38	50	39	78	71	75	52	44	65	63	67	44	51
70	84	43	56	44	82	76	79	58	49	70	68	72	50	56
75	87	50	62	51	85	80	83	64	56	75	74	76	56	63
80	90	57	68	58	89	84	87	70	63	80	79	81	63	69
85	93	65	75	66	92	88	90	77	70	85	84	86	71	76
90	95	75	83	76	95	92	94	84	79	90	89	91	79	83
95	98	86	91	87	97	96	97	92	89	95	95	95	89	91
99	100	97	98	97	99	99	99	98	98	99	99	99	98	98
100	100	100	100	100	100	100	100	100	100	100	100	100	100	100

Table A 36 Adjusted values according to the European standard of the defoliation values for *Picea abies* supplied by the separate countries (based on results of regression analysis)

Supplied value	FR	BE	DL	IT	UK-1 <sup>1)</sup>	UK-2 <sup>1)</sup>	IR	DK	ES	LX	SW	AU	FI	RO
0	0	0	0	0	0	0	0	0	0	0	0	0	0	0
1	5	1	1	5	1	1	1	1	1	1	1	5	1	1
5	22	6	5	23	3	4	3	4	4	6	5	22	6	5
10	37	12	10	38	6	8	6	8	8	12	10	37	11	11
15	48	18	15	50	9	13	9	12	12	18	15	48	16	16
20	57	24	19	58	12	17	12	16	16	23	20	57	22	21
25	64	30	24	65	15	22	16	21	20	29	25	64	27	27
30	69	35	29	71	19	26	19	25	24	34	30	69	32	32
35	74	40	34	75	23	31	23	30	29	40	35	74	38	37
40	78	46	39	79	27	36	27	34	33	45	40	78	43	42
45	81	51	44	82	31	41	31	39	38	50	45	81	48	47
50	84	56	49	85	35	45	36	44	43	55	50	84	53	52
55	86	61	54	87	40	50	41	49	48	60	55	87	58	57
60	89	65	59	89	45	56	46	54	53	65	60	89	63	62
65	91	70	64	91	50	61	51	59	58	69	65	91	68	67
70	92	75	69	93	56	66	57	65	64	74	70	92	72	72
75	94	79	74	94	62	71	63	70	69	79	75	94	77	77
80	95	83	79	96	69	77	69	76	75	83	80	95	82	81
85	97	88	85	97	76	83	76	82	81	87	85	97	86	86
90	98	92	90	98	83	88	83	88	87	92	90	98	91	91
95	99	96	95	99	91	94	91	94	93	96	95	99	96	95
99	100	99	99	100	98	99	98	99	99	99	99	100	99	99
100	100	100	100	100	100	100	100	100	100	100	100	100	100	100

<sup>1)</sup> UK-1 = UK till 1991; UK-2 = UK from 1992 onwards

Table A 36 (continued)

Supplied value	PL	SR	NO	CH	HU	LI	CR	CZ	EE	SL	BY	BU	LA
0	0	0	0	0	0	0	0	0	0	0	0	0	0
1	0	0	2	1	3	0	2	0	2	1	0	2	1
5	2	2	9	6	13	2	9	2	10	5	0	8	3
10	5	4	18	12	24	4	18	5	19	9	0	16	6
15	7	7	26	18	33	6	26	8	27	14	1	23	9
20	10	9	33	23	41	9	33	11	35	19	1	29	13
25	13	12	39	29	48	11	40	14	42	23	1	36	16
30	16	15	46	34	55	14	46	17	48	28	1	42	20
35	20	18	51	39	60	17	52	20	54	33	2	47	24
40	23	22	57	45	65	20	57	24	59	38	2	53	28
45	27	25	62	50	70	23	62	28	64	43	2	58	32
50	31	29	66	55	74	27	67	32	68	48	3	63	37
55	35	33	70	60	77	31	71	37	72	53	3	67	42
60	40	38	75	64	81	36	75	42	76	58	4	72	47
65	46	43	78	69	84	41	79	47	80	63	5	76	52
70	51	49	82	74	87	47	82	53	83	68	6	80	58
75	57	55	85	78	89	53	86	59	87	73	8	83	64
80	64	62	89	83	92	60	89	65	90	78	10	87	70
85	72	70	92	87	94	68	92	73	92	84	14	90	77
90	80	79	95	92	96	77	95	81	95	89	21	94	84
95	90	89	97	96	98	88	97	90	98	95	36	97	92
99	98	98	99	99	100	97	99	98	100	99	74	99	98
100	100	100	100	100	100	100	100	100	100	100	100	100	100

Table A 37 Adjusted values according to the European standard of the defoliation values for *Quercus robur* and *Q. petraea* supplied by the separate countries (based on results of regression analysis)

Supplied value	FR	BE	NL	DL	IT	UL-1 <sup>1)</sup>	UK-2 <sup>1)</sup>	DK	EL	PO	ES	LX	SW
0	0	0	0	0	0	0	0	0	0	0	0	0	0
1	3	3	2	1	2	1	1	1	1	6	1	1	1
5	15	13	9	4	8	4	6	3	3	25	7	7	6
10	27	24	17	8	15	8	12	6	7	41	14	13	12
15	37	33	25	13	22	12	17	9	11	53	21	19	18
20	45	41	32	17	28	16	23	12	14	61	27	25	23
25	53	49	39	22	35	20	29	16	18	68	33	31	29
30	59	55	45	26	41	24	34	19	22	73	39	36	34
35	64	60	51	31	46	29	39	23	26	77	44	42	39
40	69	65	56	36	51	33	44	27	31	81	49	47	45
45	73	70	61	40	57	38	50	31	35	84	55	52	50
50	77	74	66	45	61	43	55	36	40	86	59	57	55
55	80	78	70	50	66	48	59	40	45	88	64	62	60
60	83	81	74	55	70	53	64	45	50	90	69	67	64
65	86	84	78	61	75	58	69	51	55	92	73	71	69
70	89	87	82	66	79	63	74	56	61	94	77	76	74
75	91	89	85	71	83	69	78	62	67	95	81	80	78
80	93	92	88	77	86	75	83	69	73	96	85	84	83
85	95	94	92	82	90	81	87	76	79	97	89	88	87
90	97	96	94	88	93	87	92	83	86	98	93	92	92
95	98	98	97	94	97	93	96	91	93	99	97	96	96
99	100	100	99	99	99	99	99	98	99	100	99	99	99
100	100	100	100	100	100	100	100	100	100	100	100	100	100

<sup>1)</sup> UK-1 = UK till 1991; UK-2 = UK from 1992 onwards

Table A 37 (continued)

Supplied value	AU	RO	PL	SR	CH	HU	LI	CR	CZ	SL	MO	BU	LA
0	0	0	0	0	0	0	0	0	0	0	0	0	0
1	8	1	1	1	1	1	1	1	0	1	0	0	1
5	31	3	3	3	3	3	4	6	1	4	2	1	4
10	49	7	7	5	7	7	8	11	3	8	4	2	9
15	60	10	10	8	10	11	12	17	4	12	6	4	13
20	68	14	14	11	14	14	16	22	6	16	9	5	18
25	74	17	18	15	18	18	21	28	7	21	11	7	22
30	79	21	22	18	22	22	25	33	9	25	14	8	27
35	82	25	26	22	26	27	30	38	11	30	17	10	31
40	85	30	30	25	30	31	34	43	14	34	20	12	36
45	88	34	35	30	35	35	39	48	16	39	23	15	41
50	90	39	39	34	39	40	44	53	19	44	27	17	46
55	91	43	44	38	44	45	49	58	22	49	31	20	51
60	93	48	49	43	49	50	54	63	26	54	36	24	56
65	94	54	55	49	54	56	59	68	30	59	41	28	61
70	95	59	60	54	60	61	65	73	36	65	47	33	67
75	96	65	66	61	66	67	70	78	41	70	53	39	72
80	97	72	72	67	72	73	76	82	49	76	60	46	77
85	98	78	79	74	78	79	82	87	57	82	68	54	83
90	99	85	85	82	85	86	88	91	68	88	77	65	88
95	99	92	92	91	92	93	94	96	82	94	88	80	94
99	100	98	98	98	98	99	99	99	96	99	97	95	99
100	100	100	100	100	100	100	100	100	100	100	100	100	100



Table A 38 Adjusted values according to the European standard of the defoliation values for *Fagus sylvatica* supplied by the separate countries (based on results of regression analysis)

Supplied value	FR	BE	DL	IT	UK-1 <sup>1)</sup>	UK-2 <sup>1)</sup>	DK	EL	ES	LX	SW
0	0	0	0	0	0	0	0	0	0	0	0
1	2	2	1	3	0	1	0	2	2	1	1
5	12	10	3	14	2	3	2	8	8	5	3
10	22	19	7	25	4	7	4	16	15	10	6
15	31	27	11	35	6	10	6	24	22	14	9
20	39	35	15	43	8	14	8	30	28	19	13
25	46	41	19	50	11	18	10	37	34	24	16
30	52	47	23	57	13	22	13	43	40	29	20
35	57	53	27	62	16	26	15	48	46	34	24
40	63	58	31	67	19	30	18	54	51	39	28
45	67	63	36	71	22	35	22	59	56	44	32
50	72	68	41	75	26	39	25	64	61	49	37
55	75	72	45	79	30	44	29	68	66	54	41
60	79	76	51	82	35	49	34	72	70	59	46
65	82	80	56	85	40	55	39	76	75	64	52
70	85	83	61	88	45	60	44	80	79	69	57
75	88	86	67	90	52	66	50	84	83	74	63
80	91	89	73	92	59	72	57	87	86	79	70
85	93	92	79	95	67	79	66	91	90	84	77
90	96	95	86	96	76	85	75	94	93	90	84
95	98	98	93	98	87	92	87	97	97	95	92
99	100	100	99	100	97	98	97	99	99	99	98
100	100	100	100	100	100	100	100	100	100	100	100

<sup>1)</sup> UK-1 = UK till 1991; UK-2 = UK from 1992 onwards

Table A 38 (continued)

Supplied value	AU	RO	PL	SR	CH	HU	CR	CZ	SL	BU
0	0	0	0	0	0	0	0	0	0	0
1	2	1	0	1	1	3	2	1	1	1
5	10	5	2	3	4	13	11	3	5	3
10	19	10	4	6	8	23	20	5	10	6
15	28	15	7	10	12	33	29	8	15	9
20	35	20	10	13	16	41	37	11	20	12
25	42	25	12	17	20	48	43	14	25	16
30	48	30	15	21	25	54	50	18	30	19
35	54	35	19	25	29	60	55	21	34	23
40	59	40	22	29	34	65	61	25	39	27
45	64	45	26	34	38	69	65	29	44	32
50	68	50	30	38	43	73	70	33	49	36
55	73	55	34	43	48	77	74	38	54	41
60	76	60	39	48	53	81	78	43	59	46
65	80	65	44	54	59	84	81	48	64	51
70	83	70	50	59	64	87	84	54	69	57
75	87	75	56	65	70	89	87	60	75	63
80	90	80	63	71	75	92	90	67	80	69
85	92	85	71	78	81	94	93	74	85	76
90	95	90	79	85	87	96	95	82	90	84
95	98	95	89	92	94	98	98	91	95	91
99	100	99	98	98	99	100	100	98	99	98
100	100	100	100	100	100	100	100	100	100	100

Table A 39 *Adjusted values according to the European standard of the defoliation values for Quercus ilex supplied by the separate countries (based on results of regression analysis)*

Supplied value	FR	IT	EL	ES	CR	SL
0	0	0	0	0	0	0
1	2	4	0	1	1	1
5	8	16	1	4	6	4
10	15	29	3	8	11	8
15	22	39	4	13	17	12
20	28	48	6	17	23	16
25	34	55	8	21	28	20
30	40	61	10	26	33	24
35	46	66	12	30	39	28
40	51	71	14	35	44	33
45	56	75	17	40	49	38
50	61	78	20	45	54	42
55	66	82	24	50	59	47
60	70	84	27	55	64	53
65	74	87	32	60	68	58
70	78	89	37	65	73	63
75	82	92	43	71	78	69
80	86	94	50	76	82	75
85	90	95	59	82	87	81
90	93	97	69	88	91	87
95	97	99	83	94	96	93
99	99	100	96	99	99	99
100	100	100	100	100	100	100

## ERRATA

The titles of Fig. 43 and Fig. 47 at the bottom of pages 110 and 113 have dropped through the bottom margin. The titles should be as follows:

At page 110:

*Fig. 43 The difference between the calculated 10 years average present N deposition level and the critical N deposition level related to effects on the forest understorey for all monitoring plots*

At page 113:

*Fig. 47 The difference between the calculated 10 years average present acid deposition level and the critical acid deposition level for all monitoring plots*



